New York State Department of
Environmental Conservation
21 South Putt Corners Road
New Paltz, NY 12561

Shallow water benthic mapping:
West side Manhattan and Brooklyn waterfront

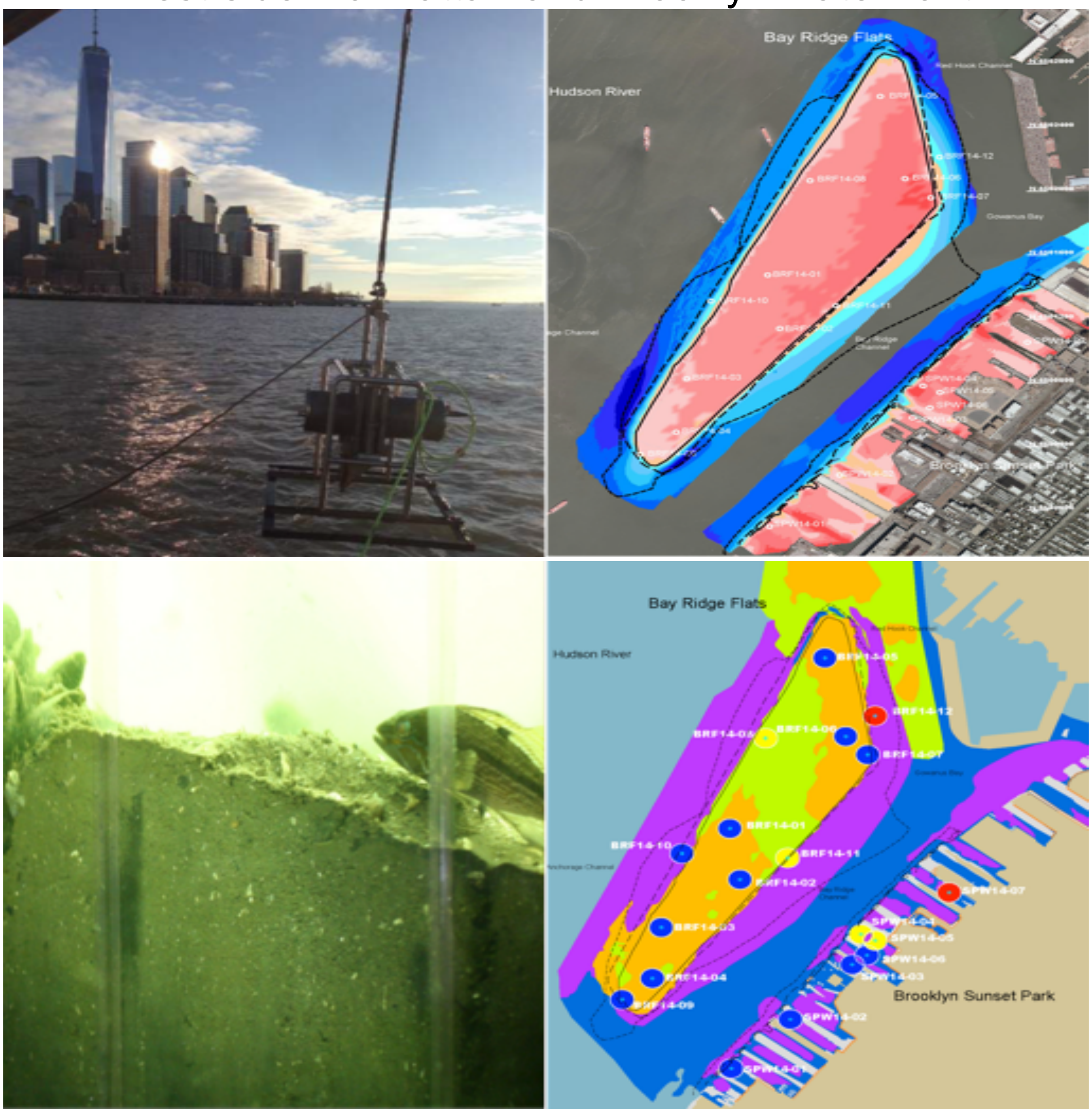

October 28, 2015

e4sciences | Earthworks, LLC
27 Glen Road, North Entrance
Sandy Hook, Connecticut 06482
P.O. Box 178, Newtown, CT 06470
(203) 270-8100, Fax (203) 364-0480
www.e4sciences.com

CH2M Hill
22 Cortlandt St. 31st Floor
New York, NY 10007
(720) 286-2000
www.ch2m.com

All interpretations are opinions based on inferences from geophysical, biological and other measurements. We cannot, and do not, guarantee the accuracy or correctness of any interpretation. We shall not, except in the case of gross or willful negligence on our part, be liable or responsible for any loss, costs, damages or expenses incurred or sustained by anyone resulting from any interpretations made by any of our officers, agents or employees.

Executive Summary

The New York State Department of Environmental Conservation (DEC) monitors the Hudson River Estuary. The New York City Department of Environmental Protection (DEP) has partnered with the DEC to map the shallow waters in the Hudson and East Rivers.

The DEP assigned e4sciences (e4) to map the sediment strata, the shoreline structures, and the benthic infaunal communities on both the western shoreline of Manhattan and the northwestern shore of Brooklyn. e4 measured the bathymetry, sonar reflectivity, seismic reflectivity, sediment chemistry, grain size, infrastructure, and benthic organisms.

e4 collected and analyzed sediment cores and grab samples to determine grain size distribution, benthic invertebrate faunal communities, and sediment chemistry. e4 collected and analyzed Sediment Profile Imagery (SPI) to determine fine-scale structures, infaunal activity, and water chemistry at the sediment-water interface and within the uppermost few (~21 cm) centimeters of sediment. e4 integrated geological, chemical, and biological data with additional mapping, acoustic and sub-bottom datasets to derive sediment accumulation rates and integrated bottom classifications in the harbor. e4 also integrated newly collected data and analyses with previous work conducted in the harbor. The current analysis included measures of change over time, to the extent that previous work spatially and analytically overlaps areas of investigation in this project.

e4 developed detailed bathymetric, acoustic-reflectivity, benthic-organism, and acoustic-character maps of the shallow portions of the Upper Bay of New York Harbor. The area of investigation is divided into eight areas:

1. Bay Ridge Flats
2. Governors Island
3. Sunset Park waterfront
4. Brooklyn Bridge Park
5. Brooklyn Navy Yard
6. West Manhattan waterfront South (Harrison St. to 17th St.)
7. West Manhattan waterfront Middle (17th St. to 57th St.)
8. West Manhattan waterfront North (57th St. to 109th St.)

The survey, SPI drop, and grab sample site results show that five areas – Bay Ridge Flats, Brooklyn Bridge Park, Sunset Park waterfront, West Manhattan waterfront South, and West Manhattan waterfront Middle – are overall healthy, lightly stressed[1] ecosystems. They represent the breadth of diverse benthic ecosystems in NY Harbor. The other three areas – Governors Island, the Brooklyn Navy Yard, and West Manhattan waterfront North – are a mixture of healthy and stressed sites. Some of the more diverse and well-established communities live in the sandier environments with better circulation. Many of the healthier communities in the three areas with a mixture of healthy and stressed sites, were observed in the physically quiet regions with lower deposition, erosion, or disturbance[2]. e4 finds healthy communities in both fine and coarse-grained

---

[1] e4 based our definition of stress on the work of Hale et al. (2007) who limited environmental stress to three measurable parameters: dissolved oxygen, salinity, and sediment composition. Because the Organism Sediment Index (OSI) captures two of these three parameters, we used OSI values to determine designations of stress level at each of our samples sites. More generally, environmental stress refers to physical, chemical, and biological forces on the productivity of species and on the development of ecosystems. When the exposure to environmental forces or stressors, such as pollution or pathogens, increases or decreases in intensity, ecological responses result (Rhoads and Germano, 1986).

[2] e4 based the definition used for disturbance throughout this report on the previous work of Don Rhoads. By Rhoads' definition, disturbance refers specifically to sediments that have been anthropogenically affected and captures both chemical contamination and physical manipulation (e.g. construction and dredging) of the harbor bottom. In e4's modified definition, we account for sediment accumulation rate (volume/area/year) and include both, but distinguish between, natural and anthropogenic processes. We relate

sediments: communities dominated by Stage I species in fine-grained sediments; communities dominated by Stage III species in coarse-grained sediments. Grain size is a controlling factor in determining the kind of benthic community observed, while physical disturbance relates most strongly to the apparent health, as indicated by the Organism Sediment Index (OSI), of the community.

e4sciences compared the current results with data collected 10 or more years ago. Seasonal spring to fall variations notwithstanding, e4sciences observed that the western shorelines of Manhattan and Brooklyn are generally healthy and have been improving since 1993. Efforts to remove polluted silts, increase park areas (with corresponding reductions in boat traffic), and clean the water have begun to show measurable success. For example, on the southwest shore of Manhattan, our study showed that the benthic environment is less stressed compared to the conditions reported by Hale et al. (2007) with healthy sites observed further northward than previously reported. This is likely the consequence of New York City's continued efforts to improve water quality with advanced sewage treatment programs and education of the public to encourage a higher quality, sustainable New York Harbor ecosystem that benefits the overall community. In addition, 400 water-acres in this area were designated the Hudson River Park and became part of the Hudson River Park Estuarine Sanctuary in 1998, which has reduced use of the shallows (less boat traffic) in this area and also contributed to increased benthic ecosystem health.

The current results, when compared with data collected 10 or more years ago, indicate that the quality of the overall benthic habitat within open water areas such as Bay Ridge Flats and Governors Island remained stabilized with many Organism-Sediment Index (OSI) values greater than 6. We found pockets of low quality habitats in Brooklyn Navy Yard, at the mouth of the Gowanus Canal, within berthing slips of West Manhattan waterfront North, and in sediment traps around the shore of Governors Island and on the slopes of Bay Ridge Flats. These areas are active both from natural tidal forces and from sediment movement related to human use of the harbor. Many have been previously identified as stressed habitats.

Analyses of the benthic communities show a strong association with sediment type, specifically grain size. Acoustic reflectivity in the orthosonographs, benchmarked by cores and grab samples, distinguishes the differences between the sandy environments and the silty environments. The more diverse and well-established communities live in the sandier environments with better circulation, corresponding to the highest observed OSI values. There are healthy communities in the siltier, finer-grained sediments, however these sites are more variable and, we hypothesize, more sensitive to sediment accumulation rates. The contour map of the black silt shows that such environments are generally restricted to the inner confines of the piers and the leeward sides of structures and outcrops, such as Governors Island. Sites with the highest rates of black silt and sediment accumulation (e.g. BNY14-02, BRF14-12) have low OSI scores.

In Bay Ridge Flats, Brooklyn Bridge Park, some sites at Governors Island, Sunset Park waterfront, West Manhattan waterfront South, and West Manhattan waterfront Middle, infaunal amphipods, gastropods, and other sediment feeders represent equilibrium stage (Stage III) or successional end-stage species. e4 found shallow-dwelling bivalves (*Mulinia lateralis*, *Tellina agilis*), grazing gastropods (*Illyanassa* sp.), and a few species of tubicolous amphipods (*Ampelisca sp.*). Stage III assemblages include maldanid, nepthyd, and lumbrinerid polychaetes, nuculanid clams, and *Molpadia* tunicates. These areas have deeply oxygenated sediment surfaces where the apparent redox discontinuity (aRPD) commonly reaches depths of over 10 cm.

---

chemical contamination with apparent redox potential discontinuity (aRPD), which is a proxy for soil oxygenation, cleanliness, and biotic irrigation.

Opportunistic benthic organisms can be found in Sunset Park waterfront, Brooklyn Navy Yard, West Manhattan waterfront North, the southern tip of Governors Island, and the western and eastern sediment traps at Governors Island (GI14-04 and GI14-08). The opportunists are the initial species to occupy organically enriched habitat. In our SPI analyses, we observed small opportunistic tube-dwelling polychaetes or oligochaetes, identified as Stage I successional species. They are among the first macrofaunal components to colonize newly disturbed sediments. These worms may reach high densities of greater than $10^5/m^2$ within a few days to weeks after disturbance. The pioneering species that colonize a disturbed bottom may vary, depending on substratum. They oxidize the sediment-water interface and they pave the way for later successional stage species (Stage II and Stage III). The pioneering species feed near the sediment surface or from the water column. They construct tube walls or shells that isolate them from the poor quality sediment often low in oxygen and high in organic content.

e4sciences identified controlling factors for the spatial distribution of the benthic communities as (a) the geological or structural substrate, (b) well-circulating cleaner water, and (c) anthropogenic disturbance. Water quality and the presence of pathogens, pollutants, and suspended sediments are important. The amount of pollutants has been reduced in the past forty years. Suspended sediment load is declining. These trends have contributed to improved benthic community health in the Upper Bay areas of New York Harbor.

e4sciences used bathymetry, sonar reflectivity, and seismic reflectivity to characterize site sediments, their properties, and their thicknesses. A contour map shows the thickness and spatial distribution of the black silt. Pleistocene sediments are exposed in Bay Ridge Flats and northeastern Governors Island. Bay Ridge Flats have retained their morphology over two hundred years.

e4sciences did not observe completely anoxic conditions in the benthic zone at any of our sample sites. In fact, e4sciences found that the areas of investigation are lightly stressed at worst, and are healthier than observed in previous work conducted in the 1970's and 1990's.

The schist of the Hartland Formation is exposed in Governors Island. The Fordham gneiss is exposed in Brooklyn Bridge Park underneath the Manhattan Bridge. Rock is relatively shallow on the west shore of Manhattan.

The fish in New York Harbor seek the areas of high vorticity. The orthosonographs show that fish were observed in areas around Governors Island, Manhattan, and Bay Ridge Flats. In fact, fish were observed in many SPI locations.

Appendices contain the raw and processed digital data with their corresponding shapefiles and metadata. The metadata describes the data type, size, and geographic extent of both the raw and processed data. The metadata follows the Federal Geographic Data Committee standards. e4sciences provided license-free viewers for side-scan sonar and sub-bottom reflection seismology.

Table of Contents

List of Figures

List of Tables

List of Plates

1.0 Introduction

The New York State Department of Environmental Conservation (DEC) monitors the Hudson River Estuary with care. The New York City Department of Environmental Protection (DEP) has partnered with the DEC to map the shallow water sediments and benthic infaunal communities in the Hudson and East Rivers.

The DEP assigned e4sciences (e4) to map the sediment strata, the shoreline structures, and the benthic communities on both the western shoreline of Manhattan and the northwestern shore of Brooklyn. e4 measured the bathymetry, sonar reflectivity, seismic reflectivity, sediment chemistry, grain size, infrastructure, and benthic organisms. e4 collected and analyzed sediment cores and grabs to determine grain size distribution, benthic invertebrate faunal communities, and sediment accumulation rates. e4 collected and analyzed Sediment Profile Imagery (SPI) to determine fine-scale structures at the sediment-water interface and within the uppermost few centimeters of sediments. e4 integrated newly collected data and analyses with previous work conducted in the harbor. The current analysis included measures of change over time, to the extent that previous work spatially and analytically overlaps areas of investigation in this project.

e4 developed detailed bathymetric maps, acoustic reflectivity, and acoustic character maps of the shallow portions of the Upper Bay of New York Harbor. Figure 1 shows an encompassing view of the study area. Figure 2 shows oblique aerial photographs of the area of investigation. The area of investigation is divided into eight regions:

1. Bay Ridge Flats
2. Governors Island
3. Sunset Park waterfront
4. Brooklyn Bridge Park
5. Brooklyn Navy Yard
6. West Manhattan waterfront South (Harrison St. to 17th St.)
7. West Manhattan waterfront Middle (17th St. to 57th St.)
8. West Manhattan waterfront North (57th St. to 109th St.)

Table 1. Project chronology. Note the dates are presented as the year, month, and date.

Task	Category	Description	Fraction	Completion date
			Portion/total	yyyy.mm.dd
0		Notice to proceed		2014.03.14
0		QA/QC plan		2014.04.30
1	Acquisition	Bathymetry, acq. & proc.	0.13	2015.05.15
2		Reflectivity, acq. & proc.	0.03	2014.10.31
3		Sub-bottom seismology, acq. & proc.	0.15	2014.10.31
4		Sediment isopach maps	0.04	2015.01.15
5		SPI, acq. & proc.	0.09	2014.12.15
6A	Sampling	Coring	0.05	2014.11.20
6B		Grab Samples	0.03	2014.11.20
6C	Analyses	Grain size	0.04	2015.01.31
6D		Lead	0.01	2015.01.31
6E		7Be/137Cs	0.02	2015.01.31
7		Invertebrates	0.09	2015.01.31
8A	Integration	Bottom classification	0.03	2014.02.28
8B		Review benthic literature	0.07	2015.02.28
8C		Interpret benthic history	0.08	2015.02.28
9		QA/QC	0.04	2015.03.15
10	Reporting	Metadata	0.00	2015.04.30
11		Viewer	0.00	2015.03.15
12		Final draft	0.10	2015.05.20
13		Digital compilation	0.01	2015.05.15
14	Review	Report review CH2MHILL		2015.05.25
15		Final report		2015.05.31
	Total		1.00	2015.05.31

1.1 Objective

The Hudson River Estuary Action Plan, introduced by NYSDEC and approved by the Governor in 1996, committed the State to, among other things, conduct a submerged habitat inventory to define areas most in need of protection for Hudson River fish, blue crab, and food chain species.

More recently, NYSDEC published a Hudson River Estuary Action Agenda (http://www.dec.ny.gov/lands/5104.html) consisting of 12 goals including:

- Goal 2: to conserve, protect, and, where possible, enhance critical river and shoreline habitats to assure that the life cycles of key species are supported for human enjoyment and to sustain a healthy ecosystem.
- Goal 3: to conserve for future generations the rich diversity of plants, animals and habitats that are key to the vitality, natural beauty and environmental quality of the Hudson River Valley.

To address the commitment of the original Action Plan, NYSDEC contracted studies in the estuary that produced digital acoustic side-scan mosaics, bathymetry, sub-bottom profiles, and sediment cores and grabs for much of the estuary. From these datasets, interpretive maps of sediment type and geological substrate were produced.

(http://www.nysgis.state.ny.us/gisdata/inventories/details.cfm?DSID=1136).

Under these same contracts NYSDEC acquired benthic invertebrate faunal community information in two pilot study areas – in the Tappan Zee and in the reach from Kingston to Saugerties (Maher and Cerrato, 2004; Strayer and Malcom, 2004). Under a separate contract, NYSDEC collected a suite of sediment samples throughout the estuary for the purposes of exploring the relationships among benthic faunal communities and contaminants found in the sediments on or in which the benthic fauna lives. The details of these studies can be found in the reports delivered under these contracts (see Maher, 2006 and Llanso et al., 2003).

Early phases of benthic mapping were limited in that detailed bathymetry was not acquired in areas of the estuary shallower than about four (4) meters, due to financial constraints. About a third of the estuary was not surveyed; however, this third is the area that includes important habitats for various species of interest. Recently, surveys were completed in the shallow portions of the estuary north from Saugerties to Troy using an interferometer side-scan system.

Studies have indicated that variations in remote sensing acoustic data can be used to characterize the sediment environment (Bell et al, 2006; Nitsche et al., 2004) and have considerable value in explaining variations in benthic macro invertebrate communities (Maher, 2006; Strayer et al., 2006; Yeung and McConnaughey 2008; Flood and Cerrato, 2010, Cerrato and Flood, 2009). The acquisition of acoustic data, sediment profile imagery and sediment samples in the shallow water areas of the estuary would extend the classification of the substrate into sediment provinces and biologically significant units begun under previous benthic mapping contracts (Bell et al., 2000; Bell et al., 2003; Bell et al., 2004a; Bell et al., 2004b; Nitsche and Kenna, 2010; Nitsche and Kenna, 2011; Kenna and Nitsche, 2011; Maher and Cerrato, 2004; Iocco et al., 2000a). Of particular importance are sediment classification and faunal unit identification in the shallow areas of the Upper Bay of New York Harbor. This work involves acoustic surveys and sediment sampling in shallow areas followed by analysis and integration with previous work including work conducted under previous NYSDEC benthic mapping contracts and under United States Army Corps of Engineers benthic surveys related to the harbor deepening project (USACE, 1999a; USACE, 1999b; USACE, 1999c; USACE, 2006; USACE, 2012; Iocco et al., 2000b).

To support these various programs in the monitoring and management of the Hudson River Estuary, the NYC DEP assigned e4sciences to perform the following:

1) Develop detailed bathymetric maps, acoustic reflectivity and acoustic character maps of the shallow portions of the Upper Bay of NY/NJ Harbor including Bay Ridge Flats, Governors Island, Hudson River Park, Brooklyn Navy Yard, Brooklyn Bridge Park and the Sunset Park waterfront.

2) Collect and analyze sediment cores and grab samples to determine grain size distribution, benthic invertebrate faunal communities, sediment chemistry, and – by integrating with other datasets – sediment accumulation rates.

3) Collect and analyze Sediment Profile Imagery (SPI) to determine fine-scale structures at the sediment-water interface and within the uppermost (~21 cm) few centimeters of sediment.

4) Integrate newly collected data and analyses with previous work conducted in the harbor.

5) Include measures of change over time in the analyses to the extent that previous work spatially overlaps areas of investigation in this project.

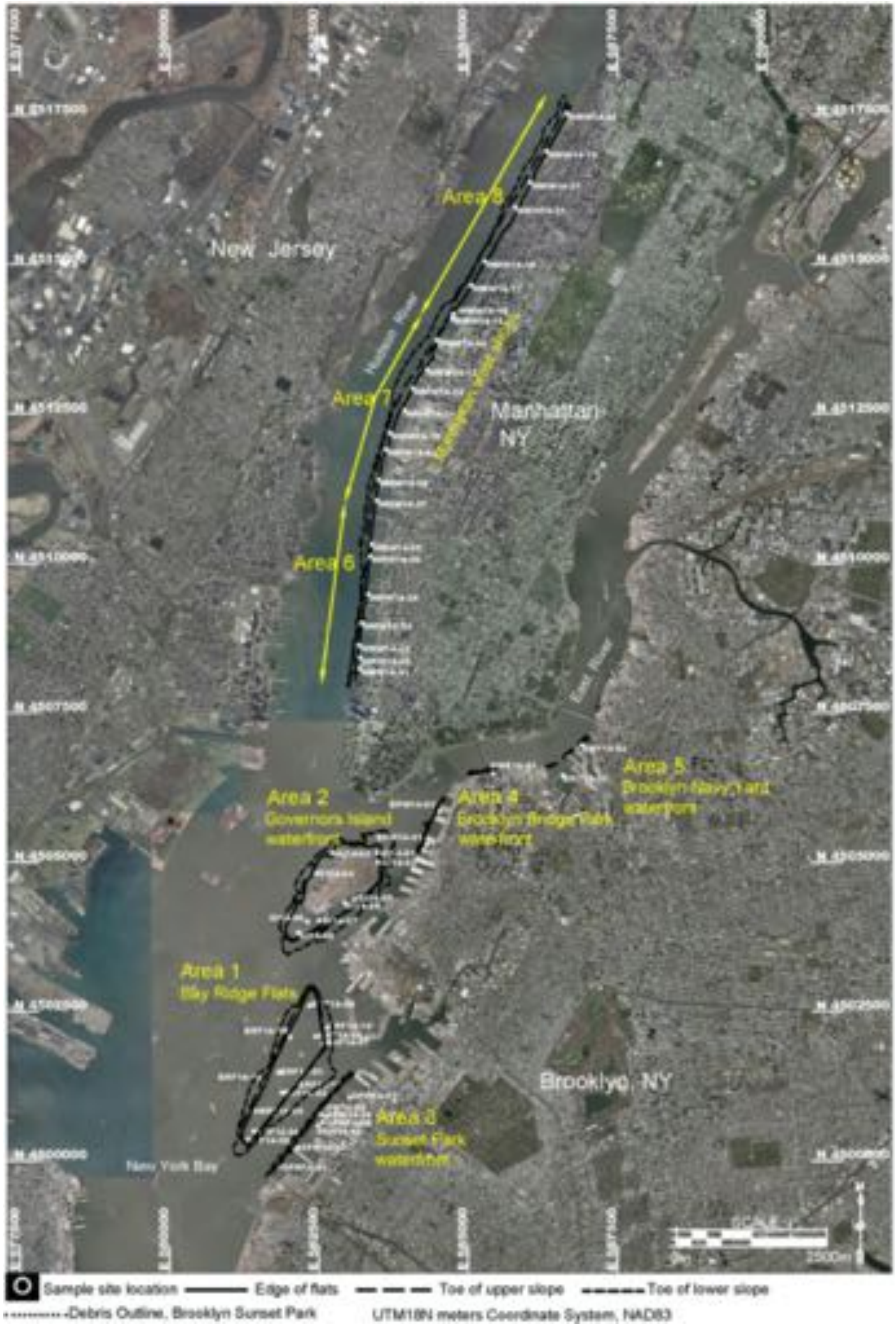

Figure 1. Location map of area of investigation and its eight subdivisions.

Figure 2. Oblique aerial photographs of the area of investigation.

2.0 Scope of work

The e4sciences team conducted the tasks and options presented in the DEC/DEP's Scope of Work, dated January 31, 2013. Appendix I contains the full version of the January 31 scope. The tasks were:

Task 1. Bathymetric surveys
Task 2. Acoustic reflectivity data
Task 3. Sub-bottom reflection seismology
Task 4. Sediment profiler imagery (SPI)
Task 5. Sediment grab samples
Task 6. Sediment cores acquisition
Task 7. Core description, grain size measurement, ^{7}Be and ^{137}Cs
Task 8. Lead concentrations in core
Task 9. Digital elevation models (DEMs), bathymetric contours, acoustic character images
Task 10. Integrate new bathymetric data with other multibeam sonar data in the harbor
Task 11. Create interpretive maps of sediment type, sediment environment
Task 12. Where feasible, provide analysis of change over time of bathymetry, acoustic character, sediment type and benthic invertebrate communities
Task 13. Provide a non-proprietary side-scan viewer
Task 14. Provide metadata describing data products produce under this contract
Task 15. Provide analysis of accuracy and precision of horizontal positioning and depth observation for data acquired under this contract
Task 16. Submit monthly progress reports summarizing progress made and problems encountered
Task 17. Contractor may publish papers or other material after first providing the Department a copy of the proposed publication
Task 18. Data collected and products generated under this contract are considered to be the property of New York State

The surveys included the shoals and aprons shown in Figure 3:

1. Bay Ridge Flats
2. Sunset Park waterfront
3. Governors Island
4. Brooklyn Navy Yard
5. Brooklyn Bridge Park
6. West shore of Manhattan

The Scope of Work specified 13 deliverables:

Deliverable 1. Hydrographic surveys
Deliverable 2. Sonar reflectivity
Deliverable 3. Sub-bottom reflection seismology
Deliverable 4. Sediment isopach map
Deliverable 5. Sediment Profile Imaging
Deliverable 6. Sediment samples
Deliverable 7. Invertebrate identification and classification
Deliverable 8. Bottom classification
Deliverable 9. Quality assurance/quality control
Deliverable 10. Metadata
Deliverable 11. Side-scan sonar viewer
Deliverable 12. Final report
Deliverable 13. Digital compilation

The remainder of Section 2 is a summary of the tasks and methods specified in the scope as e4sciences understood them. In some cases, e4sciences determined that a task or method could be conducted differently with better results. Section 3 describes the methods actually used and the work that was performed.

2.1 Deliverable 1. Hydrographic surveys – acquisition and processing

The bathymetric surveys were to result in a horizontal grid of water bottom elevations with grid spacing of one (1) meter covering the shoals and aprons shown in Figure 3. Elevations of the water bottom were to be reported relative to NAVD88 and Mean Lower Low Water (MLLW), National Tidal Datum Epoch (1983-2001). Surveys were to be conducted so as to achieve 100% coverage in the survey area with at least one (1) depth estimate for every square meter. The final data product is to include an error estimate for each depth estimate. This final report is to include a quality control (QC) analysis as described in the ACOE manual section 3-3.

All bathymetric data were to be corrected to the NAVD88 vertical datum and the Mean Lower Low Water (MLLW) vertical datum for National Tidal Datum Epoch (1983-2001) to create two (2) 1-meter resolution grids. These 1-meter grids were to be combined with existing 1-meter grids produced by NOAA in 2006 (survey H11600 at http://maps.ngdc.noaa.gov/viewers/bathymetry/) to form a continuous coverage of all areas of the Upper Bay covered by water at low tide.

These combined 1-meter grids that cover all areas of the Upper Bay were to be used to create 10-meter grids used for contouring. Finally the combined 1-meter grids were also to be used to create 30-meter grids. Grids at these various resolutions are necessary to accommodate various uses of the data products. Past experience has shown that 1-meter grids, contours based on 1-meter grids, and 10-meter grids reveal the location of features that may have great historical value. Therefore these products are quite useful for evaluating the historical treasures of New York State, but are consequently exempt from Freedom of Information Law (FOIL) in order to protect these resources.

The 10-meter gridded bathymetry was to be contoured. It is anticipated that the contours based on 10-meter grids will be available to the public.

Gridded bathymetry was to include an estimate of uncertainty for the value reported for each grid cell. The uncertainty values were to be incorporated with the depth values in a Bathymetric Attributed Grid (BAG) file (see http://www.ngdc.noaa.gov/mgg/bathymetry/hydro.html).

A key component of the analysis of new bathymetric data was to be comparison in areas of overlap with bathymetric data acquired by NOAA in 2006 and bathymetric data collected by NOAA in 2013 as well as comparisons of redundant data (such as at line crossings and multiple depth observations in the same 1-meter square) collected under this contract.

2.2 Deliverable 2. Sonar Reflectivity

e4sciences was to choose a system to measure acoustic reflectivity that provides a quantitative measure of reflectivity for every square meter of the survey area (the shoals and aprons shown in Figure 3). e4sciences was to choose a system for measuring and recording acoustic reflectivity that has a high dynamic range such that the full range of reflectivities encountered in the survey area can be recorded while maintaining a constant gain through the area of investigation.

e4sciences was to use a side-scan sonar system to acquire reflectivity. Survey tracks were to be run to ensure 100% coverage is obtained on both starboard and port transceiver arrays. This is to permit development of mosaics of reflectivity images without the blank zone that occurs directly below the tow-fish.

An orthorectified mosaic of acoustic reflectivity data was to be projected in UTM Zone 18 coordinates referenced to NAD83. The data was acquired in Edgetech's 16-bit JSF format.

The e4sciences side-scan system provided raw sonar reflectivity from the sonar system in Trident's XTF format. e4sciences provided a non-proprietary viewer to display all of the data. The XTF format was determined in consultation with John Ladd, a representative of NYSDEC in advance of the commencement of fieldwork.

In this report, e4sciences was to deliver in the digital data compendium a navigation file in an ArcMap shapefile format that includes the location, time, and number of side-scan pings such that a user can locate a given piece of raw data on a map. This file will be useful for future end users to find the side-scan data associated with a given location and, conversely the location of any given piece of side-scan data.

In the digital compendium, e4sciences was to deliver acoustic reflectivity mosaicked in GeoTIFF images. The images are to be 8-bit color scale values at a resolution of one (1) meter per pixel in a Universal Transverse Mercator Zone (UTM) 18 projection referenced to NAD83 datum.

2.3 Deliverable 3. Sub-bottom reflection seismology

In addition to surface backscatter and bathymetry, sub-bottom data is an essential tool for analyzing the sedimentary environment (e.g. depositional or erosional). Therefore, high-resolution sub-bottom data was to be acquired in every area. e4 used a high-resolution chirp system, which has minimum ringing and multiple reflection signals. The sub-bottom data was collected concurrently with the other acoustic data. The sub-bottom tracklines included "tie-lines" run perpendicular to the main survey lines.

The sub-bottom data was to be analyzed and interpreted to produce isopach maps of unconsolidated sediments over a harder base substrate.

e4sciences was to convert the sub-bottom data into standard SEG-Y data and corrected for navigation and vertical (tidal) offsets. Sub-bottom profiles were to be provided in gif images. The gif images should have either shot number or time-of-day-date annotations to permit cross-reference with a shot point map. Additionally, sub-bottom tracks and shot point locations were to be provided as separate navigation files (shapefiles in ArcMap). The shot point location shapefile permits the user of either the SEG-Y data or the gif images to locate the data or image on a map.

2.4 Deliverable 4. Sediment isopach map

In this report, e4sciences was to deliver a sediment isopach map in an ArcMap shapefile format. The associated metadata should clearly indicate the accuracy and precision of the sediment thickness estimates and describe how those estimates of accuracy and precision were obtained. If the sediment thickness could not be obtained because the top-of-Pleistocene or top-of-rock was too deep to be determined, e4sciences did not determine the sediment thickness.

2.5 Deliverable 5. Sediment Profile Imaging

Sediment profile imagery (SPI) provides useful information to characterize estuary sediment at centimeter scale. e4sciences was to collect sediment profile images at 55 sites distributed in the shoal areas (see Figure 3) based on the acoustic survey. The DEC wanted to sample areas of differing reflectivity while at the same time space the 55 sites more or less evenly along the coastline of the survey areas. In addition to collecting digital sediment profile imagery to be used in further analysis, e4sciences was to record the Prism Penetration, which provides a geotechnical estimate of sediment compaction with the profile camera prism acting as a dead weight penetrometer. A sediment grab sample was to be obtained at each SPI camera drop for analysis of grain size and macro invertebrate fauna.

The sediment profile imagery was to be analyzed for the following properties: sediment grain size, surface features, subsurface features, surface relief, and apparent color redox potential discontinuity layer.

2.6 Deliverable 6. Sediment samples

To successfully characterize and classify the river bottom using acoustic data, it was essential to obtain comprehensive ground-truth information. Sediment cores and grab samples provided these data. Besides information on surface sediment character, sediment cores provided information on the depositional history of the shallow water areas.

Previous sampling efforts have shown that some shallow areas are depositional and core samples can be taken. In other shallow areas, it might not be possible to obtain good sediment cores. The DEC thought that grab samples would provide surface information and could supplement the core data where cores cannot successfully be obtained. e4sciences collected both sediment cores and grab samples at 55 sites.

e4sciences was to provide the sampling plan/sampling strategy to DEC that provides 55 sediment cores in shoals areas as shown in Figure 3. The sediment coring was to follow after the acoustic survey and be coordinated with the sediment profile imagery acquisition. The acoustic data (backscatter/sub-bottom) was to be used to adjust the sampling strategy to optimize prospective coring results and ensure that the major different acoustic regimes were sampled. The final sampling plan must be reviewed with the DEC project manager, John Ladd, in advance of sampling. The coring strategy was to include procedures that ensured that the sediments from the water-sediment interface are included in the cores. Clear PVC core liners were to be used providing both quality and quantity of core recovery. The proposal included a description of coring and sampling procedures and in particular a description of how e4sciences would ascertain the sediment/water interface successfully.

The distribution of cores was to be based on the acoustic survey. Core penetration was not a problem. e4sciences developed a plan to obtain many more locations than were required, beyond the requested number of cores. If coring was unsuccessful at a given point, then an attempt would have been made at the next location. e4sciences used GPS positioning software to precisely record the location of all core attempts whether or not they were successful. All locations were successfully cored.

In the field at the time of coring, e4sciences was to evaluate whether or not the core recovered sediment near the sediment-water interface. If the top of the sediment core did not appear to include sediment from the sediment-water interface, a second core would have been attempted. Indicators of the recovery of sediment from the sediment-water interface may include the appearance of a more oxidized layer at the top of the core. Each of the cores included the sediment-water interface.

e4sciences was to deliver tables of:

1) The position, mean grain size, standard deviation of grain size, and other physical properties deemed useful in generating a sediment classification map.
2) The percentage value of each phi class present in the top-most sediment in each core (percentages total 100%) and the lithology of the sample as described in the above description of grain size analysis
3) Lead content at 10-cm intervals down core.
4) Beryllium-7 content of the top-most sediment in each core.
5) Cesium-137 content of the top-most sediment in each core.
6) The set of all locations where coring was attempted but a core at least one meter long was not acquired was null.

In this report, e4sciences was to deliver core descriptions and color digital images of split cores.

e4sciences was to arrange for storage of all cores in a refrigerated environment at Lamont-Doherty Earth Observatory of Columbia along with sediment cores collected during previous phases of NYSDEC's Hudson River Estuary benthic mapping project.

In this report, e4sciences was to deliver a table of:

1) The position (latitude, longitude), mean grain size, standard deviation of grain size, and gamma spectroscopy and other physical/chemical properties derived from the analysis of grab samples.
2) The percentage value of each phi class present in the sample (percentages total 100%) and the lithology of the sample as described in the above description of grain size analysis (section 2.6).
3) The observed benthic invertebrate species with relative population counts.

2.7 Deliverable 7. Invertebrate identification and classification

Grab samples for faunal analysis were to be washed through a 0.5 mm sieve, preserved in 10% buffered formalin, and stained with rose bengal. These samples were to be transferred later to 70% ethyl alcohol and sorted under a dissecting microscope. Individual organisms were to be identified to species level whenever possible, and the total for each taxa enumerated. Species counts were to be tabulated for each sediment sample. The community structure analysis was to be performed using protocols adapted from the references directed in this scope of work in Appendix I.

Individual organisms were to be identified to species level whenever possible, and the total for each taxa enumerated for each grab sample. Community structure was to be investigated using quantitative methods. The proposed methodology for sampling, species identification and community structure analysis was discussed with the DEC project manager, John Ladd.

2.8 Deliverable 8. Bottom classification

Using the suite of collected data (acoustic, optical, and sediment sample measurements), e4sciences was to classify the various bottom types encountered following the classification scheme of Bell et al. (2004b). In addition, sediment provinces were to be defined and mapped using one of the two methods outlined by Flood and Cerrato (2010): QTC-QP or ARDIS. This latter analysis included an analysis of the correlation of benthic community structure with acoustic character.

In this report, e4sciences delivers sediment type classification maps as polygon shapefiles in ArcMap. Section 3.9 of this report describes the methods of determining bottom classification maps this is also described in the associated metadata.

2.9 Deliverable 9. Quality assurance/quality control

e4sciences was to develop a set of quality assurance products as outlined in USACE manual section 3-3. The quality control includes two parts: the precision in each single measurement and the accuracy among several measurements.

2.10 Deliverable 10. Metadata

The DEC is developing a legacy dataset that will have many future uses and users. e4sciences were to prepare metadata describing the digital data products produced under this contract in accordance with the standards promoted by the Federal Geographic Data Committee (FGDC) and with detail commensurate with existing benthic mapping metadata. An example of the metadata associated with benthic mapping files at the NYS GIS Clearinghouse is:
(http://www.nysgis.state.ny.us/gisdata/inventories/details.cfm?DSID=1136).

The DEC deemed it important that e4sciences were to develop extensive and complete *Process_Description*s for each *Process_Step* in the *Lineage* section of the metadata. These *Process_Description*s explain the process without resort to commercial terminology. The end user with a basic understanding of signal processing should be able to understand the *Process_Description*s without familiarity with specific commercial products.

e4sciences was also to detail *Entity_and_Attribute_Information* including *Attribute_Definition*s and *Attribute_Domain_Values.*

2.11 Deliverable 11. Side-scan sonar viewer

In this report, e4sciences was to deliver a nonproprietary viewer that displays raw sonar files with annotations that permit the user to locate images in space on a map of side-scan tracks. e4sciences delivered a solution that permits the end user to view individual raw side-scan records as “waterfall” images. Ping numbers and date and time are to be annotated on the waterfall images so that side-scan images can be located on a shot point map (specified in Section 3.2).

2.12 Deliverable 12. Final report

e4sciences was to prepare this final report describing data acquisition, processing, and display techniques, as well as the data acquired and the results of various analyses called for in this scope of work.

2.13 Deliverable 13. Digital compilation

The following data products were to be delivered with this report such that the data can be read on a computer running Microsoft Windows:

1) Bathymetric data acquired gridded on a 1-meter grid together with a measure of uncertainty for the depth value for each grid point. This depth and uncertainty information was delivered in a Bathymetric Attributed Grid (BAG) file.

2) Bathymetric digital elevation models (DEMs) at 1-meter resolution grid spacing for the newly acquired dataset.

3) Bathymetric digital elevation models (DEMs) at 1-meter resolution grid spacing derived from merging the present survey data with survey data collected by NOAA in 2006.

4) Bathymetric digital elevation models (DEMs) at 10-meter resolution grid spacing derived from merging the present survey data with survey data collected by NOAA in 2006.

5) Bathymetric digital elevation models (DEMs) at 30-meter resolution grid spacing derived from merging the present survey data with survey data collected by NOAA in 2006.

6) Contoured bathymetry (closed polygon shapefiles in ArcMap) based on the 10-meter DEMs derived from merging of data from the present survey and the previous surveys conducted by NOAA in 2006.

7) Raw sonar reflectivity i.e. digital field records of side-scan data if reflectivity is acquired with a side-scan system or reflectivity values included in the bathymetric BAG files if reflectivity is collected with a multibeam system.

8) Reflectivity (GeoTIFF images) on a 1-meter grid

9) A ping shapefile for the side-scan with a ping every 2 minutes. The attribute tables for this shapefile should include file ID, ping #, date, time for each ping in the shapefile – only applicable if reflectivity data is collected with a side-scan system.

10) Non-proprietary viewer that can access and display raw side-scan – only applicable if reflectivity data is collected with a side-scan system.

11) A shot point shapefile for the sub-bottom with a shot point every two (2) minutes. The attribute tables for this shapefile should include file ID, shot #, date, time for each shot in the shapefile.

12) Sub-bottom profiles in SEG-Y format

13) Selected sub-bottom profiles as gif images

14) Sediment isopach map

15) Digital images from the SPI camera; table of observed properties (grain size, surface features, subsurface features, surface relief, and depth to redox potential discontinuity) along with location of each SPI drop.

16) A table in MS Excel of grain size, beryllium-7, cesium-137 and lead determinations for sediment samples collected in the survey area as well as other parameters. The table would have included the locations of any attempts to take cores where recovery was not possible, had any such cases occurred.

17) Tabulation of species counts for each macro invertebrate sample.

18) Metadata for all the above

19) Core photos in JPEG format

20) Core descriptions in PDF format

21) Maps of sediment type and sediment environment using the classification scheme of Bell et al. (2004b) and maps of sediment provinces developed from one of the numerical techniques outlined by Flood and Cerrato (2010).

22) Copies of USACE reports used in the analysis of benthic macro invertebrate and sediment temporal change.

23) Final Report including a discussion of biologic communities and change over time.

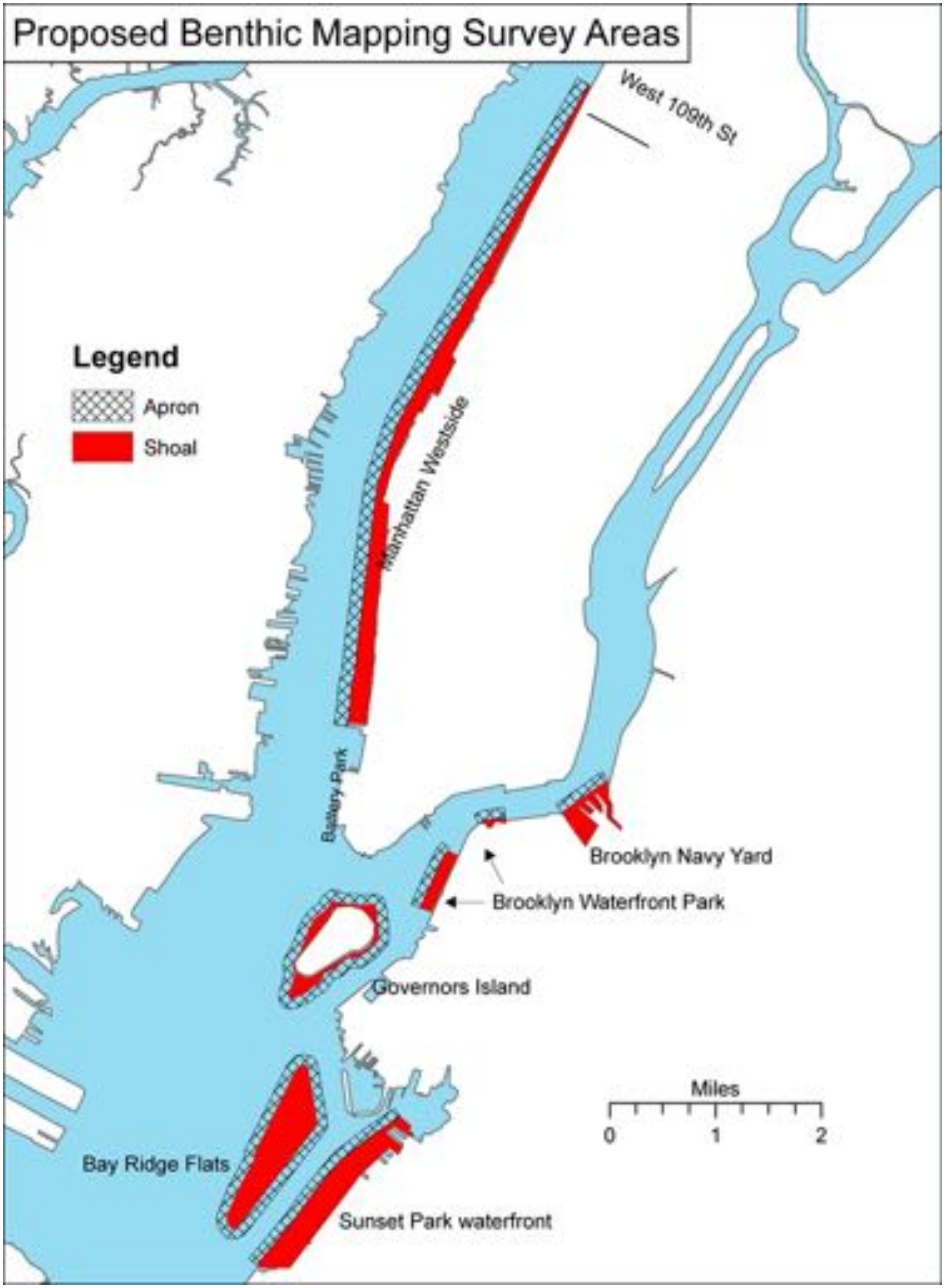

Figure 3. Location map of the extents from the scope of work.

3.0 Methodology

e4sciences reported weekly progress rather than monthly during the project.

3.1 Metadata

e4sciences created a database for accessing all the delivered data. The metadata describe the data products in accordance with the standards promoted by the Federal Geographic Data Committee (FGDC) and with detail commensurate with existing benthic mapping metadata described at the NYS GIS Clearinghouse.

e4 used ArcGIS to create the metadata, then tested the metadata files using USGS Metadata Parser (mp) to validate the FGDC standards. e4 created the files both for geophysical instruments and biological datasets following the FGDC standards. Appendix II contains the metadata files for each of the electronic data packages. The electronic data packages are organized as follows:

1) Hydrographic surveys: DEM files, and contour shapefiles for the products in this report
2) Acoustic reflectivity: side-scan data including the JSF and XTF files, and the corresponding GeoTIFF mosaics, the tracklines shapefile and ping identification shapefile are included.
3) Seismic Profiles: RAW and REAL SEG-Y data with corresponding GIF amd JPEG images for both data types. The tracklines shapefile and ping identification shapefile are included.
4) Sediment isopachs
5) SPI images
6) Biological data
7) Sediment sample: core and grab samples description and laboratory analyses
8) Bottom classification maps
9) Viewers
10) USACE reports used throughout this study
11) Referenes that includes a list of more than 800 papers for this study.

e4sciences built the database for distribution via the NYS GIS Clearinghouse system. The contact person for the data distribution was John Ladd from NYDEC. e4sciences described the data quality, process description, and processing steps in the lineage section of the metadata.

3.2 Hydrographic surveys – acquisition, processing, comparison with past data, and bathymetry analysis

3.2.1 Acquisition

The horizontal datum is the North American Datum of 1983 (NAD83). The coordinate projection system for the hydrographic data is in the Universal Transverse Mercator coordinate system zone 18N in meters (UTM18N). The vertical datum is represented in the North American Vertical Datum of 1988 in meters (NAVD88) and Mean Lower Low Water (MLLW) National Tidal Epoch (1983-2001) in meters.

e4sciences employed echosounders to measure the depth, processing translated raw depths to elevation. The crew weathered varying conditions in data collection (Figure 4) calibrating and substituting equipment accordingly.

e4sciences acquired bathymetry for the areas of investigation using two different methods: multibeam and single beam. e4 used an Edgetech 6205 interferometric multibeam echosounder (MBES) to acquire bathymetric data at 550kHz in the apron regions. Figure 5 is a photograph of the e4sciences Research Vessel *Time and Tide*. Figure 6 displays the Edgetech interferometric 6205 multibeam echosounder being set in place in the moon pool of the *Time and Tide*. The MBES was coupled with NovAtel SPAN-SE-D navigation and Northrop Grumman LCI and inertial motion control systems. Line spacing of the MBES planned acquisition lines ranged between 15 and 30m.

For the shallower flats, e4 employed HydroData, Inc. to acquire the bathymetric data. Hydrodata used an Innerspace single-beam echosounder at 200kHz (SBES) to acquire estuary bottom elevations. The SBES was coupled with a Trimble dGPS-RTK navigation system. Line spacing of the SBES survey was variable to avoid shallow obstacles and based on professional decision-making to best map the geometry of the individual areas to be surveyed.

Echosounders measure the travel time of sound from the transducer through the water column reflecting off the estuary floor and returning to the sonar receiver. This travel time depends on both the speed of sound in the water and the distance between the sonar and the estuary floor. To convert travel time to depth, time is multiplied by the speed of sound in the water.

Both types of equipment need daily calibration. Multibeam echosounders require daily patch-test calibrations of the deployment configuration, while single-beam echosounders require bar checks and latency tests. To calibrate multibeam data, e4 used an Odom Digibar Pro sound-velocity probe to measure the velocity of sound throughout the water column. The Digibar continuously records the velocity of sound every 0.5m as it is lowered through the water column. Figure 7 shows Digibar deployment aboard the *Time and Tide*. The resulting sound velocity profiles are applied to the data in post-processing. To calibrate single-beam data, e4 used a bar-check method. The bar-check method follows a similar principle, but instead of lowering a separate probe to measure the sound velocity, the crew lowers a reflective surface to a fixed depth below the transducer. Measurements are made at multiple fixed depths and sound velocity is adjusted until there is agreement between the readings from the sonar and the depth of the reflective surface.

Converting sounding depth to elevation requires knowing the elevation of the instrument or accounting for tide. For the multibeam the elevations were measured using a real-time kinematic global positioning system (RTK GPS) aided by virtual reference station (VRS) networks in the area. Tide was still evaluated for quality control and smoothing the data. During multibeam surveys, tide was primarily measured using RTK GPS.

Remote tide measurements used in multibeam acquisition are calibrated twice per day. e4 makes use of its tidal benchmark (TBM) at its marina in Jersey City, NJ. From this certified elevation, e4 measures the distance to the waterline. The e4 crew records the elevation of the waterline after subtracting this distance. Simultaneous with measuring the waterline offset at the TBM, e4 records elevation as reported by the navigation software. The e4 crew records the difference between these two measurements in the field notes. For the duration of data acquisition, the difference between the waterline elevation recorded at the tidal benchmark and the elevation recorded by the navigation software was between 0.00m and 0.03m.

To account for tide in SBES measurements, acquisition tide gauges are established from local elevation benchmarks in the area of acquisition. The crew recorded water level readings from these benchmarks at frequent intervals. In post-processing, e4 created tide files and applied them to the sounding data.

e4 used a Northrop Grumman motion sensor to measure heave, pitch, and roll of the vessel. This sensor is a tri-axial gyroscope that measures motion-induced changes at the speed of light through closed loops. As the vessel moves in the water, motion is measured, recorded, processed, and transmitted to the multibeam. The multibeam software continuously corrects for the angles of pitch and roll and the elevation changes associated with heave.

Single-beam bathymetry does not employ real-time motion correction. Instead, e4 used a filter in post-processing to remove heave, pitch, and roll artifacts.

Nancy Byrne of Hydrodata acquired the bathymetric data in the ultrashallow waters. A Certified Hydrographer and a regular team member on e4 projects, Nancy Byrne (CH#124), conducted the single-beam operations within the piers. The single-beam bathymetric data overlapped the multibeam bathymetric data in several areas. Both datasets agreed in the elevations to a difference less than 0.1m. The difference corresponds to different hydrographic transducer and frequency content of the instruments. This method also serves to independently review each measurement via two independent techniques and operators.

Figure 8 shows the coverage map for the bathymetry. The coverage is represented via the bathymetry tracklines. These appear in gray.

The horizontal datum for the hydrographic data is NAD83 and the coordinate projection system is the Universal Transverse Mercator coordinate system zone 18N in meters (UTM18N). The vertical datum is represented in the North American Vertical Datum of 1988 in meters (NAVD88) and Mean Lower Low Water (MLLW) for National Tidal Epoch (1983-2001) measured using NAVD88 meters. The metadata for each dataset describes their corresponding datum.

The bathymetric data acquired for this project is called “2015 bathymetry” in the remainder of the report, distinguishing it from historical data ranging from 1999 to 2014.

3.2.2 Processing

e4 corrected raw multibeam bathymetric results with smoothed tide values, water column sound velocity profiles, and patch test calibration values prior to editing. The crew limited beam angles to a 130° swath and applied an over-under filter to the beams. e4 removed outliers on a cell-by-cell and profile-by-profile basis. The median value of the multibeam data was used to create the XYZ files in 0.3m bins.

e4sciences applied HyPack implementation of CUBE[3] processing for estimating the uncertainty files for the multibeam bathymetry. The corresponding XYU and XYZ files are available for each area in the electronic data package. The XYU and XYZ are ASCII file format in a 3mx3m grid.

e4 gridded the XYZ data using triangulation with linear interpolation then plotted it as a surface map, reporting the resulting XYZ (northing, easting, elevation) files and grid surface maps in UTM18N projected coordinate system and NAVD88 vertical datum.

The single-beam data set was acquired with HydroData, Inc. proprietary acquisition and processing software. The HydroData, Inc. software receives and combines position and sounding

[3] CUBE (Combined Uncertainty and Bathymetry Estimator) is software that applies Bayesian statistics and modeling to multibeam data and provides uncertainty and depth estimation over a gridded surface. For more information, please check (http://ccom.unh.edu/sites/default/files/publications/ Calder_07_CUBE_User_Manual.pdf.)
The CUBE software library is licensed by HYPACK, Inc. from CCOM/JHC at the University of New Hampshire, Dr. Brian Calder.

data. The operator inputs measured offsets to account for the position of the RTK GPS antenna relative to the transducer/sounding pole. For this project, the GNSS antenna was directly above the transducer/sounding pole, so only vertical offsets were applied. HydroData used the NOAA tide station at Battery New York (station ID 8518750) for testing RTK tides.

Figure 9 shows hydrographer Nancy Byrne during single-beam data acquisition at the West side of Manhattan.

The single beam XYU files are also available as ASCII format for each of the single beam XYZ files.

3.2.3 Historical data

e4sciences has produced two historical data sets: one of bathymetric data in 2006 from NOAA and USACE and a second of bathymetric data for 2014 from NOAA, e4sciences, and USACE. e4 processed the 2006 and 2014 data including data ranging from 1999 to 2014. This is the most complete historical data set to date.

All data were compiled into 1m x 1m grids obtained with triangular linear interpolation between measurement points.

The inventory of the various datasets used to create the composite bathymetries is shown below:

- **2006 composite bathymetry**
  - NOAA Hudson H10938 (1999)
  - NOAA Hudson H10937 (1999)
  - NOAA East River H11353 (2004)
  - USACE Wallabout channel 2676 (2004)
  - NOAA NY Bay H11600 (2006)
  - NOAA NY Bay/Hudson H11395 (2006)

- **2014 composite bathymetry**
  - NOAA West Manhattan F00573 (2009)
  - NOAA Several areas F00598 (post 2012)
  - USACE NY Bay/East River 4069D (2013)
  - USACE Hudson River 4126 (2014)
  - e4 NY Bay (2014) from sub-bottom bathymetry

Note that an additional 2012 NOAA dataset was available for the study area (F00626). However, the data was acquired with single-beam equipment with no overlap between tracks and an average spacing of 150m between tracks. At the level of discretization used in this report (1m x1m cells), the resulting grid contained too many artifacts. This dataset was therefore included neither in the 2014 composite bathymetry, nor in the analysis.

3.2.3.1 Bathymetry analysis

The shallows or flats and surrounding slopes vary in bathymetry throughout the different areas. A single elevation contour cannot define these. In order to determine the outline of the flats and slopes more accurately e4 performed a bathymetry analysis on the most recent composite bathymetry for each area.

e4 computed the first and second spatial derivatives of the bathymetry data sets. e4 used the first derivative maps to obtain the contours of the edge of the flats and the bottom of the general slope.

e4 then performed a subsequent analysis of the high-definition bathymetry maps to distinguish the two slopes with different steepness, when present. In some areas, e4 identified upper and lower slopes and calculated the slope values (one vertical unit / corresponding horizontal units).

Note that most of the bathymetry analysis was performed on the 2006 composite bathymetry as it was the most complete. However, for the West Manhattan area, the 2006 dataset produced too many artifacts in the grids due to the large spacing between measurements. All bathymetry analysis for this area was therefore computed from the 2014 bathymetry.

3.2.3.2 Difference maps

Historical bathymetry data were combined in 1m x 1m grids obtained with triangular linear interpolation. The newly acquired 2015 bathymetry included single beam data, acquired with large spacing between tracks (several meters to tens of meters), and multibeam data, acquired with 100% coverage of the surveyed areas. To limit the potential artifacts created by the gridding process, the single beam data (corresponding to the ultrashallow areas) were combined in 5m x 5m grids. To conserve the high-definition of the multibeam measurements (corresponding to the deeper areas), data were combined in 1m x 1m grids, similarly to the historical bathymetry.

Difference maps were then computed between the 2015 bathymetry and the 2006 bathymetry for Brooklyn and Governor's Island, and between the 2015 bathymetry and the 2014 bathymetry for West Manhattan. For a given area, if both single beam and multibeam data were used for the 2015 bathymetry, two separate difference grids were calculated (one for the 1m x 1m grid and another one for the 5m x 5m grid). The maps presented in this report combine the results of both grids.

Figure 4. Ice encountered by the e4 crew as data was collected.

Figure 5. Field operations photos: *Time and Tide.*

Figure 6. e4's Edgetech interferometric 6205 multibeam echosounder being set in place in the moon pool of the *Time and Tide*.

Figure 7. e4 deploying the Digibar water velocity probe.

Figure 8. Coverage map for the bathymetry operations. Tracklines of the bathymetry appear in gray.

Figure 9. Hydrographer Nancy Byrne performing single-beam data acquisition at West Side Manhattan.

3.3 Sonar reflectivity – acquisition and processing

While the phase and time information from the backscatter in multibeam bathymetry quantifies the elevations of the bottom, the intensities and amplitudes measured in the backscatter waveforms reveal the roughness and the impedance of the sediments on the bottom.

e4 developed side-scan orthosonographs™ in order to distinguish materials for dredge material placement. A single side-scan orthosonograph provides two seamless aerial-photograph-like images of the area of investigation. The e4 method of processing the orthosonographs is proprietary. Using this technique, e4 differentiates bottom sediments into silt, clay, sand, and rock.

3.3.1 Orthosonograph acquisition

e4 used an Edgetech 4200 at 400kHz and an Edgetech 4125 at 600kHz to produce the orthosonographs. The side-scan sonar transmits ultrasonic waves obliquely into the water and measures the amplitude of the backscatter from the seafloor as a function of range. The reflectivity is a function of the seafloor roughness and the sediment acoustic properties. The e4 proprietary processing produces two independent orthosonographs, each insonified from the opposite direction. These reflectivity images produce a high-definition picture of the structures on the seafloor. These images are also the best means to map debris on the seafloor.

e4 acquired lines parallel and normal to the apron, with line spacing between 15m and 24m. The side-scan images produced 100% coverage with 200% redundancy and 400% overlap of the area of investigation. The two independent orthosonographs, insonified from two directions, suffice to constitute the 200% redundancy. Orthosonographs are seamless, aerial-photograph-like images that are insonified from one direction only. In fact, the data required to produce two images constitutes significantly greater overlap.

The side-scan reflectivity data were acquired at 16 bits. The 16bits data is preserved in the JSF and XTF format.

3.3.2 Processing

e4 processed all of the side-scan data with a 0.1m resolution – that is an order of resolution smaller than standard processing. e4 produced one-sided georeferenced images that can be used with any interpretation software, such as ArcGIS, AutoCAD.

e4 proprietary method for side-scan orthosonographs produces images that represent high acoustic reflectivity as bright (white) and low reflectivity areas as dark (dark brown). This differs from the common use of side-scan images in strip charts that are often inverted. e4's method produces images that are more intuitive. Acoustic shadows (areas of no reflection) are also easier to detect visually in e4's orthosonograph images as a result of this processing.

The processing applies a tine varying gain (TVG) for relative amplitude balancing based on the location of the project. All of the GeoTIFF files are created with the same TVG values throughout the project – this allows for a direct comparison of data. The mosaics are made as 8-bit images with a spatial resolution of 0.1m. The final step applies a standard sepia color scale to the mosaic images to create the GeoTIFF.

These GeoTIFFs having higher spatial resolution (0.1m) provide more information per area than would higher dynamic range mosaics at standard resolution of 1m. The high dynamic range data is available in the electronic appendix within the JSF files of the side-scan data. Mosaics of 16-bit dynamics range are possible but would lose the spatial resolution. A systematic production of both the high resolution and the high dynamic range images was beyond the scope of this project.

The electronic data package includes the 16 bit JSF and XTF files, and the processed orthosonographs in GeoTIFF format. We included a shapefile of the tracklines for the acquisition, and a shapefile that includes a table with ping number, easting, northing, time and file name for every 200 pings.

3.4 Sub-bottom reflection seismology – acquisition and processing

The e4sciences geophysical Research Vessel *Time and Tide* and its tender dock at Liberty Landing in New Jersey. The *Time and Tide* is 18m in length and fully equipped for geophysical exploration in shallow (<91m) waters. The tender was outfitted daily with sensors for acquisition in ultrashallow waters (<4m).

Figure 10 contains photographs of the geophysical survey boat with the 512i used in the investigation. e4 used the RV *Time and Tide* in the apron areas. e4 used a small tender vessel (Figure 11) in areas between piers and in the flats where water depth was less than 3m.

Figures 12, 13, and 14 show a field operation's view of Bay Ridge Flats, Brooklyn Bridge Park, and Manhattan, respectively.

3.4.1 Acquisition

e4 used an Edgetech 512i for all seismic data acquisition in the apron and flats where water depths exceeded 3m. In areas of shallow water where a smaller vessel was needed, e4 used an Edgetech 424. e4 implemented a 1-10kHz chirp for roughly 75% of sub-bottom tracklines (512i), and a 4-24kHz chirp for the other 25% (424). Sub-bottom profiling works similar to single-beam bathymetry. The much lower frequency seismic waves, however, penetrate the mudline and reflect off the strata in the subsurface. The 1-10kHz chirp penetrated through the Holocene and Pleistocene into rock. The 4-24kHz chirp had similar results. e4 interpreted the sub-bottom reflection seismic results to construct isopach maps and cross sections of the strata. Sub-bottom seismic was also crucial for the efficient placement of SPI camera sites and grab sample locations. Appendix II contains reflection seismic data and its corresponding metadata files. The seismic data available is the raw amplitude data from the chirp sonar in SEG-Y format. e4 also provides the real component of the analytic data in SEG-Y format.

Figure 15 plots the sub-bottom tracklines.

More than 900 seismic lines were acquired. The line spacing between long lines parallel to the apron toes was 15m. The line spacing for the cross lines normal to the apron toes was 152m.

3.4.2 Processing

e4 has developed a proprietary set of protocols for processing high-frequency, shallow water, reflection seismology for determination of sediments and rock in harbors.[4] e4 filters every line. The processing generates six images for every line. The six different images facilitated interpretation of the data. The only two datasets delivered in the electronic appendix are the raw envelope data and the real component of the analytical data.

The RTK system provides every trace with its proper location and elevation. Daily throughout the work, e4 tested the accuracy of the RTK against known benchmarks in each of the areas of interest. All the data is stored digitally, duplicated in real time, and transmitted to the office for processing. The benchmark for the RTK system is the NOAA tide station at the battery (station ID 8518750) with geoid12a. The processing of the data includes digital bandpass filtering, deconvolution, automated gain control (AGC) with a 300x200 sample window, the first derivative of the amplitude data, and wave-equation migration of the real analytical component of the chirp data.

The standard format of representing sub-bottom seismic data is the raw format, that is, the envelope of the chirp signal. The chirp signal has a time-varying frequency. e4's proprietary processing allows the generation of the real and imaginary components of the time-varying frequency signal. The real analytical component of the chirp data allows processing the images using wave-equation techniques. The data is migrated to depth with an initial constant velocity model derived from field water velocity measurements. The depth migration depends on the data frequency content. The 4-24kHz dataset requires a higher sample interval for the depth migration.

The electronic data package includes both the raw envelope data and the real components of the chirp signal. The electronic data package contains these data in standard SEG-Y format; the data package also includes the GIF and JPEG images of these two data format as time versus ping number or shot point. We included a shapefile of the tracklines for the acquisition, and a shapefile that includes a table with ping number, easting, northing, time, and file name for every 200 pings.

The file name structure of the files is "0510_eX_FAI_F_Date_File_FAI_DataType" where 0510 is an e4's internal data identifier; eX is either e5 for Edgetech 512i or e4 for Edgetech 424; F denotes the frequency content as H for high frequency (1-10 kHz for e5 or 4-24 kHz for e4) and M for medium frequency (0.5-6 kHz only for e5 tool); FAI is a unique field acquisition identifier; Date is the acquisition date; File is the file number of the day; and DataType is either RAW or REAL.

The navigation of the seismic data is processed using Kalman filters. The intial RTK position is 1Hz frequency. The data has a 0.25Hz repetition rate. The Kalman filter interpolates the spatial location data using the fish positioning, the speed of the boat, and the heading.

e4 measures the water column and each sediment type to accurately determine the speed of sound and density in each medium, respectively.

---

[4] William Murphy III, W. Bruce Ward, Beckett Boyd, Gary Fleming, William Murphy IV, Richard Nolen-Hoeksema, Matthew Art, and Daniel A. Rosales, High-resolution shallow geophysics and geology in the Hudson-Raritan Estuary Ecosystem Restoration, New Jersey, *The Leading Edge*, February 2011, Vol. 30, No. 2: pp. 182-190.

From the sub-bottom seismic data alone, e4 interprets each of the seismic lines. The interpretation process produces maps of the first arrival and each of the geological surfaces identified as horizons of interest. e4 correlates information from e4's own proprietary database (for more information on e4sciences' database, please contact our main office) of borings and samples throughout the area to benchmark and identify each of the geological horizons of interest. These interpreted lines produced independent cross sections, sediment classification maps, and isopach maps for the geologic strata of interest. During this project, e4 identified the silt horizon, sand horizon, and clay horizons. e4 interpreted the Pleistocene-Holocene interface in portions of Bay Ridge Flats and Governors Island. This interface dips strongly and is not visible in any of the other areas. Some of the penetration of the seismic data was compromised due to the presence of organic-rich sediments at the mudline.

The seismic data has additional quality problems due to the presence of heave in the area. e4 records the heave correction values in the headers of the JSF files. However, not all the heave was correctable. Other acquisition techniques could be implemented for future data acquisition in this environment.

3.4.3 Interpretation

After the seismic-based maps are complete, we combine them with the coring and the sonar reflectivity to produce the best-integrated solution for the stratigraphy and sediment classification. The sediment isopach maps were delivered as shapefiles in ArcMap, and their correspondent metadata are available in Appendix II.

Figure 10. The Edgetech 512i being lowered into the water for seismic data acquisition.

Figure 11. Field operations photos: Dib boat.


Figure 12. Field operations photos: Bay Ridge Flats.

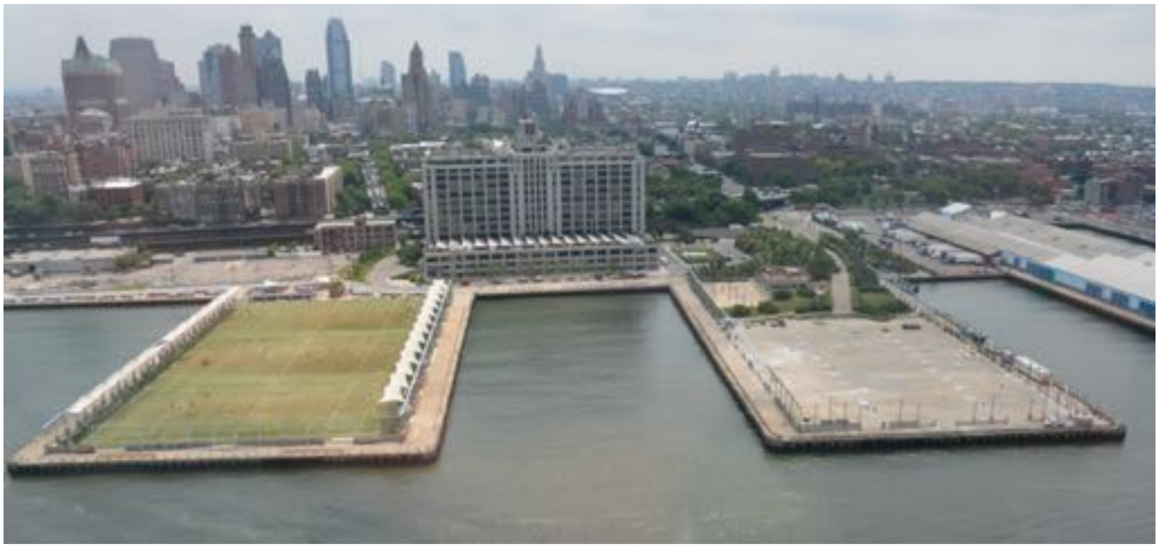

Figure 13. Field operations photos: Brooklyn Bridge Park.

Figure 14. Field operations photos: Manhattan.

Figure 15. Seismic tracklines.

3.5 Sediment isopach maps

e4sciences produced isopach maps from the reflection seismology seismic data. The isopach map corresponds to the silt sediments; we refer to this as acoustic silt. This is the most consistent horizon that occurs in portions of all the areas of investigation. These sediment isopach maps correspond to single instrument result that is reflection seismology.

The acoustic silt responds to sonar depending on seasons, its hydrocarbon content, organic material content, thickness, and age. Even in sandy areas, where it forms a thin veneer, the acoustic silt is still easily detected (Murphy et al., 2004).

The acoustic silt layer also has different properties in the seismic: 1) it is followed by a strong multiple ghost in the near surface and little to no penetration of the sound source, 2) it has a transparent behavior with smaller amplitude changes followed by a strong reflection and in some cases no more penetration of the sound source. These two characteristics are associated with absorption of energy in the side-scan data also.

These sediment isopach maps are the input to the sediment type and geological substrate maps (section 3.9). e4sciences correlate these maps with core samples, proprietary core database, and orthosonograph maps to identify the acoustic silt as black silt, gray silt, or silt.

These sediment isopach maps were delivered as shapefiles in ArcMap. These shapefiles and their correspondent metadata are available in Appendix II.

The mapping of the benthic layer is concentrated on the first 30cm below the water-bottom. This is equivalent to the first 5 samples in the 1-10kHz dataset and 10 samples in the 4-24kHz dataset. The maps and cross sections in this report go deeper than 25 meters below 0 MLLW. The maximum amount of acoustic silt throughout the area of investigation is 3 meters.

The sediment deposits are thicker than the volume of interest. We can see down to 25m below MLLW. In very few of the lines acquired did we see the bottom of sediment and top of rock.

e4sciences recommends to acquire more acoustic data at different seasons (i.e. winter/summer) and more core sampling at the same time to better understand the acoustic properties of the shallow layer and its corresponding classification as black silt versus organic-rich content silt.

3.6 Sediment Profile Imaging – acquisition and processing

3.6.1 Areas of investigation

e4 was assigned six survey areas. We subsequently divided West Manhattan into three separate areas. Table 2 shows the area names used in this report and lists the number of sites per area.

Table 2. Sampling sites per regions.

	Survey area in this report	SOW survey areas	Sites
1	Bay Ridge Flats	Bay Ridge Flats	12
2	Governors Island	Governors Island	9
3	Sunset Park waterfront	Sunset Park waterfront	7
4	Brooklyn Bridge Park	Brooklyn Park waterfront	3
5	Brooklyn Navy Yard	Brooklyn Navy Yard	2
6	West Manhattan waterfront South	Hudson River Park and North	6
7	West Manhattan waterfront Middle	Hudson River Park and North	8
8	West Manhattan waterfront North	Hudson River Park and North	8
			55

3.6.2 Sampling sites

e4 collected sediment cores and grab samples at 55 sites in the shallows, while separately conducting the SPI imaging at 52 sites. Figure 16 shows the SPI on deck during operations. The SPI did not achieve penetration at three sites.

The original assigned number of sampling sites averaged approximately one site per 490m of shoreline length. This original distribution is also equivalent to averaging one site per 18 hectares. The actual ranges are in Table 3. Deeming Sunset Park waterfront to be underrepresented based on area, e4 added one site to Sunset Park waterfront and subtracted one site from Governors Island. The sampling sites per area of investigation are shown in Table 4.

Figure 17 shows deployment of the SPI imaging equipment.

Table 3. Sampling sites and density analysis per site as per scope.

Areas	Actual number of sites		Shoreline length	Total Area	Actual length per site		Actual area per site	
	Original	Actual			Original	Actual	Original	Actual
			m	hectares	m	m	hectares	hectares
Bay Ridge Flats	12	12	5878	250	490	490	20.8	20.8
Governors Island	10	9	4763	114	476	529	11.4	12.7
Sunset Park waterfront	6	7	3166	160	528	452	26.7	22.9
Brooklyn Bridge Park	3	3	1443	43	481	481	14.3	14.3
Brooklyn Navy Yard	2	2	860	32	430	430	16.0	16.0
West Manhattan waterfront	22	22	10,885	415	495	495	18.9	18.9
Totals	55	55	26,995	1014	491	491	18.4	18.4

Table 4. Sampling sites per survey area. Note that there are two different prefixes for Brooklyn Bridge Park.

Areas	Site name prefix	Number of core sites	Number of grab – infaunal sites	Number of SPI sites
Bay Ridge Flats	BRF-14	12	12	12
Governors Island	GI-14	9	9	7
Sunset Park waterfront	SPW-14	7	7	7
Brooklyn Bridge Park	BPW-14 (south of Brooklyn Bridge)	2	2	2
	BMB-14 (north of Manhattan Bridge)	1	1	0
Brooklyn Navy Yard	BNY-14	2	2	2
West Manhattan waterfront South	WMW-14	6	6	6
West Manhattan waterfront Middle	WMW-14	8	8	8
West Manhattan waterfront North	WMW-14	8	8	8
Total		55	55	52

3.6.3 Sampling site selections

Prior to selecting sites, e4 interpreted the available orthosonographs, seismic, and bathymetry at each region to identify probable areas of silt, sands, gravels, boulders, riprap, debris fields, and areas unsafe for navigation. Table 5 lists the actual sites selected and achieved for the sampling.

Table 5. Sampling sites in each study region.

Region	Sample site	Latitude	Longitude	Easting	Northing	Recovered core length
		DD MM.mmmmmmm	DDD MM.mmmmmmm	UTM18N m	UTM18N m	cm
Bay Ridge Flats	BRF14-01	40 40.2096872	074 01.5560875	582,328.0	4,502,599.0	26.0
	BRF14-02	40 39.9343261	074 01.7844012	582,012.0	4,502,086.0	32.0
	BRF14-03	40 39.9338745	074 01.4742112	582,449.0	4,502,090.0	45.0
	BRF14-04	40 39.8672439	074 01.3928428	582,565.0	4,501,968.0	13.0
	BRF14-05	40 39.5905374	074 01.8461648	581,932.0	4,501,449.0	22.0
	BRF14-06	40 39.4238721	074 01.8883226	581,876.0	4,501,140.0	38.0
	BRF14-07	40 39.2550846	074 02.1938107	581,449.0	4,500,823.0	39.0
	BRF14-08	40 39.0764974	074 02.2325733	581,398.0	4,500,492.0	30.0
	BRF14-09	40 38.9546794	074 02.0789089	581,617.0	4,500,269.0	21.0
	BRF14-10	40 39.5363807	074 02.1564048	581,496.0	4,501,344.0	6.0
	BRF14-11	40 39.9997486	074 01.2744952	582,729.0	4,502,215.0	24.0
	BRF14-12	40 38.9926007	074 02.4133247	581,145.0	4,500,334.0	42.0
Governors Island	GI14-01	40 41.5815035	074 00.7287028	583,465.0	4,505,150.0	46.0
	GI14-02	40 41.4981538	074 00.7157317	583,485.0	4,504,996.0	24.0
	GI14-03	40 41.5848267	074 01.2456237	582,737.0	4,505,148.0	31.5
	GI14-04	40 41.4043984	074 01.4492212	582,454.0	4,504,811.0	31.5
	GI14-05	40 40.8701032	074 01.6735637	582,149.0	4,503,819.0	23.0
	GI14-06	40 40.9681073	074 01.5656376	582,299.0	4,504,002.0	38.0
	GI14-07	40 40.9761197	074 01.4263578	582,495.0	4,504,019.0	56.0
	GI14-08	40 41.1345780	074 01.1180165	582,926.0	4,504,317.0	12.0
	GI14-09	40 41.1622005	074 00.9976130	583,095.0	4,504,370.0	41.0
Sunset Park waterfront	SPW14-01	40 38.7529191	074 01.9320858	581,828.0	4,499,898.0	36.0
	SPW14-02	40 38.9253073	074 01.7025060	582,148.0	4,500,220.5	31.0
	SPW14-03	40 39.1181348	074 01.4619634	582,483.0	4,500,581.0	31.0
	SPW14-04	40 39.2253991	074 01.4266898	582,530.5	4,500,780.0	26.0
	SPW14-05	40 39.2027756	074 01.3720176	582,608.0	4,500,739.0	42.0
	SPW14-06	40 39.1506252	074 01.4050695	582,562.5	4,500,642.0	38.0
	SPW14-07	40 39.3706025	074 01.0849663	583,009.0	4,501,054.0	46.0
Brooklyn Bridge Park	BPW14-01	40 41.6536571	074 00.1311232	584,305.0	4,505,293.0	40.0
	BPW14-02	40 41.9512055	073 59.9747030	584,519.0	4,505,846.0	43.0
	BMB14-01	40 42.2894120	073 59.3368115	585,410.0	4,506,482.0	13.5
Brooklyn Navy Yard	BNY14-01	40 42.2642755	073 58.5090486	586,576.0	4,506,449.0	39.0
	BNY14-02	40 42.5367443	073 58.2718958	586,904.0	4,506,957.0	36.0
West Manhattan waterfront South	WMW14-01	40 43.2467488	074 00.9108207	583,174.0	4,508,228.0	36.0
	WMW14-23	40 43.4629007	074 00.9047926	583,178.0	4,508,628.0	NA
	WMW14-02	40 43.3471858	074 00.8993941	583,188.0	4,508,414.0	44.0
	WMW14-03	40 43.6647948	074 00.8748171	583,216.0	4,509,002.0	48.0
	WMW14-04	40 43.9230098	074 00.7942694	583,324.0	4,509,481.0	44.0
	WMW14-05	40 44.2670750	074 00.7664461	583,356.0	4,510,118.0	35.0
	WMW14-06	40 44.3723389	074 00.7506774	583,376.0	4,510,313.0	43.0
West Manhattan waterfront Middle	WMW14-07	40 44.7679385	074 00.6815746	583,465.0	4,511,046.0	33.0
	WMW14-08	40 44.9569333	074 00.6602966	583,491.0	4,511,396.0	41.0
	WMW14-09	40 45.2284663	074 00.5574759	583,630.0	4,511,900.0	29.0
	WMW14-10	40 45.3783710	074 00.5097595	583,694.0	4,512,178.1	46.0
	WMW14-11	40 45.5848925	074 00.3332475	583,938.0	4,512,563.0	52.0
	WMW14-12	40 45.7796963	074 00.2336659	584,074.0	4,512,925.0	31.0
	WMW14-13	40 45.9517380	074 00.0647470	584,308.0	4,513,246.0	46.0
	WMW14-14	40 46.2161116	073 59.9477475	584,467.0	4,513,737.0	48.0
West Manhattan waterfront North	WMW14-15	40 46.4527132	073 59.7451205	584,747.0	4,514,178.0	41.0
	WMW14-16	40 46.4101427	073 59.7599811	584,727.0	4,514,099.0	37.0
	WMW14-17	40 46.7075588	073 59.5279729	585,047.0	4,514,653.0	31.0
	WMW14-18	40 46.9212014	073 59.3590642	585,280.0	4,515,051.0	11.5
	WMW14-19	40 47.9112782	073 58.6093324	586,313.0	4,516,895.0	36.5
	WMW14-20	40 48.2496171	073 58.3644262	586,650.0	4,517,525.0	37.0
	WMW14-21	40 47.6298194	073 58.8085214	586,039.0	4,516,371.0	31.0
	WMW14-22	40 47.4098315	073 58.9918102	585,786.0	4,515,961.0	59.0

e4 distributed samples among the areas of sands and silts in the shallows and upper slope, while excluding areas of coarse gravel, boulders and debris, and other unsafe areas. Table 6 lists the analyses conducted for each site.

Table 6. Analyses performed at each site

Region	Sample site	Sediment	Infaunal	SPI
Bay Ridge Flats	BRF14-01	yes	yes	yes
	BRF14-02	yes	yes	yes
	BRF14-03	yes	yes	yes
	BRF14-04	yes	yes	yes
	BRF14-05	yes	yes	yes
	BRF14-06	yes	yes	yes
	BRF14-07	yes	yes	yes
	BRF14-08	yes	yes	yes
	BRF14-09	yes	yes	yes
	BRF14-10	yes	yes	yes
	BRF14-11	yes	yes	yes
	BRF14-12	yes	yes	yes
Governors Island	GI14-01	yes	yes	no, area of pipe debris & gravel, no penetration
	GI14-02	yes	yes	yes
	GI14-03	yes	yes	no, area of gravel, no penetration
	GI14-04	yes	yes	yes
	GI14-05	yes	yes	yes
	GI14-06	yes	yes	yes
	GI14-07	yes	yes	yes
	GI14-08	yes	yes	yes
	GI14-09	yes	yes	yes
Sunset Park waterfront	SPW14-01	yes	yes	yes
	SPW14-02	yes	yes	yes
	SPW14-03	yes	yes	yes
	SPW14-04	yes	yes	yes
	SPW14-05	yes	yes	yes
	SPW14-06	yes	yes	yes
	SPW14-07	yes	yes	yes
Brooklyn Bridge Park	BPW14-01	yes	yes	yes
	BPW14-02	yes	yes	yes
	BMB14-01	yes	yes	no, rock & gravel, no penetration
Brooklyn Navy Yard	BNY14-01	yes	yes	yes
	BNY14-02	yes	yes	yes
West Manhattan waterfront South	WMW14-01	yes	yes	no, pipe in area, substituted WMW14-23
	WMW14-23	no	no	yes
	WMW14-02	yes	yes	yes
	WMW14-03	yes	yes	yes
	WMW14-04	yes	yes	yes
	WMW14-05	yes	yes	yes
	WMW14-06	yes	yes	yes
West Manhattan waterfront Middle	WMW14-07	yes	yes	yes
	WMW14-08	yes	yes	yes
	WMW14-09	yes	yes	yes
	WMW14-10	yes	yes	yes
	WMW14-11	yes	yes	yes
	WMW14-12	yes	yes	yes
	WMW14-13	yes	yes	yes
	WMW14-14	yes	yes	yes
West Manhattan waterfront North	WMW14-15	yes	yes	yes
	WMW14-16	yes	yes	yes
	WMW14-17	yes	yes	yes
	WMW14-18	yes	yes	yes
	WMW14-19	yes	yes	yes
	WMW14-20	yes	yes	yes
	WMW14-21	yes	yes	yes
	WMW14-22	yes	yes	yes

In the field, e4 made changes in the SPI imaging based on the grab-sampling and sediment-coring results. One site was eliminated from Governors Island. The Manhattan Bridge site, BMB-14-1, was not appropriate for SPI because it consists primarily of rock and coarse gravel. One site in Westside Manhattan, WMW-14-01, was moved to avoid infrastructure during the SPI imaging.

e4 conducted CHEM-SPI analyses at 52 sites. The CEM-SPI is a unique adaptation of the standard SPI device. The CHEM-SPI is the most advanced system of its kind. This system, developed by Robert Aller of Stony Brook, and Dr. Qingzhi Zhu, incorporates electrochemical sensors that measure the elemental content of porewater in sediment strata. Aller and Zhu pioneered the development of planar optode sensors for in situ (SPI hyperspectral camera system – CHEM-SPI) measurement of solute, solid, and microbial enzyme activity distributions. Aller and Zhu have a patent pending (Aller RC, Zhu Q, 2005, Optical pH sensor. US Patent Application number: US10/973,663). The CHEM-SPI system allows direct quantitative confirmation of bio-geochemical patterns previously inferred qualitatively from color patterns in visible SPI images.

Jaime Soto-Neira redesigned and updated the earlier model of CHEM-SPI electronics as described in Fan et al, 2011.[5] One of Soto-Neira's innovations is a web camera inside the unit. The camera and auxiliary webcam were controlled via a deckside computer connected via a waterproof ethernet cable. The video could be watched in real time. The total imaging window is 15 x 22cm.

Dr. Bruce Ward and/or William Murphy 4 from e4sciences supervised the operation. Dr. Robert C. Aller, Dr. Qingzhi Zhu and Jaime Soto-Neira, all from Stony Brook University, performed the CHEM-SPI measurements.

e4 conducted the initial sampling at Bay Ridge Flats on the anchored *Time and Tide*. Because of the difficulties sampling in New York Harbor due to winds, tidal currents, and extremely busy marine traffic, e4 used a 20m steel self-spudding utility boat, the *Samantha Miller*, for all remaining sampling. The large vessel ensured not only the safety of the crew, but also the best possible results. The self-spudding setup allowed re-sampling at each site without loss of time or repositioning.

3.6.4 CHEM-SPI system and sensors

The crew deployed Fe^{2+}, O_2 and pH polymer sensing strips, with one or two strips of polymers on the side of the window. O_2 and pH reactions are reversible and the strips could be kept in place for multiple deployments. The Fe^{2+} strip reaction is irreversible and the strip is removed after one deployment. Because the Fe^{2+} strip is on the outside of the window, it provides measurements approximately 2cm deeper than the bottom of the glass window.

[5] Fan, Y., Q.Z. Zhu, R.C. Aller, D.C. Rhoads. 2011. An *in situ* multispectral imaging system for planar optodes in sediments: example high resolution seasonal patterns of pH. Aquatic Geochem. 17: 457-471.
Zhu, Q.Z., R.C. Aller, and Y. Fan. 2005. High-performance planar pH fluorosensor for two-dimensional pH measurements in marine sediment and water. Environ. Sci. Technol. 39: 8906-8911.
Zhu, Q.Z., R.C. Aller. 2012. Two-dimensional dissolved ferrous iron distributions in marine sediments as revealed by a novel planar optical sensor. Mar. Chem. 136-137: 14-23.
Zhu, Q.Z., R.C. Aller, and Y. Fan. 2005. High-performance planar pH fluorosensor for two-dimensional pH measurements in marine sediment and water. Environ. Sci. Technol. 39: 8906-8911.

Figure 18 shows two configurations of the sensor strips on the SPI window.

The crew deployed CHEM-SPI imaging at 52 sites and sediment cores and grab samples at 55 sites in the shallows, conducting the SPI imaging separately from the other sampling. Only at three sites could SPI images not be obtained. The crew conducted CHEM-SPI imaging of Bay Ridge Flats on the anchored *Time and Tide* prior to sediment sampling. To adjust the color and the weights to avoid poor penetration, the crew collected a Ponar grab sample prior to deployment of the CHEM-SPI. CHEM-SPI was deployed after sediment sampling at remaining sites off the *Samantha Miller.* In all, the crew deployed or cast CHEM-SPI imaging two to three times at each site.

Steps in the deployment of CHEM-SPI were:

1. Spud down or anchor at site.
2. Measure bottom temperature and conductivity prior to deployment.
3. Cast 1: Video record on way down. Acquire visible images.
4 Bring to deck. Place sensor strips on window. Adjust collar height and weights if penetration was too great or too little.
5. Cast 2: Video record on way down. Acquire visible images. Let sensor sit required time. Turn on appropriate light.
6. Bring to deck. Place sensor strips on window.
7. Cast 3. Video record on way down. Acquire visible images.
8. Bring to deck. Secure.
9. Raise spud or anchor, move to next site.

Jaime Soto-Neira normalized the visible images in the lab. Qingzhi Zhu calibrated the CHEM-SPI images against strips exposed to standard solutions in the lab.

3.6.5 CHEM-SPI interpretation

Dr. Pam Neubert performed the profile image analysis using Image Pro Premiere (Media Cybernetics) software. Appendix II contains digital sediment profile images and a table summarizing the analyses.

The interpretation consisted of a determination of the following parameters:

Sediment grain size – Grain size followed the Wentworth classification system and was assigned visually. Major modal class for each image was determined by comparison to a standard set of images for which mean grain size has been determined in the laboratory.

Surface features – The presence of certain surface features was recorded. These included bedforms, physically or biologically dominated habitats, shell, worm pits, detritus, or anthropomorphic material.

Subsurface features – Images were evaluated for subsurface features such as worm tubes or shell hash that reveal a great deal about physical and biological processes influencing the bottom. Methane gas voids were noted and enumerated along with sediment layering.

Surface relief – Boundary roughness was measured across the prism faceplate (15cm width).

Apparent color redox potential discontinuity (aRPD) Layer – This parameter is an important estimator of benthic habitat quality (Rhoads and Germano, 1986; Diaz and Schaffner, 1988), providing an estimate of the depth to which sediments appear to be oxidized. This is a measurement based on the change in color resulting from the transition of oxidized sediment to anoxic sediment in an image.

Image analysis results were entered into a Microsoft Excel database that contains the site number and UTM coordinates of the site location. From the metrics measured above (methane presence or absence, aRPD, successional stage, and anoxia at the surface) OSI was calculated following the protocol of Rhoads and Germano (1986).

As defined in Rhoads and Germano (1986) the Organism-Sediment Index (OSI) calculations were developed to standardize comparison of habitat quality and have a consistent index that can be compared among and between habitats. The OSI utilizes a combination of four factors (methane presence or absence, successional stage, depth of aRPD and anoxia presence or absence). Values for OSI range from -10 (poorest quality habitats) to +11 (highest quality habitats). The OSI has been used to map disturbance gradients and to follow ecosystem recovery after disturbance abatement. For estuarine and coastal bay benthic habitats in the northeastern United States, OSI values greater than 6 indicate good habitat conditions and are generally associated with bottoms that are not heavily influenced by stress. Stressors can be natural environmental factors, or they may result from the activities of humans. In this report, we use the word disturbed to distinguish between natural stressors and anthropogenic stressors, after Rhoads. Stress is largely a consequence of organic loading (eutrophication) that can change sediment texture and dramatically reduce oxygenation of sediments and water column (anoxia and/or hypoxia). However, it may also be due to physical disturbance of the bottom from either dredging or construction and human use of the shallows for other activities such as, shipping and boating. The value for defining stressed from non-stressed bottom varies depending on region (e.g. Diaz et al. 2004). The formulation of the OSI and contribution of each component are scaled to reflect the increasing importance of bioturbation, sediment mixing mediated by organisms, and other biogenic activity, such as structure building, in defining benthic habitat quality. In NY Harbor, OSI < 6 defines stressed habitat, $6 < \text{OSI} < 8$ defines intermediate habitat, and OSI > 10 defines habitat that is not stressed.

Small opportunistic tube-dwelling polychaetes or oligochaetes, identified as Stage I successional species by Rhoads and Germano (1982)[6], are among the first macrofaunal components to colonize newly disturbed sediments. These worms may reach high densities of greater than $10^5/m^2$ within a few days to weeks after disturbance (McCall, 1977; Rhoads et al., 1978). The pioneering species that colonize a disturbed bottom may vary with substratum but are the initial species to occupy organically enriched habitat; as they oxidize the sediment-water interface, they pave the way for later successional stage species (Stage II and Stage III). Most pioneering species feed near the sediment surface or from the water column and they construct tube walls or shells that isolate them from the poor quality sediment often low in oxygen and high in organic content (Rhoads and Germano 1982). In the absence of further disturbance, Stage I assemblages are replaced by Stage II infaunal amphipods, gastropods, and other sediment feeders then subsequently equilibrium stage (Stage III) or successional end-stage species. Typical species appearing in the intermediate Stage II assemblage include but are not limited to shallow-dwelling bivalves (e.g. *Mulinia lateralis*, *Tellina agilis*), grazing gastropods (e.g. *Illyanassa* sp.), and a few species of tubicolous amphipods (e.g. *Ampelisca sp.*). Examples of Stage III assemblages have been described as including maldanid, nepthyd, and lumbrinerid polychaetes, nuculanid clams, and *Molpadia* tunicates. These Stage III species complexes are associated with a deeply

[6] Rhoads, D.C. and J.D. Germano. 1986. Interpreting long-term changes in benthic community structure: a new protocol. *Hydrobiologia* 142:291-308. Diaz, R.J. and L.C. Schaffner. 1988. Comparison of sediment landscapes in the Chesapeake Bay as seen by surface and profile imaging. pp. 222-240. In: M. P. Lynch and E. C. Krome, eds. Understanding the estuary; Advances in Chesapeake Bay research. Chesapeake Res. Consort. Pub. 129, CBP/TRS 24/88. Maher, Nicole P., 2006. A New Approach to Benthic Biotope Identification and Mapping. Ph.D. Thesis. Marine Sciences Research Center, Stony Brook University, Stony Brook, NY. 181 pp. (copies of thesis can be obtained from Dissertation Express http://disexpress.umi.com)

oxygenated sediment surface where the redox commonly reaches depths of more than 10cm (Rhoads and Germano 1982).

Benthic community successions are not necessarily linear. Any combination of stages can occur together. Sites are classified as Successional Stage I on III have Stage I assemblages occurring at the same place and time as Stage III. For example a SPI image may reveal a large numbers of small polychaetes at or near the sediment surface along with active Stage III feeding burrows occurring at depth.

> *"In summary, the sedimentary effects of equilibrium species in shallow water environments appear to be: (1) The transfer of both water and particles over vertical distances of up to 10-20 cm. (2) Intensive particle mixing produces homogeneously mixed fabrics; many of the particles at and below the sediment surface may be in the form of fecal pellets. (3) Head-down feeding produces void spaces (feeding pockets) at depth within the bottom. (4) Surface microtopography may be featureless and planar if tidal resuspension 'smoothes-over' biologically produced features at the sediment surface; in the absence of this smoothing effect, the surface may be covered with numerous feeding pits, and fecal or excavation mounds."* (Rhoads and Germano, 1982)

Figure 16. Field operations: SPI (camera on deck).

Figure 17. Field operations photos: SPI imaging.

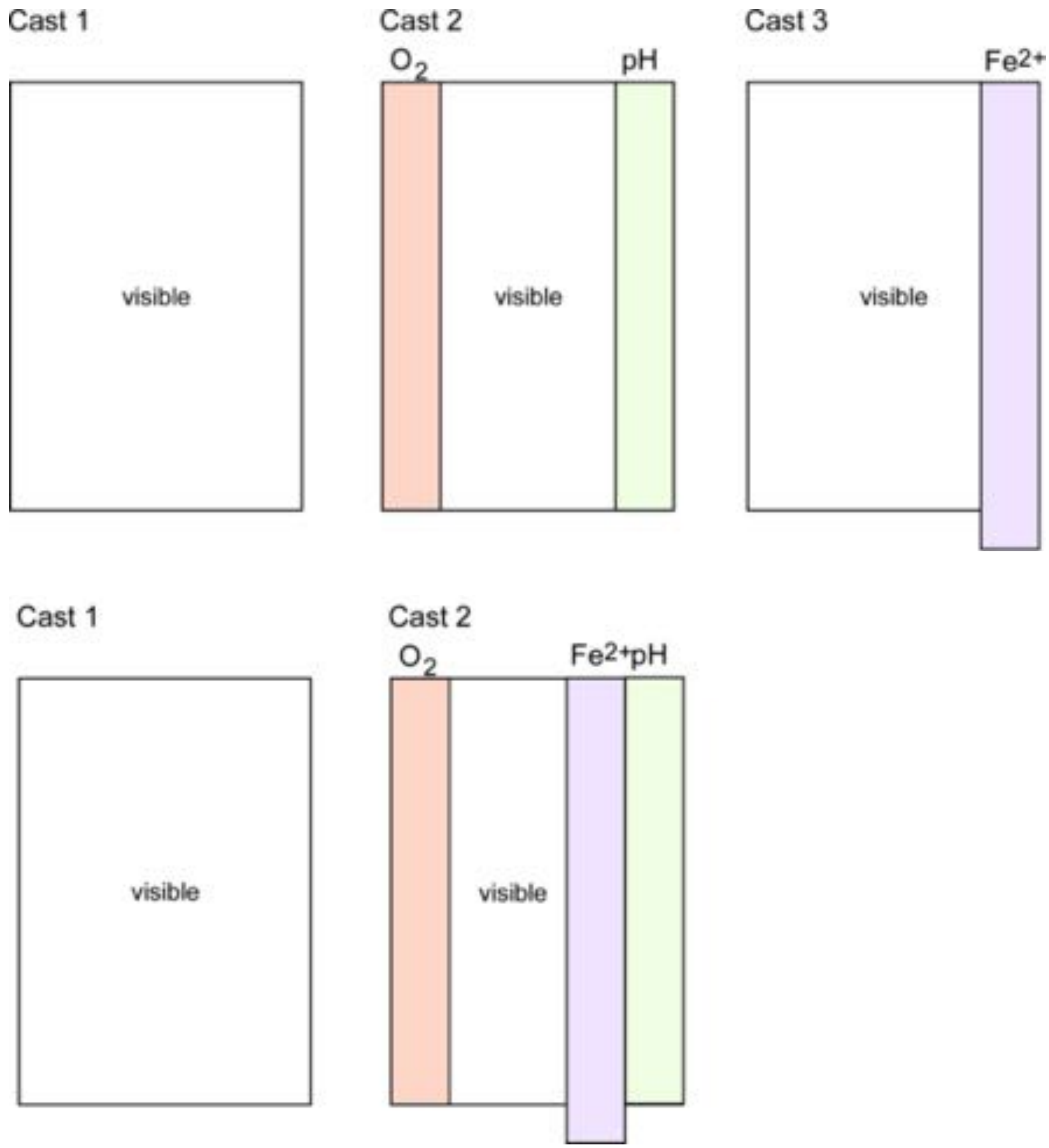

Figure 18. Two configurations of the sensor strips on the SPI window. The top shows sensor configuration for three casts per site. The bottom is for two casts at each site. The sensor strips are transparent.

3.7 Sediment samples

3.7.1 Sediment cores acquisition and processing

e4 collected push cores at 55 sites and sampled sediment cores at the same time as the grab samples. James Trotta and Bruce Ward oversaw the sampling and collected the push cores.

Figure 19 shows the e4-acquired benthic samples.

The crew verified all actual locations on-site using a Trimble dGPS system. At each site, the captain spudded the vessel as close as possible to the planned location. Once the vessel was stable, the crew took the first grab sample. The core samples were obtained after the Ponar samples. e4 collected the cores with a push-core system, using sterile clear 2 ¾" polycarbonate tubes. Such tubes are optically clearer than PVC and other plastic sampling tubes. This allows one to confirm the sediment-water interface is sampled. The crew advanced the cores as deep as possible, and a minimum of 10cm of recovery was required. The crew repeated core attempts until it obtained sufficient recovery. The core sample was then compared to the Ponar results to ensure the recovery of the sediment-water interface. After samples were collected, e4 photographed the tubes with emphasis on the sediment-water interface and stored the cores at 34°C.

Prior to splitting the cores, e4 logged each core continuously for properties useful in sediment classification. Immediately after splitting the cores into two halves, one for archiving and one for working, e4 photographed both halves then visually described them. e4 depicted a graphic interpretive log next to the digital image that includes grain size, bed thickness, contacts, sedimentary structures, mineralogy, coring-induced sediment deformations, color and lithologic accessories including organic carbon, plant matter, diagenetic features, macrofossils, and anthropogenic content. e4 sealed the split cores in airtight plastic wrap. At the end of the project, the cores were delivered and archived in the refrigerated environment with other sediment cores collected during previous phases of the NYSDEC Hudson River Estuary benthic mapping project at Lamont-Doherty Earth Observatory of Columbia University.

3.7.2 Sediment grabs acquisition and processing

James Trotta and Bruce Ward oversaw the collection of push cores and of the grab samples and maintained the chain of custody for the samples. Pam Neubert oversaw the mobilization and training for the infaunal sampling. Sarah Boucher and Ally Sullivan, both of Stantec, collected the infaunal samples in the field. e4 collected the grab samples with a Ponar grab sample device.

At each site, the captain spudded the vessel as close as possible to the planned location. Once the vessel was stable, the crew collected the first grab sample with a 6"x6" Ponar grab sampler (in a few problematic areas, a 9"x9" grab sampler was used). Ponar samples were repeated until sufficient recovery (at least 80% full) for the benthic infauna sample. The crew then repeated the sampling until sufficient recovery for the grain size, ^{7}Be and ^{137}Cs analyses. The crew cleaned the grab sampler between attempts.

e4 deployed two grab samples: the first for infaunal organisms, the second for sediment samples. e4 kept the infaunal samples if recovery was greater than 80% of the sample. Immediately after sampling, infaunal samples were washed through a 500-micron mesh sieve and preserved in 10% buffered formalin. The second deployment targeted sediment – the top 5cm were sampled for isotopes.

3.7.3 Grain size analysis sieves and hydrometer

The methods followed Folk (1974) and standard ASTM protocols. TerraSense, LLC, conducted the measurements in collaboration with e4laboratories, a division of e4sciences.

Grain size samples were stored in sterile 12oz glass or plastic jars. Samples were transferred to TerraSense for grain size analysis.

Grain size was reported in the Krumbien Phi scale of the Uden-Wentworth grain-size classes as described in Folk (1974). The coarse fraction (>-6.0 to 4.0Phi) was measured by standard sieve analyses at one Phi increments. The fines (4.0 to 9.5Phi) were determined in half Phi increments. The first increment (4.5Phi) was done by sieve analyses and the remainder by hydrometer.

Major rain size classes

	Wentworth Size Class	Size	
		Phi	mm
Gravel	Gravel	< -1.0	>2.0
Sand	Sand	-1.0 to 4.0	2.0 to 0.0625
Mud	Silt	4.0 to 8.0	0.0625 to 0.0039
	Clay	>8.0	<0.0039

3.7.4 Logging the sediment cores for lead

e4 performed a full elemental analysis on sediment cores, paying special attention to all metal [most importantly lead (Pb)] content of the sediment cores using a ThermoNiton XL3t 950 GOLDD+ XRF analyzer. This device is capable of measuring the concentrations of elements as light as magnesium (Mg), as heavy as uranium (U), and every element in between. This device uses helium gas to decrease the minimum detection limit (MDL) and increase the accuracy of the readings. At the start and end of each session the soil standard NIST 279a (San Joaquin soil) was measured. The precision or variation between the analyses was approximately 1%. The analyses varied less than 2% from the published value of the standard.

The analyses followed protocols established in Kenna et al. (2011a) and Nitsche et al. (2010). e4 made the analyses using the proprietary geology mode, which is included in the manufacturer's software. The geology mode is a normalized calibration scheme that is compliant with EPA Method 6200. Lead, for example, is quantified by monitoring its characteristic X-ray emissions at 10.55keV (La1) and 12.61keV (Lb1), and each measurement was conducted for a period of at least 120 seconds.

e4 contained the sediment cores with plastic wrap immediately after splitting them and recorded XRF measurements every 5cm down the core. XRF measurements always included Pb concentration, but also included other metals (see previous paragraphs). All of this data is contained in Appendix V (Table 42), and Pb concentrations are highlighted in individual figures, also in Appendix V.

3.7.5 ^{7}Be and ^{137}Cs analyses

The ^{7}Be content of the topmost sediment in each grab sample was measured as soon as possible after taking the grab sample in time to determine whether any ^{7}Be existed at the time the core was taken. The time between obtaining a core and ^{7}Be measurement must be less than one (1) year.

^{137}Cs is a man-made radionuclide that was not present in the environment prior to 1950 and allows additional constraints to be placed on the age of the surface material. ^{137}Cs levels were also determined in the topmost sediment in each core.

The analysis of these radionuclides followed the protocol outlined in Nitsche and Kenna (2010). One variation from their method that we recommend is to sample the top 5cm as opposed to the top 1cm of each core. This increases the likelihood of capturing the whole ^{7}Be inventory at each site. Dr. Kirk Cochran[7] also recommends that the samples be dried and ground before analyses. This ensures a more homogeneous sample.

TestAmerica dried, homogenized and ground the surficial sediment samples. The samples were weighed wet and then dried to determine water content and dry bulk density. TestAmerica reported the results as activity per gram of dried sediment. Samples were analyzed for ^{7}Be (477keV) and ^{137}Cs (662keV) by counting the samples on a Canberra 3800 mm2 germanium gamma detector for ~ 24 hours. Excess ^{7}Be was corrected for radioactive decay from core collection to the time of counting.

[7] Cochran, J.K., D.J. Hirschberg and H. Feng. 2006. Reconstructing sediment chronologies in the Hudson River Estuary. In: The Hudson River Estuary (J.S. Levinton, J.R. Waldman, eds.) Cambridge University Press, pp. 65-78.

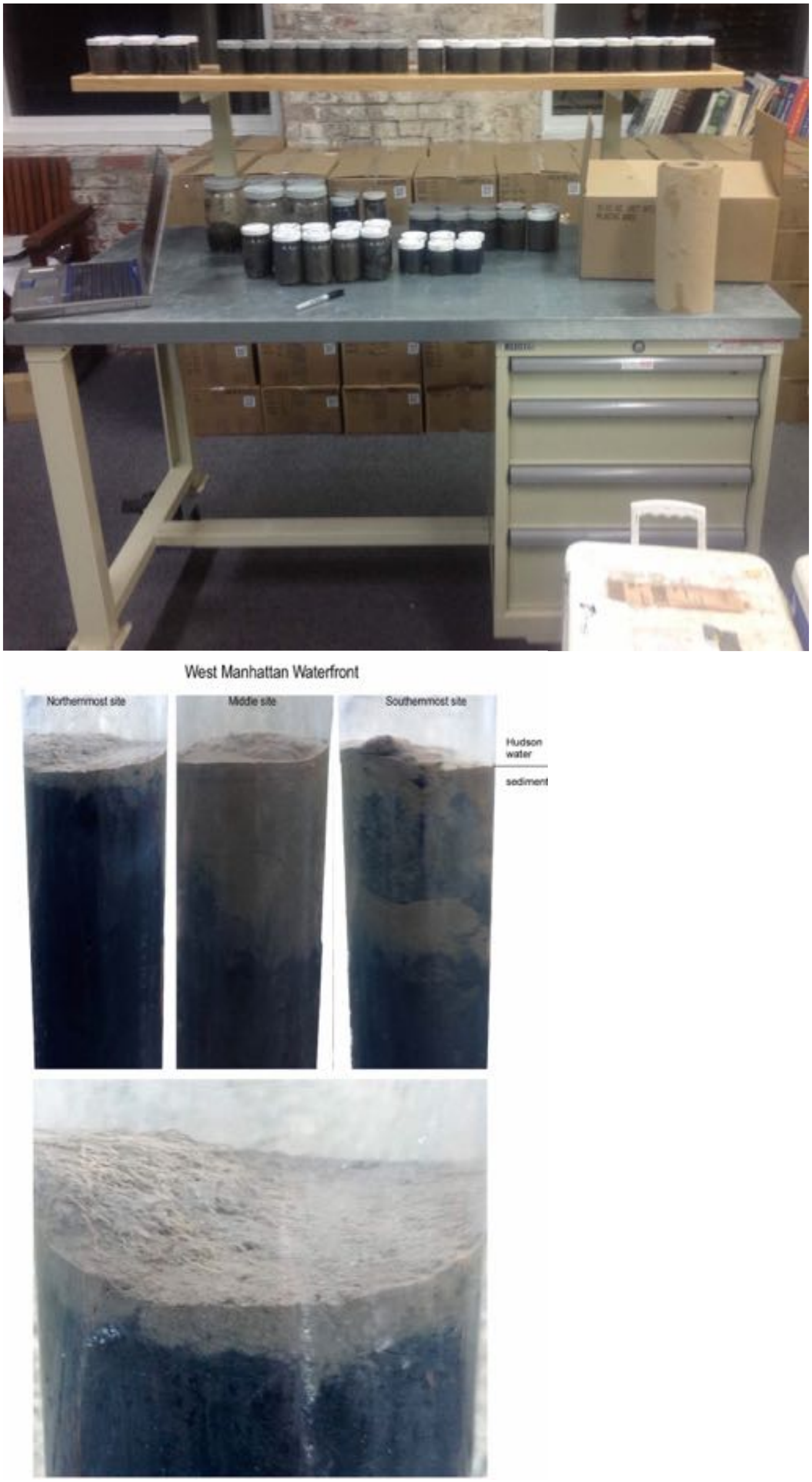

Figure 19. e4-acquired benthic samples.

3.8 Invertebrate identification and counts

3.8.1 Benthic infaunal community analysis

Dr. Pam Neubert QA/QC'ed the data and evaluated the benthic invertebrate data for community analysis. She calculated standard univariate metrics that include Shannon-Weiner diversity, Pielou's Evenness, log series Fisher's alpha, taxa richness, abundance, and number of organisms per meter squared. Multivariate analysis include Analysis of Similarity (ANOSIM), principal component analysis, and Bray-Curtis similarity. Using results from both multi- and univariate analyses, she compared community structure of each of the 55 sites to the biotopes defined within Maher (2006) "A New Approach to Benthic Biotope Identification and Mapping."

The infauna team is pictured in Figure 20 performing invertebrate sampling.

Adams et al. 1998 developed a benthic index of biotic integrity (B-IBI) for the mid-Atlantic region for tidal rivers and estuaries. This B-IBI incorporated five benthic macroinvertebrate metrics: 1) average number of taxa, 2) average number of pollution sensitive organisms, 3) average abundance, 4) average number of pollution tolerant organisms, and 5) biomass. Each metric is scored by assigning a value. Each metric is scored with 5 (the highest, best quality value), moderately impaired sites are scored with 3, and 1 is assigned to highly impacted characteristics. An average score is calculated to generate the mid-Atlantic tidal B-IBI score from each of these five scores at an individual site.

3.8.2 Community Metrics Definitions

Shannon-Weiner index: The Shannon-Weiner index has been a popular diversity index in ecological literature. The Shannon-Weiner index quantifies the uncertainty associated with the proportion of characters (i.e. species) and the ability to predict how many characters may be represented as well as the certainty of predicting which character will be next in the series. Most frequently the Shannon-Index is calculated using the natural logarithm, but the base of the logarithm used when calculating the Shannon entropy can be chosen freely. Shannon himself discussed logarithm bases 2, 10 and *e*, and these have since become the most popular bases in applications that use the Shannon entropy.

Abundance: The number of individuals observed at a sampled location.

Species richness: The number of species observed at a sampled location.

Pielou's Evenness: Pielou's Evenness or species evenness is defined as a diversity index and a measure that quantifies the equality of the ecological community in numerical form. Evenness is measured on a scale of 0 to 1. If a population is highly even it will have a value near 1 and if there is a dominant species that has a higher abundance relative to other species then the community would be highly uneven with a value closer to 0.

Log Series Fisher's alpha: Fisher's logarithmic series model (Fisher et.al., 1943) relates the number of species and the number of individuals in those species. It is a parametric diversity index that assumes that species abundance follows log distribution.

Bray-Curtis Similarity: This is a statistic used to quantify the compositional similarity and dissimilarity between different locations/sites/samples at each site.

Multidimensional scaling (MDS): This metric is a means of visualizing the level of similarity of individual samples/sites/locations within a dataset. It refers to a set of related ordination techniques used in information visualization, in particular to display the information contained in a distance matrix.

Principal component analysis (PCA): PCA is a statistical procedure that uses orthogonal transformation to convert a set of observations of possibly correlated variables into a set of values of linearly uncorrelated variables. The first principal component has the largest possible variance and each succeeding component has the next highest variance. The principal components are orthogonal eigenvectors of the covariance matrix that is symmetric.

3.8.3 Infauna Samples

Immediately after acquisition, e4 processed the infauna samples. e4 washed grab samples for faunal analysis through a 0.5mm sieve, preserved in 10% buffered formalin, and stained with rose bengal. e4 then shipped these samples to EcoAnalyst for classification.

EcoAnalysts transferred the samples to 70% ethyl alcohol and sorted them under a dissecting microscope. Individual organisms were identified to species level whenever possible, and the total for each taxa enumerated. After EcoAnalyst sorted samples using a 500-micron mesh sieve, they separated samples into major taxonomic groups. After primary sorting, the taxonomists analyzed the samples and identified the organisms to lowest practical taxonomic level, typically genus and species. The team has a Taxonomy QC requirement of a 10% re-identification to determine and maintain 90% efficacy. The final report includes a complete metrics report, a taxa report, a sorting efficacy report, and a community similarity report.

3.8.4 Post-field infaunal sorting, enumeration, and identification of 55 samples

e4 shipped the infaunal samples to EcoAnalysts. The biologist at EcoAnalysts sorted individual benthic organisms and identified organisms to the species level whenever possible, and enumerated the total for each taxa. The biologist performed taxonomic identifications from infaunal organisms to the lowest practical taxonomic level.

The 10% QA/QC re-sort of samples assures 90% efficacy removal of organisms. Samples were stained with rose bengal. Full sample sorts were performed. After sorting, the biologist enumerated and identified resulting organisms to lowest practical taxonomic level (LPTL) with oligochaetes enumerated only. A species list by site with a QA/QC report for sorting is an electronic data deliverable.


Figure 20. The infauna team performing invertebrate sampling in Brooklyn Bridge Park**.**

3.9 Bottom classification

3.9.1 Bottom classification

Final bottom classification maps were derived by combining site-specific OSI values with the sediment type maps to produce a single bottom classification map. Both of these data sets are provided in the electronic data delivery and a description of their uses is included in the metadata.

The bottom classification was based on a combination of a) sediment type and geological substrate maps, b) Organism-Sediment Index (OSI) values, and c) species population and diversity surfaces and maps.

e4 combined sub-bottom and orthosonograph datasets using manual and automatic data processes, described above (Sections 3.3-3.5), to characterize the type and extent of sediments throughout NY Harbor and the Lower Hudson River. These results were tied to grain size analyses from grab samples collected in the study area and to orthosonograph evidence of anthropogenic materials [e.g., fallen piers, debris fields, and dredged areas – similar to Bell et al. (2004), but described in greater detail below]. In combination, these results provide a comprehensive picture of sediment type and environment within the study region. These sediment type and geological substrate maps formed the basis of e4's bottom classification maps in each area.

Flood and Cerrato (2010) reported that previous researchers found that "province variables such as visually derived backscatter patterns" explained 13-48% more benthic community variation than the 132 QTC Multiview sonar-derived variables that they presented. Further, they stated that there was nothing in their 2010 study to suggest that their 132 sonar-derived variables can displace province variables as the primary set of variables used to characterize bottom type – benthic faunal relationships. They thus concluded that, despite not considering province variables derived from the visual interpretation of backscatter maps in their 2010 report, visually determined province variables remain a critical element in the analysis of benthic community structure. Based partly on Flood and Cerrato's (2010) own conclusions, and partly on experience working in and around NY Harbor, e4sciences based our bottom classification algorithm on the visual interpretation of processed sub-bottom seismic and orthosonograph data. To the extent they are not proprietary, e4's data collection, analysis and processing methods for both backscatter (orthosonograph) and seismic data are described in detail above (sections 3.3 and 3.4). As mentioned in these sections, e4's side-scan image processing produces intuitive orthosonographs, similar to aerial photographs, which can be visually analyzed and compared to other datasets, such as sub-bottom seismic data. e4 interprets each dataset independently. After each dataset is interpreted, e4 produces a combined interpretation for all the independent measurements.

3.9.1.1 Bell's classification

This section reviews Bell et al. (2004) and the reasoning for deviating from their algorithm. e4 based the geologic substrate interpretation partially on Bell et al. (2004). e4 also used multiple acoustic sensors for interpretation of the harbor floor.

Bell et al (2004) recognized 5 major groups of bottom interpretation for the Hudson River:

1) Sedimentary environments based on backscatter and subbottom;
2) Grain size based on cores, grab samples and SPI;

3) Morphology based on bathymetry;
4) Anthropogenic features based on the acoustic data; and
5) Habitats based on the acoustic data.

Our approach to item 1 will be discussed last because it drives e4's sediment type and geologic substrate classification algorithm.

e4 followed an approach analogous to that of Bell et al. (2004) for the grain size measurements (item 2). e4 simplified the morphology based on bathymetry (item 3) to distinguish the shallows, the deeper channel, and the slopes in between.

e4 also identified anthropogenic features (item 4) in an approach analogous to that of Bell et al. (2004); however, we grouped the anthropogenic features together as one group in the bottom classification.

For item 5, Bell et al. (2004) encountered two habitats easily recognizable in the geophysical data; shell beds and submerged aquatic vegetation. Neither of these facies was encountered in this study.

In the sedimentary environment (item 1) classification, Bell et al. distinguished the following four classes:

1) Depositional
2) Erosional/non depositional
3) Dynamic environment
4) Unknown

Bell et al. (2004) define deposits characterized by low backscatter and a variety of sediment thickness and draping relations as depositional. They also group bedforms, including scours, as dynamic. Erosional/non depositional subclasses represent areas where subsurface strata appear to be truncated, where rock is exposed, or where there is no clear thickness of the depositional classes.

Although e4 used similar backscatter and cross-cutting relationships in the bottom classification, we did not follow the scheme of Bell et al. because the groupings of depositional and dynamic can be misleading.

e4 has found that all sedimentary bodies are depositional. Generally, the use of the term "dynamic" implies active movement, but active requires defining a time frame in which activity occurs. For example, the whole of the harbor is "active" on a geologic timescale, while black silt deposits are more active than anything else in the harbor but display no active morphology because the sediment is a thin, draping deposit. There is a periodicity to sand wave movement in which the waves can lie dormant for weeks-months or weeks-years while other sediments accumulate on top of them. To accurately define activity, a time scale for the activity must be specified. None of the studies of the benthic environment in NY Harbor, this one included, have captured enough data to accurately define such time scales. As a result e4sciences did not use the approach of Bell et al. (2004) in our sediment type and bottom geologic substrate classifications and maps.

e4sciences' imaging of the harbor floor over the last 15 years has shown that one of the most dynamic sediment deposits are the low-backscatter "depositional" black silt deposits. Black silt can be stirred easily. It can move with any and all water movement whether it is by tidal, wind-forced or from vessel traffic. Deposits can change daily.

On the other hand it is not uncommon in the NY Harbor for the "dynamic" sand waves to have a thin deposition of black silt over them. The movement of such sand waves is episodic. We lack the temporal data to constrain the time scale of the episodic movement. The presence of these bedforms does not mean that they are actively dynamic or that active sedimentation is going on.

3.9.1.2 e4sciences's algorithm for geologic bottom classification

e4sciences' approach is to first identify and separate hard-bottom areas from areas of sediment. From a benthic perspective this separates areas of sediment where infaunal communities are possible from areas where only epifaunal communities are possible. Although we identified the hard-bottom areas we did not evaluate the attachment communities because they were not included in the scope of work for benthic infaunal communities analysis. e4 recommends that epifauna and attachment communities be included in future analysis of New York harbor and Hudson River benthos.

e4's process is first to interpret single-tool data to produce hypothesis maps and cross sections. Interpreted maps should be considered testable hypotheses. These were tested against each other and sediment samples, SPI images, aerial photographs, and historic boring and sample data.

Hard-bottom areas include piles, collapsed piers and surrounding debris, accumulations of debris, sunken vessels, rock exposures, and rip rap. Intact piers are not included. All of these may have small pockets of sediment but are dominated by hard surfaces, These also have cryptic habitats or cavities. Rip rap is separated out as a special case. Rip rap can be considered either a hard bottom or as an endmember of the sediment (coarse gravel). It is most commonly used in NY Harbor as shoreline armor. Rip rap along with piles and bulkheads are the main features in the intertidal zone.

The hard-bottom areas typically are characterized by areas of both strong backscatter and acoustic shadows. Acoustic shadows are areas of no backscatter. Sediment layers may onlap onto the hard-bottom areas.

The non hard-bottom areas are areas of sediment. There are older sediments exposed through erosion by currents or dredging. In the sediment regions we first identified the more obvious bottom coverage. These include areas of net erosion and the bedforms of the end-member sediment types: black silt and sand. Areas of net erosion include most of the truncated exposed subsurface strata of Bell et al. (2004). Bell et al.'s (2004) approach to erosional surfaces in the harbor was similar to e4's, which was partially based on Bell et al.'s (2004), and our results – as expected for this class – are similar.

The black silt signal is frequency and temperature dependent. A single tool identifies the presence of silt. A single tool interpretation (i.e. seismic isopachs – reflection wavefield) is used in conjunction with core measurements and grab samples to guide the classification of acoustic silt as black silt.

The black silt in the orthosonographs (backscatter wavefield) appears evenly dark to black (low backscatter wavefield). The evenness is a reflection of the smooth surface. The reflection is also a function of the bottom morphology and direction of illumination (i.e. east, west, north, or south). In areas where the silt is thin, the dark areas are patchy where cobbles, boulders, and irregular surfaces emerge through the silt. In patchy areas, for the purpose of this bottom classification, e4 selected the dominant sediment as the sediment type, for example in sand waves where black silt is in the trough – the sediment type is sand; sand waves with black silt in the crest – the sediment type is black silt.

From repeated imaging and sampling over the last 15 years e4 has shown that layers of black silt as thin as 2cm can be identified in orthosonographs. Black silt deposits in NY Harbor can range from being thin (a few mm in samples) to being greater than 3m thick. This sediment commonly forms drapes and also infills deep areas.

Most of the bedforms occur in areas of sand or coarser grains. The large scale ripples or waves in the Harbor also prove to be sand. In the lower harbor, the ripples and waves are typically fine sand. These ripples have strong backscatter and areas of acoustic shadows (no backscatter). In many cases the subbottom data shows that beneath the undulating surface there are sand deposits characterized by low-angle strata that climb to the surface. These apparent truncated stratal horizons are dominantly depositional even though they may appear as an erosion feature.

Once the more obvious bottom sediment types are identified, the interpretations are tested against available grab sample, core, SPI, and boring data. The remaining sediment areas involve more interpretation and correlation from known areas that have been sampled. We map out the stratigraphy in the subbottom profiles by tracing strata horizons from known historic borings and cores and using principles of superposition and cross-cutting relationships. We use subbottom interpretation to calibrate our visual investigation of the orthosonographs, which we used as a starting point for the production of our base sediment type and geologic substrate maps.

3.9.1.3 Incorporation of infaunal community information

In addition to sub-bottom and side-scan analysis, e4 included results from the study of benthic infaunal communities in NY Harbor and the Lower Hudson River in the bottom classification. Unlike Flood and Cerrato (2010) who incorporated primarily species distributions and observed benthic species in their report, we incorporated benthic community indicators to the bottom classification. These parameters capture community health and benthic infaunal habitat quality in addition to simple observations of the types of benthic species observed. Further, e4 provided maps showing the distribution of sample site benthic indicators overlain on our sediment type and geologic substrate maps for both the whole harbor and specific study areas of the project. We found that this approach provided simple, at-a-glance associations between the benthic and geologic environments in NY Harbor and improved upon the sonar-biologic associations first presented by Flood and Cerrato (2010). We say improved because we do not present potentially misleading statistics for quantitative associations from a limited density of samples. Without significant coverage of biological sampling there is a need to extend or extrapolate the limited biological data throughout the area of investigation. This is especially true in an exploratory or reconnaissance study such as this. For this study there is, on average, one sampling site per 18 hectares. Such a low geographic density of samples precludes direct contouring of the sample attributes and limits the usefulness of statistical approaches to geographic relationships required for mapping. To achieve the desired quantitative associations between sediment types and benthic communities, e4 recommends examining a small area with a very high density of samples. This is something e4 recommends for future work on the NY Harbor benthos.

e4's maps provide visual associations without the introduced error inherent in performing statistics on a limited suite of samples. e4 incorporated benthic community health into its bottom classification maps by mapping, only where appropriate, and examining two key biologic indicators, organism density and OSI. These are described below.

Organism density maps plot the total number of individuals per meter squared. This data is presented either as a surface, or as a location-dependent plot of the relevant indicators as numbers. This data provides a counterpoint to the single OSI values calculated for each site and highlights the heterogeneity of benthic habitats in NY Harbor.

Based on detailed mapping and analysis of the many biologic indicators measured or observed in our SPI analyses, e4 determined that the biologic parameter that best captured benthic community environments in the study region was OSI (in part, because it incorporates so many key biologic indicators). After detailed examinations of both the OSI and organism density parameters, we determined that OSI best and most simply captured the relevant information on the health of the benthic communities sampled in this study. In our final bottom classification maps, the key biologic indicator of OSI is shown overlain on our geologic and sediment-type maps.

e4 created a final bottom classification map based on all of the data that we acquired. We examined the Bell et al. (2004) and Flood and Cerrato (2010) approaches. We adopted some of the sediment type classifications from Bell et al. (2004), but found that neither the Bell et al. (2004) nor Flood and Cerrato (2010) approaches could be adopted by e4 directly because they would not honor all of the data or accurately represent the sediment type. Flood and Cerrato's (2010) approach was especially problematic given its reliance on 132 "sonar-derived" variables that are attributes of each backscatter image, but otherwise divorced from the measurable characteristics of the seafloor. As much as possible, e4 strives to accurately represent all data and associate interpretations with measurable, repeatable results. For this and other reasons, including e4's boring database throughout New York harbor of which we made extensive use, e4 based our sediment type and bottom classification algorithms on the direct interpretation of sub-bottom orthosonograph and seismic images and data directly. We also improved the techniques presented by Bell et al. (2004) and Flood and Cerrato (2010) by combining the sediment classification and OSI results for benthic communities on one map. This produced an at-a-glance association between benthic community indicators of habitat quality and infaunal health (rather than solely species-based community type), location in the harbor, and sediment type/geologic substrates.

3.9.2 Literature review of benthic community

Carmela Cuomo, PhD, prepared the benthic literature review. The full collection of papers used in the review is included in the digital portion of this report. The benthic literature search was undertaken in an effort to document the known historical and present state of the benthos of the Hudson River estuary in order to elucidate the changes – physical, chemical, geological and biological – that have occurred within the estuary since the arrival of European settlers to the present. This represents an enormous amount of literature—tens of thousands of papers. The report in Appendix III focuses primarily on the parts of the watershed that feed into the areas known today as the Brooklyn Navy Yards, the tidal flats off of Brooklyn, the upper and lower areas of the lower Hudson River, and the developments along the Hudson.

Pam Neubert, PhD, prepared the epifanual literature review. The review is included in her report in Appendix IV.

3.9.3 Integration of acquired data and benthic literature

Task 8C combined the historical data in the literature and the analyses of the physical and biological data acquired in the shallow water benthic surveys into a comprehensive overview of the history of the benthic communities.

The 1995 NOAA study set a benchmark for the benthic community health (Iocco et al., 2000a). The interesting part of the NOAA study was that they conducted a repeat of the June study in October. The June-1995 results show a range of OSI values, including some that indicate stressed environments. The October-1995 results show ecosystems consistent with our observations in November.

We compared the November-2015 to the October-1995 data (Iocco et al., 2000a), noting that the comparison is subject to variability month-to-month. The results of this comparison are described in detail in Section 4.5 and further discussed in Dr. Neubert's epifaunal literature review (Appendix IV, Figures 5-7). Additional historic data is provided in Figure 61 from Hale et al., (2007) and in Dr. Cuomo's benthic literature review (Appendix III).

3.10 QA/QC

The importance of the accuracy and completeness of the investigations cannot be overstated. QA/QC has three steps:

1) Preparation
2) Accuracy through redundancy
3) Independent review

At e4, QA/QC standards are designed to align with USACE ER 1110-1-12 Engineering & Design Quality Management, and Engineering Manual 1110-2-1003. The QA/QC process is a series of checks and balances that maximize accuracy and completeness of the following:

a) measured and observed data
b) entry of the measured data onto graphic sections and into databases
c) reference frame for the observed data
d) plotting of the data
e) reporting of the data
f) archival of the data

The QA/QC process begins with a series of daily habits and protocols that govern the observation, processing, interpretation, and reporting of data. The Independent Technical Review (ITR) does not replace QA/QC. The ITR is a post-report review that cannot undo all of the inaccuracies and omissions in the observations, measurements, and input of data.

A primary step in all procedures is that multiple sources of data are constantly being combined in a single reference frame. Each data set is acquired and processed independently and then it is correlated in a single reference frame. Dr. Bruce Ward is the quality control officer (QCO). He continually reviews the combination of these data.

All members of the team are qualified geologists, scientists, drillers and captains with a minimum of four years experience in description, drilling practice and/or geo-referenced electronic data gathering. All are familiar with surface and subsurface measurements, safety procedures, teamwork, surveying benchmarks, observing and recording boring data, vertical and horizontal datum, map making, digital photography, event recording, objective description, note taking, and data backups.

Prior to the fieldwork, the team met, reviewed and debated the procedures. The key members of the e4sciences team visited the *Tide and Time* and reviewed the data. They walked through the location procedures to improve coordination and to determine potential hazards.

a) Operations and maintenance manuals
b) Aerial photographs and historical drawings
c) Chain of custody for historical document electronic reproduction
d) Coordinate systems and datum
e) Tie-ins to local benchmarks
f) Three-dimensional terrain model of the system
g) Hard copies of data to be used in the field inspection
h) Checklists for each system
i) Checklists for equipment and inspection procedures
j) Data backup and transportation
k) Backup note taking procedures
l) Define naming conventions for all types of recorded data
m) CAD/GIS drawings
n) Experience with the event-based recording

This meeting prepared the team to cover all of the expected phenomena at the site. The team tried to anticipate the unexpected, as well as criticize the planned procedures in order to eliminate surprise and omissions. Nomenclature and numbering systems were reviewed. The Team Leader conducted the meeting, and the Quality Control Officer observed. This step ensured that fieldwork would not be repeated. The preparation must be complete.

The fundamental practice of the e4sciences team is to acquire independent and redundant data in single reference frame:

a) Redundant data
b) More data than is defined in scope of work
c) Process each data set independently
d) Compile all data
e) Plot data in a single reference frame

All data was duplicated at the end of every day. The redundant data copies were divided up among the crew and transported in separate vehicles.

3.11 Side-scan viewer

e4 provided license-free viewers for all of the sonar XTF and JSF data as part of the digital compilation and final report.

e4sciences provided a license free viewer for the sub-bottom seismic profiles. The viewer displays SEG-Y files.

3.12 Final report

The main report contains an executive summary, description of methodology, results, and appendices containing data. Particular focus is placed on the bottom maps for bathymetry, sediment classification, and benthic environment. Oversized (44”x30”) plates replot the key maps and cross sections for presentation and discussion purposes.

e4sciences produced a comprehensive report for each of the eight areas of investigation. The deliverables include:

1. Main report
2. Digital data (where appropriate includes ArcGIS shapefiles)
3. Data readers for hydrography, sonar, reflectivity, and sub-bottom data
4. Hydrographic output in XYZ/XYU files and DEM files.
5. Oversized plates

All algorithms used in creating sediment classification maps were made explicit in the report in section 3.9 and self-evidently displayed on each map.

e4 compiled eight reports for the eight areas of investigation into a single report for simplicity. However, e4 configured the cumulative report such that it can be broken down into eight independent reports.

3.13 Digital compilation

We organized and prepared the raw and processed data in an electronic data package with metadata. Metadata describes how to access the database. Every data point has a location and time associated with it.

The seismic and the sonar viewers are included in the compilation

The hydrography and reflectivity data are listed in XYZ and XYU files.

The side-scan orthosonographs are GeoTIFFs.

The raw sonar and seismic data are listed as XTF/JSF and SEG-Y, respectively.

The SPI database includes the digital photographs and the annotations of the characteristics observed in the images.

The excel spreadsheets for the cores, samples, and SPI images are included in the database.

All of the color and contour maps are in Shapefiles.

Each core description and digital core photograph is standardized in color, scale, and designations, and available in PDF and JPEG format, respectively.

3.13.1 Additional products

In addition to the electronic products from the scope of work, the electronic data package also includes:

1. 200% side-scan orthosonograph coverage at 0.1m resolution
2. Real component of the seismic data, 924 seismic lines averaging 400m
3. Definition of waterfront morphology by data analysis through breaks in the slope at the edge of shallow and at the base of slope aprons.
4. Complete compose bathymetry map for 2006 and 2014.
5. Difference map for bathymetry including historical bathymetries from 2006 and 2014
6. 1^{st} and 2^{nd} derivative maps of bathymetry to show the changes in bathymetries
7. Complete XRF core measurements every 5cm for several elements
8. Data interpretation with e4sciences' proprietary core data
9. Shapefiles for data tracklines
10. Explicit bottom classification to take advantage of the quality of data acquired
11. Extensive report including 8 area reports describing all of the results
12. SPI chemistry (oxygen, pH, Fe) in the SPI results.

4.0 Results

4.1 Morphology

4.1.1 2015 Bathymetry

Figure 21 and Figure 22 plot the bathymetric results for Brooklyn and Manhattan, respectively. The shallower elevations are in red, and the deeper elevations in blue.

The range in bathymetry is elevations +1 to -20m MLLW (National Tidal Epoch 1983-2001). The flats are mostly shallower than an elevation of -5m. The channels vary from -12 to -20m. In Bay Ridge Flats and Governors Island, the flats may be as deep as -11m.

The bathymetries are displayed as average values on a regular grid in MLLW (National Tidal Epoch 1983-2001). If both single beam and multibeam data were used for the 2015 bathymetry, two separate difference grids were calculated (one for the 1m x 1m grid and another one for the 5m x 5m grid). Figure 8 shows the coverage map for the bathymetry. All bathymetry plots are in elevations. In Appendix II, we delivered 10m x 10m grids and 30m x 30m grids in MLLW. Also we delivered in Appendix II the same data in NAVD88. All grids were obtained using a triangular linear interpolation between data points.

4.1.2 2014 Bathymetry

e4 produced a 2014 composite bathymetry for the area of investigation. The dataset consists of hydrographic surveys from NOAA: F00573 (2009) and F00598 (2012), USACE: 4069D (2013) and 4126 (2014), and e4sciences (2014). The bathymetry from e4sciences was computed from a sub-bottom survey.

Figures 23 and 24 plot the 2014 bathymetries for Brooklyn and Manhattan, respectively.

e4 studied the bathymetry by producing derivative maps to examine the slope, the first derivative, and the change in slope, the second derivative. Figure 25 plots the first and second derivatives for Manhattan with the 2014 data. In the slope plot, the color bar is set to show a negative slope from east to west in green and a positive slope from east to west in red. In the change in slope plot, the color bar is set to blue for declining slope and red for increasing slope from east to west.

e4 subtracted the historical 2014 data from the 2015 data for Manhattan waterfront. Figure 26 is the difference map between the two bathymetries. Red is increasing elevation, and blue is decreasing elevation.

4.1.3 2006 Bathymetry

e4 produced a 2006 composite bathymetry for the area of investigation. The dataset consists of hydrographic surveys from NOAA: H10937 and H10938 (1999), H11353 (2004), H11600 (2006) and H11395 (2006), and USACE: 2676 (2004).

Figures 27 and 28 plot the 2006 bathymetries for Brooklyn and Manhattan, respectively.

Figure 29 plots the first and second derivatives for Brooklyn with the 2006 data.

e4 subtracted the 2006 data from the 2015 data for Brooklyn waterfront. Figure 30 is the difference map between the two bathymetries. Red is increasing elevation, and blue is decreasing elevation.

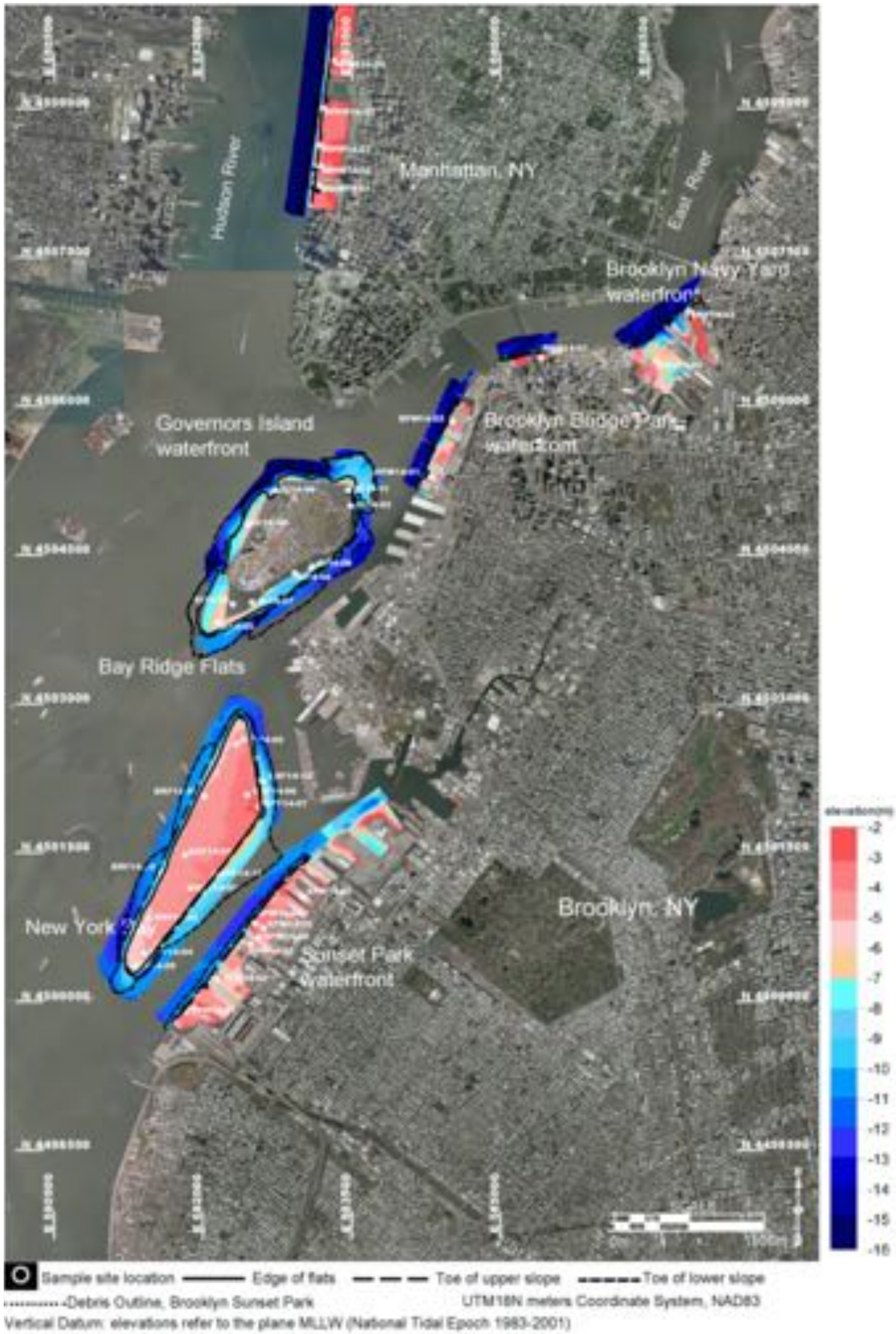

Figure 21. 2015 combined single and multibeam bathymetries in Brooklyn northwest including Governors Island. Single and multibeam data acquired by e4sciences were combined in 5m x 5m and 1m x 1m grids, respectively, using a triangular linear interpolation.

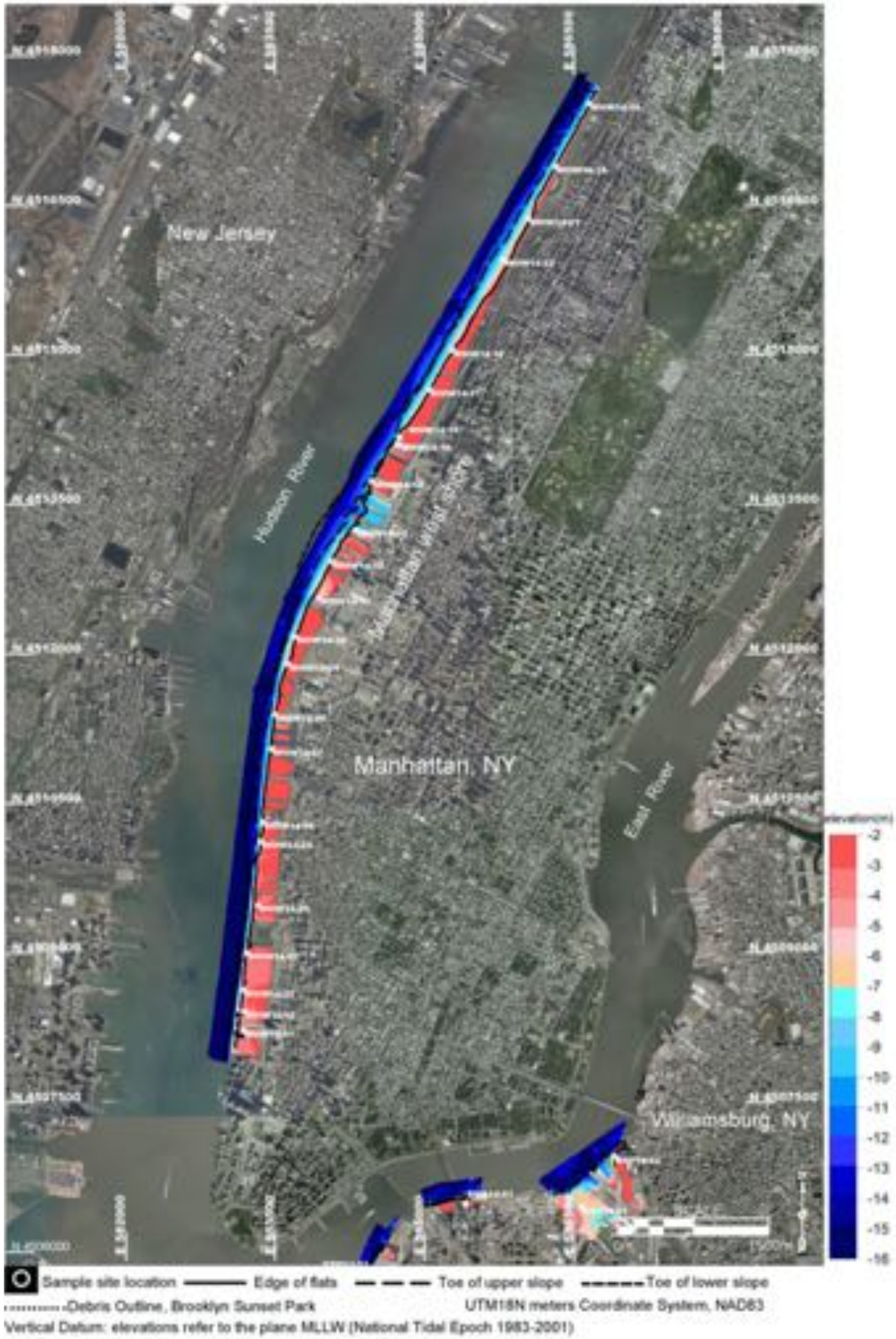

Figure 22. 2015 combined single and multibeam bathymetries in West Manhattan shoreline. Single and multibeam data acquired by e4sciences were combined in 5m x 5m and 1m x 1m grids, respectively, using a triangular linear interpolation.

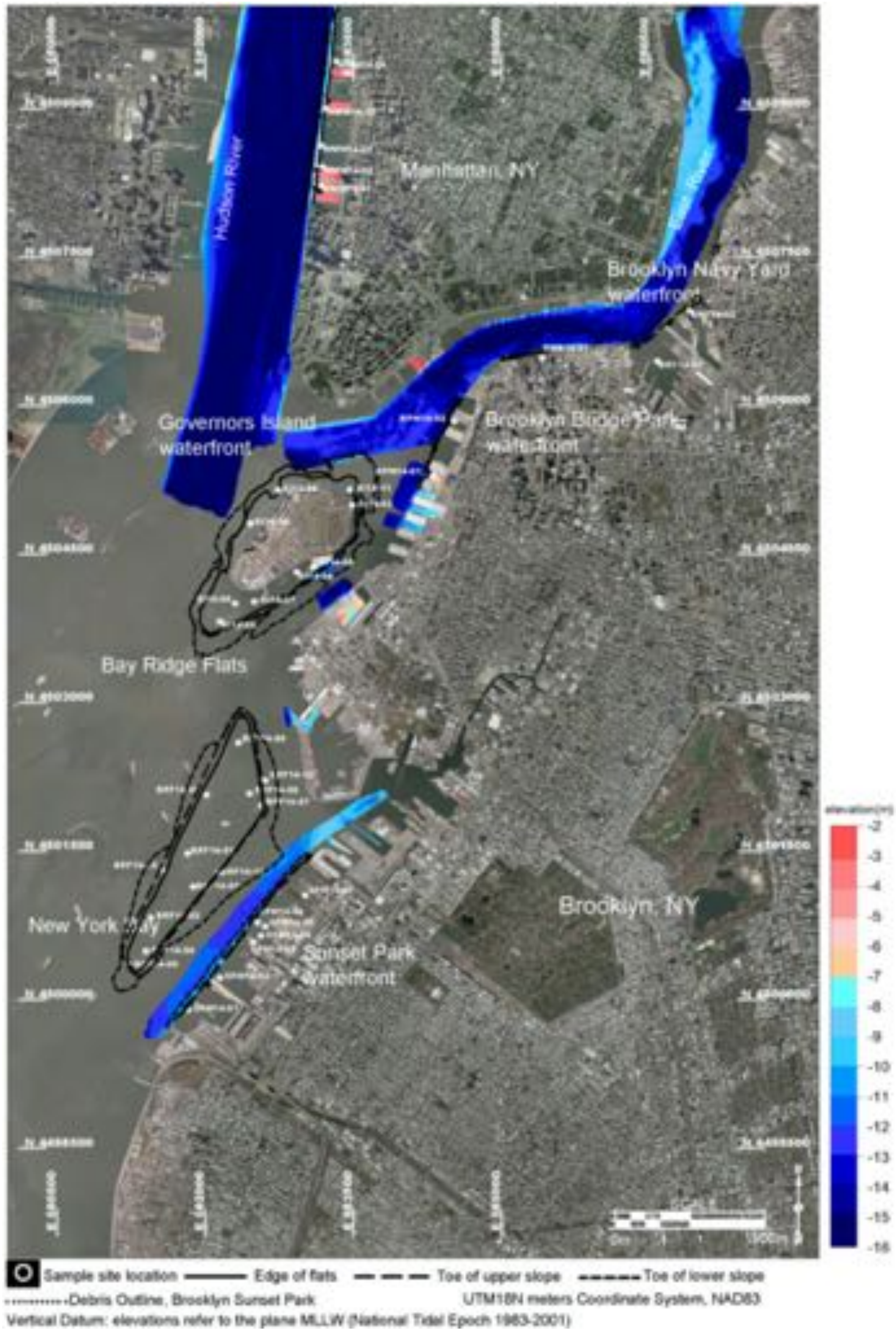

Figure 23. 2014 composite bathymetry in Brooklyn northwest including Governors Island. Data from NOAA, USACE and e4sciences were combined in a 1m x 1m grid using a triangular linear interpolation. NOAA bathymetry includes surveys F00573 (2009) and F00598 (2012). USACE bathymetry includes surveys 4069D (2013) and 4126 (2014). e4sciences bathymetry includes bathymetry computed from sub-bottom data (2014).

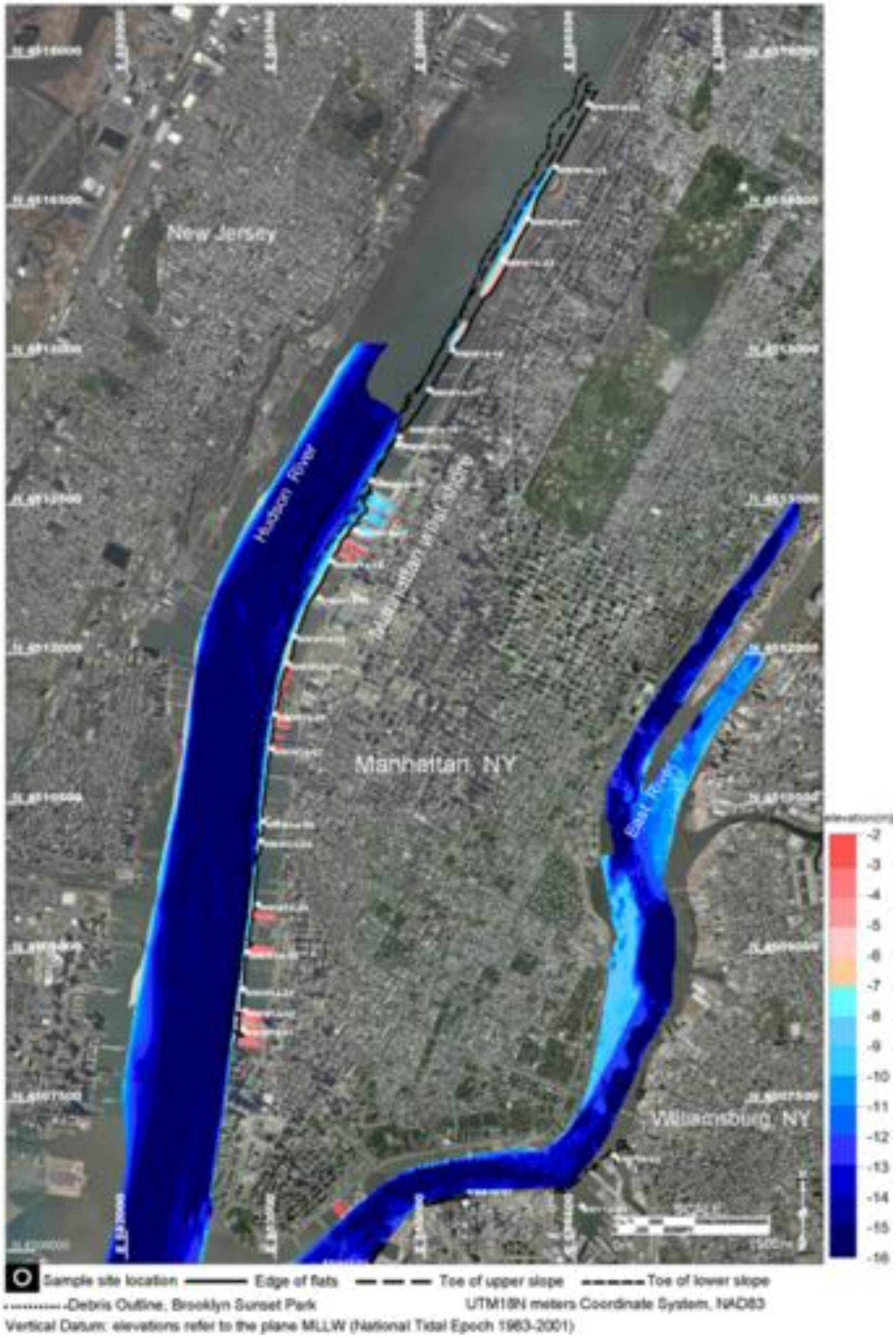

Figure 24. 2014 composite bathymetry in Manhattan West shoreline. Data from NOAA and USACE were combined in a 1m x 1m grid using a triangular linear interpolation. NOAA bathymetry includes surveys F00573 (2009) and F00598 (2012). USACE bathymetry includes surveys 4069D (2013) and 4126 (2014).

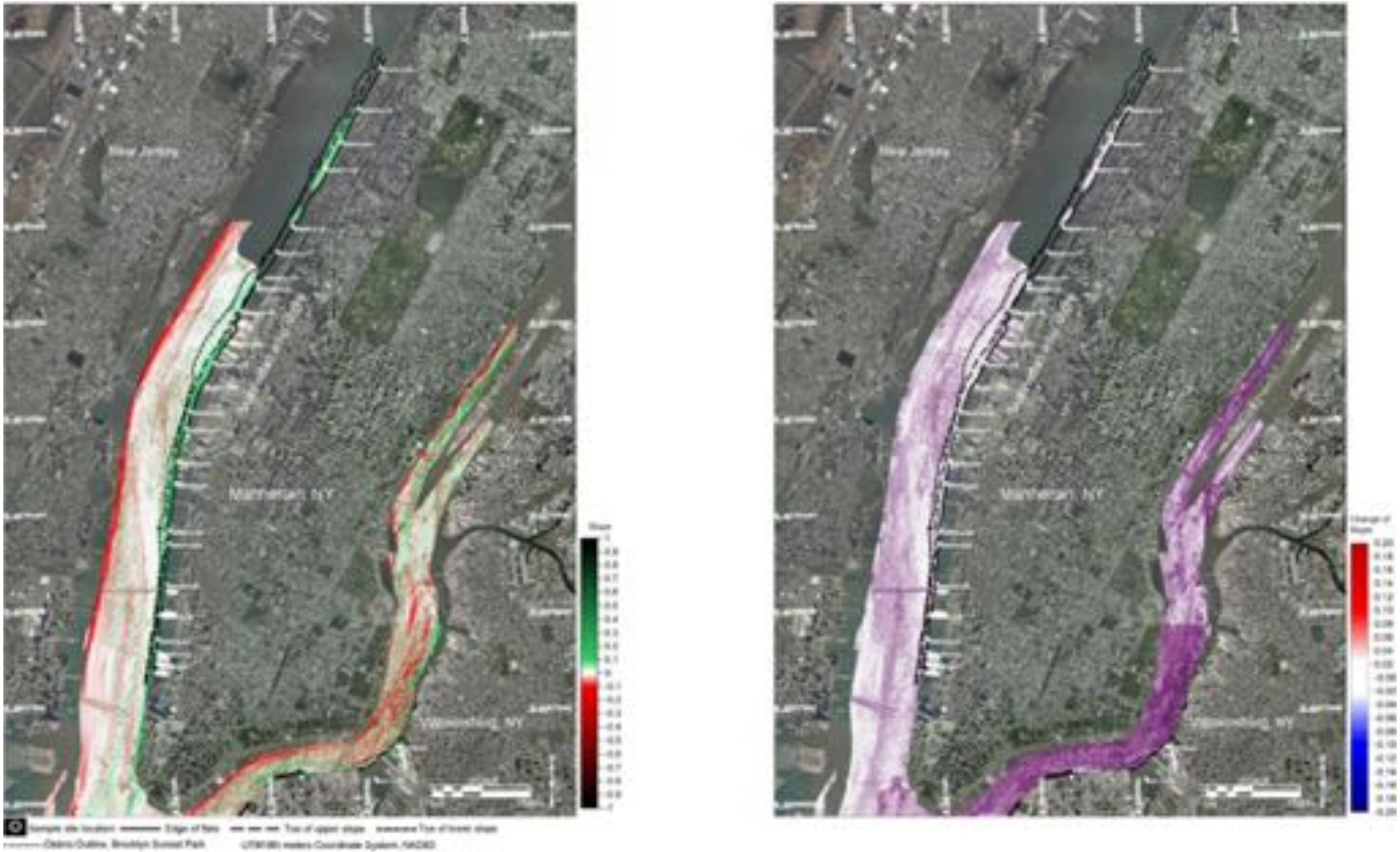

Figure 25. Derivative maps for 2014 composite bathymetry in Manhattan West shoreline. Data from NOAA and USACE were combined in a 1m x 1m grid using a triangular linear interpolation. NOAA bathymetry includes surveys F00573 (2009) and F00598 (2012). USACE bathymetry includes surveys 4069D (2013) and 4126 (2014). (Left) 2D first order derivative filter – slope. (Right) 2D second order derivative filter – change in slope.

Figure 26. Difference map of bathymetry elevation 2015 minus 2014 bathymetry of West Manhattan. The 2015 bathymetry includes combined single and multibeam bathymetries from e4sciences. The 2014 bathymetry includes NOAA surveys F00573 (2009) and F00598 (2012) and USACE surveys 4069D (2013) and 4126 (2014). The map displays both results of the difference in bathymetry for the 5m x 5m grid in the ultrashallow area, and the 1m x 1m grid in the deeper area. All grids were obtained with triangular linear interpolations.

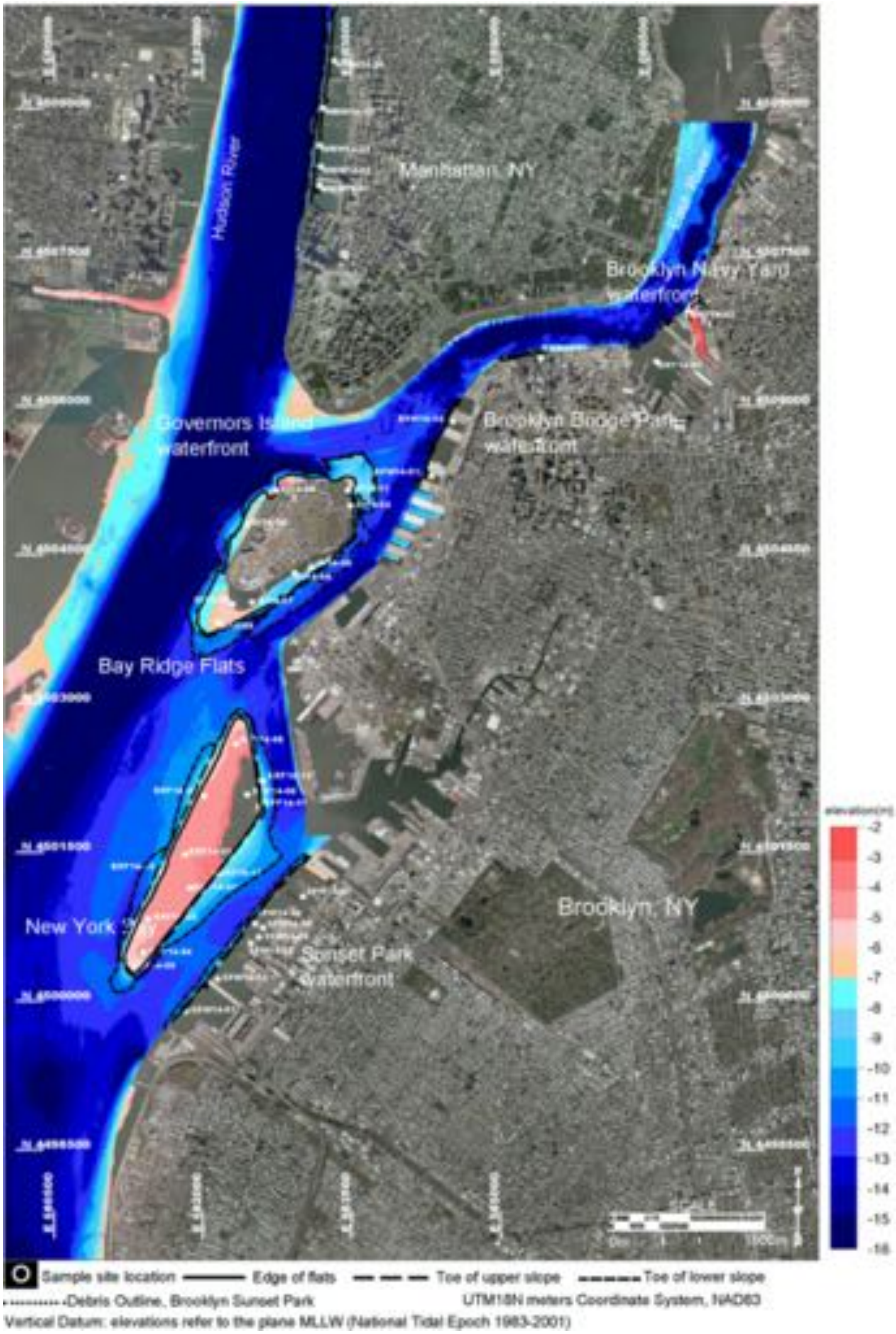

Figure 27. 2006 composite bathymetry in Brooklyn northwest including Governors Island. Data from NOAA and USACE were combined in a 1m x 1m grid using a triangular linear interpolation. NOAA bathymetry includes surveys H10938 (1999), H11353 (2004), H11395 (2006) and H11600 (2006). USACE bathymetry includes survey 2676 (2004).

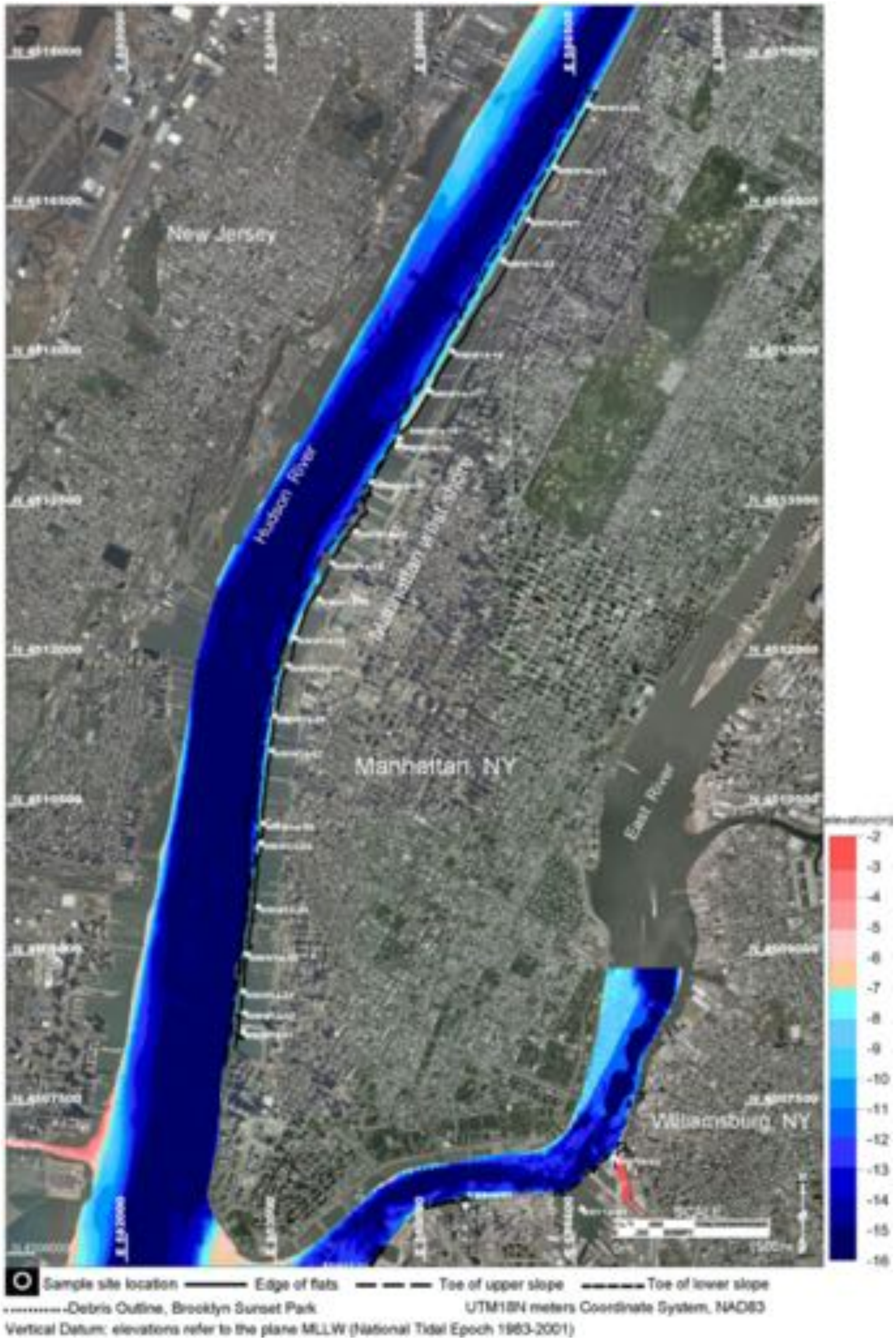

Figure 28. 2006 composite bathymetry in west Manhattan shoreline. Data from NOAA and USACE were combined in a 1m x 1m grid using a triangular linear interpolation. NOAA bathymetry includes surveys H10938 (1999), H10937 (1999), H11353 (2004) and H11395 (2006). USACE bathymetry includes survey 2676 (2004).

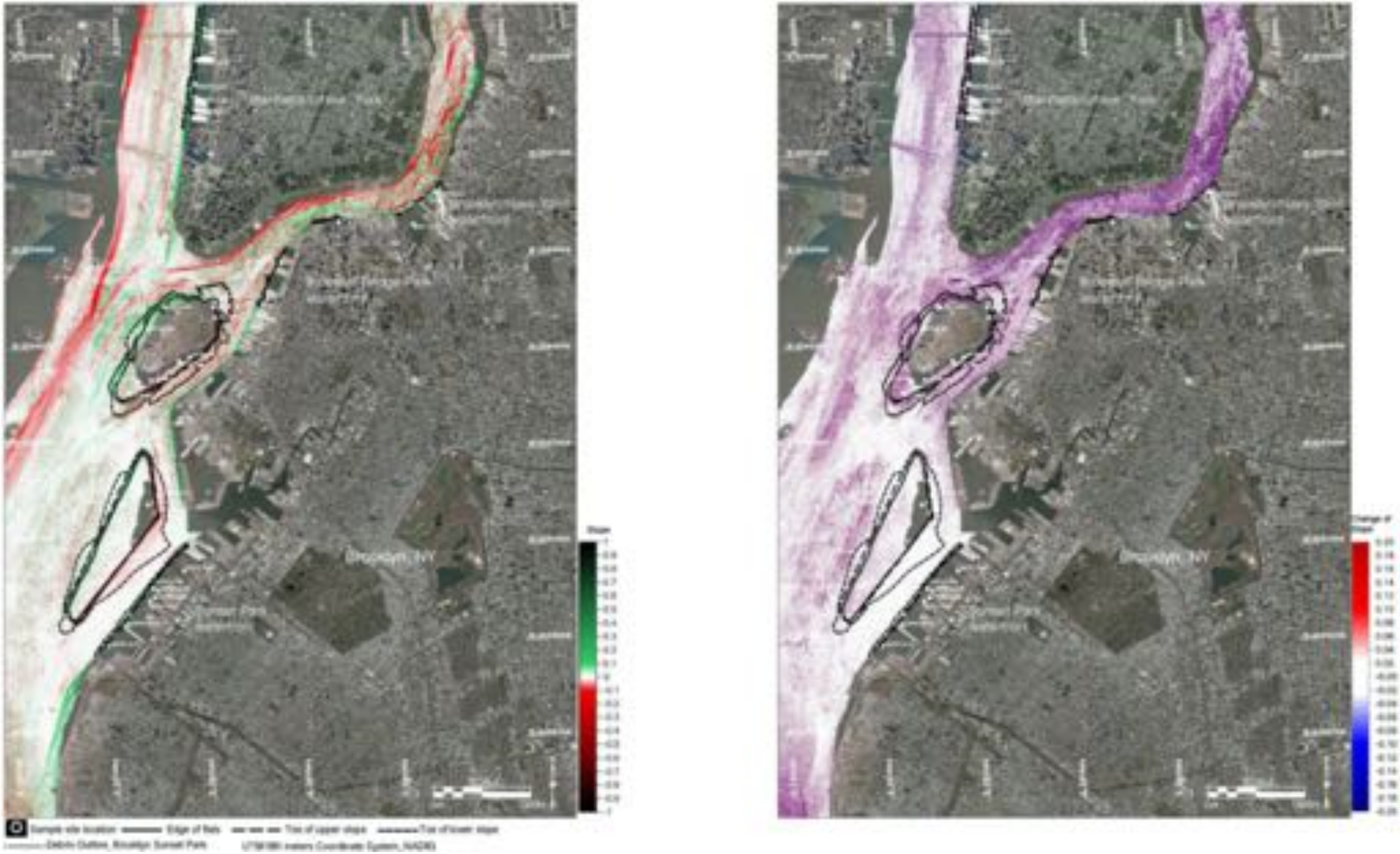

Figure 29. Derivative maps for 2006 composite bathymetry for Brooklyn northwest including Governors Island. Data from NOAA and USACE were combined in a 1m x 1m grid using a triangular linear interpolation. NOAA bathymetry includes surveys H10938 (1999), H11353 (2004), H11395 (2006) and H11600 (2006). USACE bathymetry includes survey 2676 (2004). (Left) 2D first order derivative filter – slope. (Right) 2D second order derivative filter – change in slope.

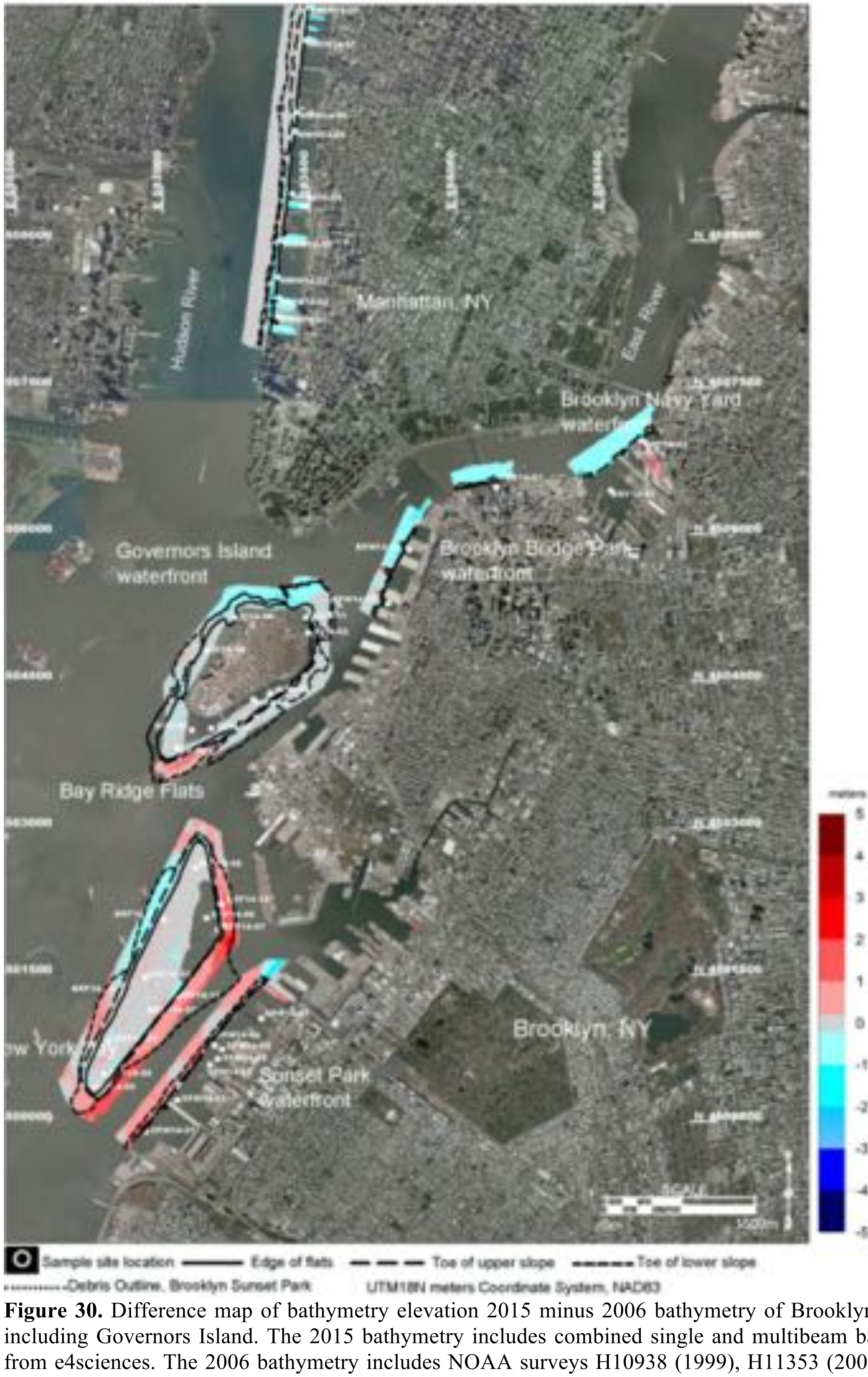

Figure 30. Difference map of bathymetry elevation 2015 minus 2006 bathymetry of Brooklyn northwest including Governors Island. The 2015 bathymetry includes combined single and multibeam bathymetries from e4sciences. The 2006 bathymetry includes NOAA surveys H10938 (1999), H11353 (2004), H11395 (2006) and H11600 (2006), and USACE survey 2676 (2004). The map displays both results of the difference in bathymetry for the 5m x 5m grid in the ultrashallow area, and the 1m x 1m grid in the deeper area. All grids were obtained with triangular linear interpolations.

4.2 Sediments

4.2.1 Orthosonographs

e4 produced side-scan orthosonographs™ for Brooklyn and Manhattan areas of investigation. Orthosonographs are twin images: one insonified from the east and south, and a second insonified from the west and north. The color represents the acoustic reflectivity of the bottom. Two factors contribute to reflectivity: the fractional difference in the acoustic impedance at the water-sediment interface, and the angle of incidence of the sonar and the bottom slope. The bright white colors are clean sand, Pleistocene clay, or rock. The steeper is the angle of incidence, then the brighter the color. The darker colors represent silts and organic-rich fine-grained sediments.

Figures 31 and 32 plot the orthosonographs insonified from the east and from the west for Brooklyn waterfront including Governors Island. The dark brown to black areas define the extent of the black silt.

Figures 33 and 34 plot the orthosonographs insonified from the east and from the west for the Manhattan waterfront. The dark brown to black areas define the extent of the black silt.

4.2.2 Core descriptions

e4 obtained 55 sediment cores of 15 to 60cm in length. The limited length of core was due solely to refusal at the hard sand layer, gravel, or rock. Figure 35 shows the location map of the core boring locations in Brooklyn. Figure 36 shows the location map of the core boring locations in Manhattan.

Figure 37 is an example of a core photograph showing the archival half of the core along with the core description for the working half of the core.

The sediment cores benchmark both the interpretation of the side-scan orthosonographs and the sub-bottom reflection seismology.

4.2.3 Isopach map of acoustic silt

Figure 38 plots the isopach map for the thickness of acoustic silt in Brooklyn including Governors Island.

Figure 39 plots the isopach map for the thickness of acoustic silt in Manhattan.

4.2.4 Grab samples

e4 obtained 55 grab samples. Figures 40, 41, and 42 show various examples of the grab samples. Figure 40 shows a sandy sample from Bay Ridge Flats. Figure 41 shows a mixed sample from Bay Ridge Flats. Figure 42 shows black silt sample from Bay Ridge Flats.

4.2.5 Sediment grain size and chemistry

e4 measured the grain size at each site. Appendix II contains the grain size curves.

e4 tested the sediment samples for Fe, S, Hg, Zn, Pb, As, Mn, ^{7}Be, and ^{137}Cs. Appendix II lists the chemical abundances.

4.2.6 Geological map and cross sections

Figure 43 displays a geological map of the area of investigation. Figure 44 plots regional bedrock cross-sections normal to the Brooklyn and Manhattan shorelines.

Figure 31. Side-scan orthosonograph of Brooklyn northwest including Governors Island insonified from the east.

Figure 32. Side-scan orthosonograph of Brooklyn northwest including Governors Island insonified from the west.

Figure 33. Side-scan orthosonograph of Manhattan insonified from the east.

Figure 34. Side-scan orthosonograph of Manhattan insonified from the west.

Figure 35. Core location map for Brooklyn northwest including Governors Island.

Figure 36. Core location map for West Manhattan.

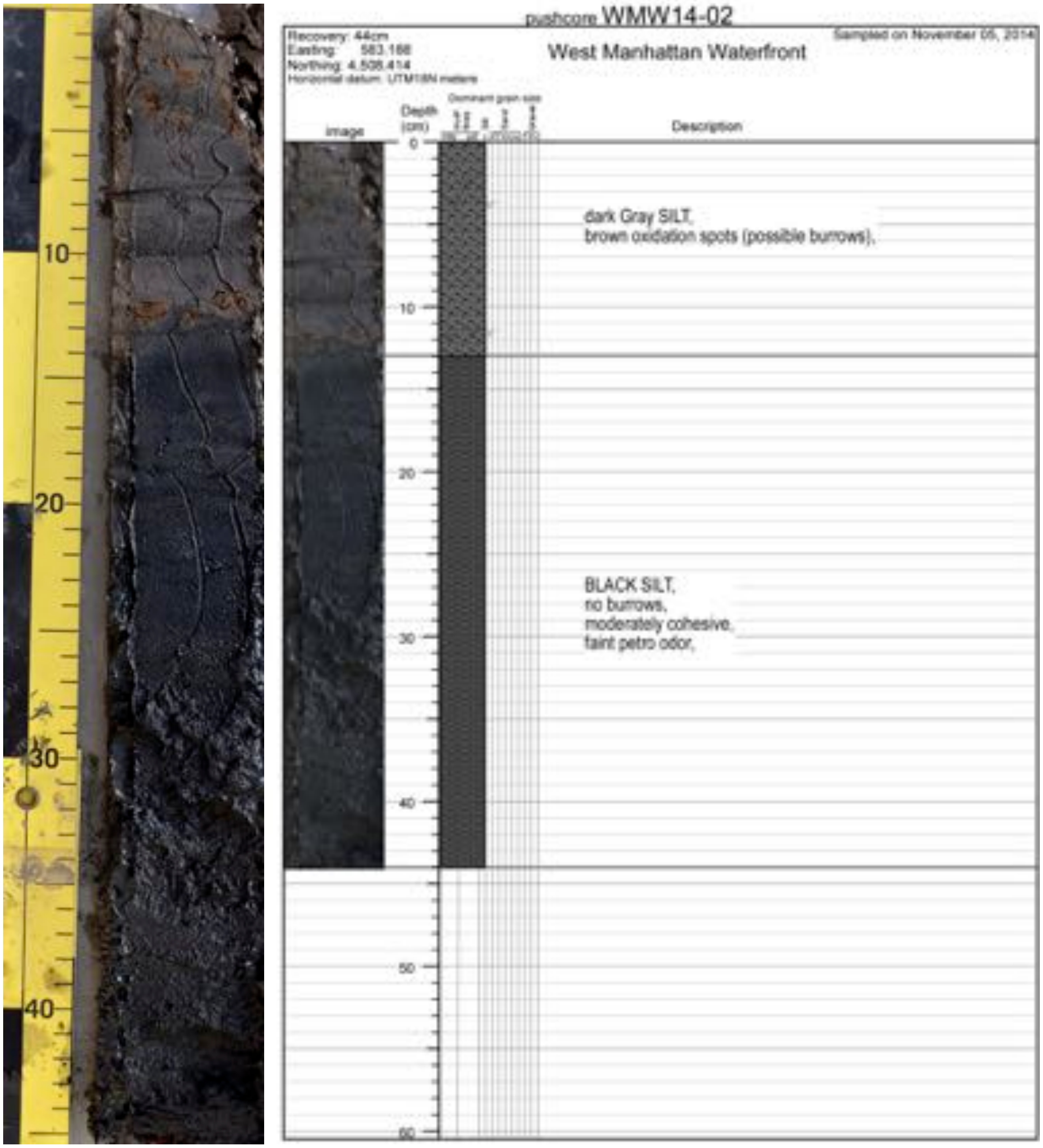

Figure 37. Push core WMW14-02: (Left) Photograph of the archival split, (Right) the core description.

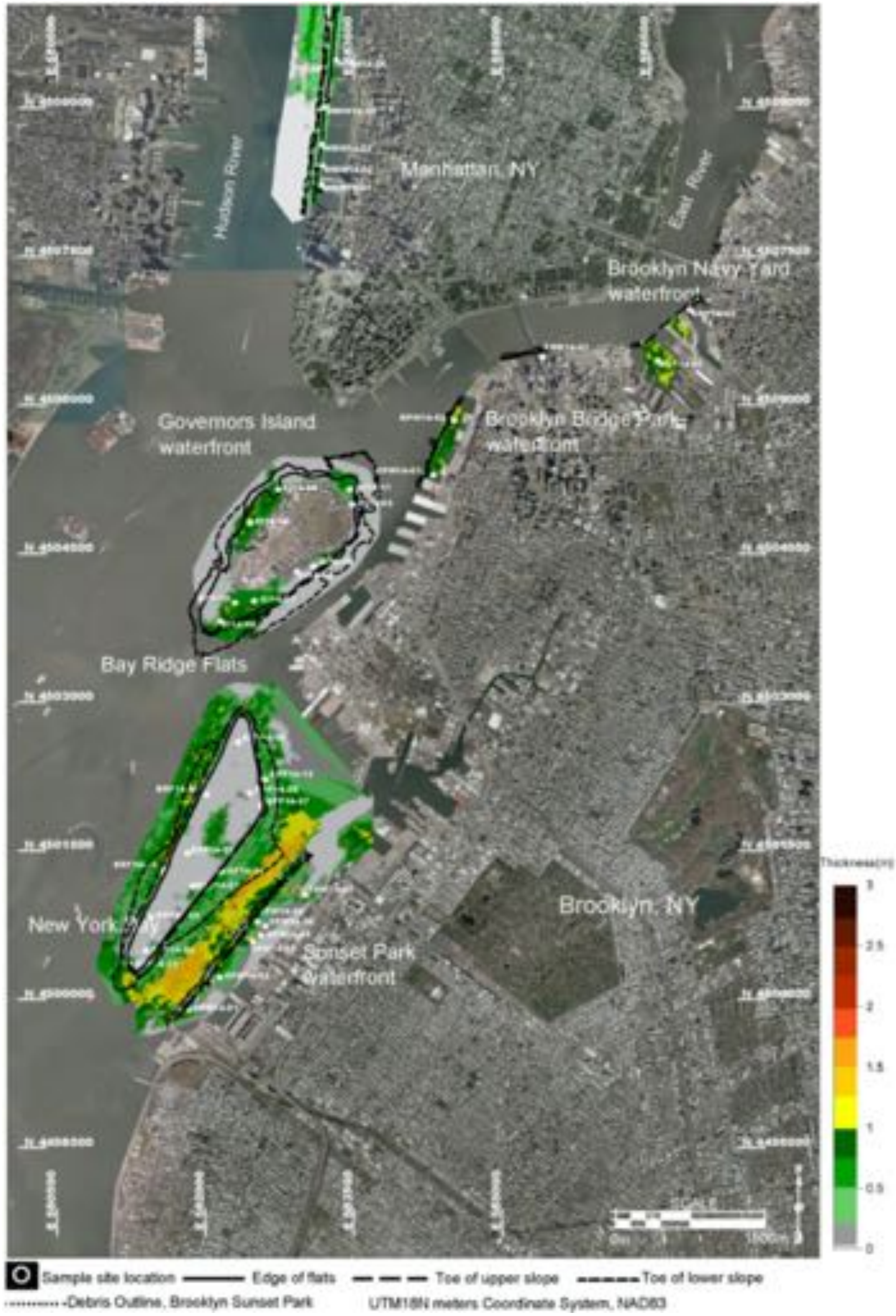

Figure 38. Isopach map of thickness of acoustic silt in northwest Brooklyn including Governors Island.

Figure 39. Isopach map of thickness of acoustic silt in Manhattan.


Figure 40. Bay Ridge Flats grab sample, BRF14-03.


Figure 41. Bay Ridge Flats grab sample, BRF14-08.

Figure 42. Bay Ridge Flats grab sample, BRF14-07.

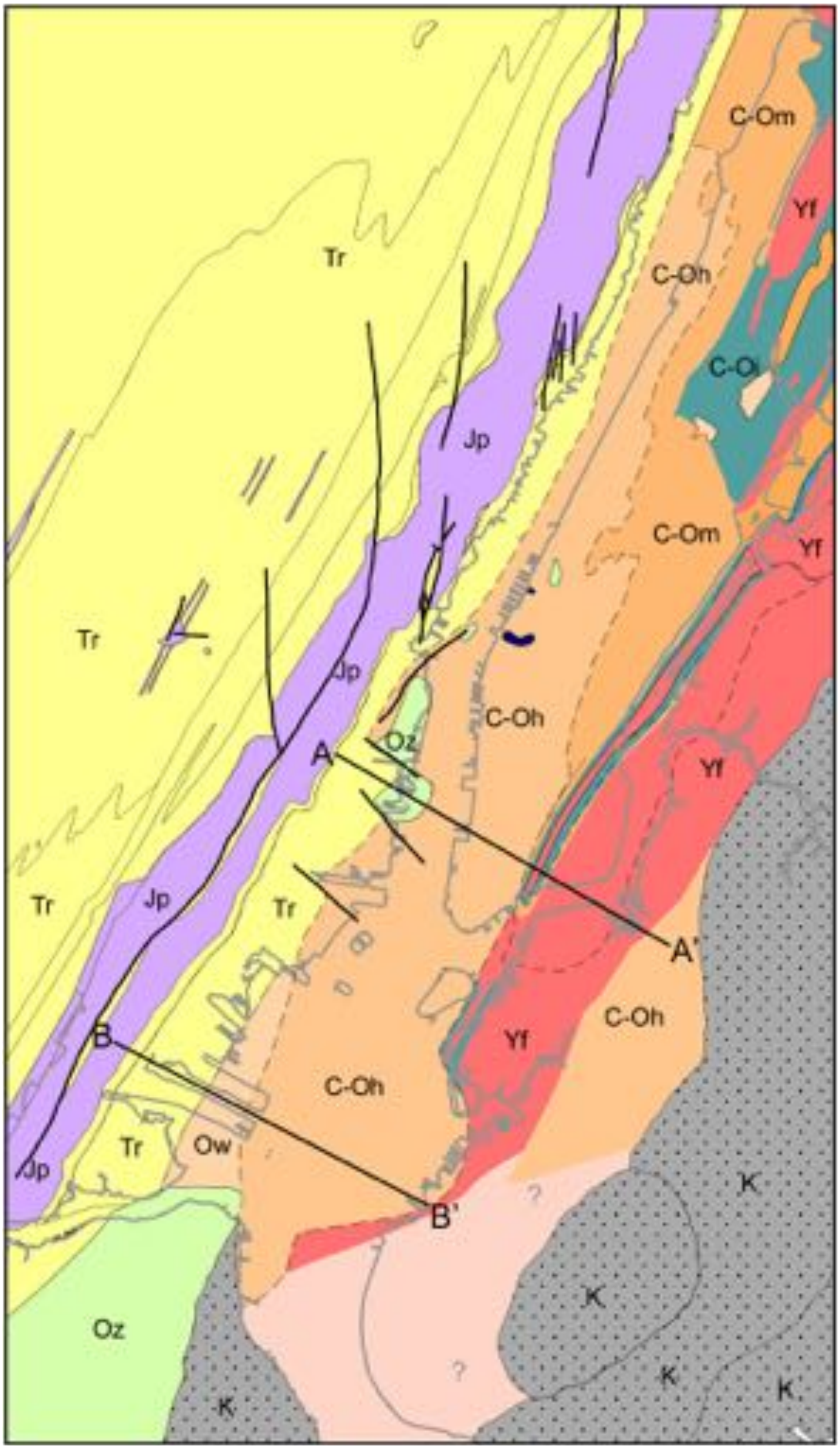

Figure 43. Geological map of the area of investigation. The key and the cross sections, A-A' and B-B', are displayed in Figure 44. After Baskerville 1992 and 1994; Drake et al., 1996; Merguerian and Baskerville, 1987; and Merguerian and Merguerian, 2004.

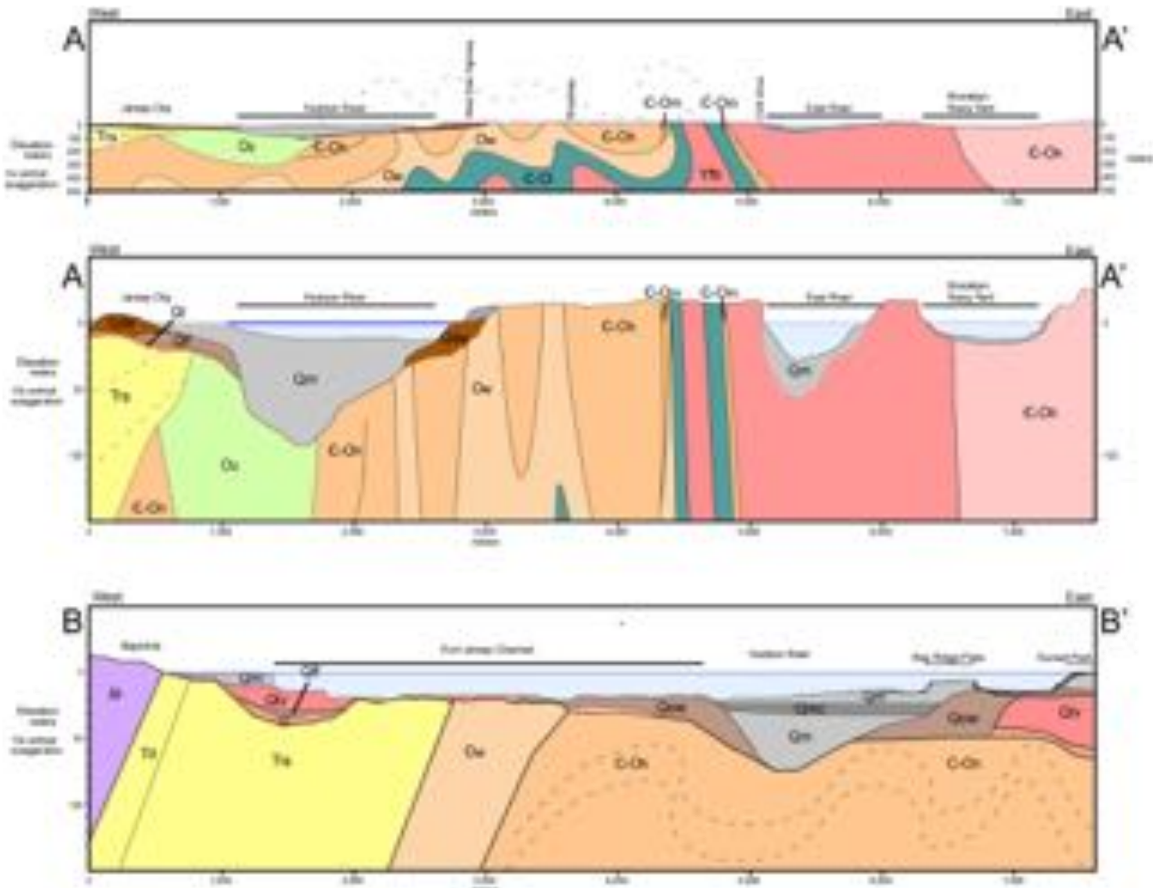

Geological Age		Rock or sediment type	Formation
Cretaceous	K	sediments over deep bedrock	Coastal Plain Group
Jurassic	Jp	diabase	Palisades Sill
Triassic-Jurassic	Tr	sandstones and shales	Newark Basin Group
Ordovician	Oz	serpentinite	Serpentinite
Cambrian-Ordovician	Ow	schist	Walloomsac Formation
	C-Om		Hartland Formation
	C-Oh		Manhattan Schist
	C-Oi	marble	Inwood Marble
PreCambrian	Yf	gneiss	Fordham Gneiss
	?	undifferentiated metamorphics	

Figure 44. Geological cross sections normal to the Brooklyn and Manhattan shorelines. The key at the bottom also applies to the map in Figure 43. Cross section after Lovegreen 1974; Baskerville 1992 and 1994; Drake et al., 1996;Moss, 2010; and e4 data.

4.3 Fauna

4.3.1 SPI interpretation

The Chemistry Sediment Profile Imager (CHEM-SPI) provides a photograph of at least the first 10cm below the sediment-water interface and vertical logs of oxygen, iron, and sulfide. Appendix II contains the results of the SPI analysis including photographs, chemistry, and interpretation. Figure 45 shows the real positions for the CHEM-SPI drops in Brooklyn. Figure 46 shows the real positions for the CHEM-SPI drops in West Manhattan.

The Organism-Sediment Index, OSI, is an indicator of benthic health based on the results of the SPI camera. The OSI ranges from negative ten (-10) to positive eleven (11). Positive eleven is a healthy, thriving habitat, and negative ten is the lowest quality habitat, devoid of healthy life. Figure 47 presents a schematic representation of the succession stages.

Figures 48 through 52 show examples of the SPI images at Governors Island with pH and O_2. These images show the details of bioturbation and chemical mixing to an extent never measured before. The O_2 scale is a relative saturation scale. In water, oxygen saturation is the percentage of dissolved oxygen (O_2) in the water relative to the maximum amount of oxygen that will dissolve in the water at that salinity, temperature and pressure under stable equilibrium. Well-aerated water without oxygen producers or consumers is 100 % saturated.

Of the 151 images collected for sediment profile analysis, 106 were analyzable, and none of these analyzed images had negative OSI values. Negative values indicate the lowest quality habitat. Most images showed that the sediment was oxidized with both Stage I and III communities.

Bay Ridge Flats (BRF) was characterized by having the majority of sites with an OSI value of 11.

Of the 27 analyzable images from BRF, only three had values below the “stressed” site OSI threshold of 6. For estuarine and coastal bay benthic habitats in the northeastern United States, OSI values greater than 6 indicate good habitat conditions and are generally associated with bottoms that are not heavily influenced by environmental stressors, either physical or chemical, natural or anthropogenic (e.g. Diaz et al. 2004).

Of the Governors Island (GI) sites, 9 of the 18 analyzable images had values below the OSI 6 threshold. These drops took place in sediment traps with high sediment accumulation rates. Otherwise, the benthic communities around GI are healthy and stable.

Sunset Park waterfront (SPW) had only one site of five with OSI below the threshold of 6. SPW is a great example of the healthy communities that can be observed even in silty regions when the benthic organisms that colonize such environments are left undisturbed.

e4 was only able to acquire SPI images at two of three intended sites in Brooklyn Bridge Park (BBP) area. Both of the sites at which SPI was able to be acquired had OSI calculated values greater than 6.

Of the six images acquired in Brooklyn Navy Yard (BNY), three had values below the OSI threshold of 6, and three images had values greater than 6. The three with values less than six were taken in an area with high sediment accumulation rates and frequent dredging. We hypothesize that the large difference between the two BNY sites is due to frequent disturbance at the stressed site.

All images of the twenty-one analyzable images acquired in the south of West Manhattan waterfront (WMW) had OSI values greater than 6, with 9 of the 11 sites having an OSI value of 11. This is a major improvement since 2007.

WMW middle had 2 of 14 sites with an OSI value lower than 6, and WMW North had 4 of the 11 analyzable images with values lower than OSI 6. The lower values are in the berths for ships and boats. These results show healthy benthic habitat extending northward of previous observations along the WMW shoreline. We hypothesize that the low OSI values for the northernmost sites in WMW may be due to physical disturbance from the narrowing of the benthic shelf and increased human use of the shallows north of the Hudson River Estuarine Sanctuary.

Major modal grain size had a phi class that was predominantly greater than 4 throughout the eight surveyed areas.

Successional Stage analysis showed that most sites had both opportunistic species (Stage I) and higher successional stage species (Stage III). No methane or anoxia was observed at any of the analyzed sites. Surface roughness tended to result from biological activity.

Numerous images from the eight areas studied showed organism burrows, feeding voids, and both epifauna and infauna. These patterns were analyzed holistically for the entire New York Harbor/Upper West Side Manhattan ecosystem. The more open water areas such as Bay Ridge Flats and Governors Island that receive a greater tidal flushing from Raritan Bay and offshore waters tended to have overall higher OSI values and larger particle size sediment texture (sand).

The sites within berthing slips of West Manhattan waterfront North region and Brooklyn Navy Yard were composed largely of accumulated black silt and receive more limited flushing due to the overall engineering of these structures. Healthy sites were also observed in areas dominated by black silt and other fine-grained sediment, but these sites were more variable and, we hypothesize, may be more susceptible to physical disturbance and any change in sedimentation rate. Areas within berthing slips have often been previously dredged, and may therefore act as sediment traps. Sediments that have low oxygen and are organically enriched typically show lower OSI and sediment quality than sandier, oxidized sediments that have higher biodiversity and organism-sediment activity. However, the most important factor related to benthic community health (high OSI) appears to be physical disturbance of the sediment substrate. That is, the more physical disturbance that occurs in a given area, the lower the OSI values associated with benthic communities in that area. This finding appears to be partially independent of the substrate itself, implying that physical disturbance of the sediment may more strongly influence benthic habitat quality, as measured by OSI, than sediment type.

Figure 45. Location map of CHEM-SPI positions in Brooklyn northwest including Governors Island.

Figure 46. Location map of CHEM-SPI positions in West Manhattan.

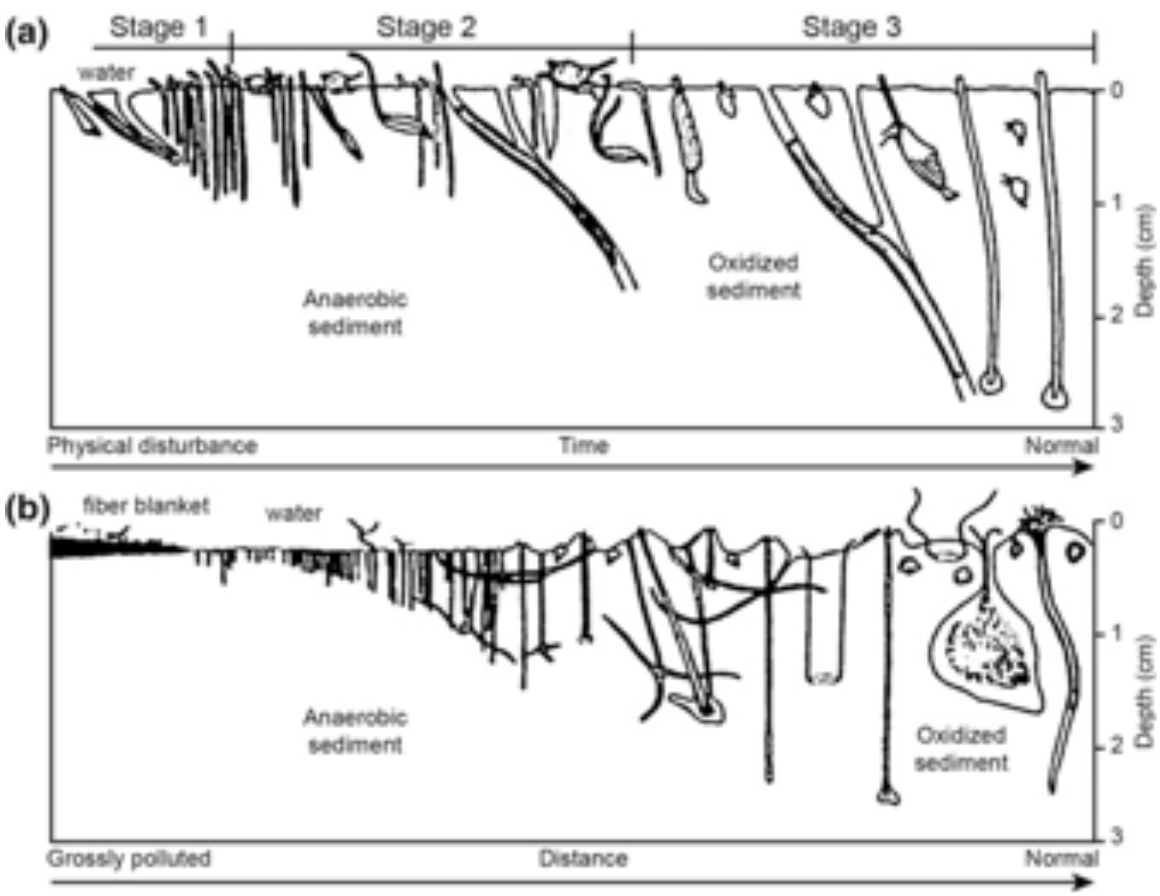

Figure 47. Schematic representation of benthic succession stages. Animal-sediment response to organic enrichment [taken from Rhoads and Germano (1982) and based on models presented in Rhoads et al. (1978) and Pearson and Rosenberg (1978)]. Most marine communities are mixtures of these, although the greater the organic enrichment the more likely the movement toward Stage I communities. It should be noted that once a system moves toward the left part of the diagram, more carbon is stored in the sediments creating an environment that further favors Stage I type communities. Benthic ecosystems in much of the present day Hudson River are dominated by Stage I and Stage II communities (Taken from Cuomo, Cochran & Turekian, 2014 "Chapter 4: Geochemistry of Long Island Sound" in *Long Island Sound: Prospects for the Urban Sea*, Latimer, et al., editors, Springer-Verlag Publishers.)

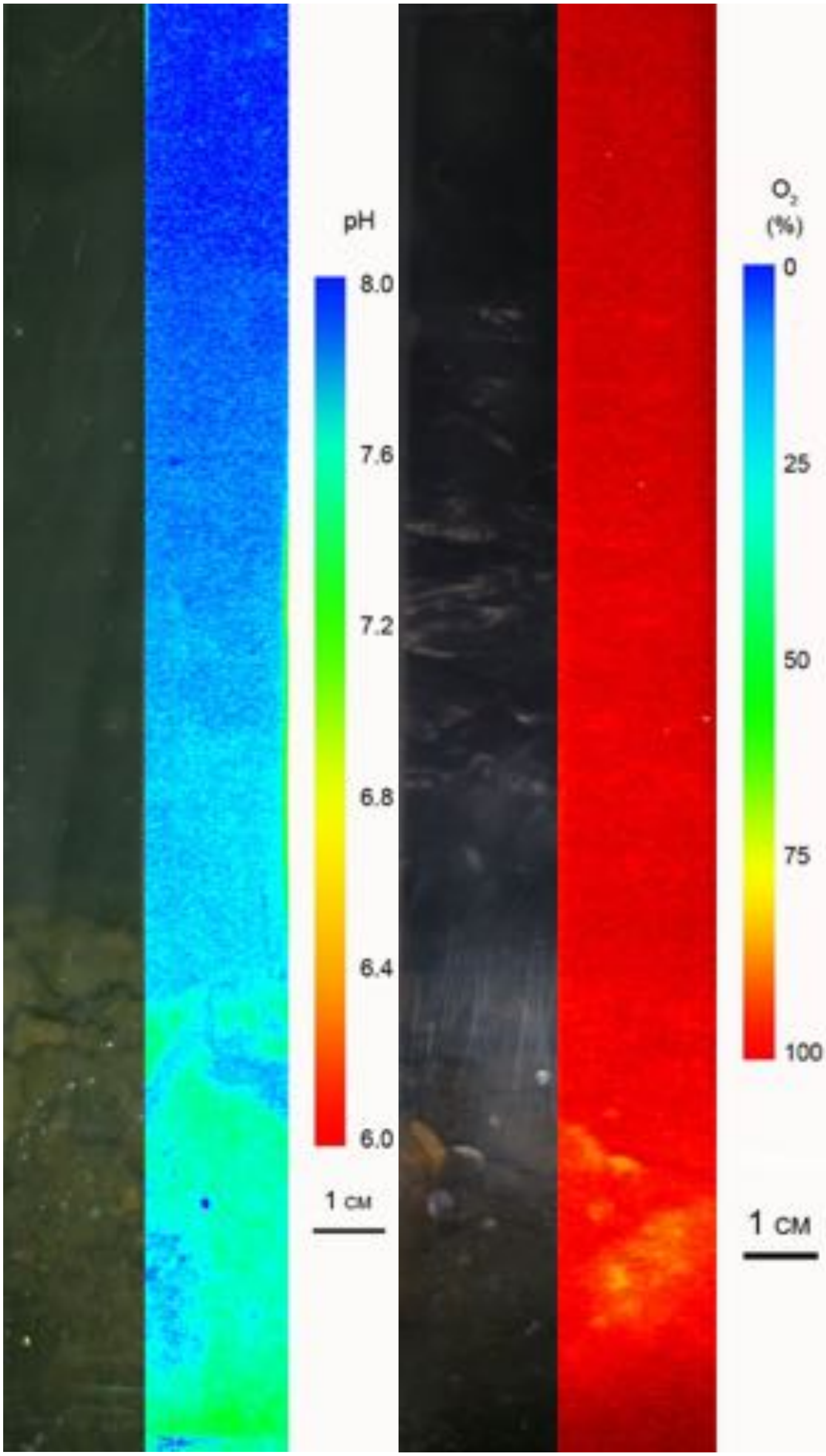

Figure 48. CHEM-SPI images at GI14-02. (Left) pH. (Right) O_2. The O_2 scale is a relative saturation scale. In water, oxygen saturation is the percentage of dissolved oxygen (O_2) in the water relative to the maximum amount of oxygen that will dissolve in the water at that salinity, temperature and pressure under stable equilibrium. Well-aerated water without oxygen producers or consumers is 100 % saturated.

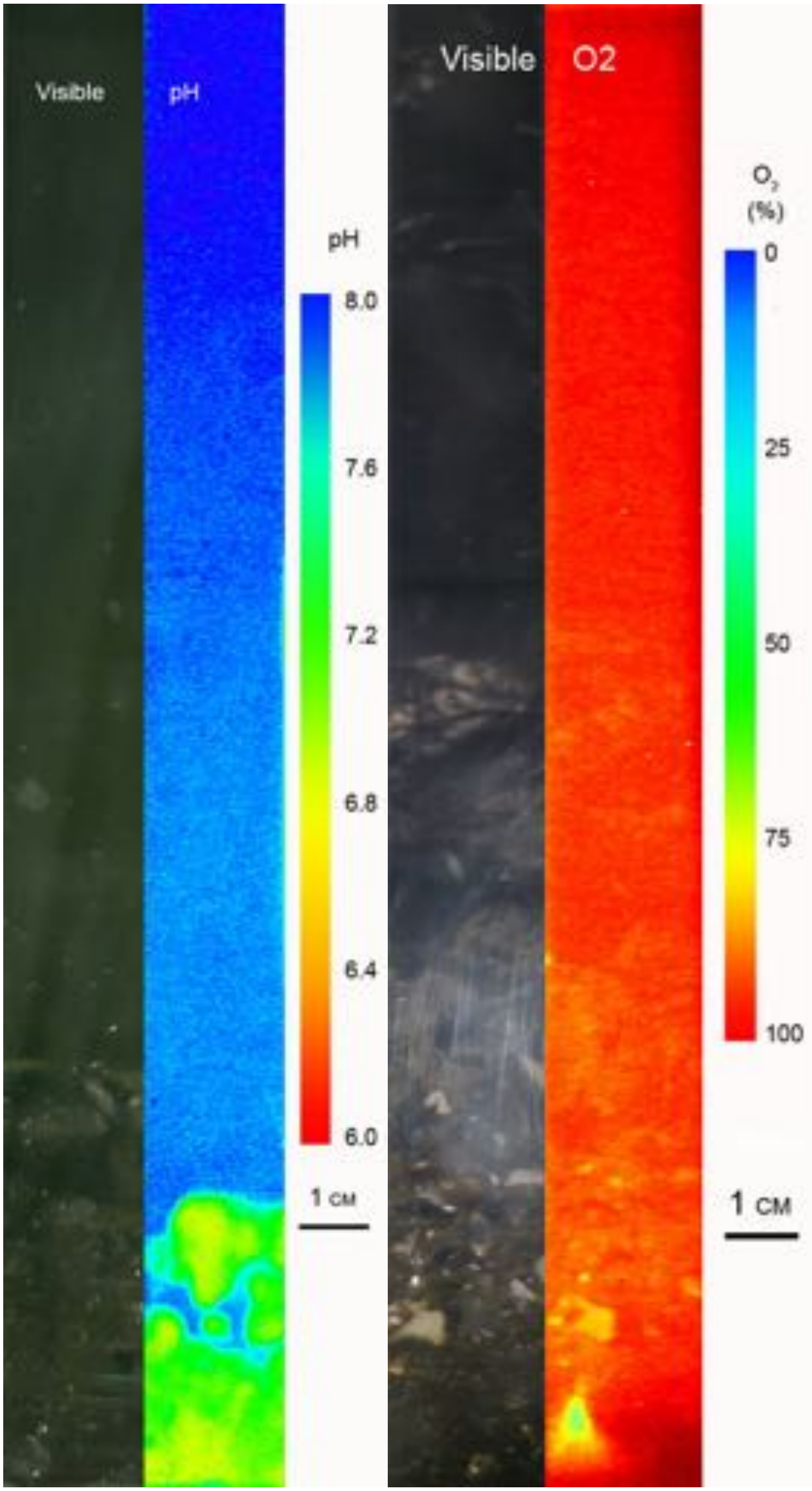

Figure 49. CHEM-SPI images at GI14-05. (Left) pH. (Right) O_2. The O_2 scale is a relative saturation scale. In water, oxygen saturation is the percentage of dissolved oxygen (O_2) in the water relative to the maximum amount of oxygen that will dissolve in the water at that salinity, temperature and pressure under stable equilibrium. Well-aerated water without oxygen producers or consumers is 100 % saturated.

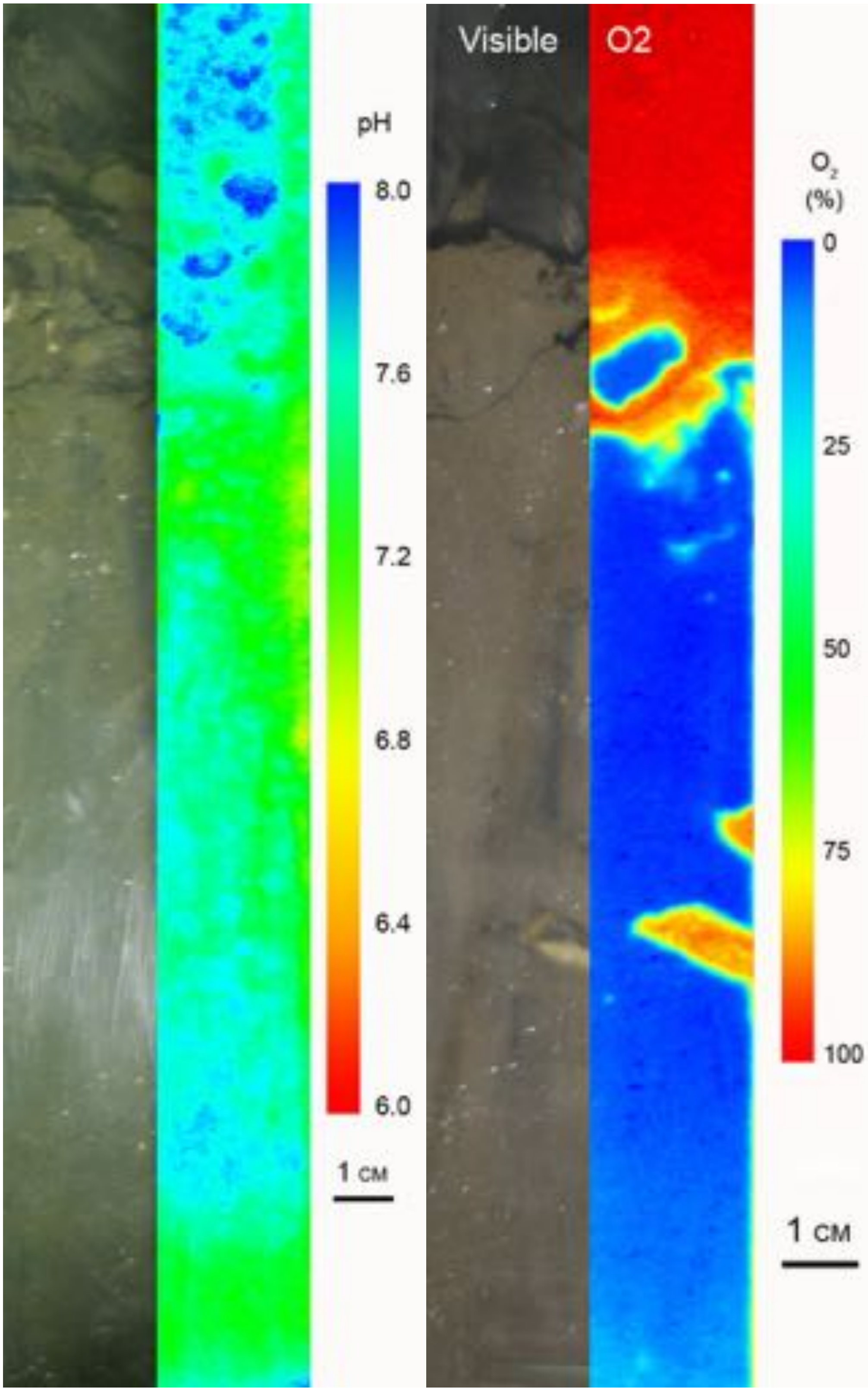

Figure 50. CHEM-SPI images at GI14-06. (Left) pH. (Right) O_2. The O_2 scale is a relative saturation scale. In water, oxygen saturation is the percentage of dissolved oxygen (O_2) in the water relative to the maximum amount of oxygen that will dissolve in the water at that salinity, temperature and pressure under stable equilibrium. Well-aerated water without oxygen producers or consumers is 100 % saturated.

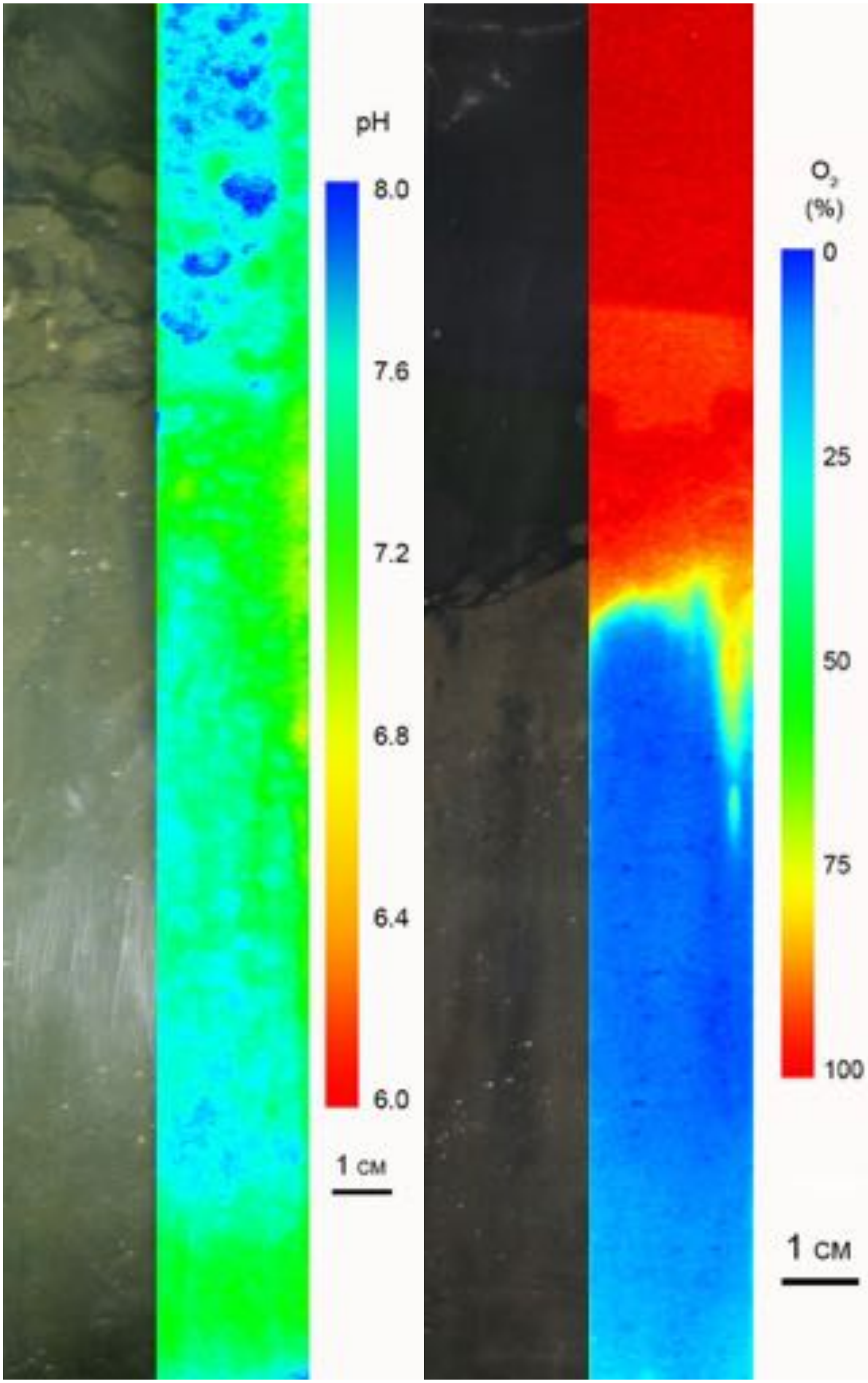

Figure 51. CHEM-SPI images at GI14-07. (Left) pH. (Right) O_2. The O_2 scale is a relative saturation scale. In water, oxygen saturation is the percentage of dissolved oxygen (O_2) in the water relative to the maximum amount of oxygen that will dissolve in the water at that salinity, temperature and pressure under stable equilibrium. Well-aerated water without oxygen producers or consumers is 100 % saturated.

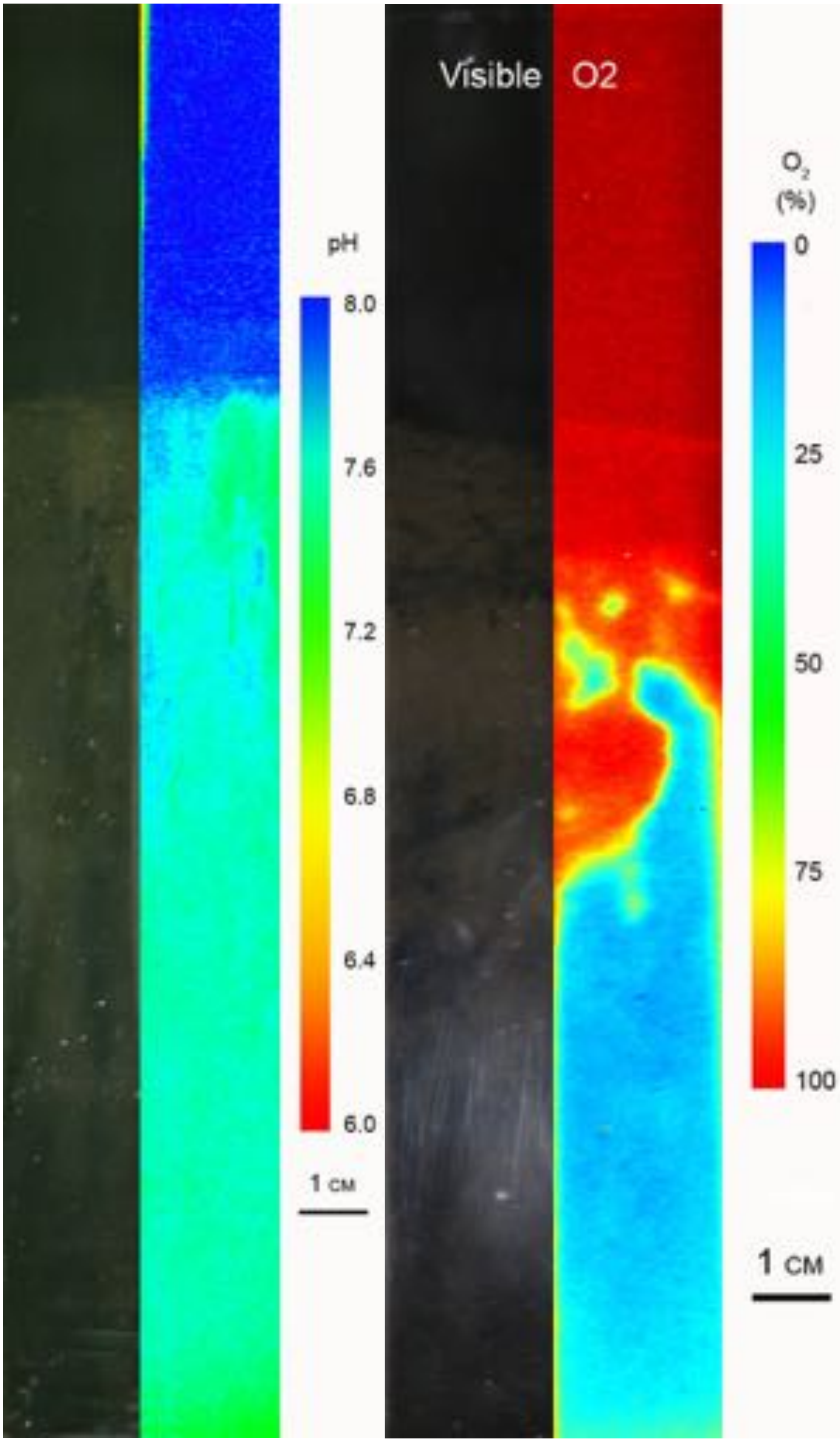

Figure 52. CHEM-SPI images at GI14-09. (Left) pH. (Right) O_2. The O_2 scale is a relative saturation scale. In water, oxygen saturation is the percentage of dissolved oxygen (O_2) in the water relative to the maximum amount of oxygen that will dissolve in the water at that salinity, temperature and pressure under stable equilibrium. Well-aerated water without oxygen producers or consumers is 100 % saturated.

4.3.2 Biological samples and analyses

Taxonomic identifications from infaunal organisms were performed to the lowest practical taxonomic level. These data were entered into PRIMER + Version 6.0 and analyzed for both univariate and multivariate benthic community metrics. Table 7 lists the univariate metrics such as species richness, abundance, Pielou's Evenness, Log Series Fisher's alpha, and Shannon-Weiner diversity. Table 7 lists the results from Brooklyn and Governors Island waterfronts.

Table 7. Benthic infaunal abundance and diversity community metrics in the Brooklyn and Governors Island waterfronts.

Site	Species Richness	Abundance ($0.05m^2$)	Abundance ($1m^2$)	Pielou's Evenness	Log Series Fisher's alpha	Shannon-Weiner Diversity (loge)
BMB-14-01 (BBP)	18	175	3500	0.694	5.032	2.007
BNY-14-01	12	73	1460	0.647	4.085	1.609
BNY-14-02	13	346	6920	0.321	2.668	0.822
BPW-14-01	8	28	560	0.736	3.742	1.530
BPW-14-02	11	74	1480	0.638	3.574	1.529
BRF-14-01	10	199	3980	0.481	2.218	1.107
BRF-14-02	13	395	7900	0.495	2.581	1.269
BRF-14-03-02	16	252	5040	0.461	3.801	1.278
BRF-14-04	9	462	9240	0.567	1.585	1.246
BRF-14-05	8	139	2780	0.418	1.845	0.869
BRF-14-06	10	174	3480	0.682	2.306	1.571
BRF-14-07	4	5	100	0.961	9.284	1.332
BRF-14-08	16	268	5360	0.438	3.731	1.215
BRF-14-09	18	304	6080	0.588	4.187	1.698
BRF-14-10	12	103	2060	0.620	3.519	1.542
BRF-14-11	15	393	7860	0.521	3.091	1.410
BRF-14-12	12	106	2120	0.711	3.479	1.767
GI-14-01	15	171	3420	0.622	3.959	1.685
GI-14-02 (02)	15	361	7220	0.313	3.160	0.848
GI-14-03	10	73	1460	0.550	3.135	1.266
GI-14-04	12	507	10140	0.503	2.205	1.251
GI-14-05	11	173	3460	0.461	2.615	1.106
GI-14-06	17	374	7480	0.398	3.668	1.127
GI-14-07	9	32	640	0.773	4.163	1.699
GI-14-08	17	172	3440	0.529	4.683	1.500
GI-14-09	18	504	10080	0.484	3.647	1.398
SPW-14-01	8	12	240	0.952	10.489	1.979
SPW-14-02	9	33	660	0.787	4.077	1.730
SPW-14-03	14	67	1340	0.811	5.390	2.140
SPW-14-04	10	64	1280	0.758	3.324	1.746
SPW-14-05	7	58	1160	0.521	2.082	1.014
SPW-14-06	14	38	760	0.823	8.007	2.172
SPW-14-07	6	18	360	0.754	3.152	1.351

Overall, univariate benthic community metrics were similar among locations. Governors Island, Bay Ridge Flats and a few of the WMW locations that had higher percentages of sandy sediment had higher abundances of individuals, some with more than 10,000 per m^2. Areas that had fine sediments with predominantly black silt had lower species richness and abundances. Evenness ranged from a low of 0.398 to a high of 1.0. Stations with high evenness scores tended to have few species with low abundances, such as WMW 14-07, which was a site composed of >95% black silt although sediments were not anoxic as seen in sediment profile images. Species diversity as measured with Shannon-Weiner and log series alpha was generally typical of anthropogenically influenced estuarine habitats. SPW had low abundances but relatively high proportional species richness and, therefore, had log series alpha and Shannon-Weiner diversity values higher than other regions samples. BRF had higher abundances and greater species richness but in proportion diversity metrics were lower than SPW. BRF diversity metrics were more similar to GI and WMW sites. Table 8 lists the results from the Manhattan waterfront.

Table 8. Benthic infaunal abundance and diversity community metrics on the Manhattan waterfront.

Site	Species Richness	Abundance (0.05m2)	Abundance (1m2)	Pielou's Evenness	Log Series Fisher's alpha	Shannon-Weiner Diversity (loge)
WMW-14-01	12	41	820	0.817	5.709	2.029
WMW-14-02	3	10	200	0.730	1.453	0.802
WMW-14-03	11	45	900	0.678	4.642	1.625
WMW-14-04	13	121	2420	0.655	3.694	1.681
WMW-14-05	10	87	1740	0.699	2.917	1.609
WMW-14-06	14	76	1520	0.503	5.041	1.328
WMW-14-07	3	6	120	1.000	2.388	1.099
WMW-14-08	5	38	760	0.533	1.541	0.858
WMW-14-09	10	110	2200	0.473	2.673	1.090
WMW-14-10	21	578	11560	0.438	4.273	1.334
WMW-14-11	11	164	3280	0.478	2.658	1.147
WMW-14-12	8	64	1280	0.458	2.413	0.952
WMW-14-13	7	44	880	0.687	2.346	1.336
WMW-14-14	13	369	7380	0.499	2.625	1.279
WMW-14-15	16	325	6500	0.515	3.529	1.428
WMW-14-16	10	50	1000	0.731	3.759	1.683
WMW-14-17	20	777	15540	0.504	3.746	1.509
WMW-14-18	10	118	2360	0.650	2.608	1.498
WMW-14-19	9	117	2340	0.534	2.272	1.174
WMW-14-20	9	140	2800	0.495	2.146	1.088
WMW-14-21	18	266	5320	0.515	4.362	1.488
WMW-14-22	13	588	11760	0.426	2.353	1.092

4.3.3 Bray-Curtis similarity analysis

A Bray-Curtis similarity analysis was performed using PRIMER + Version 6.0 and unweighted pair-group method using arithmetic averages. This type of similarity analysis is a statistic used to quantify the compositional similarity and dissimilarity between different locations, sites, and samples. Figure 53 shows results of a Bray-Curtis analysis performed to compare all sites from the eight different areas sampled as part of this study. By observing similarities among sites, habitats can be classified based on their sedimentary characteristics, abundances and species richness. Original data was transformed to the 4th root to downweight abundant species relative to rare species.

Based on the Bray-Curtis analysis there are two main groups (Group A and Group B) that have a mix of site locations within these clusters (Figures 53 and 54). The clusters represent differences in sediment characteristics that are directly related to abundances and species richness. Sandier sites such as those found at BRF and GI along with siltier WMW south sites formed Group A while siltier sites found in WMW north, BNY, and the siltier GI and BRF sites formed Group B. Sites such as BMB14-01, and WMW14-07, which had few individuals and species, formed outliers to the remaining dataset. Sites with a higher percentage of clay also tended to be part of Group A or formed small branched group outside of either Group A or Group B

4.3.4 Multidimensional scaling

Multidimensional scaling shows patterns of similarity based on the Bray-Curtis 4th root analysis in two dimensions. Multidimensional scaling attempts to preserve rank order of the similarities between samples and used the Kruscal Stress Formula with a minimum stress of 0.01. As shown in Figure 54, the majority of sites shared at least 25% similarity with the two large clusters (Group A and Group B) having at least 48% similarity. Few sites had 70% or greater similarity to each other and those sites that did have the greatest similarity also had similar grain size distribution (either sandy or silty sediments).

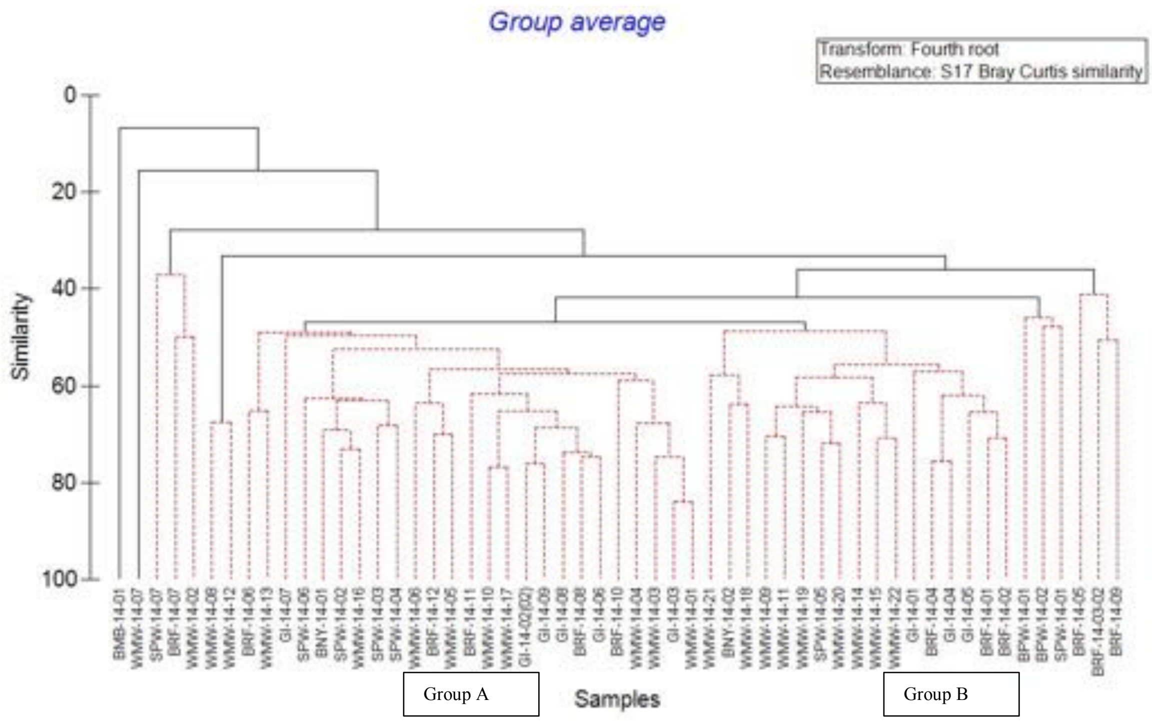

Figure 53. Bray-Curtis Analysis (4th Root Transformed)

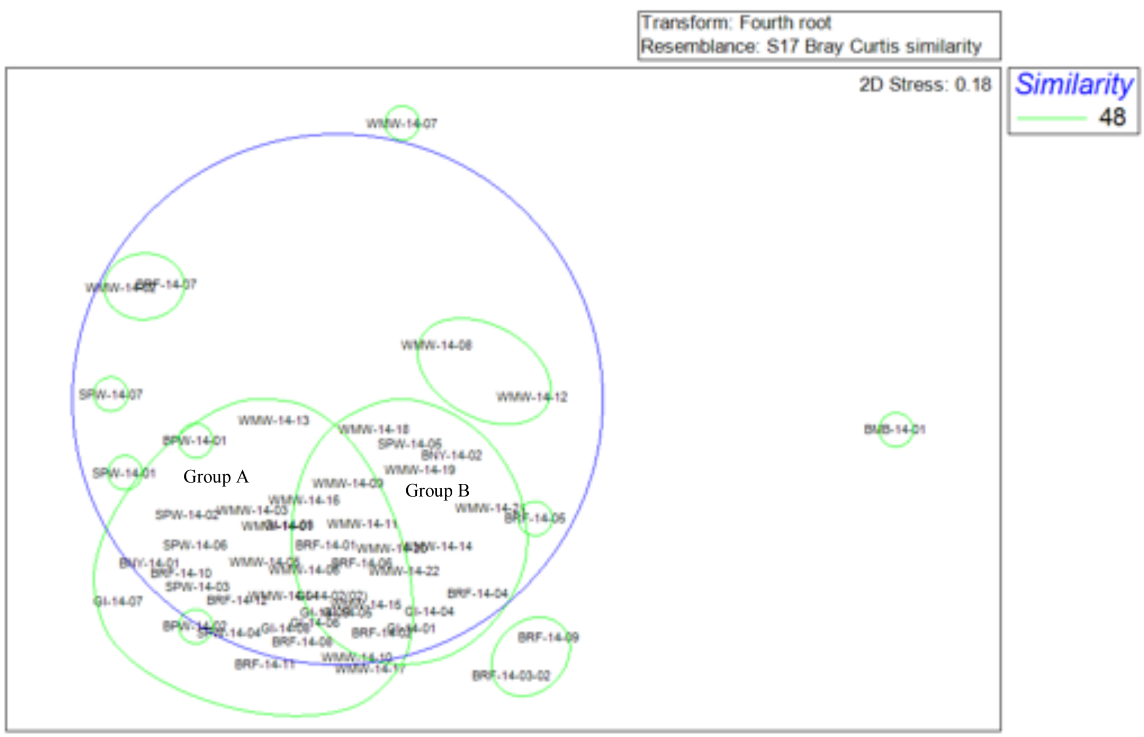

Figure 54. MDS plot of Bray-Curtis Cluster Analysis (4th Root Transformed Data). The green contours group sites with 48% or greater similarity. The blue contour groups 25% similarity.

4.3.5 Principal component analysis

Principal component analysis is another statistic that can be useful to understand benthic community similarities among and between locations.

Principal component analysis was performed on transformed data and was analyzed by comparing both two (2D) and three (3D) dimensional aspects. Pricipal component analysis is a way to visualize how the data being analyzed groups.

For two-dimensional analyses (Figure 55), PC1 and PC2 are used to graph the components. For three-dimensional analyses (Figure 56), PC1, PC2, and PC3 are used for comparison purposes. Adding PC3 can assist with further differentiating groups based on their similarities. Figures 56 and 57 show both 2D and 3D PCA results comparing the sites sampled as part of the lower Hudson River habitat assessment study. In addition, using PRIMER + version 6.0, species vectors that contribute to the groupings can be plotted and shown in these figures. The longer the vectors in PRIMER PCA figures the greater the influence these species have with regard to the groupings formed.

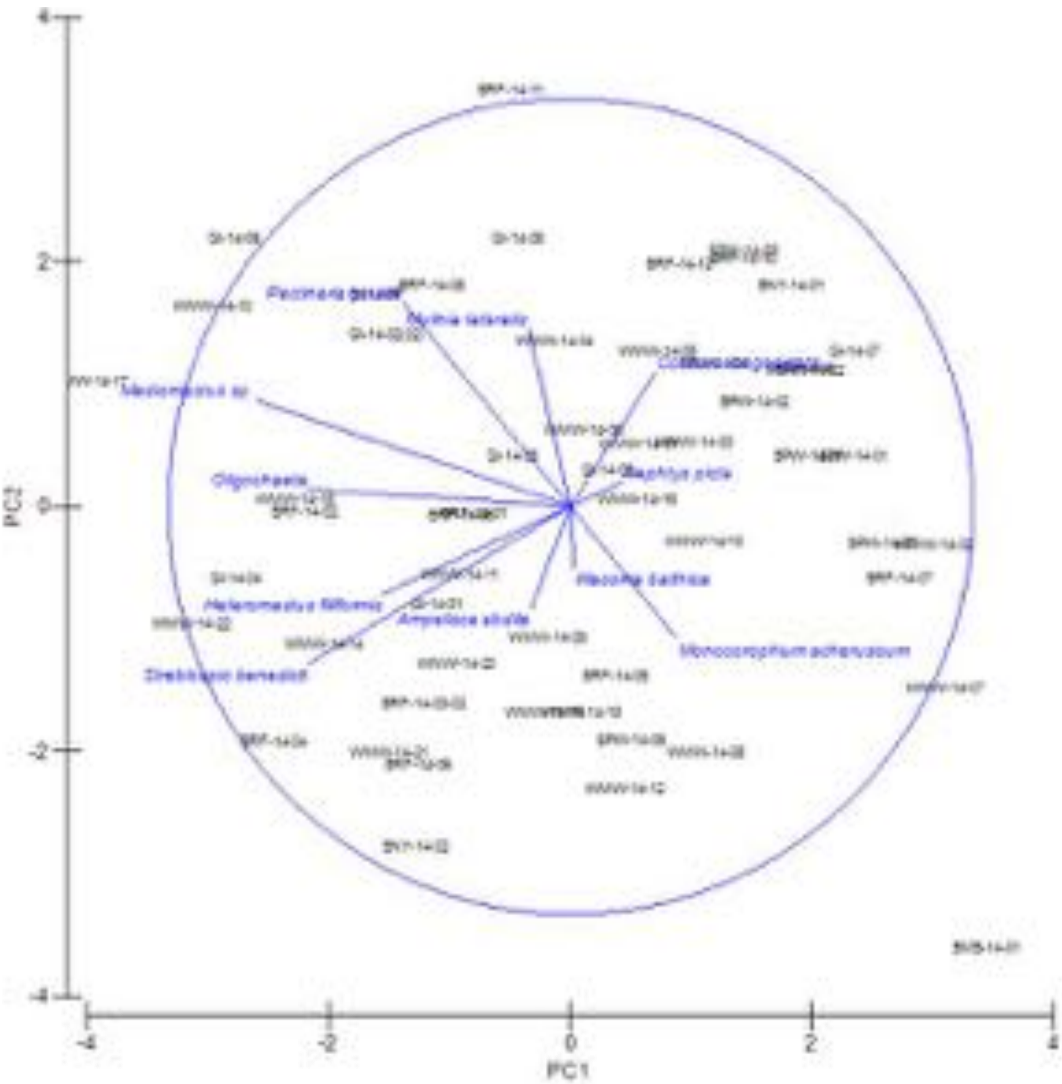

Figure 55. 2D principal component analysis results.

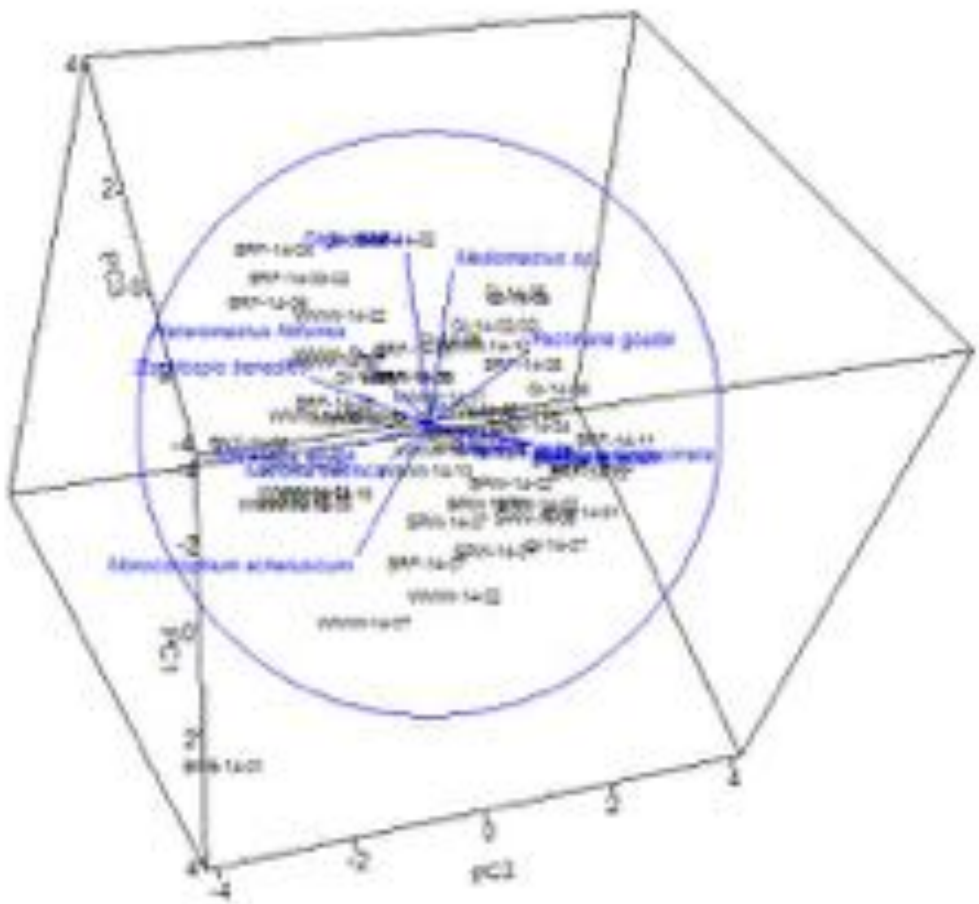

Figure 56. 3D principal component analysis results.

Higher abundances of Stage I organisms tended to best represent the WMW south and GI site groupings while sandy site species representatives grouped together in areas characterized by siltier sediments. Sites that had sandier mud with presences of Stage II amphipods and gastropods tended to group together but separate from the siltier sites. Assuming the null hypothesis, all sites observed and analyzed would have the same benthic species composition independent of sediment texture. This hypothesis is rejected, as it was clear that sediment texture affects species successional stage through their tolerance levels of siltier or sandier sediment as well as lower oxygen and higher organic content conditions in areas where the sediments are dominated by fine-grained sediment.

Principal component analysis does not directly reveal which of the original variables analyzed explains the most variability in a dataset. Rather, it reduces the dimensionality of that dataset and clusters similar datapoints together along the principal components. By deductive reasoning, the factors contributing to this clustering can then be determined.

4.4 Bottom classification

4.4.1 Sediments

Figures 57 and 58 form the base map for the bottom classification based on the sediment distribution in the area of investigation. The substrate types include black silt, silt, clay, sands, gravel, rock, and structures or debris. Dominant sediment type is sand. Black silt is the second most dominant type. Pleistocene clay is observed on the eastside (Buttermilk Channel flats) of Governors Island and other Pleistocene sediments are observed in Bay Ridge Flats. The schist of the Hartland Formation is exposed in the flats of Governors Island. The Fordham gneiss is exposed in Brooklyn Bridge Park. The structures consist of nonrock hard bottoms of piles, fallen piers, debris, and bulkheads. Within the structures, riprap is called out separately. The riprap, piles, and bulkheads are the main substrates in the intertidal zones. Areas beneath intact piers were not included in this study.

4.4.2 Organisms

On each of the bottom classification maps (Figures 59 and 60), the table of biologic indicators lists a) the OSI, b) the organism density as number of individuals per meter squared, and c) the diversity defined as the number of species observed in a sample.

4.4.3 Sediment and OSI

e4 considered as a principal objective a stress-based evaluation of the sediments and biological community within the area of investigation. Stress is defined as a force per unit area from environmental sources (e.g., salinity, temperature, currents) and anthropogenic sources (e.g., construction, pollution). The Organism-Sediment Index (OSI) calculations were developed to standardize comparison of habitat quality and have a consistent index that can be compared among and between habitats. The OSI utilizes a combination of four factors: a) methane presence or absence, b) successional stage, c) depth of aRPD and d) anoxia presence or absence. In the e4 analysis, we added grain size from the SPI and surface roughness, and penetration depth. Values for OSI range from -10, poorest quality habitats, to +11, highest quality habitats.

e4 has classified observed OSI values according to stress designation. e4 defined "stress" based on OSI as <6 - stressed, 6-8 - intermediate, and >8 - not stressed. Based on previous work (e.g. Diaz et al., 2004), we consider that that these designations were appropriate for the benthic habitats studied in NY Harbor.

The OSI values are plotted on the bottom classification maps in Figures 59 and 60. Sites in red are stressed. Sites in yellow are intermediate. Sites in blue are not stressed.

In the area of investigation, the calculated OSI values range from 2.5 to 11. The lowest value 2.5 was observed on the eastern coast of Governors Island, in the piers. We calculated a value of 3 on the western side of Governors Island and on the south end of Governors Island. Another value of 3 was calculated for the westside of Manhattan in the north. Low OSI values correspond to regions of the harbor with high use and/or high sediment accumulation. These are areas of frequent physical change where the benthic community is likely to be disturbed or to experience natural stressors. The low OSI values associated with areas of frequent physical change and/or disturbance were interpreted as indicative of poorer quality benthic habitat with “stressed” benthic communities.

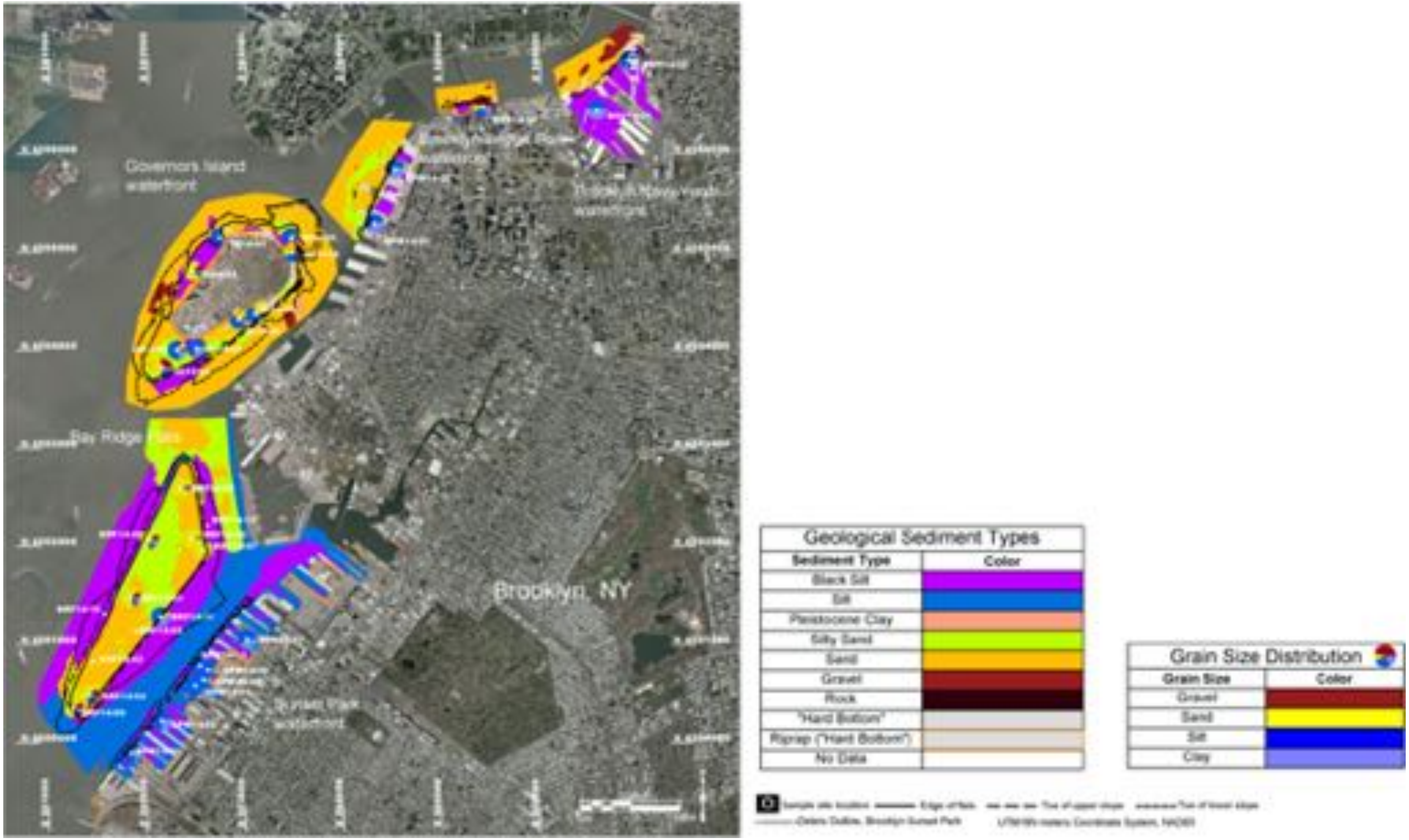

Figure 57. Bottom sediment type and geological substrate map for Brooklyn northwest including Governors Island.

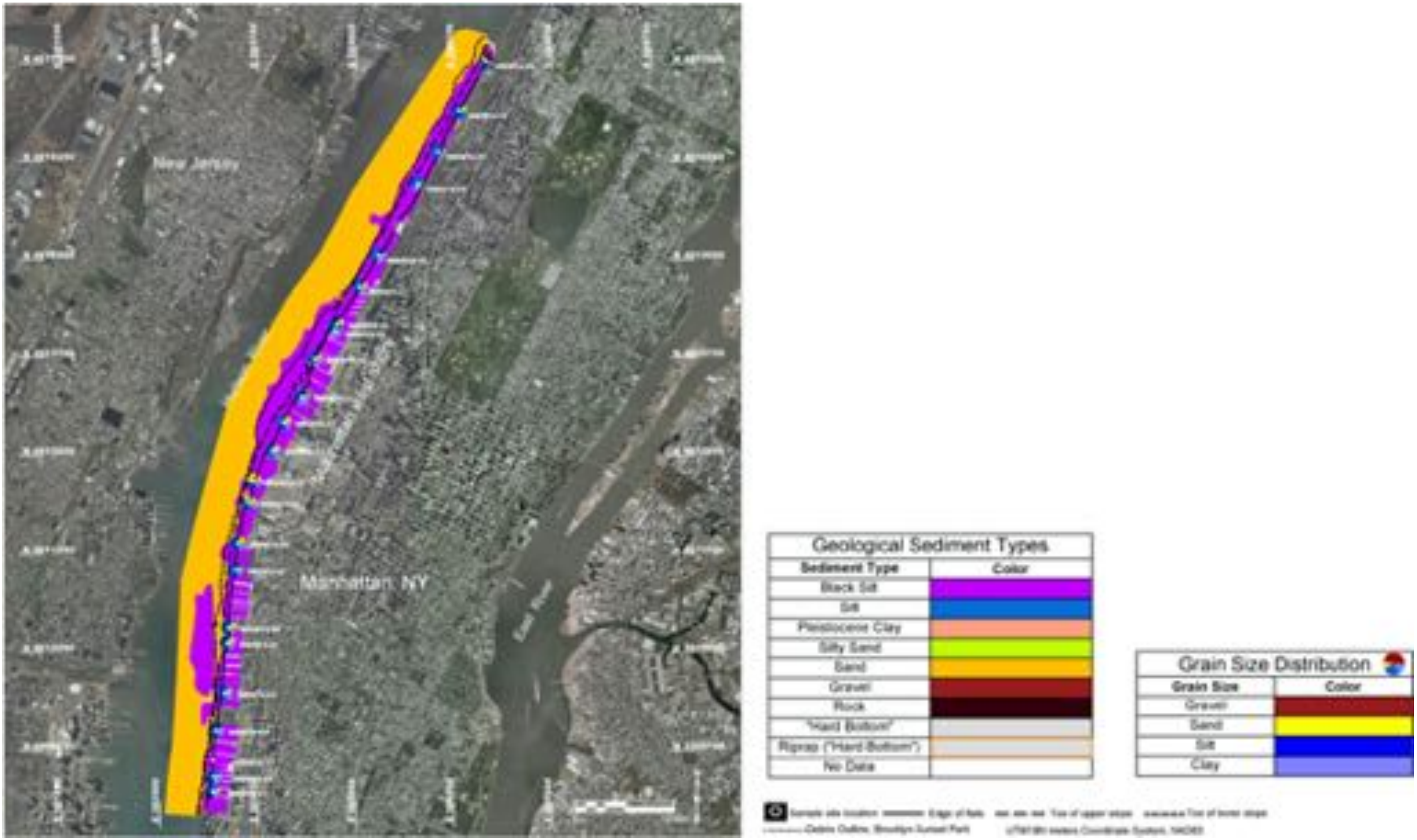

Figure 58. Bottom sediment type and geological substrate map for West Manhattan.

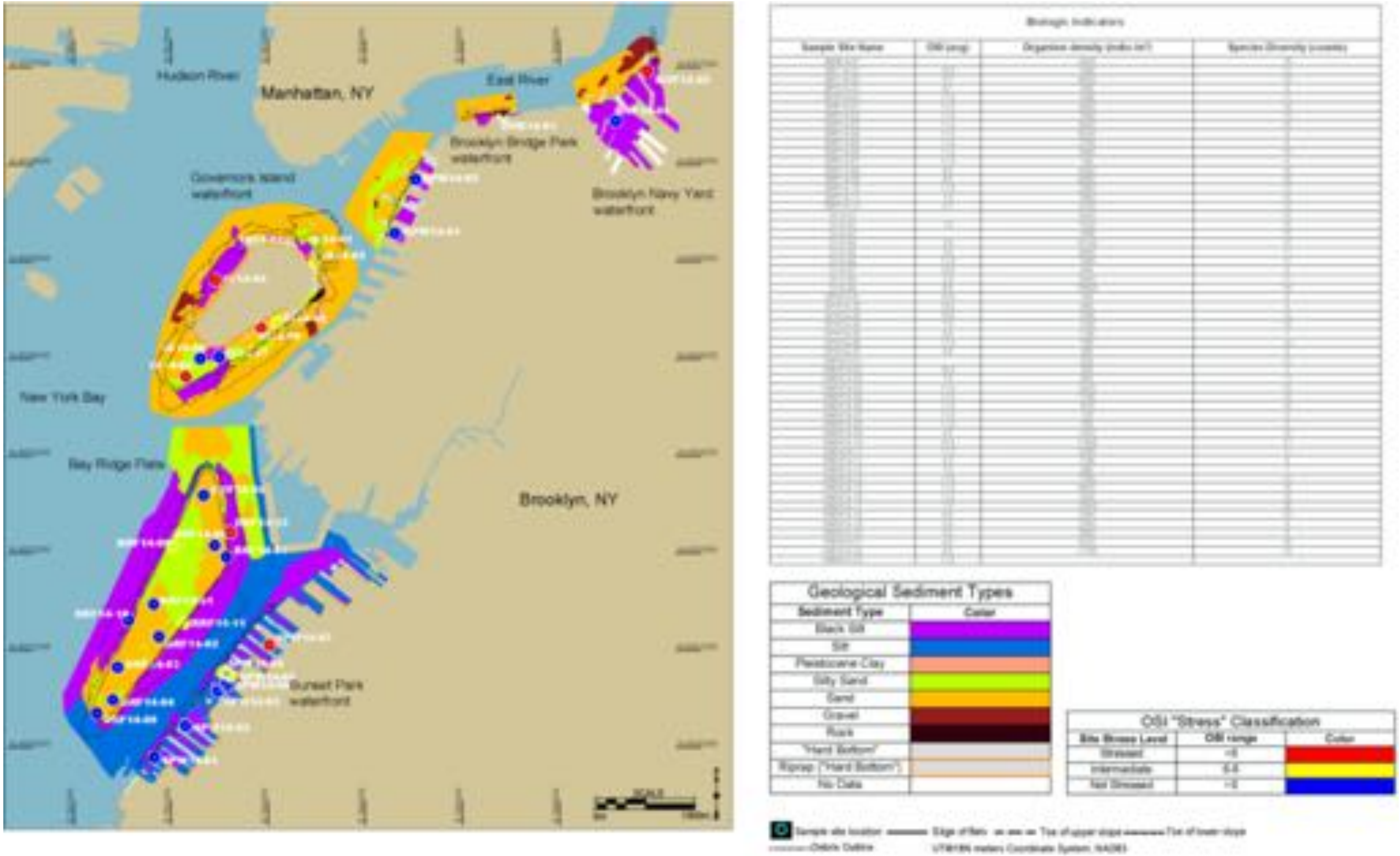

Figure 59. Bottom classification map, Brooklyn northwest including Governors Island.

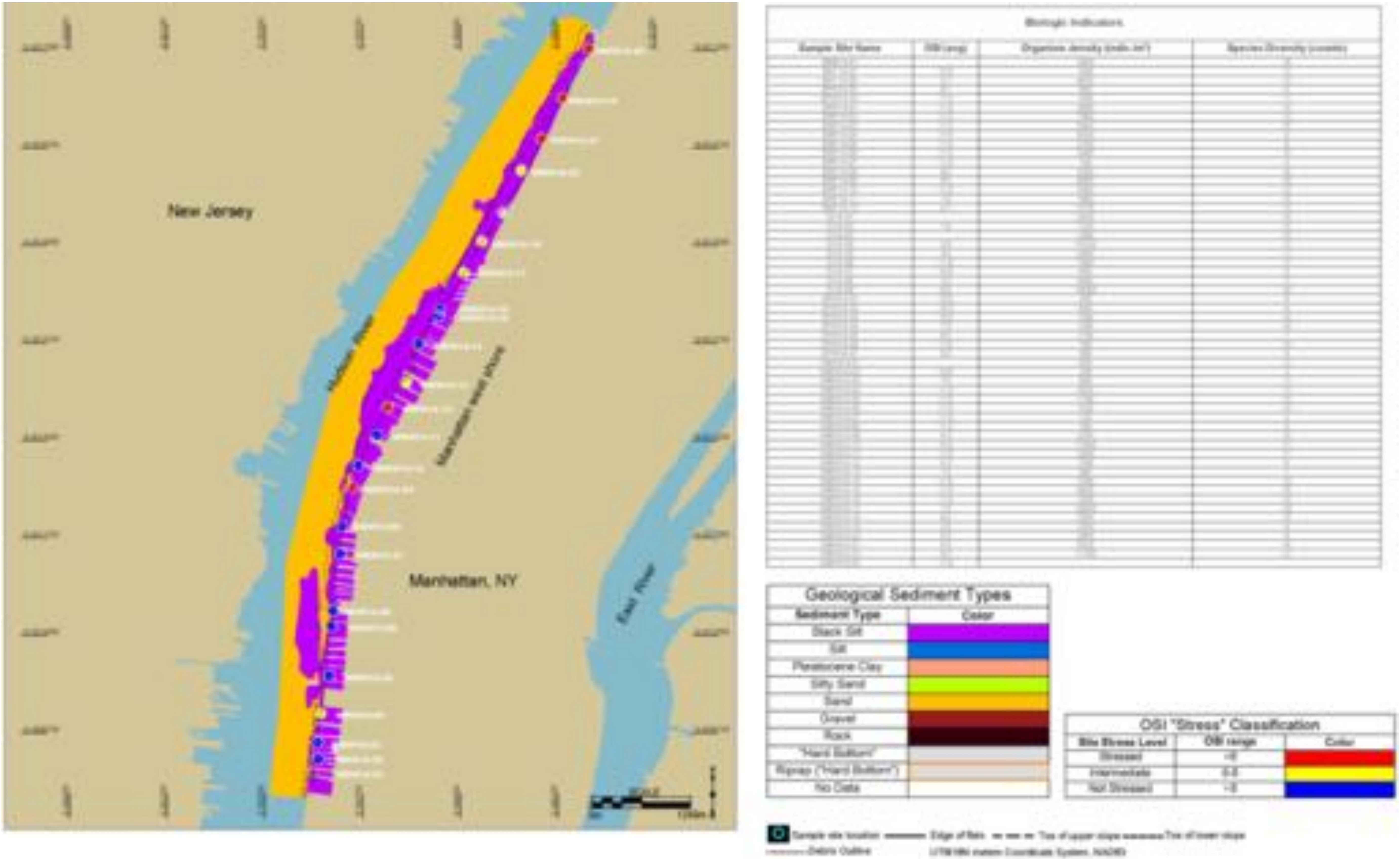

Figure 60. Bottom classification map, West Manhattan.

4.5 Observations with respect to previous studies

The benthos in the Hudson River estuary consists of three primary types: an infaunal and epifaunal soft-sediment community, an epibenthic hard-ground community, and an epibenthic attachment community. Many refer to this last group as "fouling communities" because they are often found growing on artificial structures (e.g. piers, pilings, docks, ship hulls, boat lines, etc.). The organisms comprising these communities are varied and commonly include tunicates, bryozoans, mussels, sponges, arthropods, and a variety of macroalgae.

The first group has been the focus of this project and will be discussed after the second and third groups. The techniques in this study are not adequate for the study of the hard-ground and attachment community. In some of the berth areas hard substrates make up a significant portion of the bottom.

The second group of benthic invertebrates identified from the literature consists of epibenthic hard-ground communities (Blackford 1885, 1887, 1888; Franz 1982; Ingersoll 1881; Ravit et al. 2011; Slagle et al. 2002; Slagle, Carbotte, Nitsche, Ryan, & Bell 2004). These hard-ground bottoms historically existed throughout the greater Hudson River estuary and were composed primarily of oysters and other calcifying organisms. Today natural occurrences of these organisms are very limited in scope but there are ongoing oyster restoration efforts in the lower Hudson River that show some promise. A significant number of organisms that form hard-ground communities are active filter-feeders. These organisms play an important role in an ecosystem because they are able to efficiently filter out particulates (including phytoplankton and clay particles) from the water column, reducing the amount of suspended material in the water column. There have historically been problems with oysters in this area (Blackford 1887; Farley 1988; Bricelj et al. 1992; DePaola, Kaysner, Bowers, & Cook 2000; Mackenzie 2007), as well as in other areas within United States coastal waters, resulting from the presence of diseases (MSX and Dermo). Restoration of oyster reefs has recently been attempted in the Hudson River with mixed results (Stringer 2002; Berger, Haseltine, Boehm, & Goreau 2006; Dalton 2006; Harris & Mass, 2008; Ravit et al., 2011; Grizzle, Ward, Lodge, Suszkowski, & Mosher-Smith 2012).

The third group of benthic invertebrates identified within the Hudson River—particularly in the areas investigated for this report—consists of attached epibenthic organisms, such as tunicates, mussels, barnacles, sponges, some macroalgae, and calcified tube-dwelling polychaete worms (Ayers 1951; Gosner 1969; Able & Duffy-Anderson 2005; Abdus-Samad 2013). These attachment communities, usually found on piers, pilings, docks, lines, and other man-made structures, consist primarily of filter-feeding organisms. Many of these filter-feeders are highly efficient and are capable of filtering a very large volume of water over the course of a day. Like other filter-feeders, they are able to remove particulates from the water column. Given that a majority of them are located within 3m of the surface, not only are they able to remove particulates from the water column, but their production of pseudofeces and feces effectively repackages the smaller particulates that they ingest and releases them as larger particulates that fall to the bottom near where they live. Such sediments are often colonized by a large number of infaunal organisms, which, in turn, support fish communities and other larger organisms. The literature reveals that some work has been done documenting the fish and benthic communities living at the base of the piers and pilings in the area of interest (Able, Manderson, & Studholme 1998; Able & Duffy-Anderson 1999, 2005, 2006; Duffy-Anderson, Manderson, & Able 2003; Grothues & Able 2010). However, little documentation of or research on the attachment communities exists. Additionally, members of attachment communities—especially tunicates—are known to create a three-dimensional biological habitat that, in turn, serves to increase biodiversity in an area. Despite this, attachment communities are often removed from piers and other man-made structures because they are considered nuisance organisms. The attachment communities in the Hudson River estuarine system have not been the focus of much attention although it is possible that the organisms within these communities play an important role in removing particulates and other materials from the water column and transporting them to the sediments.

The construction of piers and other marine structures has facilitated the establishment of attachment communities consisting of tunicates, barnacles, sponges, mussels, bryozoans and species associated with them (e.g. shrimp, blue-crab, macroalgae). These communities consist primarily of filter-feeding organisms and may play a role in water-column nutrient, plankton, and sediment removal in the lower Hudson and its associated rivers.

The microflora (such as phytoplankton) of the Hudson River and its sediment have most likely changed over time. Sandy, well-oxygenated sediments generally have different microflora than terrigenous sediments with a high sediment-oxygen demand.

Hypoxic and anoxic sediments are associated with anaerobic organic matter decomposition and the release of ammonia and sulfide into bottom waters.

Recent mitigation of historic and modern contaminants in the Harbor has contributed to improved benthic habitats, especially on the West Side of Manhattan. Mitigation includes limiting and monitoring municipal and industrial discharges, atmospheric inputs, non-point source runoff, hazardous waste sites, landfills, combined sewer overflows, and spills

The first group of infaunal benthic organisms consists of more than 180 benthic taxa that have been identified in this region. Infaunal macroinvertebrates commonly found within the New York Harbor system include polychaete worms, oligochaetes, snails, bivalves, and amphipods. Common epifauna include hydrozoans, anemones, tunicates, tubiculous amphipods, bivalves, gastropods, and crabs.

Our overview is that the shallow waters nearshore Brooklyn and Manhattan provide very good habitat for a variety of species. The control of sewage outfalls, drainage outfalls, and the removal of black silt have improved water and habitat quality. The greatest concern remains the black silt between the piers both in Brooklyn and Manhattan. The shallow waters in Bay Ridge Flats have remained good habitat since 1995 (Iocco et al., 2000a). Only the east and south flats of Governors Island have shown some diminution of habitat. The report continues, focusing on each of the areas with the region of investigation.

Combining benthic infaunal habitat results with sediment profile image analysis has been a core to our understanding of organism-sediment interactions and defining habitat quality for over 30 years. Calculation of a biotic integrity index such as sediment profile OSI further provides a mechanism to determine the habitat recovery and value within areas being investigated. Maher (2006) developed five different biotopes for lower New York Harbor but she targeted habitat such as living oyster reefs, and her locations were not similar to those in our current study. However, her results similarly suggested that sediment type is a key driver to understanding benthic community structure, and that the types of communities present can tolerate different percentages of gravel, sand, silt, and clay even though some species are found only in certain types of sediment texture.

Our study showed that sites sampled in marinas and boat slips along the shorelines of upper and mid-west side Manhattan and sites sampled in active boat slips/marinas on the Brooklyn shoreline had siltier sediments.

Assuming the null hypothesis, all sites observed and analyzed would have the same benthic species composition independent of sediment texture. This hypothesis is rejected, as it was clear that sediment texture affects species successional stage through their tolerance levels of siltier or sandier sediment as well as lower oxygen and higher organic content conditions in areas where the sediments are dominated by fine-grained sediment. However, sediment profile image analysis and OSI calculations suggested that most of the sites throughout our sampled areas supported relatively healthy benthic habitats (although composed of different communities of various successional stages) for an anthropogenically-affected estuary. Methane within the sediment column was absent from all sites analyzed. Sediments were oxygenated at the surface although some sites in upper West Manhattan and Brooklyn had shallow aRPD depths. Throughout the eight areas sampled, OSI values were generally greater than 6, which is the threshold suggested by Rhoads and Germano (1986); below this value benthic habitat quality should be considered marginal or poor. Evidence of opportunistic, intermediate, and end-stage successional species tubes, burrows, traces, and voids was observed at the sites sampled in this 2014 study. While the lower New York Harbor ecosystem is extensively disturbed, the benthic communities at the time of sampling, aside from a few outlier sites showed mainly healthy communities with high OSI values. However, the healthiest communities were found in regions with well-established benthic habitat or in parts of the harbor where disturbance and/or natural stressors are limited for various reasons.

e4sciences compared the current results with data collected 10 or more years ago. Seasonal spring to fall variations notwithstanding, e4sciences observed that the western shorelines of Manhattan and Brooklyn are generally healthy and have been improving since 1993 (EPA/902-R-03-002).

In 1995, NOAA collected two seasons of sediment profile images throughout New York Harbor (June and October). However, OSI was not calculated. These results were provided to e4sciences by Dr. Pam Neubert and are available in Iocco et al. (2000a and 2000b). Analysis of this historical data and habitat quality and correlation with the 2014 dataset allowed us to make a comparison over a 20-year period. Sites that overlapped with the 2014 study were extracted from the database and OSI was calculated by Dr. Pam Neubert from the metadata provided by NOAA. This allowed for a direct comparison of habitat quality from the 1995 and 2014 datasets, although the number of sites that overlapped was limited to only a few in the Sunset Park waterfront and Governors Island areas. The October-1995 data showed less stressed habitat than was observed in the June-1995 data. Improved habitat quality is likely related to temporal changes in water and sediment quality related to cooling temperatures and higher oxygen concentrations. Although collecting measurements twice a year is better than once a year, it is still not frequent enough to determine the overall improvement of habitat quality. The table for the calculated values of OSI based on NOAA 1995 dataset including their position is available in the electronic data package under the biological data section.

Because of the temporal variation, we decided to compare the November-2014 data with the October-1995 instead of with the June-1995 data. The comparison between November-2014 and October-1995, while not perfect, is better. Comparison with these historical results emphasizes the importance of conducting short-term studies to establish the seasonal variability of benthic community stress in NY Harbor. It also shows that the results presented here can only be considered as a single snapshot in time and are subject to both short- and long-term variability from changing environmental stressors. e4 recommends conducting further short-term studies to establish a truer baseline of the health of benthic communities in NY Harbor.

Hale et al. (2007) calculated “stressed” and “not-stressed” habitats based on benthic seafloor conditions and community structure using EMAP and USEPA criteria. Their definition of stressed described bottom conditions that featured eutrophied sediments that were low in oxygen and characteristically dominated by opportunistic (Stage I) species. Non-stressed habitats had greater sediment oxygenation, higher successional stage species and mixed sediment texture with larger grain size particles. Hale et al. (2007) results were similar to those determined as part of our 2014 study but with some important differences. In 1995, the area around Bay Ridge Flats and Governors Island (mixed sandy and silty sediments) showed results that suggested these habitats were not stressed or were in transition between stressed and not-stressed – similar to our 2014 results (Iocco et al., 2000b). Samples from Bay Ridge from the Hale et al. (2007) and our 2014 study were both classified as not stressed. Sites sampled from upper West Manhattan shorelines were stressed for the Hale et al. (2007) and our 2014 study. However, it appeared that sites within southwest Manhattan for the 2014 study showed improved sediment quality when compared to Hale et al. (2007) results, with healthy habitats observed further north in 2014 than in Hale et al. (2007). Additionally, Hale et al. (2007) showed that areas such as Jamaica Bay, Kill van Kull, Arthur Kill and Queens (excluded from this study) were areas of stressed benthic community habitat while areas in more open water such as the outer portion of Raritan Bay, Bay Ridge Flats, and around Governors Island and Sandy Hook were less stressed or not-stressed (Figure 61).

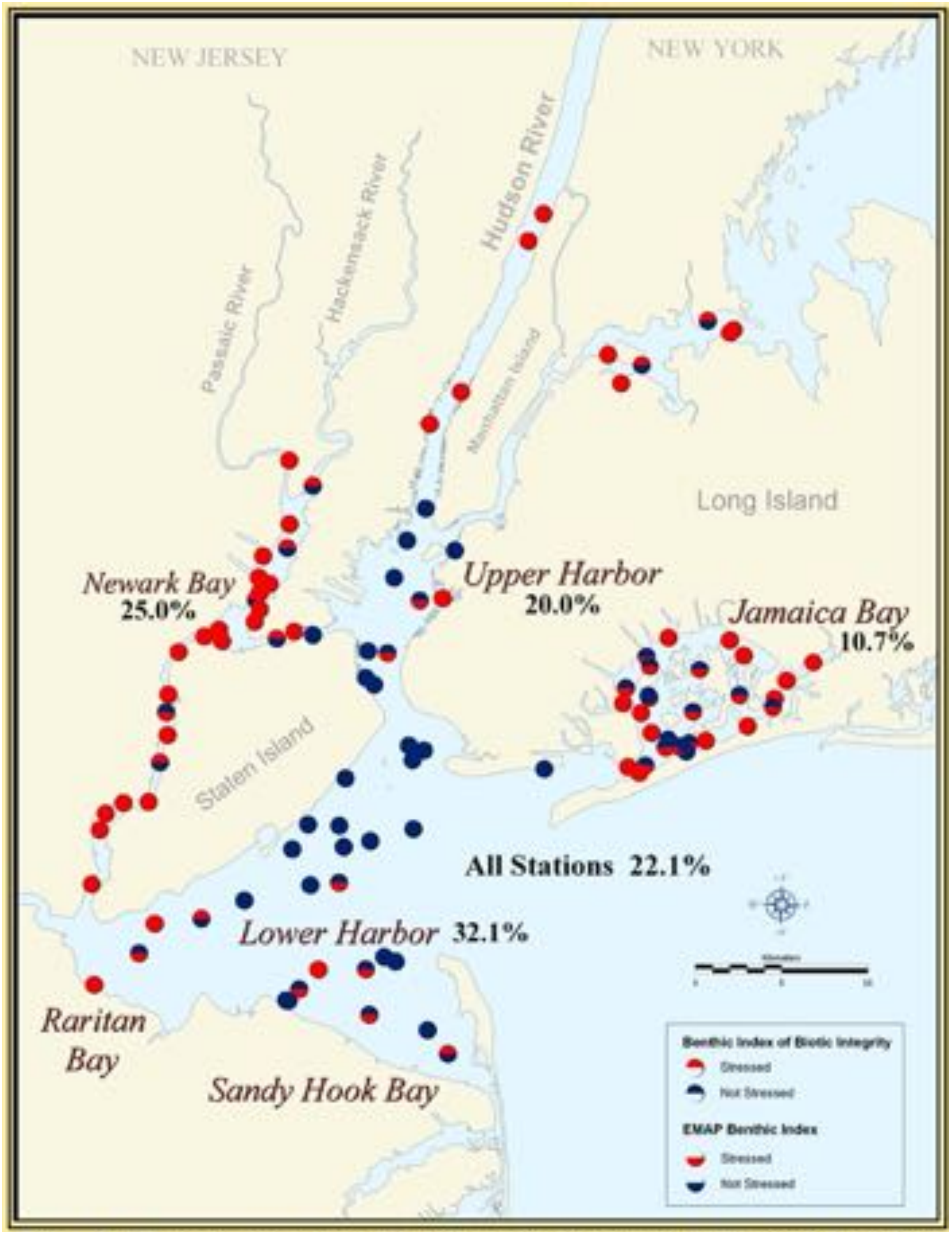

Figure 61. NYNJ harbor from Hale et al., 2007.

5.0 Area Reports

5.1 Area Report 1. Bay Ridge Flats

5.1.1 Morphology (Bathymetry, bathymetry analysis)

Figure 62 is a location photograph for Bay Ridge Flats. Note that this is an anchorage. Oil barges anchor around the flats waiting for access to piers in the Arthur Kill.

Figure 63 is the bathymetry for the Bay Ridge Flats. Single and multibeam data from e4sciences (2015) were combined in 5m x 5m and 1m x 1m grids, respectively, using a triangular linear interpolation. Historical data from NOAA survey H11600 (2006) were combined in a 1m x 1m grid using a triangular linear interpolation. 2D first and second order derivative filters were applied to the historical bathymetry. Figure 64 plots the derivative maps for the historical bathymetry. Figure 65 is the difference map between 2015 and 2006. The map displays both results of the difference in bathymetry for the 5m x 5m grid in the ultrashallow area, and the 1m x 1m grid in the deeper area.


Figure 62. Location photo for Bay Ridge Flats.

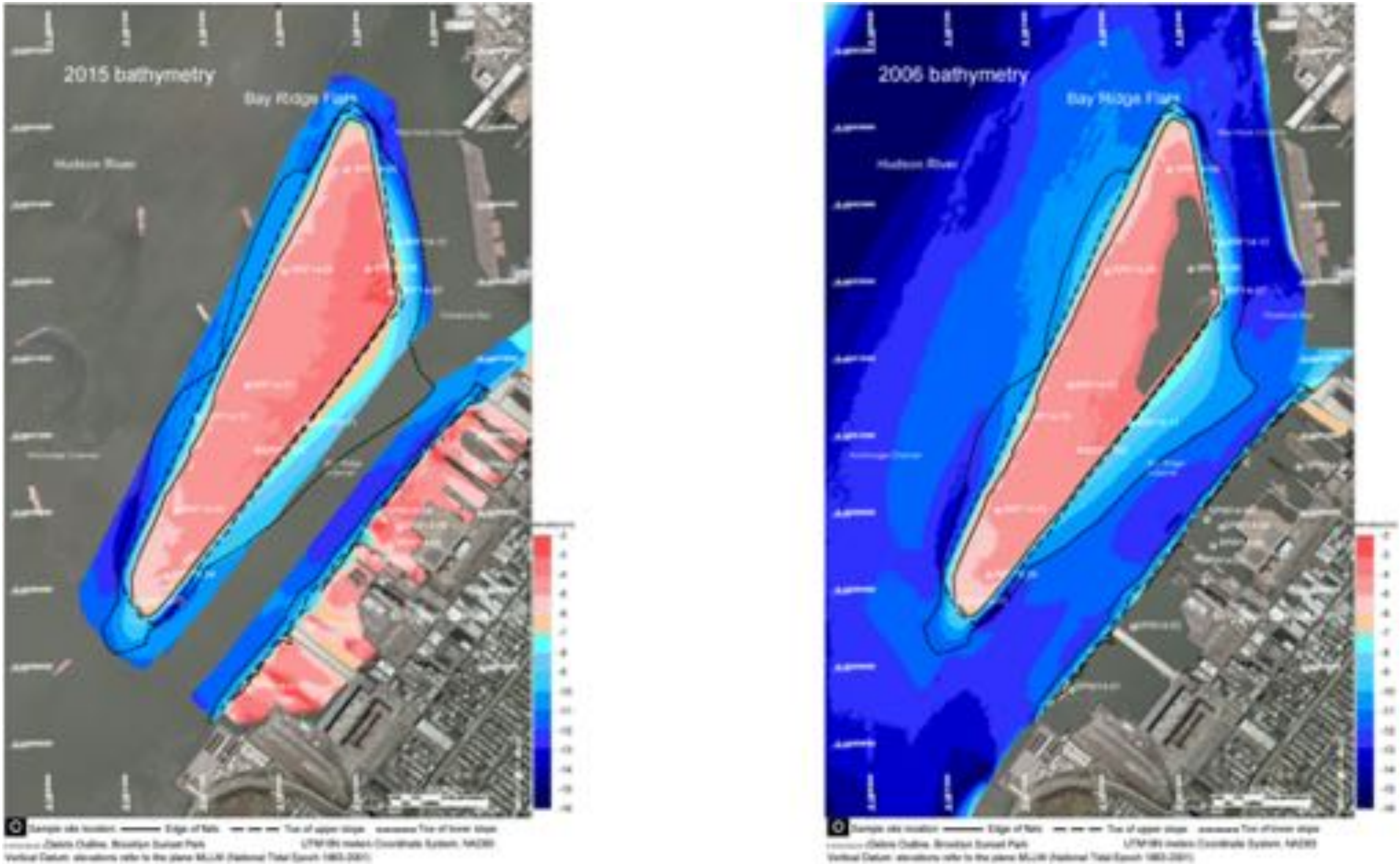

Figure 63. Bathymetric and location map for Bay Ridge Flats. (Left) Single and multibeam data from e4sciences (2015) were combined in 5m x 5m and 1m x 1m grids, respectively, using a triangular linear interpolation. (Right) Data from NOAA survey H11600 (2006) were combined in a 1m x 1m grid using a triangular linear interpolation

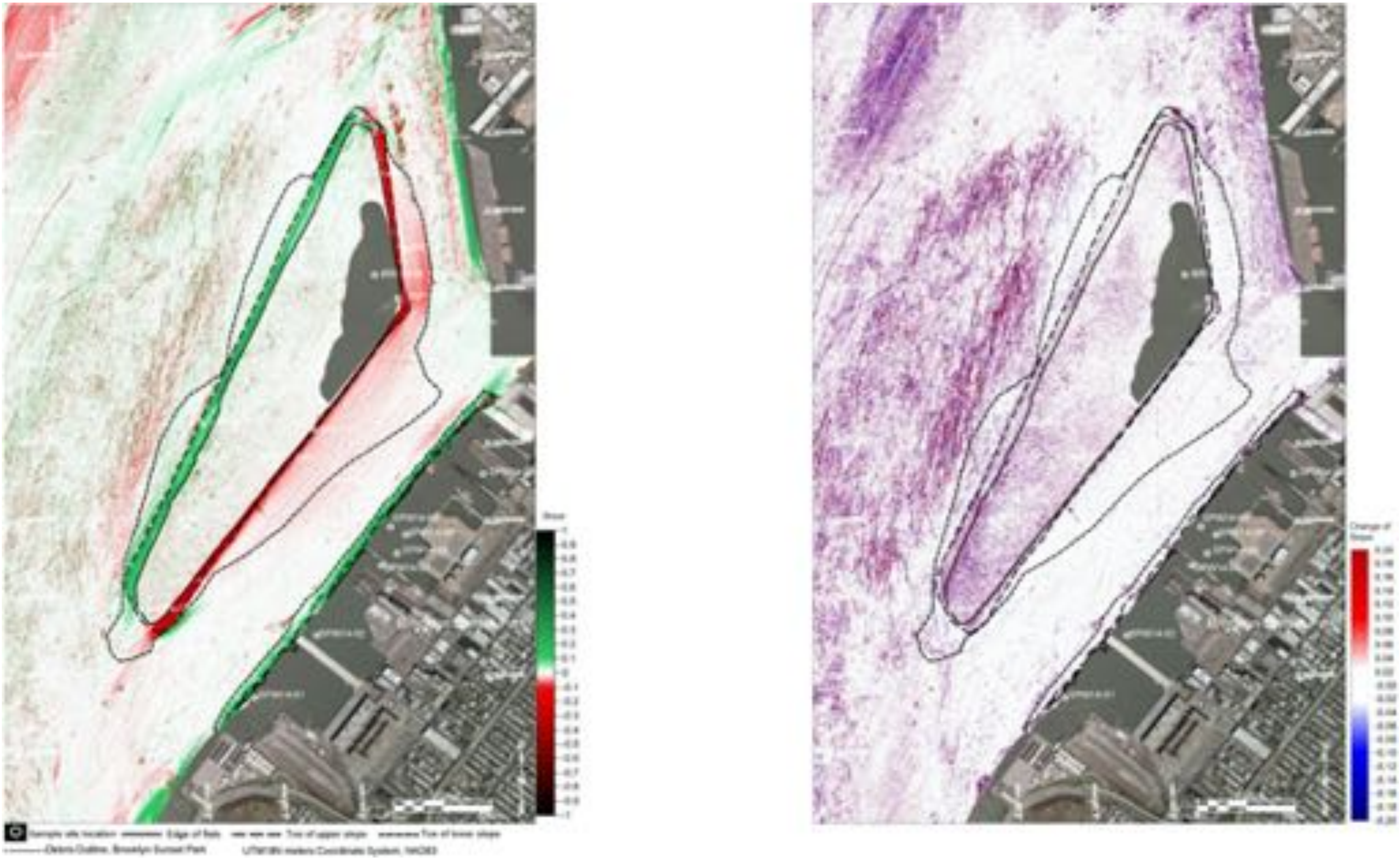

Figure 64. Bathymetric analysis for Bay Ridge Flats (derivative maps for Area 1). Data from NOAA survey H11600 (2006) were combined in a 1m x 1m grid using a triangular linear interpolation. (Left) 2D first order derivative filter – slope. (Right) 2D second order derivative filter – change in slope. The NOAA survey H11600 was incomplete in the shallowest water.

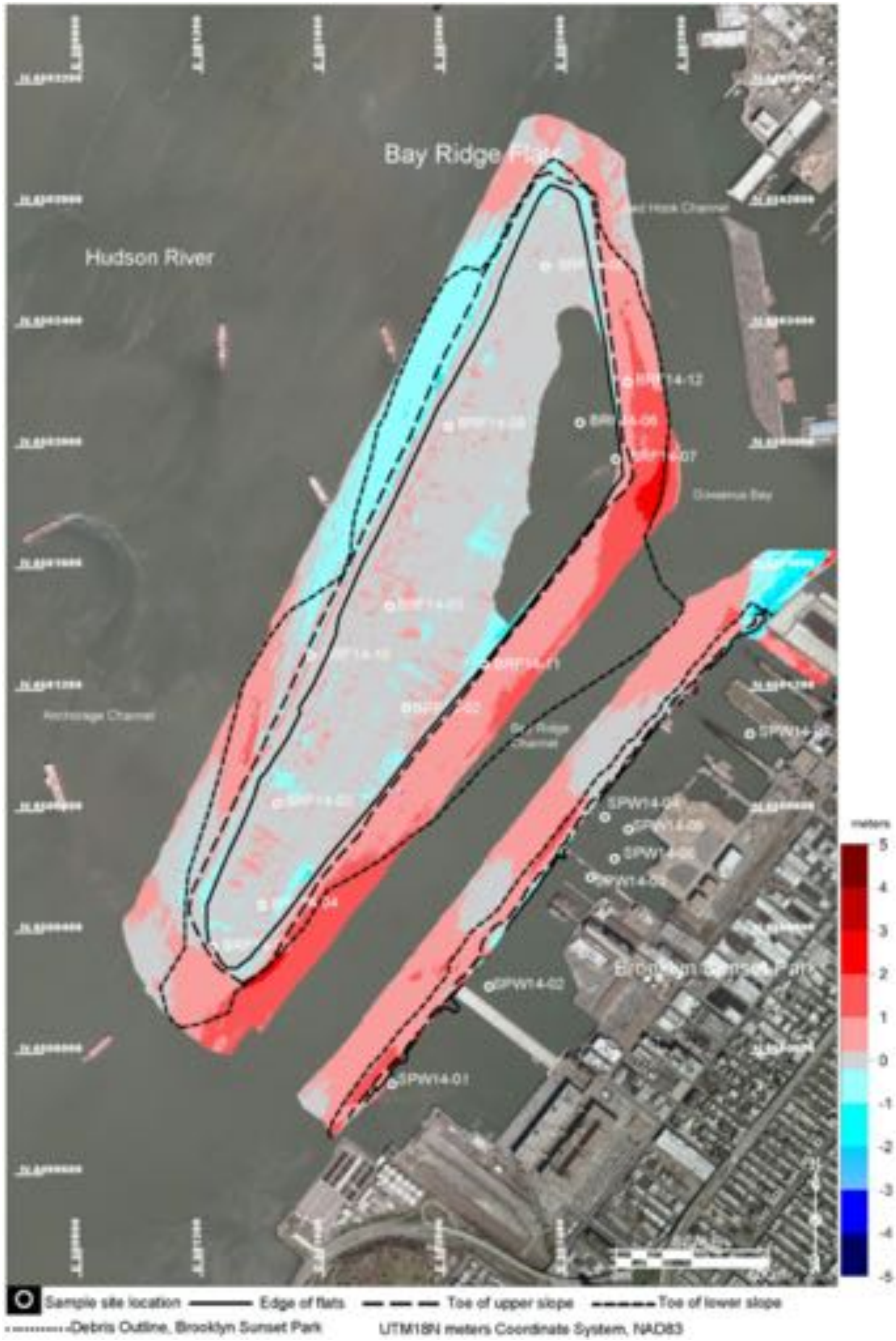

Figure 65. Bathymetry elevation difference map 2015 minus 2006 for Bay Ridge Flats. The 2015 bathymetry includes combined single and multibeam bathymetries from e4sciences. The 2006 bathymetry includes NOAA survey H11600. The map displays both results of the difference in bathymetry for the 5m x 5m grid in the ultrashallow area, and the 1m x 1m grid in the deeper area. All grids were obtained with triangular linear interpolations. The NOAA survey H11600 was incomplete in the shallowest water.

5.1.2 Sediments (side-scan, seismic, cross sections, isopachs, grab samples)

Figure 66 is the side-scan orthosonograph for Bay Ridge Flats insonified from the west. Figure 67 is its pair insonified from the east.

Figure 68 is a sub-bottom seismic cross section from south to north through the Bay Ridge Flats. Figure 69 is the acoustic silt isopach. The acoustic silt is relatively thin on Bay Ridge Flats.

Table 9 lists the grain size mean and standard deviation. The grain sizes are expressed in the Krumbien phi scale. Size ranges define limits of classes that are given names in the Wentworth scale (or Udden-Wentworth) used in the United States. The Krumbein *phi* (φ) scale, a modification of the Wentworth scale created by W. C. Krumbein in 1937, is a logarithmic scale computed by the equation, $f = \log_2 D/D_o$, where ϕ is the Krumbein phi scale, D is the diameter of the particle, D_o is a reference diameter, equal to 1 mm (to make the equation dimensionally consistent). This equation can be rearranged to find diameter, using ϕ, $D = D_o\,2^{-phi}$.

Table 9. Bay Ridge Flats grain size

Sample	Mean	Median	Std. Deviation
	Φ		
BRF14-01	3.0	2.0	2.5
BRF14-02	2.5	2.0	2.5
BRF14-03	1.7	1.5	2.0
BRF14-04	3.2	2.0	3.3
BRF14-05	1.8	2.0	1.5
BRF14-06	2.0	2.0	0.6
BRF14-07	2.0	2.0	0.6
BRF14-08	3.8	2.5	3.5
BRF14-09	2.8	2.0	2.8
BRF14-11	7.7	7.5	2.5
BRF14-12	8.3	8.0	3.0

Table 10 lists the chemical measurements for lead, beryllium, and cesium.

Table 10. Bay Ridge Flats Pb, ^{7}Be, and ^{137}Cs

Sample	Sample Date	Sample Time	Pb (ICPMS)	^{7}Be	^{7}Be Qualifiers	^{137}Cs	^{137}Cs Qualifiers
			mg/Kg	pCi/g		pCi/g	
BRF14-01	11/3/14	9:49	24	-0.037	U	-0.017	U
BRF14-02	11/3/14	8:39	19	0.002	U	0.024	U
BRF14-03	11/3/14	8:16	10	0.000	U	0.008	U
BRF14-04	11/4/14	14:07	30	0.201	U	0.043	U
BRF14-05	11/3/14	13:01	11	-0.023	U	0.000	U
BRF14-06	11/3/14	11:58	17	-0.053	U	-0.008	U
BRF14-07	11/3/14	10:51	18	0.217	U	0.000	U
BRF14-09	11/4/14	14:49	15	0.013	U	0.030	U
BRF14-11	11/3/14	10:16	37	0.271	U	0.044	U
BRF14-12	11/3/14	11:30	31	-0.061	U	0.084	U
U = Result is less than the sample detection limit							

Table 11 lists the measurements of compressional-wave velocity that are necessary for seismic processing and interpretation.

Table 11. Bay Ridge Flats acoustic velocity

Sample	Average P Velocity	Average P Velocity
	[m/s]	[ft/s]
BRF14-02	1,593.7	5,227.4
BRF14-05	1,706.4	5,597.0
BRF14-06	1,748.0	5,733.5
BRF14-09	1,631.7	5,351.8
BRF14-11	1,557.6	5,109.0

Table 12 lists the results of X-ray fluorescence on additional elements.

Table 12. Bay Ridge Flats XRF

Sample	S Avg	S Max	Fe Avg	Fe Max	Hg Avg	Hg Max	Zn Avg	Zn Max	Pb Avg	Pb Max	As Avg	As Max	Mn Avg	Mn Max
Push-Core	ppm													
BRF14-01	3,906.29	5,313.43	15,013.70	20,174.42	< LOD	< LOD	98.92	188.36	109.25	186.06	15.73	15.73	177.36	304.75
BRF14-02	5,245.50	15,737.73	17,738.38	24,939.11	< LOD	< LOD	130.76	213.95	106.38	211.12	17.71	20.22	181.48	269.31
BRF14-03	3,096.36	4,950.77	13,796.05	16,847.40	< LOD	< LOD	56.03	83.98	31.00	45.56	10.95	13.99	220.40	284.50
BRF14-04	2,239.28	2,865.69	11,686.13	12,717.35	< LOD	< LOD	40.16	60.97	20.04	28.38	9.17	9.17	166.23	233.83
BRF14-05	2,241.88	3,389.26	20,901.45	46,843.80	< LOD	< LOD	48.93	70.71	26.94	38.17	< LOD	< LOD	212.04	227.18
BRF14-06	1,780.62	2,808.40	11,174.61	14,466.30	< LOD	< LOD	52.21	93.86	28.23	52.59	< LOD	< LOD	171.49	255.81
BRF14-07	1,021.64	1,862.40	12,348.68	17,056.47	< LOD	< LOD	40.73	54.63	26.78	40.61	< LOD	< LOD	248.27	386.69
BRF14-08	3,174.25	4,320.71	14,787.27	20,220.61	< LOD	< LOD	112.86	203.67	100.65	212.11	18.29	18.29	173.79	214.78
BRF14-09	1,860.32	2,148.96	10,619.49	13,478.30	< LOD	< LOD	35.29	56.03	24.19	38.40	< LOD	< LOD	175.05	196.55
BRF14-11	1,630.15	2,774.42	14,706.83	17,326.03	< LOD	< LOD	69.23	116.66	37.56	50.70	8.89	9.79	165.87	243.62
BRF14-12	1,532.34	2,320.06	14,958.38	17,675.26	< LOD	< LOD	59.16	73.62	31.54	37.74	< LOD	< LOD	206.54	280.93
*<LOD = below Limit Of Detection														

Figure 66. Bay Ridge Flats orthosonograph insonified from the west.

Figure 67. Bay Ridge Flats orthosonograph insonified from the east.

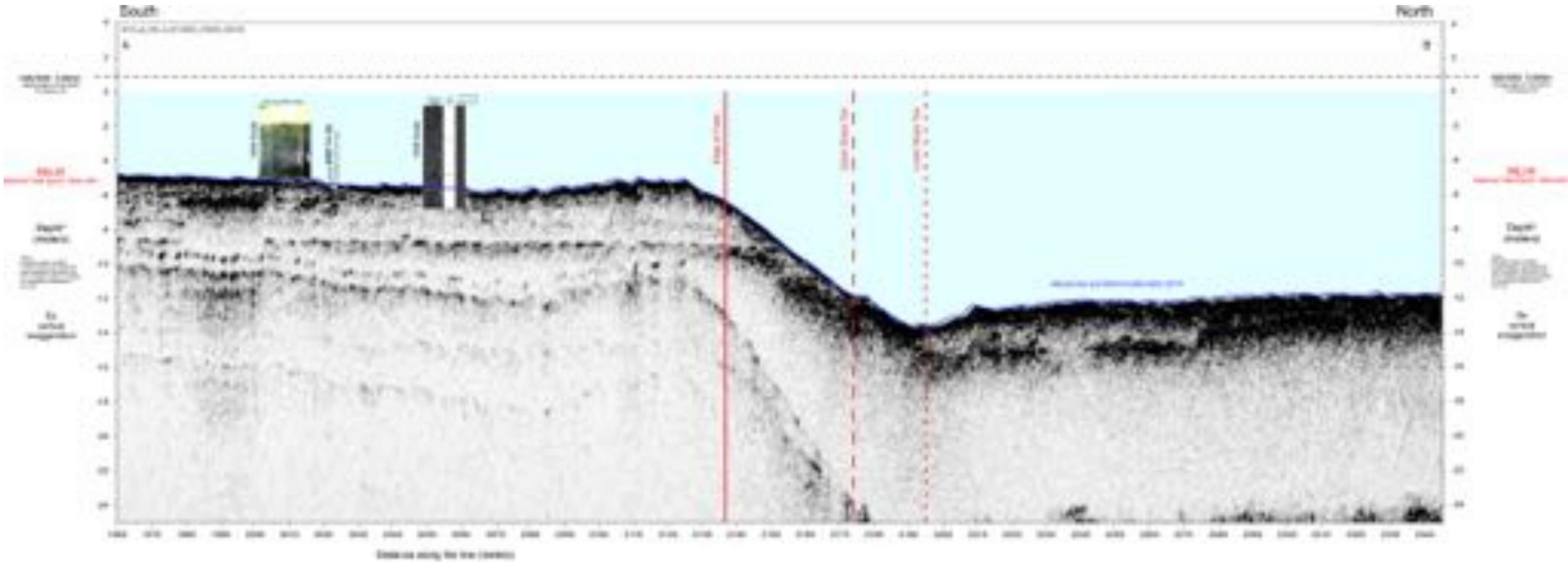

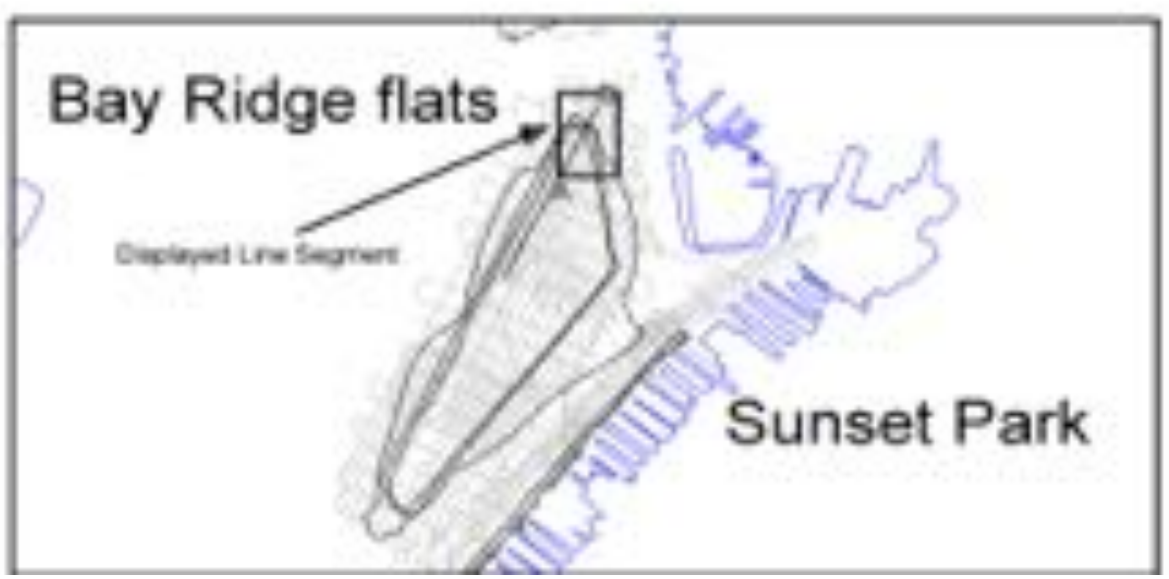

Figure 68. Seismic cross section, Bay Ridge Flats.

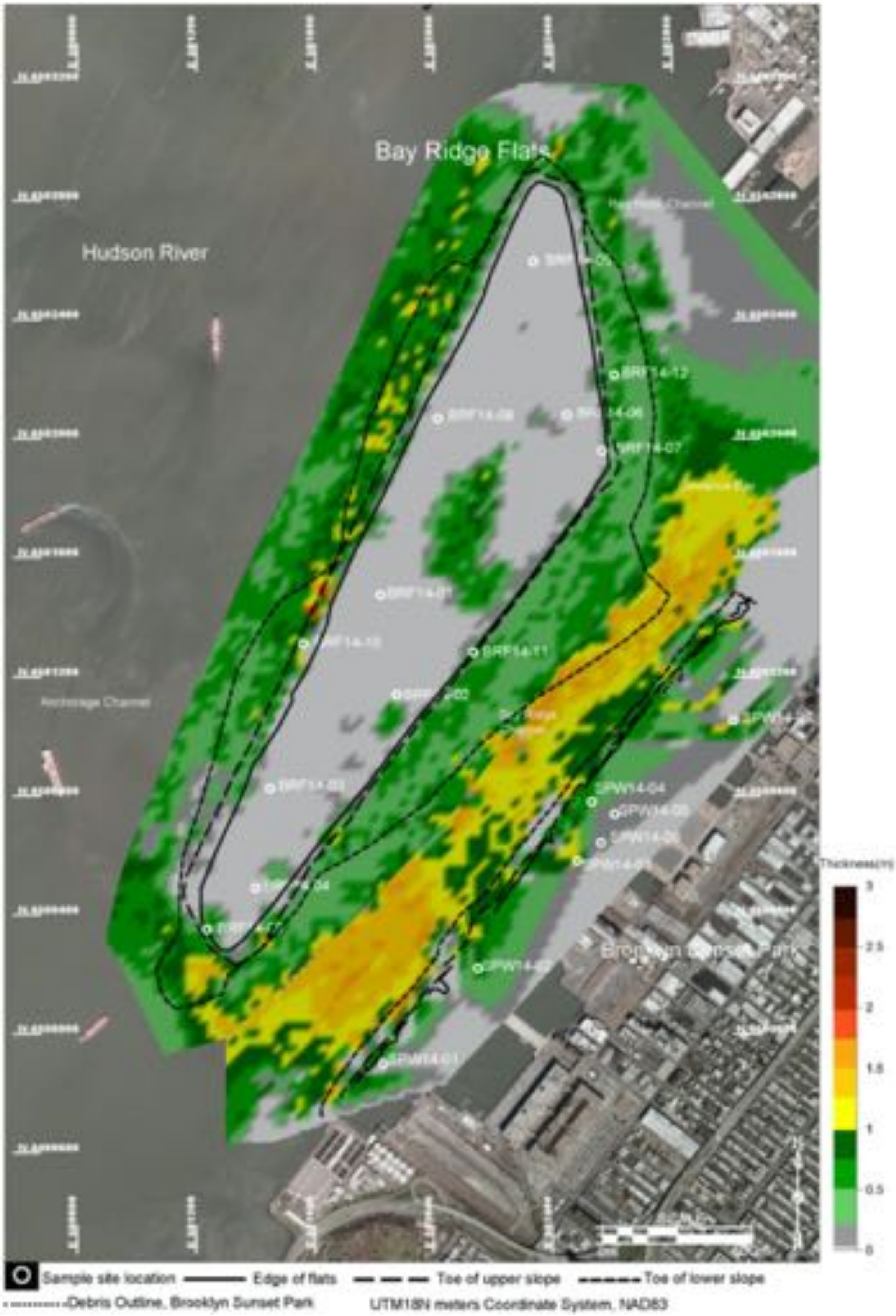

Figure 69. Acoustic silt isopach map for Bay Ridge Flats.

5.1.3 Bottom classification (SPI, benthic classification)

Figure 70 displays the geological and structural substrate for Bay Ridge Flats. Figure 71 plots the density of individual organisms per square meter as a TINed surface connecting the sample sites in area 1. Figure 72 plots the composite bottom classification.

Bay Ridge Flats (BRF) provides mooring and anchorage for boats kept in New York Harbor. Twenty-eight images were analyzed from BRF. Sediment texture at this location from grab samples was predominantly sand and more similar to the sediment found at Governors Island (GI) than the sites sampled within active berths and marinas around the Manhattan and Brooklyn areas such as SPW sites, which were located directly across from BRF sampled locations. Mean camera penetration depth was 11.20cm and also similar to the penetration in sandier sediment locations at GI. The aRPD depth at BRF was either shallow with less than 1.5cm or had a deep aRPD >3.75cm. Epifauna and methane were not observed at BRF sampled sites but bivalve shellhash was present at nearly all sites sampled. Major modal grain size was 3 to 4 phi class. Sediments were oxidized at the surface and small worm tubes were present. Only three sites had an OSI value less than 6; most sites had OSI values ranging between 7 and 11. Surface roughness was attributed to both physical and biological factors (sand waves, disturbance from anchorage as well as biological activities). Microvoids were present at nearly all sites and successional stage for this location was classified as I on III – Stage I assemblages are occurring at the same place and time as evidence of Stage III organisms. Of the six samples analyzed for sediment texture from BRF grabs, these samples had >65% sand with some samples containing >90% sand.

The benthic fauna of the Upper Bay-Brooklyn Harbor waterfront contains an abundance of pollution-tolerant polychaetes, arthropods and mollusks, very similar in composition to those found in the Lower Hudson River-Upper Bay complex (Bell et al. 2003) although with slightly more pollution-sensitive organisms present. These organisms are associated with the tidal flats located throughout this western edge of this region as well as with the more extensive Bay Ridge Flats. Oyster restoration projects have begun in this region—near Governors Island and on the Bay Ridge Flats where oyster beds were once found (Blackford 1887) — and have met with limited success (Stringer 2002; Dalton 2006; Harris & Mass, 2008; Grizzle et al., 2012; Ravit et al. 2011). These reefs do not appear to have increased organism diversity or abundance at these sites. The Bay Ridge Flats oyster reefs were dominated by polychaetes, although several gastropods, small mud crabs and tunicates were also found associated with the reefs. Tunicates are also part of the fouling communities located on and within the piers and pilings on the Brooklyn waterfront (NY DEP 2007).

Overall, BRF represents a stable, well-established benthic community in a largely healthy and supportive environment. Low OSI values corresponded to sediment traps with high accumulation rates on the slopes of the Flats. The communities in BRF show high OSI values despite boat traffic and heavy use of the shallows in this area. This supports our hypothesis that established benthic communities in well-circulated, coarse-grained sediments are less sensitive to disturbance than apparently healthy communities in siltier, less well circulated environments (e.g. SPW).

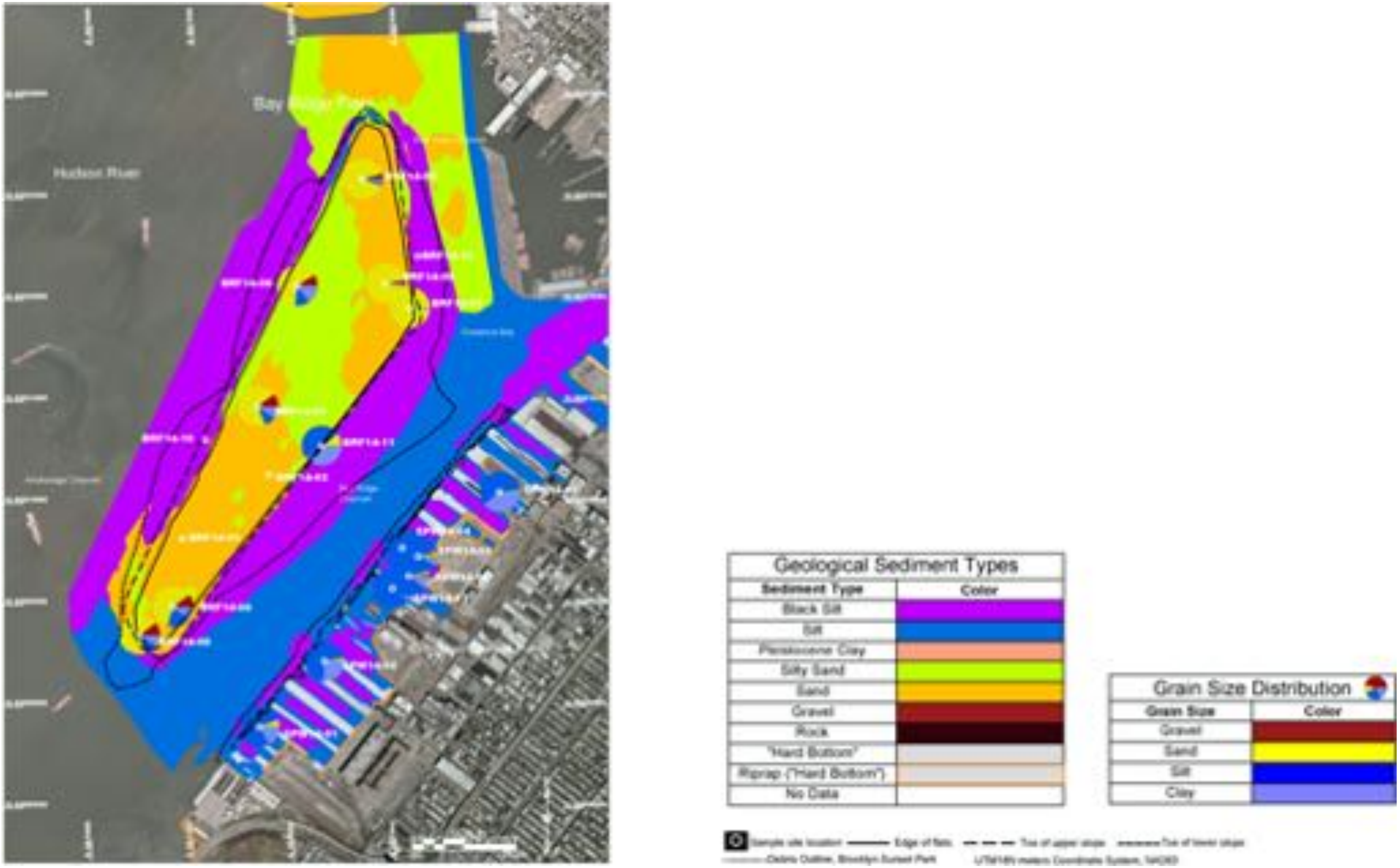

Figure 70. Bottom sediment type and geological substrate map for Bay Ridge Flats.

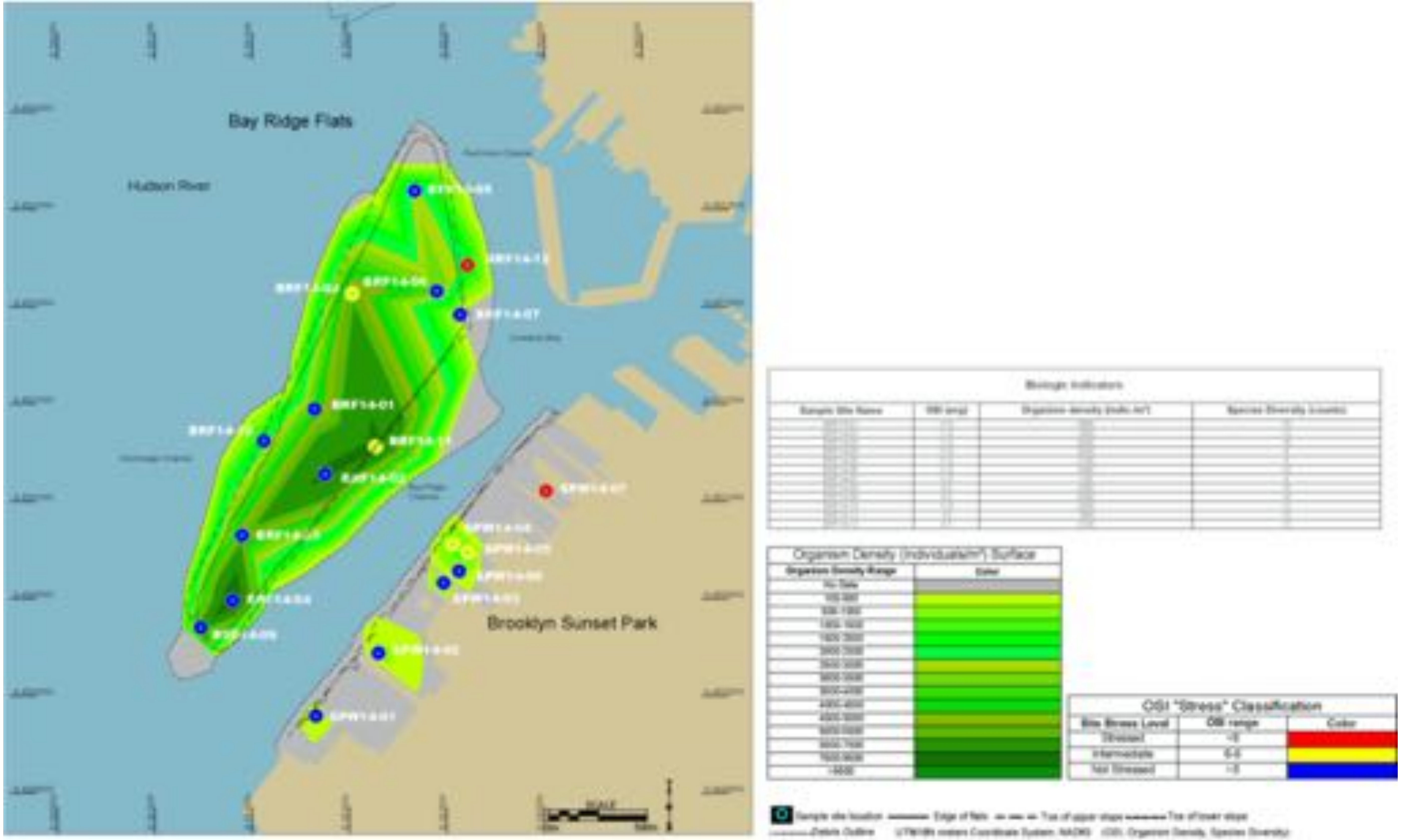

Figure 71. Organism density map for Bay Ridge Flats. The numbers at each site represent the triplet (OSI, organism density per square meter, diversity as total number of species). In the cases of no measurement the space is left blank.

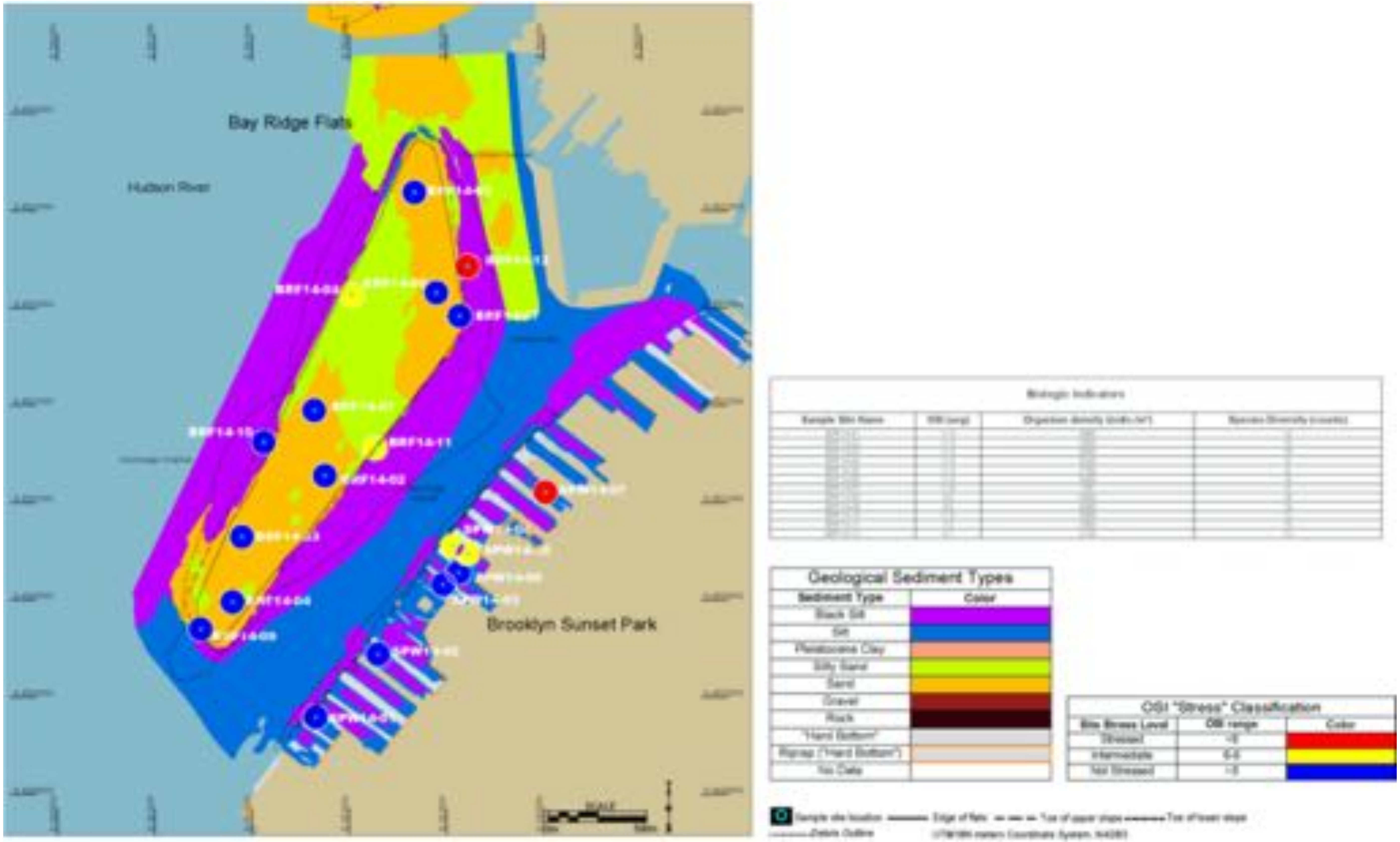

Figure 72. Composite bottom classification map for Bay Ridge Flats.

5.2 Area Report 2. Governors Island

5.2.1 Morphology (Bathymetry, bathymetry analysis)

Figure 73 is a location photograph for Governors Island. Note the structures include the vents for Brooklyn-Manhattan tunnel on the northern tip of the island and piers on the east side of the island.

Figure 74 is the bathymetry for the Governors Island. Multibeam data from e4sciences (2015) were combined in a 1m x 1m grid, using a triangular linear interpolation. Historical data from NOAA surveys H11353 (2004), H11395 (2006) and H11600 (2006) were combined in a 1m x 1m grid using a triangular linear interpolation. 2D first and second order derivative filters were applied to the historical bathymetry. Figure 75 plots the derivative maps for the 2006 historical bathymetry. Figure 76 is the difference map between 2015 and 2006.

Figure 73. Location photo for Governors Island.

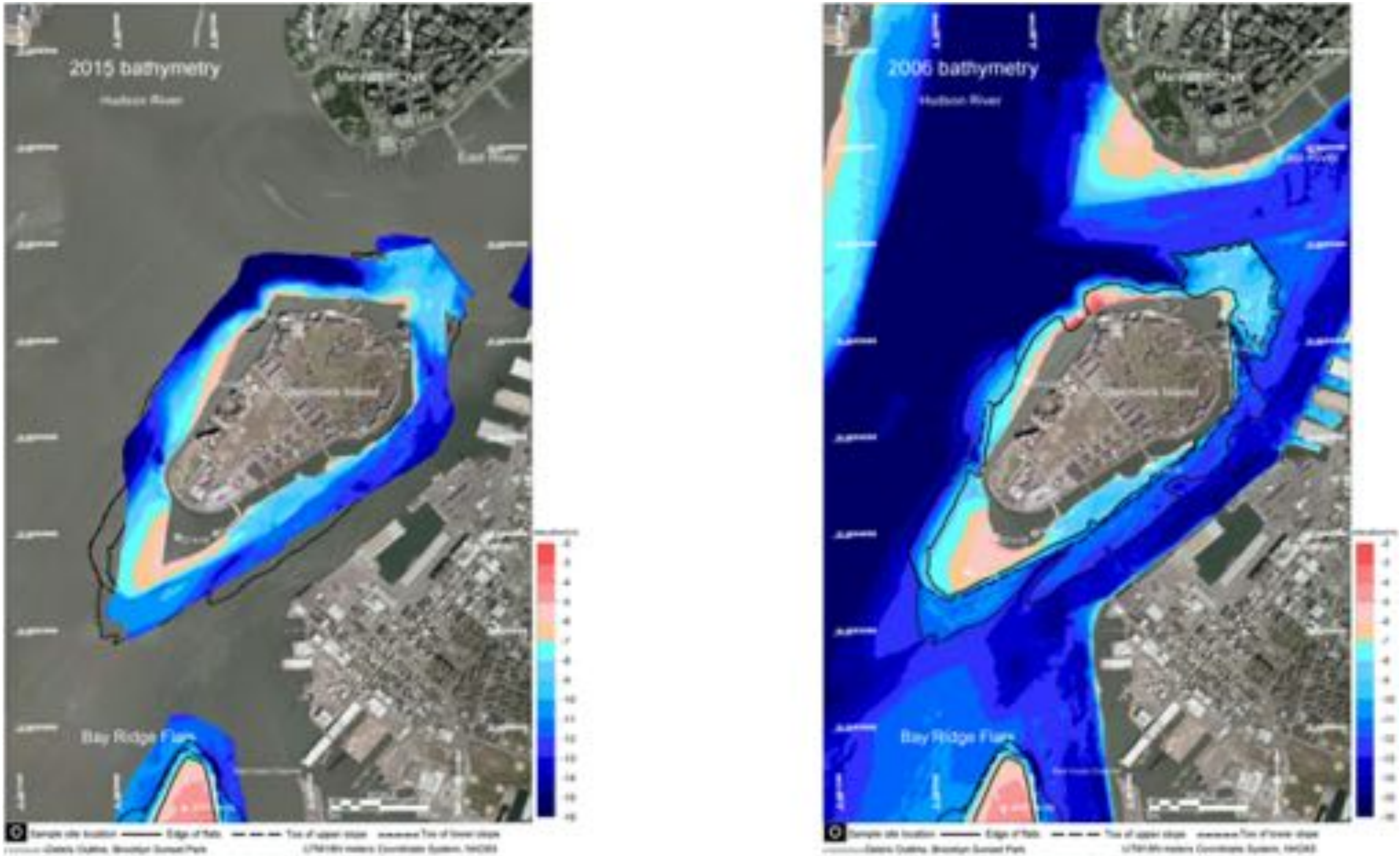

Figure 74. Bathymetric and location map for Governors Island. (Left) Multibeam data from e4sciences (2015) were combined in a 1m x 1m grid, using a triangular linear interpolation. (Right) Historical data from NOAA surveys H11353 (2004), H11395 (2006) and H11600 (2006) were combined in a 1m x 1m grid using a triangular linear interpolation.

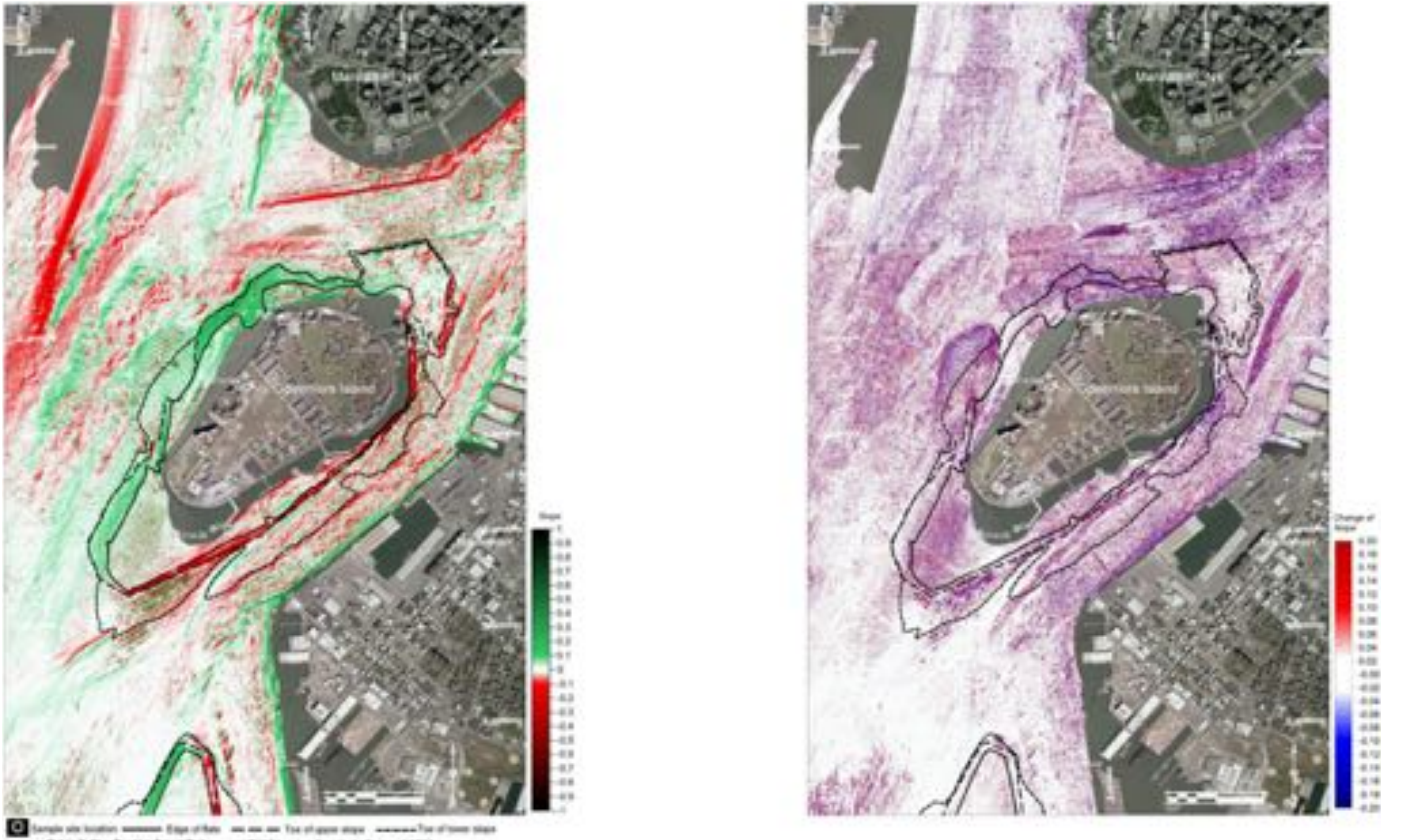

Figure 75. Bathymetric analysis for Governors Island (derivative maps for Area 2). Data from NOAA surveys H11353 (2004), H11395 (2006) and H11600 (2006) were combined in a 1m x 1m grid using a triangular linear interpolation. (Left) 2D first order derivative filter – slope. (Right) 2D second order derivative filter – change in slope.

Figure 76. Bathymetry elevation difference map 2015 minus 2006 for Governors Island. The 2015 bathymetry includes multibeam bathymetry from e4sciences. The 2006 bathymetry includes NOAA survey H11600. Data were combined in a 1m x 1m grid using a triangular linear interpolation.

5.2.2 Sediments (side-scan, seismic, cross sections, isopachs, grab samples)

Figure 77 is the side-scan orthosonograph for Governors Island insonified from the west. Figure 78 is its pair insonified from the east. Please note that the sediments in the south are finer-grained than those in the north.

Figure 79 is a sub-bottom seismic cross from south to north through the eastern shore of Governors Island. Figure 80 is the acoustic silt isopach. The acoustic silt is relatively thin on North Governors Island. In between the piers and on the southern end leeward of the East River outflow the acoustic silt thickens.

Table 13 lists the grain size mean and standard deviation. Note the variation of mean size and standard deviation with location.

Table 13. Governors Island grain size

Sample	Mean	Median	Std. Deviation
	Φ		
GI14-01	7.5	7.5	2.0
GI14-02	3.5	3.0	2.0
GI14-03	6.3	6.5	2.8
GI14-04	2.5	2.5	2.4
GI14-05	2.7	2.0	4.5
GI14-06	6.3	6.0	2.5
GI14-07	7.5	7.0	2.0
GI14-08	5.2	6.0	2.8
GI14-09	6.2	6.5	3.0

Table 14 lists the concentrations for lead, beryllium, and cesium.

Table 14. Governors Island Pb, ^{7}Be, and ^{137}Cs

Sample	Sample Date	Sample Time	Pb (ICPMS)	^{7}Be	^{7}Be Qualifiers	^{137}Cs	^{137}Cs Qualifiers
			mg/Kg	pCi/g		pCi/g	
GI14-01	11/4/14	11:22	140	0.000	U	-0.037	U
GI14-02	11/4/14	12:18	59	-0.337	U	0.064	U
GI14-03	11/4/14	13:55	210	-0.256	U	0.001	U
GI14-04	11/4/14	14:17	71	0.041	U	0.000	U
GI14-05	11/4/14	14:46	77	0.419	U	0.154	U
GI14-06	11/4/14	15:14	41	0.636	U	0.145	U
GI14-07	11/4/14	15:34	48	1.110	U	0.255	U
GI14-08	11/4/14	15:58	65	0.000	U	0.000	U
GI14-09	11/4/14	16:22	54	-0.062	U	0.038	U
U = Result is less than the sample detection limit							

Table 15 lists the measurements of acoustic compressional-wave velocity.

Table 15. Governors Island acoustic velocity

Sample	Average P Velocity	Average P Velocity
	[m/s]	[ft/s]
GI14-01	1,493.3	4,898.1
GI14-02	1,524.3	4,999.7
GI14-03	1,490.5	4,889.0
GI14-05	1,523.4	4,996.9
GI14-06	1,485.8	4,873.6
GI14-07	1,482.0	4,861.0
GI14-08	1,523.5	4,997.0
GI14-09	1,505.4	4,937.6

Table 16 lists the results of the XRF measurements.

Table 16. Governors Island XRF

Sample	S Avg	S Max	Fe Avg	Fe Max	Hg Avg	Hg Max	Zn Avg	Zn Max	Pb Avg	Pb Max	As Avg	As Max	Mn Avg	Mn Max
Push-Core	ppm													
GI14-01	2,974.03	3,971.36	15,819.13	19,413.60	< LOD	< LOD	155.56	196.52	139.89	178.85	15.86	18.72	108.41	149.62
GI14-02	3,856.75	4,486.02	18,453.66	19,953.37	< LOD	< LOD	192.10	216.43	174.76	201.76	14.67	14.67	130.15	149.60
GI14-03	4,602.69	5,852.25	17,986.40	20,625.94	< LOD	< LOD	197.93	254.26	173.61	229.84	24.41	41.13	146.44	243.03
GI14-04	3,583.18	4,042.68	18,121.25	19,375.03	< LOD	< LOD	133.44	175.62	158.06	179.33	18.79	21.37	180.48	208.94
GI14-05	3,904.35	4,701.13	15,599.52	17,946.26	< LOD	< LOD	102.08	135.12	66.75	104.56	13.44	13.44	205.86	217.63
GI14-06	3,587.79	4,994.55	17,306.54	20,355.61	< LOD	< LOD	145.19	200.10	119.73	185.24	16.78	21.91	160.03	228.85
GI14-07	2,678.17	3,803.88	18,158.75	34,489.82	< LOD	< LOD	135.22	163.61	99.02	130.43	15.37	16.97	163.77	529.69
GI14-08	4,428.24	4,977.45	16,909.33	18,283.09	< LOD	< LOD	143.26	190.45	122.75	166.44	< LOD	< LOD	189.86	214.36
GI14-09	2,392.57	3,190.34	16,643.77	19,494.71	< LOD	< LOD	69.16	84.31	36.13	46.92	< LOD	< LOD	182.14	262.19

*<LOD = below Limit Of Detection

Figure 77. Governors Island orthosonograph insonified from the west.

Figure 78. Governors Island orthosonograph insonified from the east.

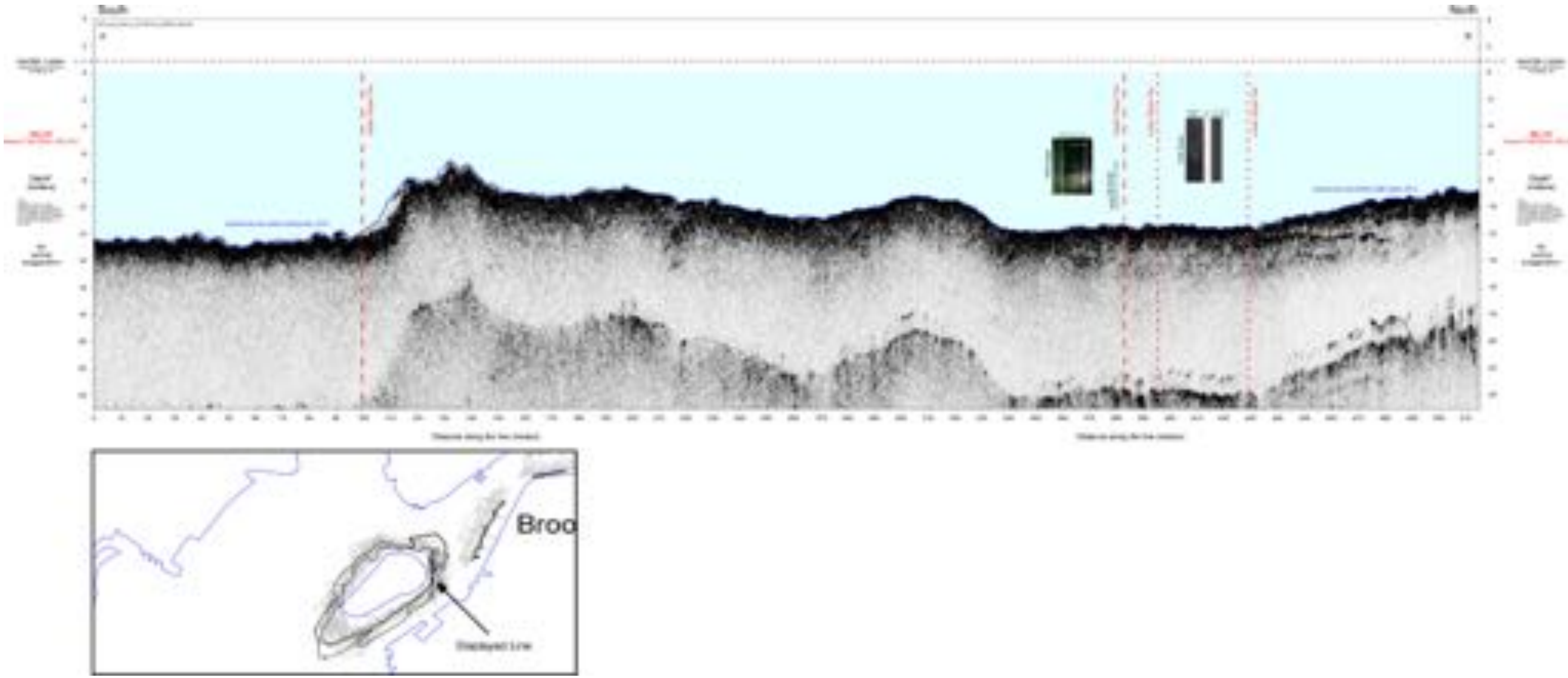

Figure 79. Seismic cross section, Governors Island.

Figure 80. Acoustic silt isopach map, Governors Island.

5.2.3 Bottom classification (SPI, benthic classification)

Figure 81 displays the geological and structural substrate for Governors Island. Figure 82 plots the density of individual organisms per square meter. Data in GI were too sparse to plot as a TIN at this scale accurately. The data are displayed as point values corresponding to each sample location overlain on the slope toes derived from e4's bathymetric analysis. Figure 83 plots the composite bottom classification.

Eighteen analyzable images were collected from around Governors Island (GI). Sediment type tended to have a higher percentage sand and gravel and was more similar to the sediment of Bay Ridge Flats (BRF) than the sediment sampled in the slips and marinas around Brooklyn and Manhattan. Camera depth had a lower average penetration value of 10.81cm than the drops deployed within the slips and marinas. The aRPD tended to be shallower at the GI sites with aRPD values ranging between 0.5 to 3.0 and only two sites had aRPD measured depths >3.75cm. There were bits of shellhash, including oyster shellhash, present at 7 of the 18 sites analyzed. Major modal grain size tended to be in the 3 to 4 phi class size range. Neither anoxia at the surface nor methane was present. Small, Stage I worm tubes were commonly found in the analyzed images. Nine of the 18 sites had an OSI value greater than 6. The other sites had OSI values ranging from 2 to 4. These lose OSI values corresponded with sediment traps with high rates of sediment accumulation due to tidal action in the area. Both physical and biological processes were responsible for surface roughness. Four sites had successional stage classified as I-II; feeding voids were absent and a shallow aRPD was typically shallow. Six sites were classified as having only Stage I organisms (small opportunistic species) present. The remaining sites at GI were classified as Stage I on III – Stage I assemblages are occurring at the same place and time as evidence of Stage III organisms. Epifauna was not observed. Surface roughness was attributed to both physical and biological factors. Overall, GI presents a more complex picture than other areas within the harbor. It offers a wide diversity of substrates for benthic organisms, not all of which support infauna. Tides and currents around GI are also complex producing a dynamic environment with episodic movement of both sand and black silt. This contributes to the wide range of OSI values observed at the sites sampled in GI.

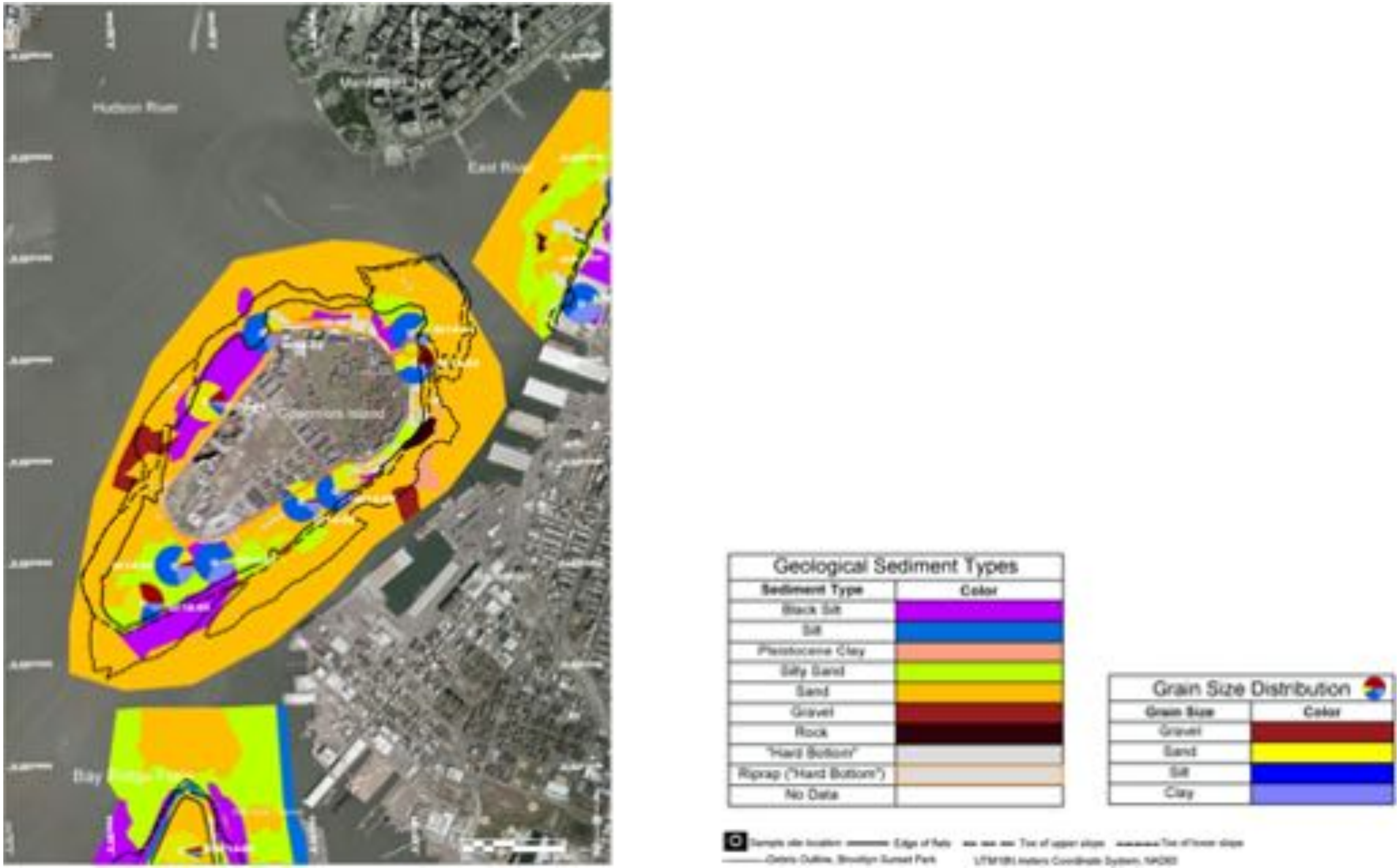

Figure 81. Bottom sediment type and geological substrate map for Governors Island.

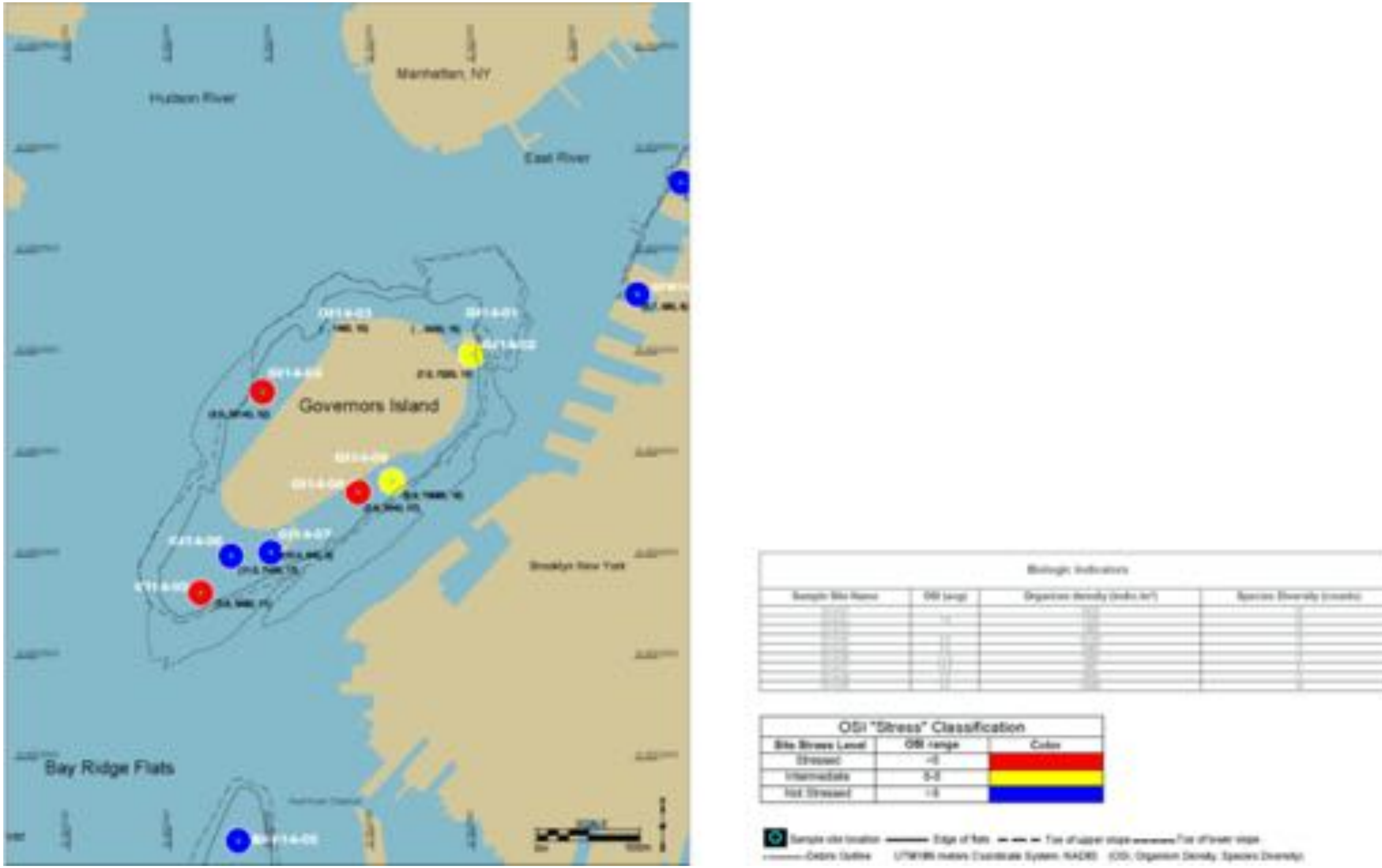

Figure 82. Organism density map for Governors Island. The numbers at each site represent the triplet (OSI, organism density per square meter, diversity as total number of species). In the cases of no measurement the space is left blank.

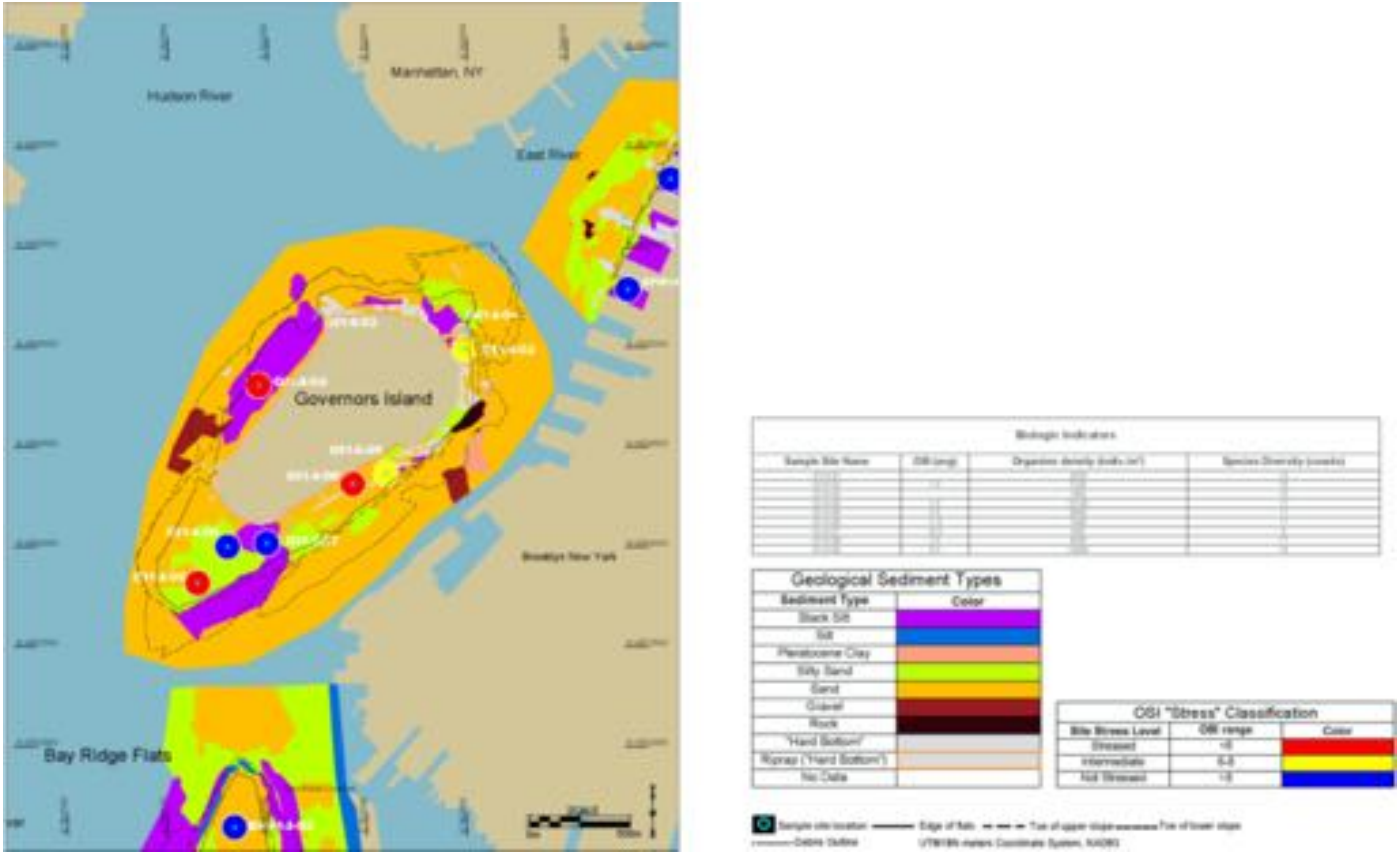

Figure 83. Composite bottom classification map for Governors Island.

5.3 Area Report 3. Sunset Park waterfront

5.3.1 Morphology (Bathymetry, bathymetry analysis)

Figure 84 is a location photograph for Sunset Park waterfront. Note the structures include Pier 5 at the mouth of the Gowanus Canal through Pier 39 near the Brooklyn Army Terminal.

Figure 85 is the bathymetry for the Sunset Park waterfront. Single and multibeam data from e4sciences (2015) were combined in 5m x 5m and 1m x 1m grids, respectively, using a triangular linear interpolation. Historical data from NOAA survey H11600 (2006) were combined in a 1m x 1m grid using a triangular linear interpolation. 2D first and second order derivative filters were applied to the 2006 historical bathymetry. Figure 86 plots the derivative maps for the 2006 historical bathymetry. Figure 87 is the difference map between 2015 and 2006. The map displays both results of the difference in bathymetry for the 5m x 5m grid in the ultrashallow area, and the 1m x 1m grid in the deeper area. All grids were obtained with triangular linear interpolations.

Figure 84. Location photo for Sunset Park waterfront.

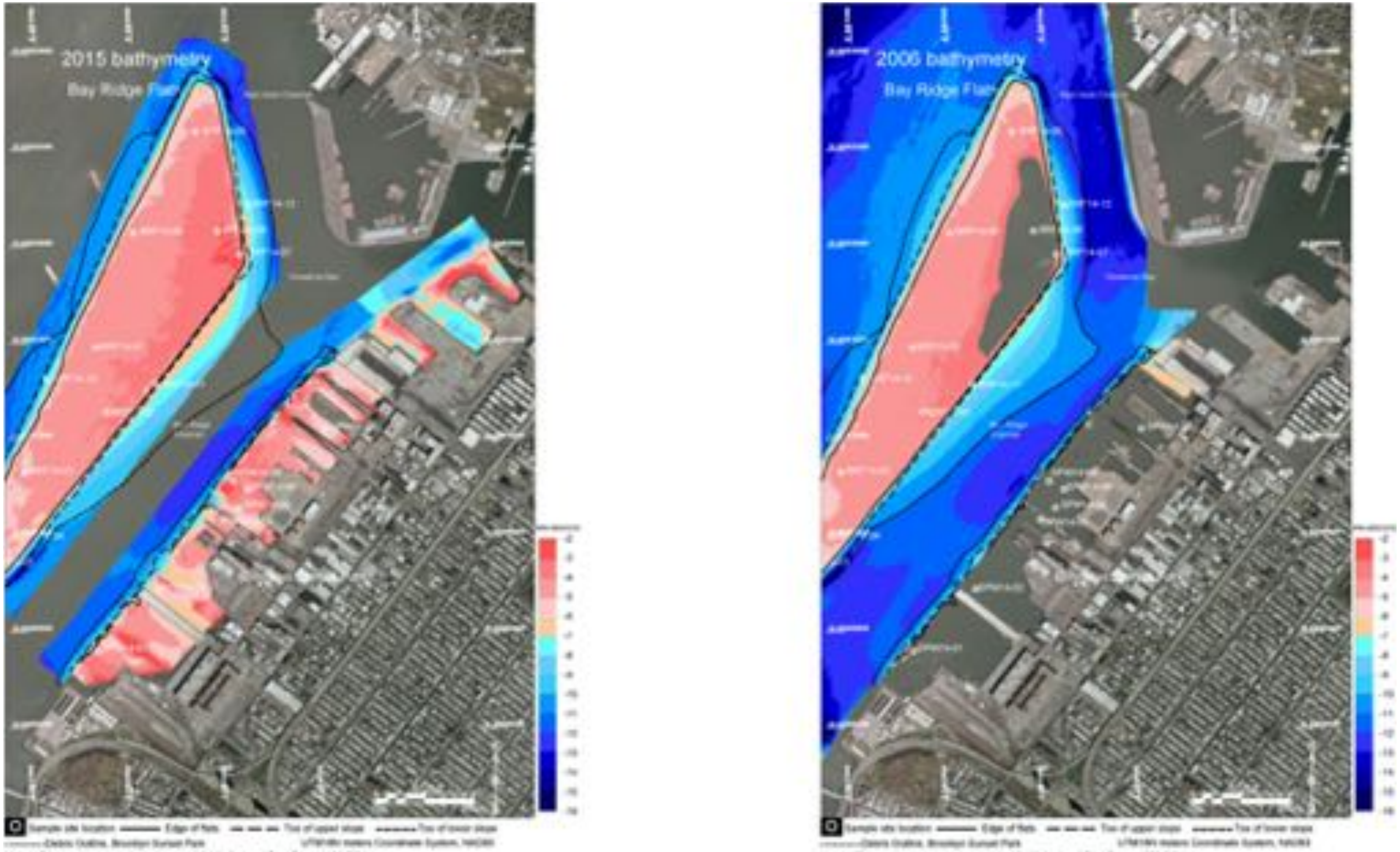

Figure 85. Bathymetric and location map for Sunset Park waterfront. (Left) Single and multibeam data from e4sciences (2015) were combined in 5m x 5m and 1m x 1m grids, respectively, using a triangular linear interpolation. (Right) Historical data from NOAA survey H11600 (2006) were combined in a 1m x 1m grid using a triangular linear interpolation.

Figure 86. Bathymetric analysis for Sunset Park waterfront (derivative maps for Area 3). Data from NOAA survey H11600 (2006) were combined in a 1m x 1m grid using a triangular linear interpolation. (Left) 2D first order derivative filter – slope. (Right) 2D second order derivative filter – change in slope.

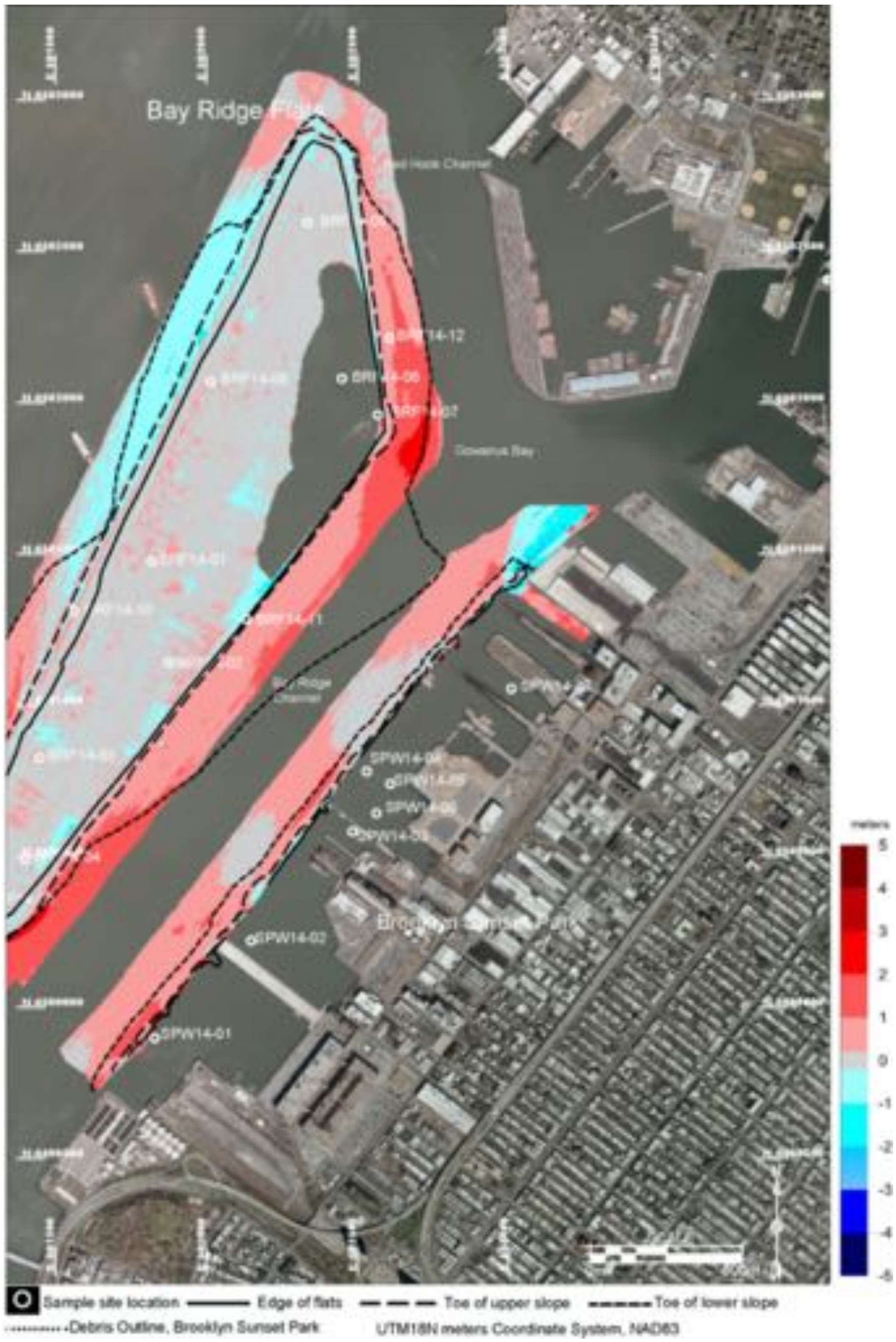

Figure 87. Bathymetry elevation difference map 2015 minus 2006 for Sunset Park waterfront. The 2015 bathymetry includes single and multibeam bathymetries from e4sciences. The 2006 bathymetry includes NOAA survey H11600. The map displays both results of the difference in bathymetry for the 5m x 5m grid in the ultrashallow area, and the 1m x 1m grid in the deeper area. All grids were obtained with triangular linear interpolations.

5.3.2 Sediments (side-scan, seismic, cross sections, isopachs, grab samples)

Figure 88 displays the orthosonograph of Sunset Park waterfront insonified from the west and north. Figure 89 is its pair insonified from the east and the south.

Figure 90 is a sub-bottom seismic cross from west to east through the Sunset Park waterfront. Figure 91 is the acoustic silt isopach. The acoustic silt is thicker in between the piers.

Table 17 lists the grain size mean and standard deviation. Note the variation with location is small. The materials in the piers are fine-grained.

Table 17. Sunset Park waterfront grain size

Sample	Mean	Median	Std. Deviation
	Φ		
SPW14-01	6.8	6.5	1.5
SPW14-02	7.7	7.0	1.8
SPW14-03	6.5	6.5	0.5
SPW14-04	6.2	6.5	0.5
SPW14-05	6.5	6.5	0.5
SPW14-06	6.5	6.5	0.5
SPW14-07	7.8	7.0	2.0

Table 18 lists the measurements of lead, beryllium, and cesium.

Table 18. Sunset Park waterfront Pb, ^{7}Be, and ^{137}Cs

Sample	Sample Date	Sample Time	Pb (ICPMS)	^{7}Be	^{7}Be Qualifiers	^{137}Cs	^{137}Cs Qualifiers
			mg/Kg	pCi/g		pCi/g	
SPW14-01	11/3/14	15:37	34	0.338	U	0.148	U
SPW14-02	11/3/14	16:14	32	0.000	U	0.145	U
SPW14-03	11/4/14	6:40	28	0.022	U	0.008	U
SPW14-04	11/4/14	7:11	29	-0.003	U	0.086	U
SPW14-05	11/4/14	7:42	32	0.935	U	0.162	U
SPW14-06	11/4/14	8:12	34	0.832	U	0.211	
SPW14-07	11/4/14	8:21	29	0.114	U	0.163	U
U = Result is less than the sample detection limit							

Table 19 lists the measurement of compressional-wave velocity.

Table 19. Sunset Park waterfront acoustic velocity

Sample	Average P Velocity	Average P Velocity
	[m/s]	[ft/s]
SPW14-03	1,481.3	4,858.7
SPW14-04	1,483.2	4,865.0
SPW14-06	1,479.5	4,852.7
SPW14-07	1,482.7	4,863.4

Table 20 lists the XRF results for other elements observed in the sediments.

Table 20. Sunset Park waterfront XRF.

Sample	S Avg	S Max	Fe Avg	Fe Max	Hg Avg	Hg Max	Zn Avg	Zn Max	Pb Avg	Pb Max	As Avg	As Max	Mn Avg	Mn Max
Push-Core	ppm													
SPW-14-01	2,148.59	3,914.40	14,615.30	17,756.87	< LOD	< LOD	59.32	81.07	31.39	37.12	9.62	10.59	140.34	187.08
SPW14-02	1,270.33	1,763.53	12,857.72	14,605.44	< LOD	< LOD	52.31	58.65	28.56	34.01	7.94	7.94	121.66	146.52
SPW14-03	1,974.69	2,632.70	16,574.39	21,316.04	< LOD	< LOD	67.08	83.35	31.93	39.20	10.55	10.55	139.96	156.02
SPW14-04	1,826.67	2,644.13	15,466.89	18,883.17	< LOD	< LOD	59.34	69.31	32.23	36.34	8.79	9.12	101.70	118.63
SPW14-05	2,336.31	2,966.14	14,415.59	17,928.88	< LOD	< LOD	74.59	101.87	41.64	51.17	< LOD	< LOD	103.59	149.82
SPW14-06	2,318.50	2,966.04	15,288.10	19,245.40	< LOD	< LOD	64.21	78.96	32.61	39.32	< LOD	< LOD	124.29	161.35
SPW14-07	2,228.24	3,181.63	14,417.87	16,261.55	< LOD	< LOD	56.23	65.43	31.90	41.29	< LOD	< LOD	117.97	156.93
*<LOD = below Limit Of Detection														

Figure 88. Sunset Park waterfront orthosonograph insonified from the west.

Figure 89. Sunset Park orthosonograph insonified from the east.

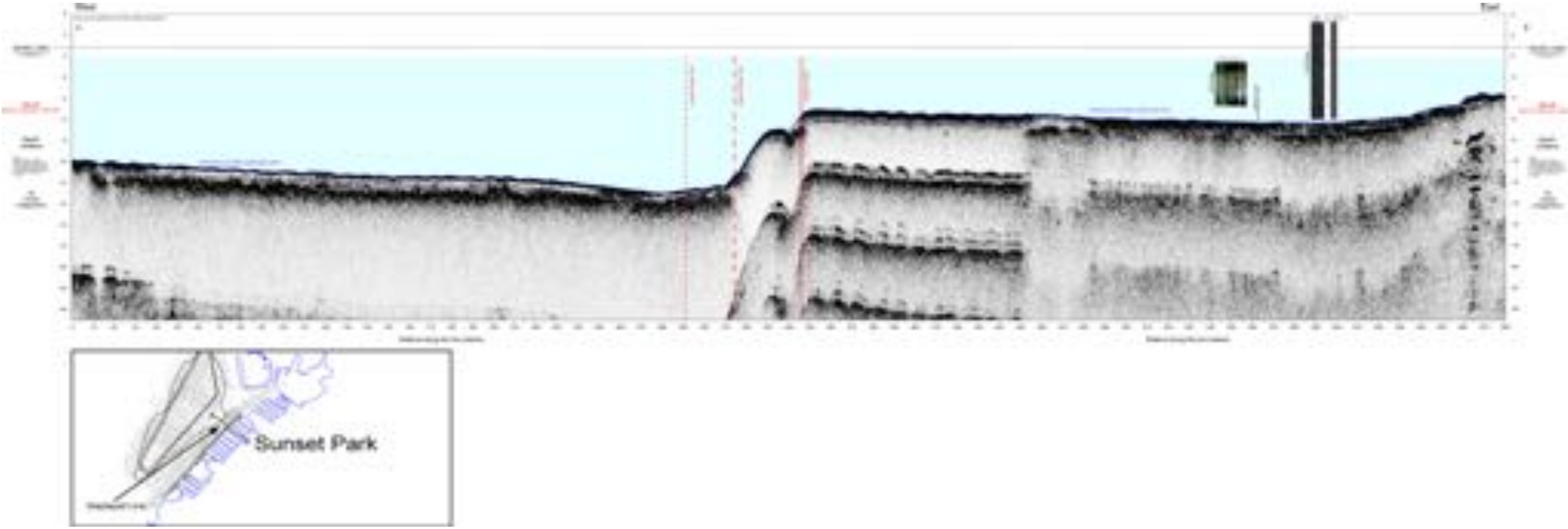

Figure 90. Seismic cross section, Sunset Park waterfront.

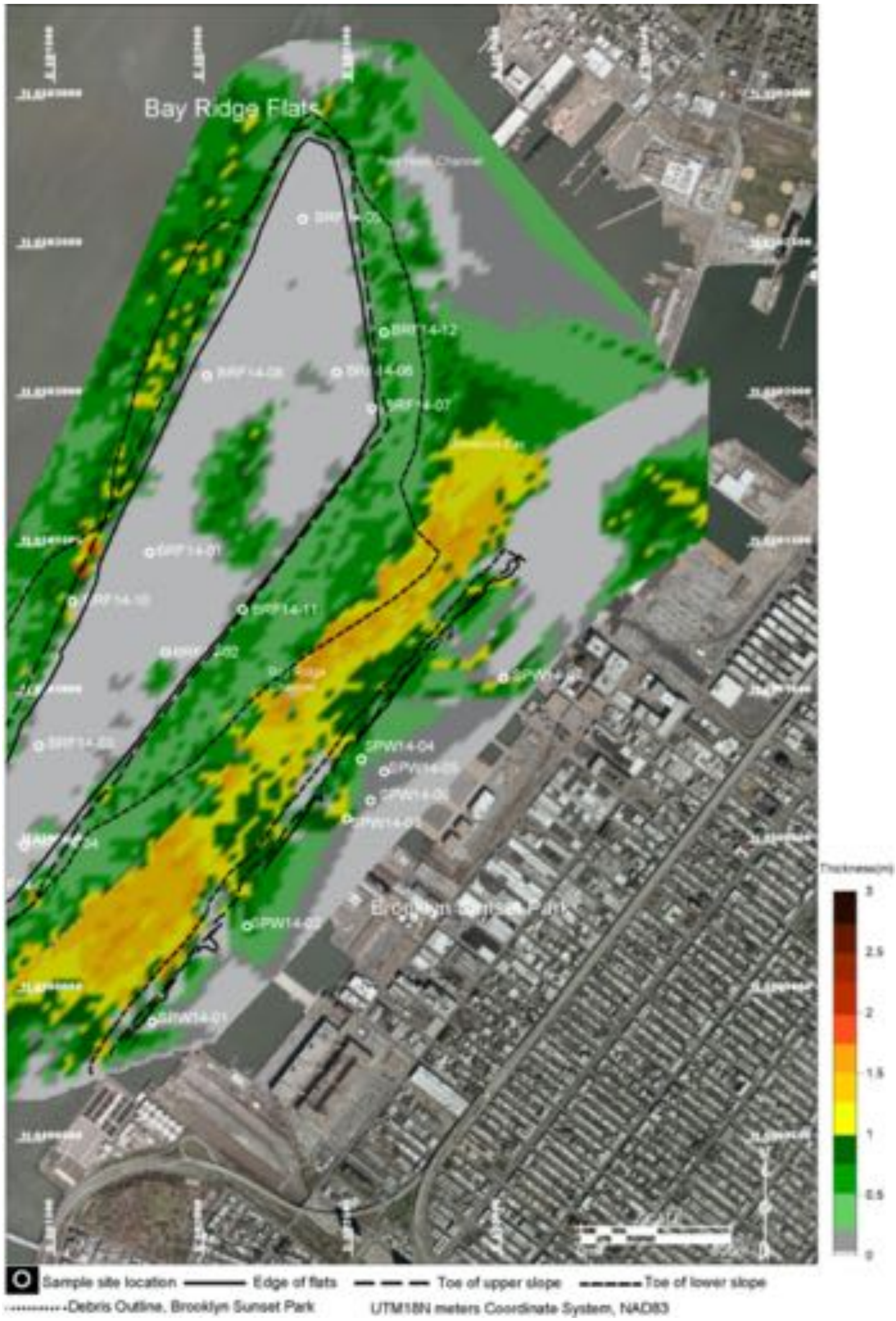

Figure 91. Acoustic silt isopach map for Sunset Park waterfront.

5.3.3 Bottom classification (SPI, benthic classification)

Figure 92 displays the geological and structural substrate for Sunset Park waterfront. Figure 93 plots the density of individual organisms per square meter. Figure 94 plots the composite bottom classification.

Fourteen analyzable images were collected at Sunset Park waterfront (SPW). Average SPI camera penetration was approximately 12cm and the most frequent aRRD category for images was 3.01 to 3.75cm depth. Only one site had an aRPD measurement shallower than 2.0cm at SPW. Epifaunal mud snails (*Illyansa obsoleta*) were observed at 6 of the 14 sites sampled. Major modal grain size was >4 phi class for the fourteen images analyzed. No anoxia at the surface or methane was present in the SPW images. Surface roughness was attributed to biological activities. Small, Stage I worm tubes were visible and numerous and with aRPD depths greater than 3.75cm. The benthic communities at Sunset Park Waterfront were attributed a successional stage of I on III – stage I assemblages are occurring at the same place and time as evidence of stage III organisms – with feeding voids visible in 5 of the 14 images. Several burrows (small and large) were also observed. SPW images were collected from between actively occupied boat slips. OSI values for the 14 sites were greater than 6, with 7 of the 14 sites having high OSI values of 10 or greater. Evidence of boating activity such as clay clasts at the surface from lower sediment layers was observed within the analyzed images. Sediment texture samples collected from benthic grabs at the SPW sites were composed predominantly of more than 93% silt and clay.

The Gowanus Canal (a designated Superfund site) and the Gowanus Bay area represent one of the most impacted areas within the Upper Harbor-Brooklyn Flats region. Benthos in the Gowanus Canal, while limited because of the highly toxic nature of the sediments, consists primarily of pollution-tolerant tubiculous amphipods and polychaetes (capitellids and spionids) (Gardner, Nystroem, & Aulisio 2007; Farrell 2012). Fouling organisms, including blue mussels, barnacles, bryozoans, isopods, and crabs (e.g. Pacific shore crab and a green crab) have been found in Gowanus Bay, associated with pilings and other hard surfaces (Drake & Kim 2011; Farrell 2012).

Despite this history of pollution, we observed sites with high OSI values in SPW. These generally correspond to areas with moderate sediment accumulation and thick layers of old black silt into which benthic infaunal organisms can burrow. High organism density in this area of opportunistic, Stage I organisms is encouraging for the potential progress this indicates toward a healthier harbor. Attempts to limit sediment movement and disturbance in this are would encourage these sites to continue progressing toward stronger, better established benthic habitat.

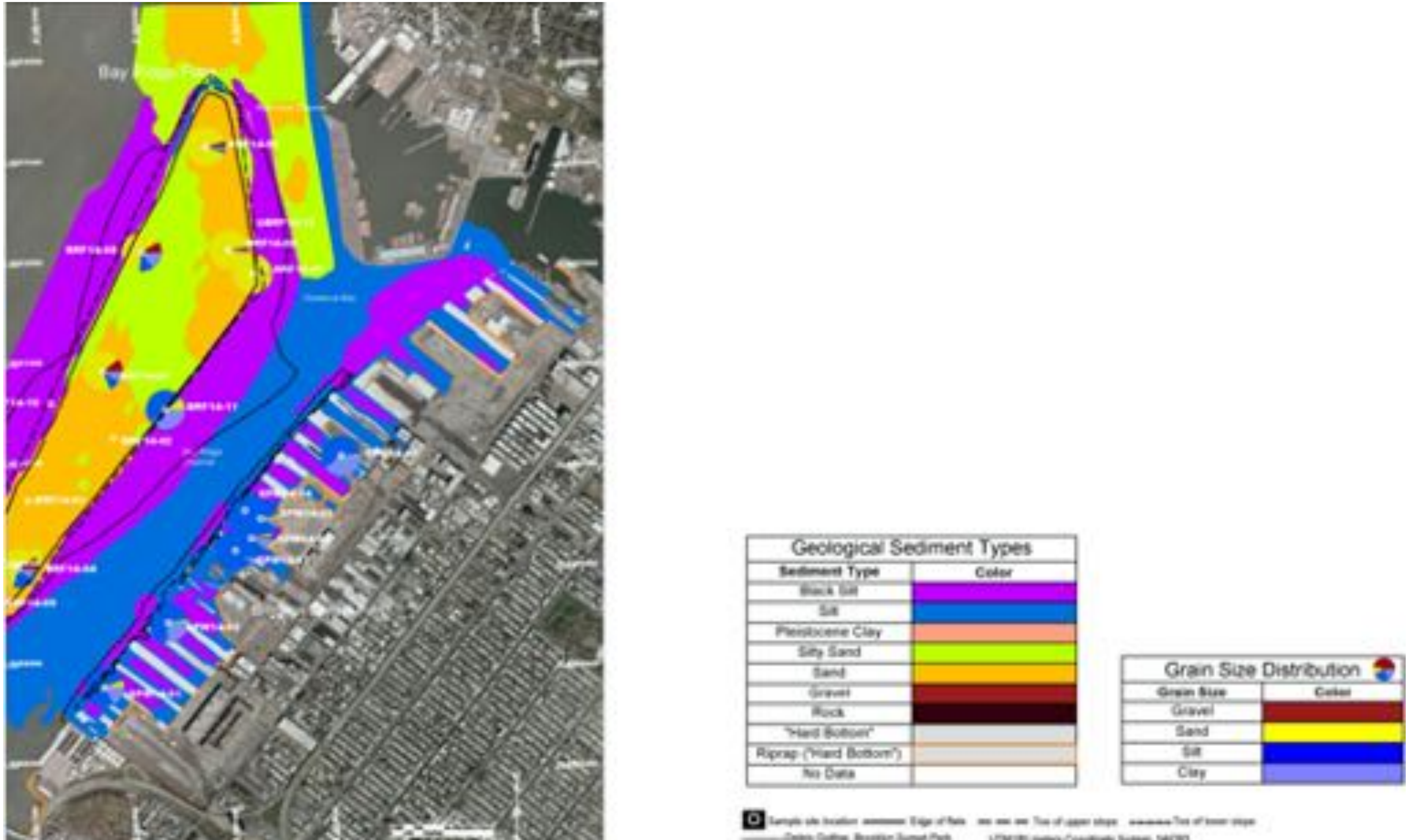

Figure 92. Bottom sediment type and geological substrate map for Sunset Park waterfront.

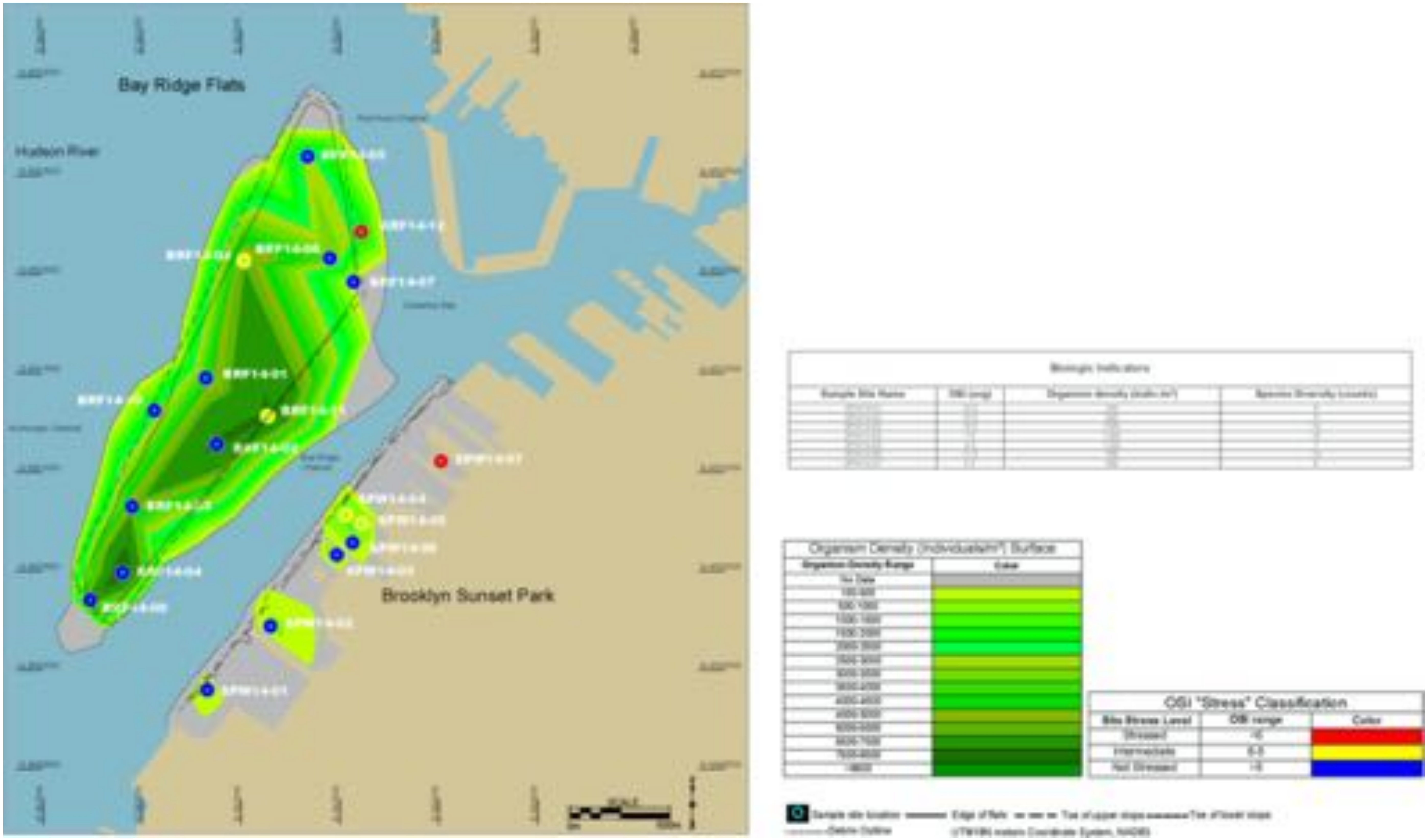

Figure 93. Organism density map for Sunset Park waterfront. The numbers at each site represent the triplet (OSI, organism density per square meter, diversity as total number of species). In the cases of no measurement the space is left blank.

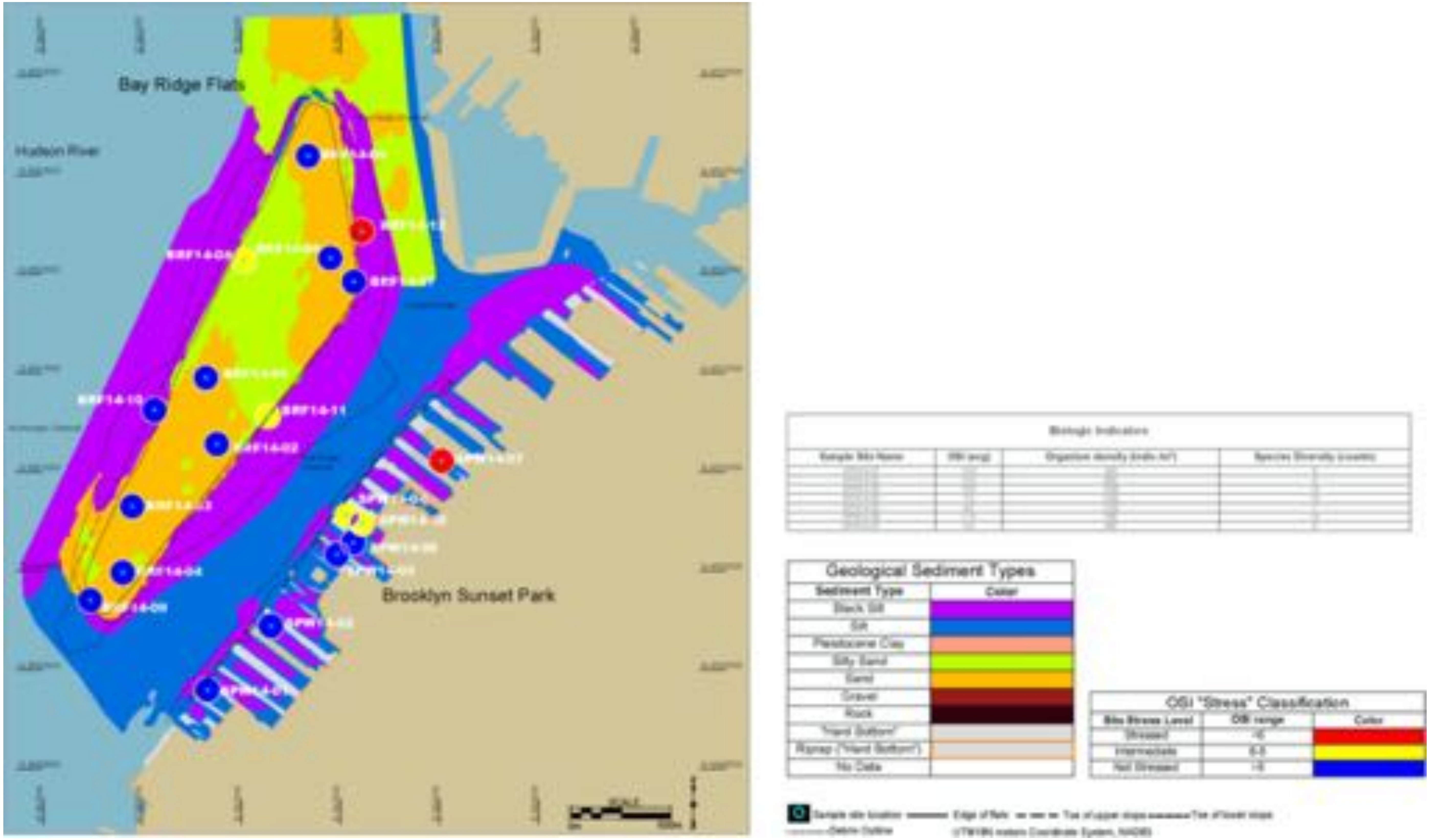

Figure 94. Composite bottom classification map for Sunset Park waterfront.

5.4 Area Report 4. Brooklyn Bridge Park

5.4.1 Morphology (Bathymetry, bathymetry analysis)

Figure 95 is a location photograph for Brooklyn Bridge Park. Note the structures include piers and bridge abutments for the Brooklyn Bridge and Manhattan Bridge.

Figure 96 is the bathymetry for the Brooklyn Bridge Park. Single and multibeam data from e4sciences (2015) were combined in 5m x 5m and 1m x 1m grids, respectively, using a triangular linear interpolation. Historical data from NOAA survey H11353 (2004) were combined in a 1m x 1m grid using a triangular linear interpolation. 2D first and second order derivative filters were applied to the 2006 historical bathymetry. Figure 97 plots the derivative maps for the bathymetry. Figure 98 is the difference map between 2015 and 2006. The map displays both results of the difference in bathymetry for the 5m x 5m grid in the ultrashallow area, and the 1m x 1m grid in the deeper area. All grids were obtained with triangular linear interpolations.

Figure 95. Location photo for Brooklyn Bridge Park.

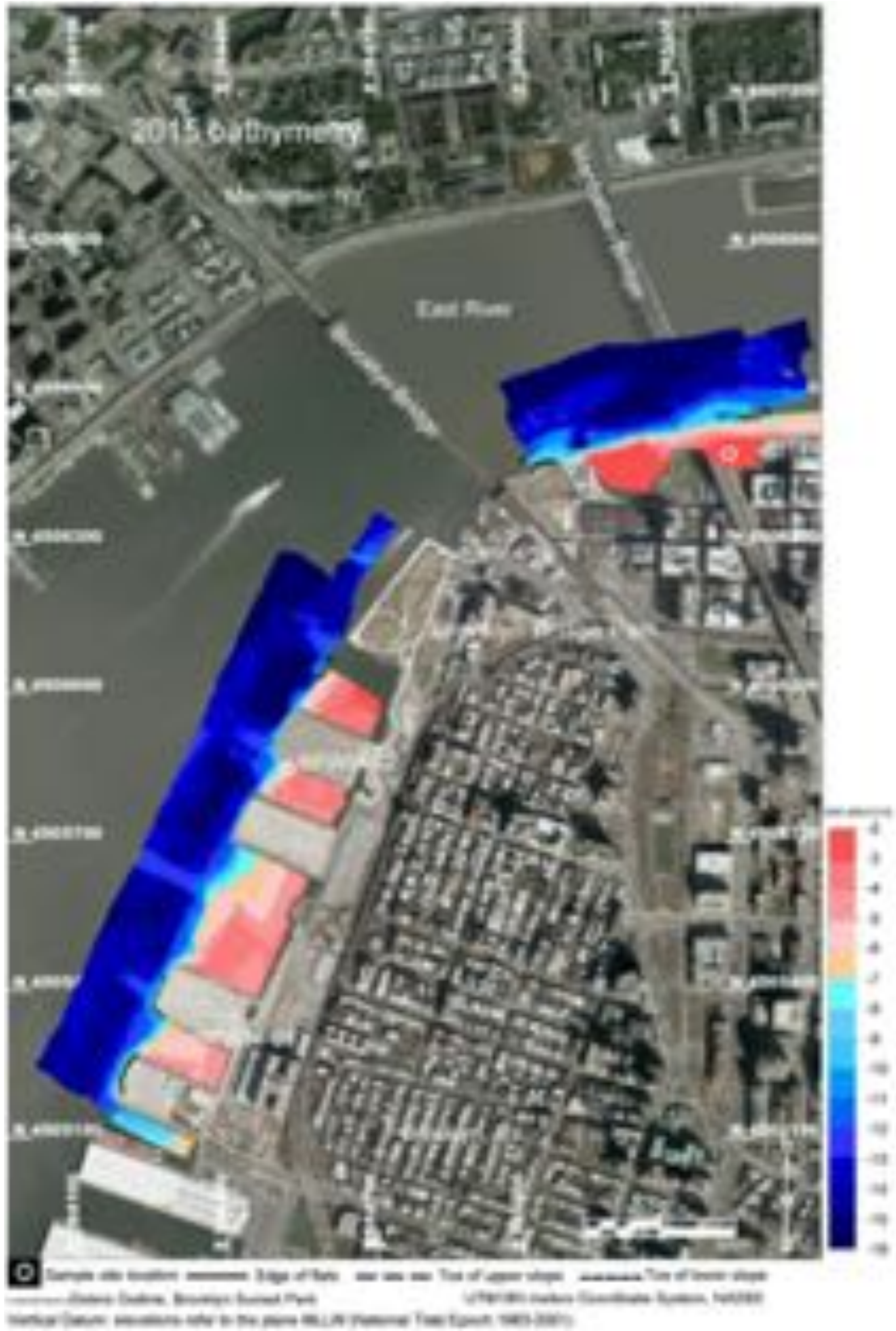

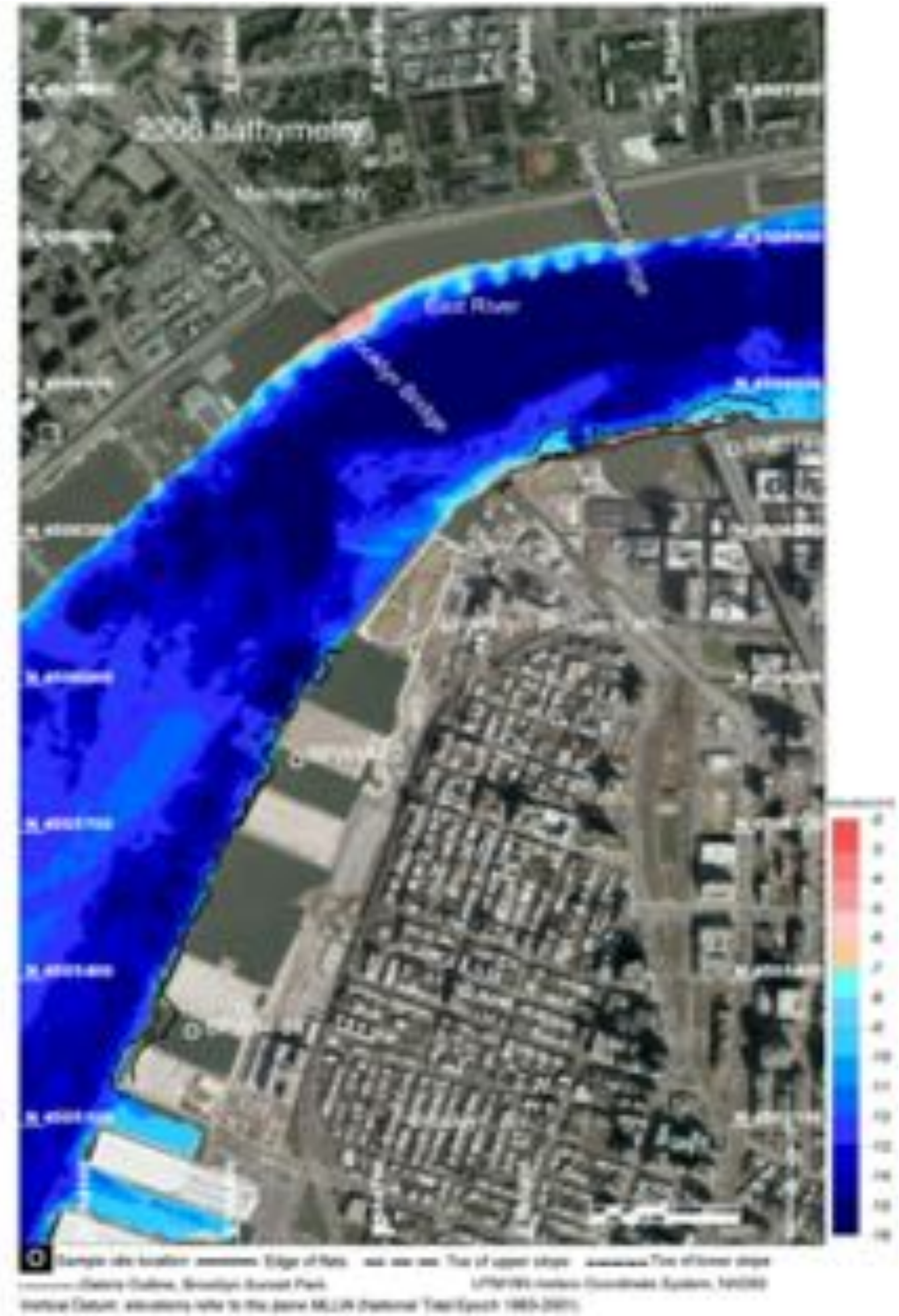

Figure 96. Bathymetric and location map for Brooklyn Bridge Park. (Left) Single and multibeam data from e4sciences (2015) were combined in 5m x 5m and 1m x 1m grids, respectively, using a triangular linear interpolation. (Right) Historical data from NOAA survey H11353 (2004) were combined in a 1m x 1m grid using a triangular linear interpolation.

Figure 97. Bathymetric analysis for Brooklyn Bridge Park (derivative maps for Area 4). Data from NOAA survey H11353 (2004) were combined in a 1m x 1m grid using a triangular linear interpolation. (Left) 2D first order derivative filter – slope. (Right) 2D second order derivative filter – change in slope.

Figure 98. Bathymetry elevation difference map 2015 minus 2006 for Brooklyn Bridge Park. The 2015 bathymetry includes single and multibeam bathymetries from e4sciences. The 2006 bathymetry includes NOAA survey H11353 (2004). The map displays both results of the difference in bathymetry for the 5m x 5m grid in the ultrashallow area, and the 1m x 1m grid in the deeper area. All grids were obtained with triangular linear interpolations.

5.4.2 Sediments (side-scan, seismic, cross sections, isopachs, grab samples)

Figure 99 displays the orthosonograph of Brooklyn Bridge Park insonified from the west and north. Figure 100 is its pair insonified from the east and the south.

Figure 101 is a sub-bottom seismic cross from west to east through the Brooklyn Bridge Park. Figure 102 is the acoustic silt isopach.

Table 21 lists the grain size mean and standard deviation. Note the large variation of mean size and standard deviation with location.

Table 21. Brooklyn Bridge Park grain size

Sample	Mean	Median	Std. Deviation
	Φ		
BMB14-01	2.2	2.0	6.3
BPW14-01	7.8	7.5	2.0
BPW14-02	7.7	7.5	2.5

Table 22 lists the measurements of lead, beryllium, and cesium.

Table 22. Brooklyn Bridge Park Pb, ^{7}Be, and ^{137}Cs

Sample	Sample Date	Sample Time	Pb (ICPMS)	^{7}Be	^{7}Be Qualifiers	^{137}Cs	^{137}Cs Qualifiers
			mg/Kg	pCi/g		pCi/g	
BMB14-01	11/4/14	13:05	450	0.203	U	0.000	U
BPW14-01	11/4/14	9:32	40	0.613	U	0.421	
BPW14-02	11/4/14	12:36	43	0.761	U	0.137	U
U = Result is less than the sample detection limit							

Table 23 lists the measurement of compressional-wave velocity.

Table 23. Brooklyn Bridge Park acoustic velocity

Sample	Average P Velocity	Average P Velocity
	[m/s]	[ft/s]
BMB14-01	1,532.1	5,025.4

Table 24 lists the XRF results for other elements observed in the sediments.

Table 24. Brooklyn Bridge Park XRF

Sample	S Avg	S Max	Fe Avg	Fe Max	Hg Avg	Hg Max	Zn Avg	Zn Max	Pb Avg	Pb Max	As Avg	As Max	Mn Avg	Mn Max
Push-Core	ppm													
BMB14-01	5,296.20	5,923.88	15,614.15	15,696.94	< LOD	< LOD	178.10	190.50	308.06	314.05	32.46	32.46	107.60	115.13
BPW14-01	1,596.65	2,312.32	15,013.30	17,434.42	< LOD	< LOD	58.44	71.99	34.08	45.09	< LOD	< LOD	194.31	254.15
BPW14-02	1,757.67	3,169.48	16,927.78	18,856.64	< LOD	< LOD	67.87	76.13	34.90	52.51	8.72	8.72	208.66	285.54
*<LOD = below Limit Of Detection														

Figure 99. Brooklyn Bridge Park orthosonograph insonified from the west.

Figure 100. Brooklyn Bridge Park orthosonograph insonified from the east.

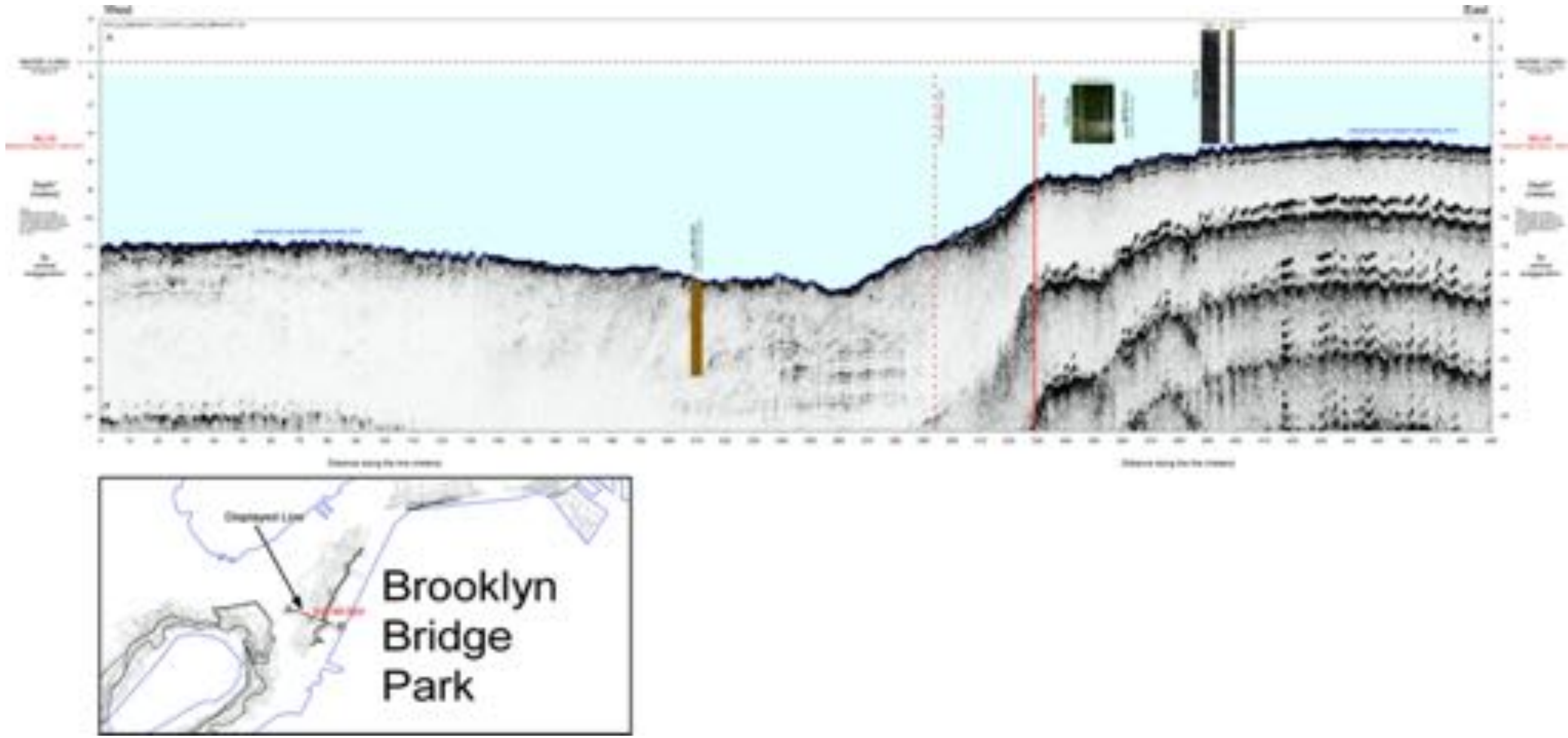

Figure 101. Seismic cross section, Brooklyn Bridge Park. The boring BC-98-029 is a USACE boring acquired in 1998. For more information regarding this boring, please contact e4sciences, LLC.

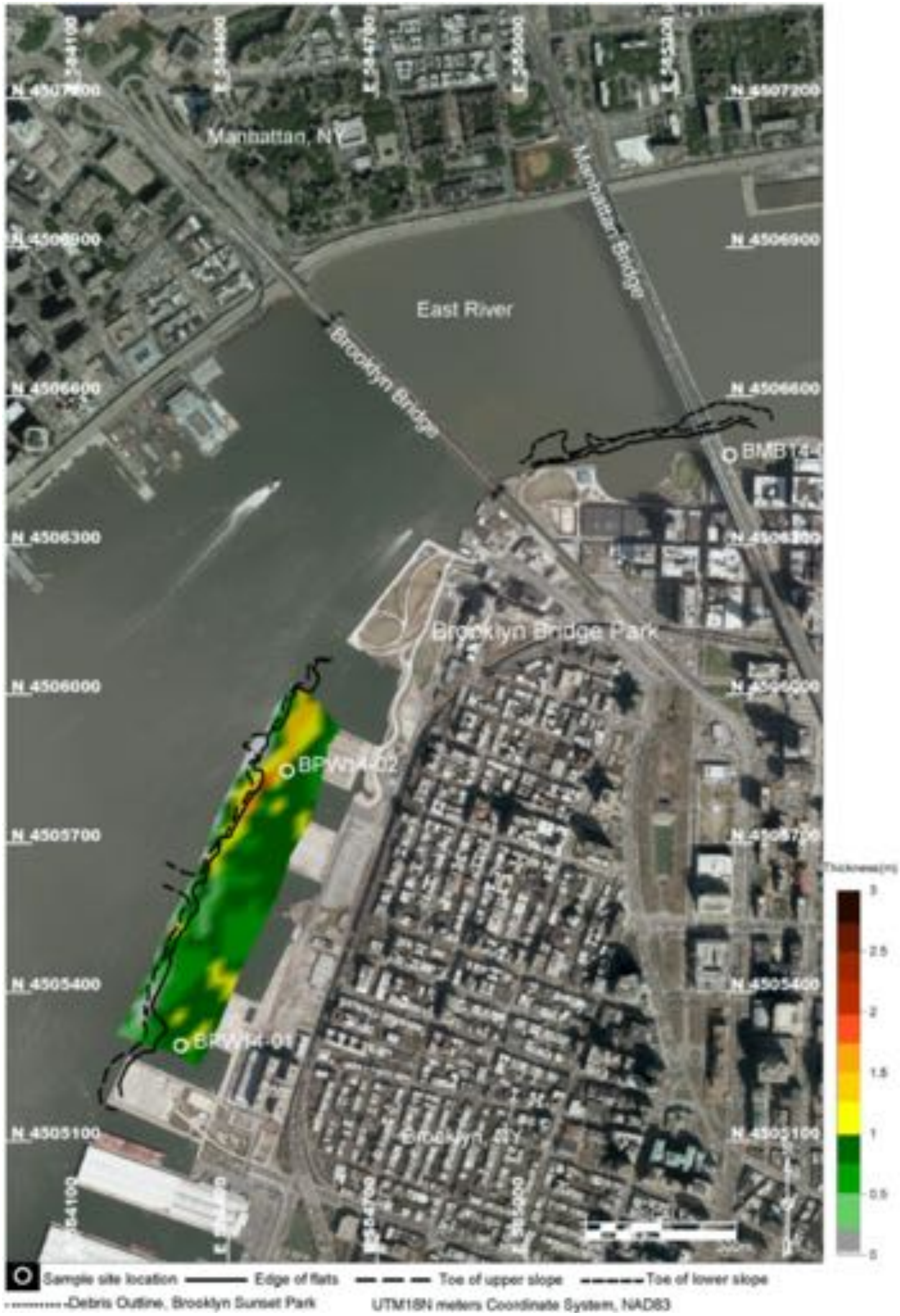

Figure 102. Acoustic silt isopach map for Brooklyn Bridge Park.

5.4.3 Bottom classification (SPI, benthic classification)

Figure 103 displays the geological and structural substrate for Brooklyn Bridge Park. Figure 104 plots the density of individual organisms per square meter. Figure 105 plots the composite bottom classification.

Six analyzable images were collected at the Brooklyn Bridge Park (BBP) area. Average penetration depth at the BBP sites was approximately 13cm. Five of the six drops analyzed had an average SPI camera penetration depth greater than 3.0 with one drop having an aRPD value of 2.99cm. Major modal grain size was >4 phi class for the six sites analyzed. No anoxia at the surface or methane was present in the BBP images. Surface roughness was attributed to biological activities. Small worm tubes and microvoids were visible in the analyzable images. Successional stage for the six images was attributed to I on III – Stage I assemblages are occurring at the same place and time as evidence of Stage III organisms. Burrows were visible in half the images but no epifauna were observed. Three samples were taken from benthic grabs to analyze for sediment texture. Two of the three samples were >95% fine sediment (silt and clay) while the third location contained 41% fine sediment, 46% gravel with 12% sand. Sediment type at BBP was patchy and sites closer to nearshore had more gravel and sand than sites located further into the Harbor. Both sites in BBP with calculated OSI values were not stressed and had high OSI values. BBP provides another example of the apparently healthy benthic communities that can establish themselves – even at contaminated sites – if left largely undisturbed by large-scale sediment movement.

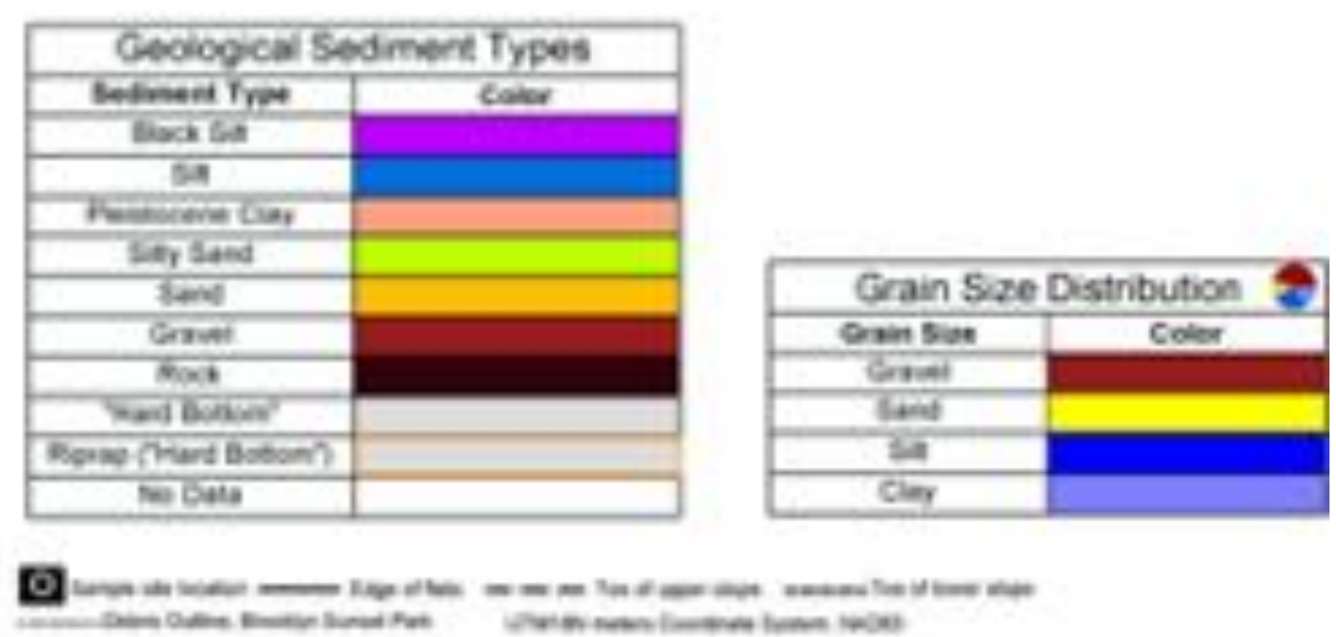

Figure 103. Bottom sediment type and geological substrate map for Brooklyn Bridge Park.

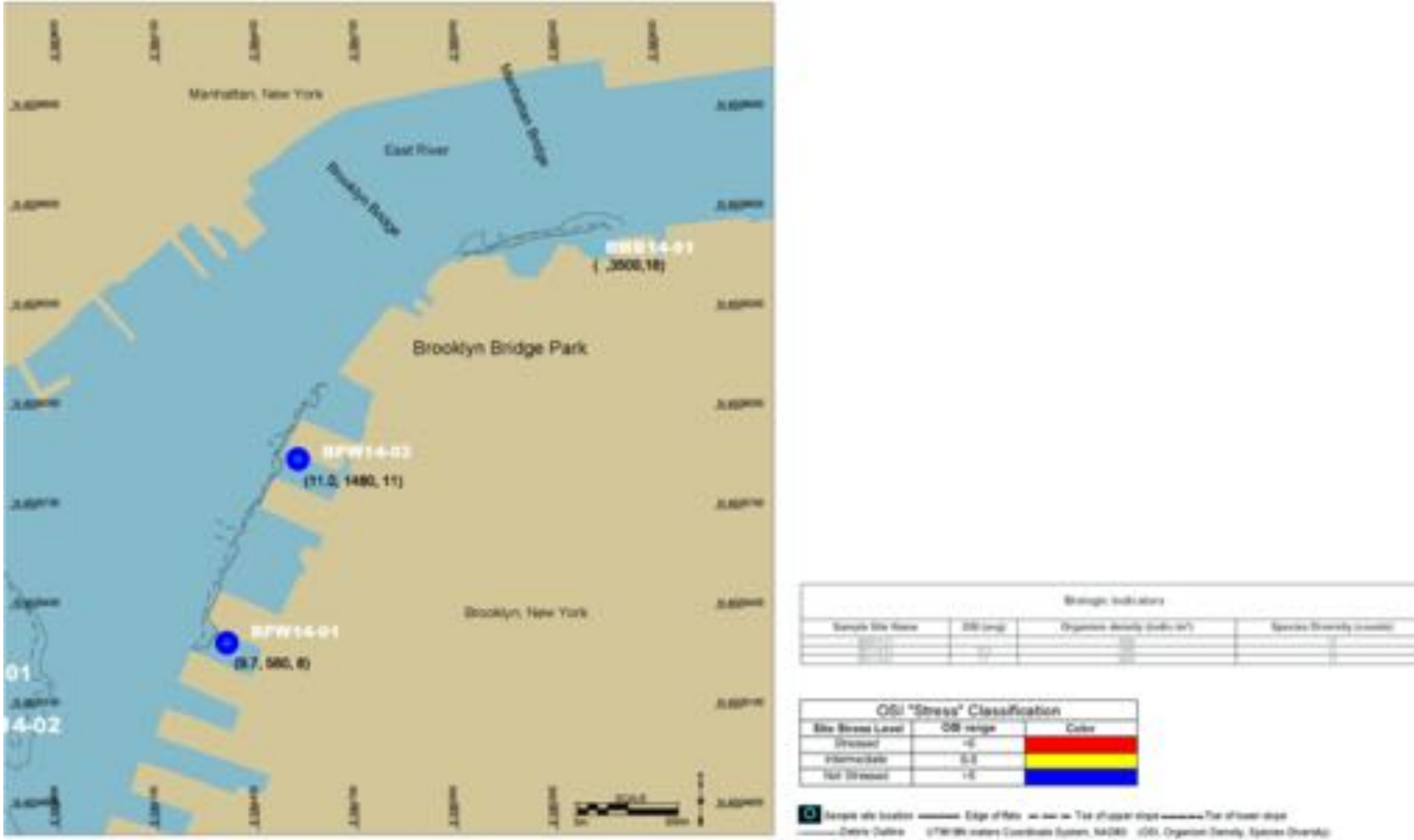

Figure 104. Organism density map for Brooklyn Bridge Park. The numbers at each site represent the triplet (OSI, organism density per square meter, diversity as total number of species). In the cases of no measurement the space is left blank.

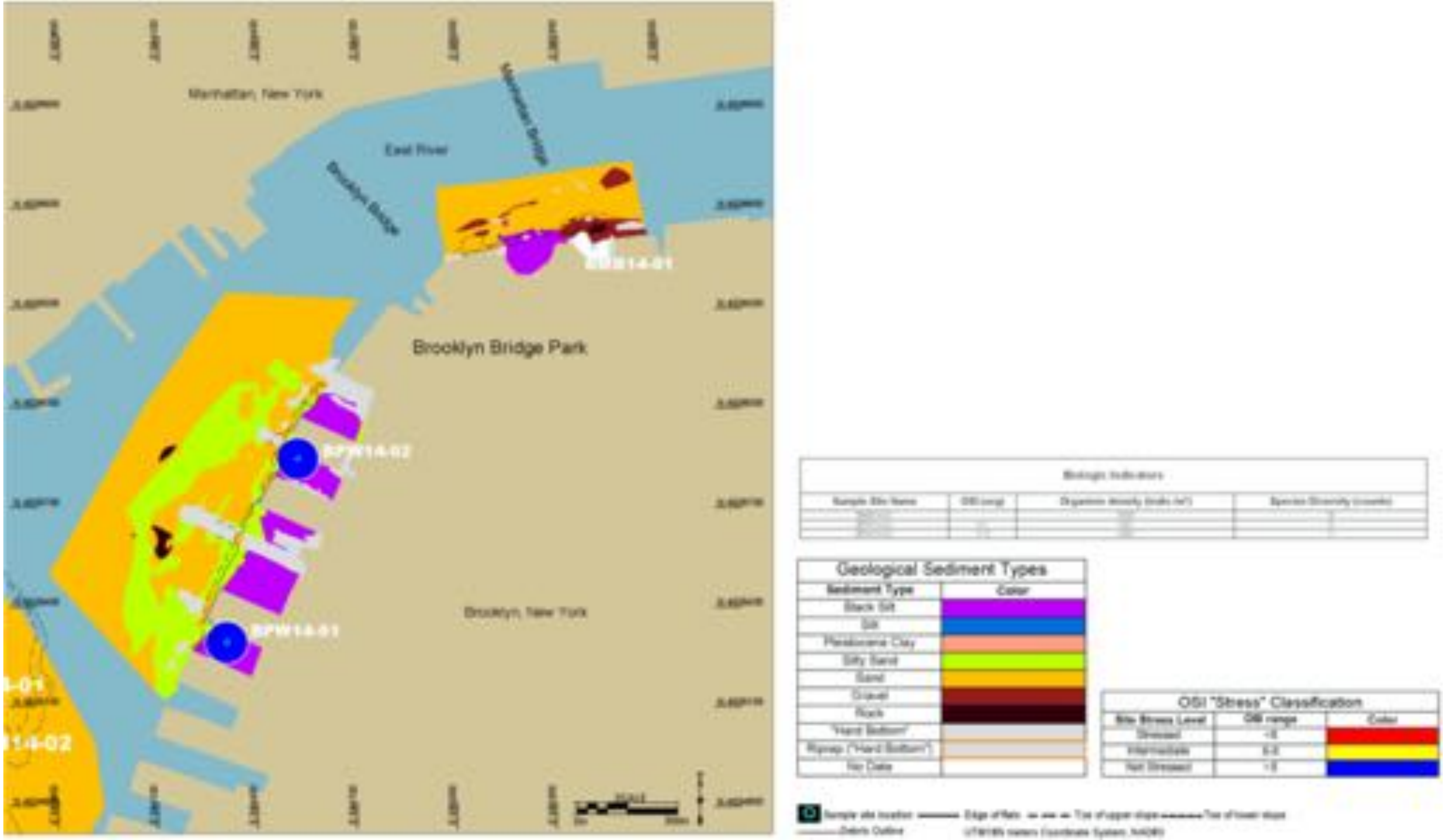

Figure 105. Composite bottom classification map for Brooklyn Bridge Park.

5.5 Area Report 5. Brooklyn Navy Yard

5.5.1 Morphology (Bathymetry, bathymetry analysis)

Figure 106 is a location photograph for the Brooklyn Navy Yard. Note the structures include piers with slips in between the piers.

Figure 107 is the bathymetry for the Brooklyn Navy Yard. Single and multibeam data from e4sciences (2015) were combined in 5m x 5m and 1m x 1m grids, respectively, using a triangular linear interpolation. Historical data from NOAA survey H11353 (2004) and USACE survey 2676 (2004) were combined in a 1m x 1m grid using a triangular linear interpolation. 2D first and second order derivative filters were applied to the 2006 historical bathymetry. Figure 108 plots the derivative maps for the bathymetry. Figure 109 is the difference map between 2015 and 2006. The map displays both results of the difference in bathymetry for the 5m x 5m grid in the ultrashallow area, and the 1m x 1m grid in the deeper area. All grids were obtained with triangular linear interpolations.


Figure 106. Location photo for the Brooklyn Navy Yard.

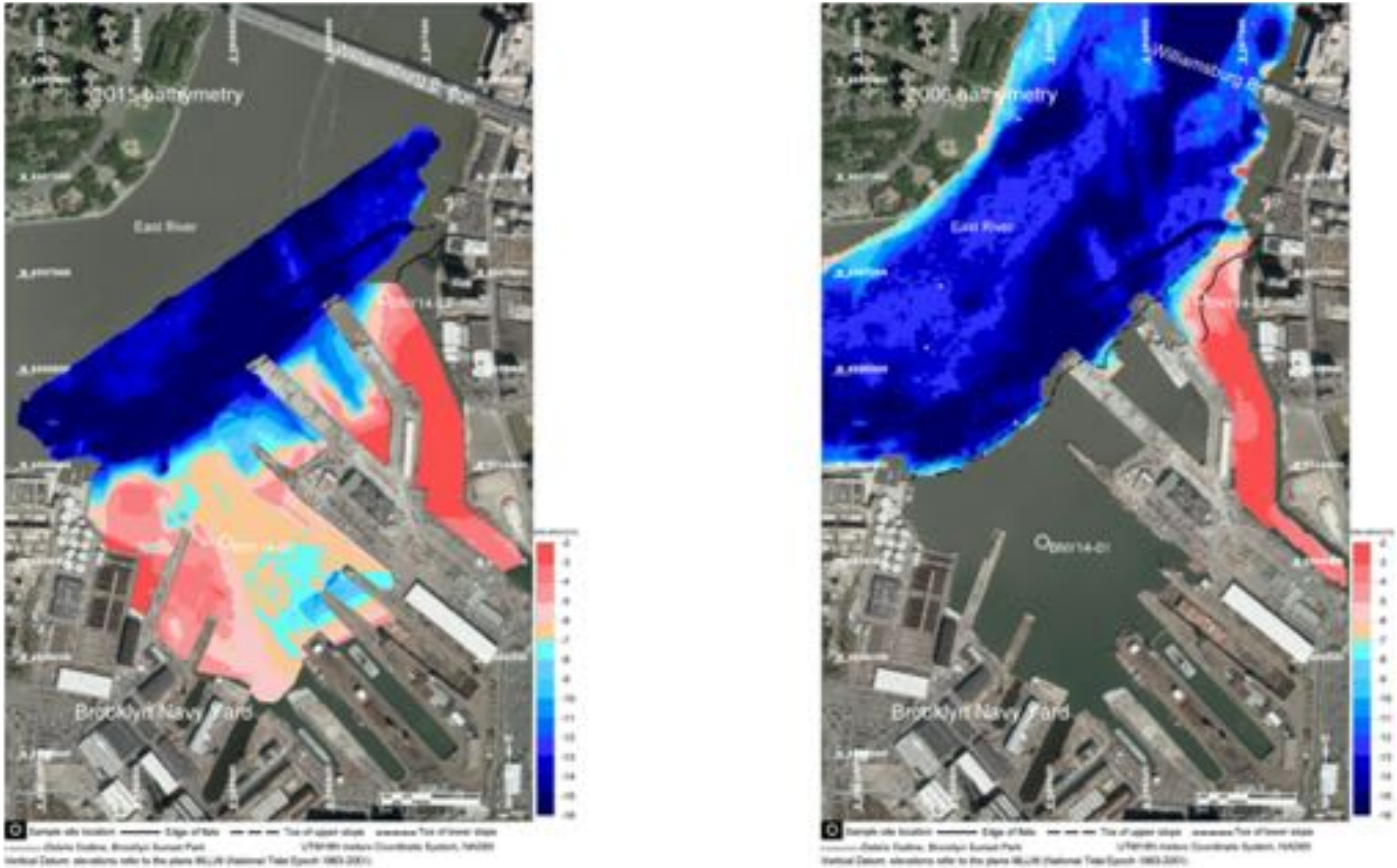

Figure 107. Bathymetric and location map for the Brooklyn Navy Yard. (Left) Single and multibeam data from e4sciences (2015) were combined in 5m x 5m and 1m x 1m grids, respectively, using a triangular linear interpolation. (Right) Historical data from NOAA survey H11353 (2004) and USACE survey 2676 (2004) were combined in a 1m x 1m grid using a triangular linear interpolation.

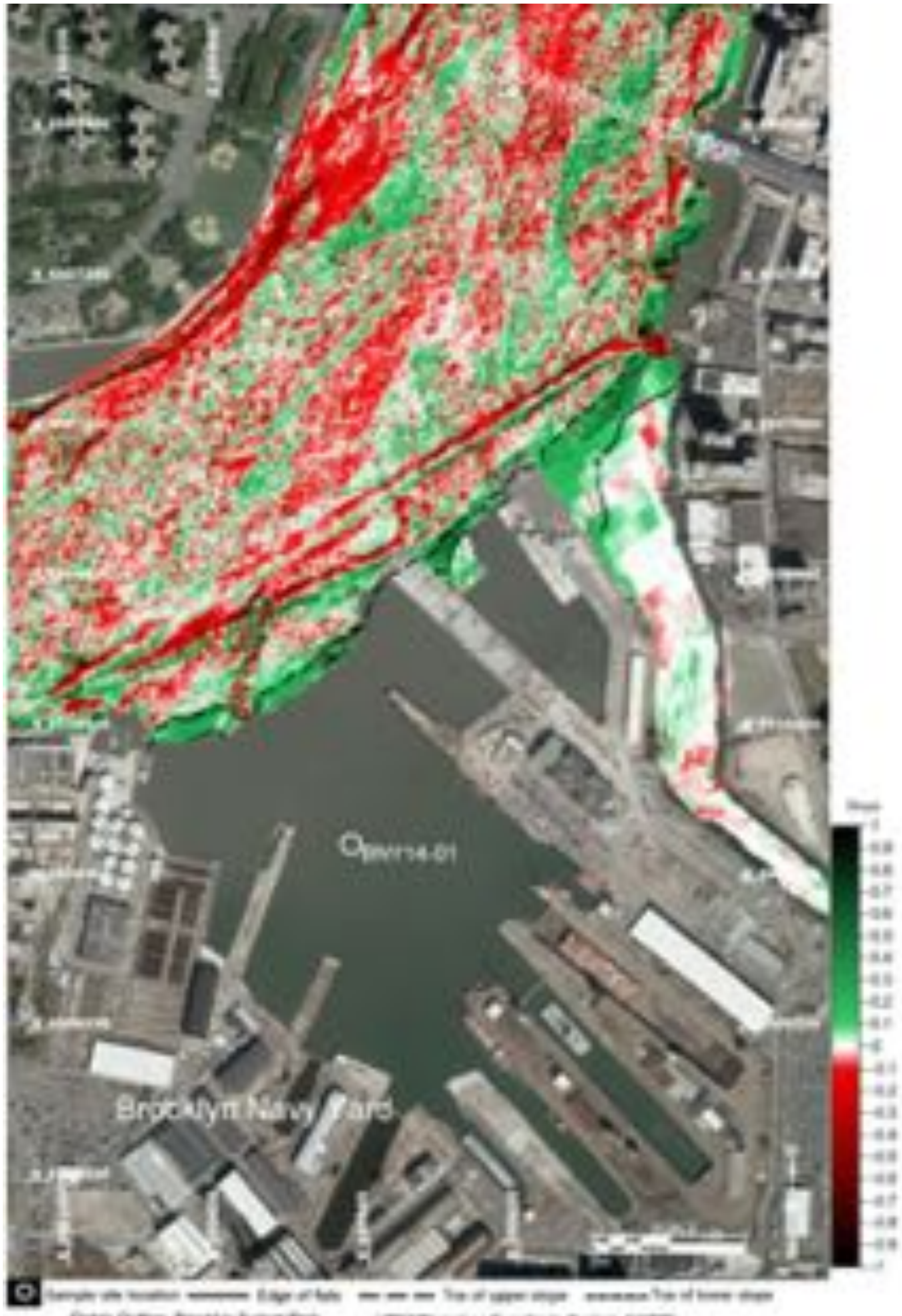

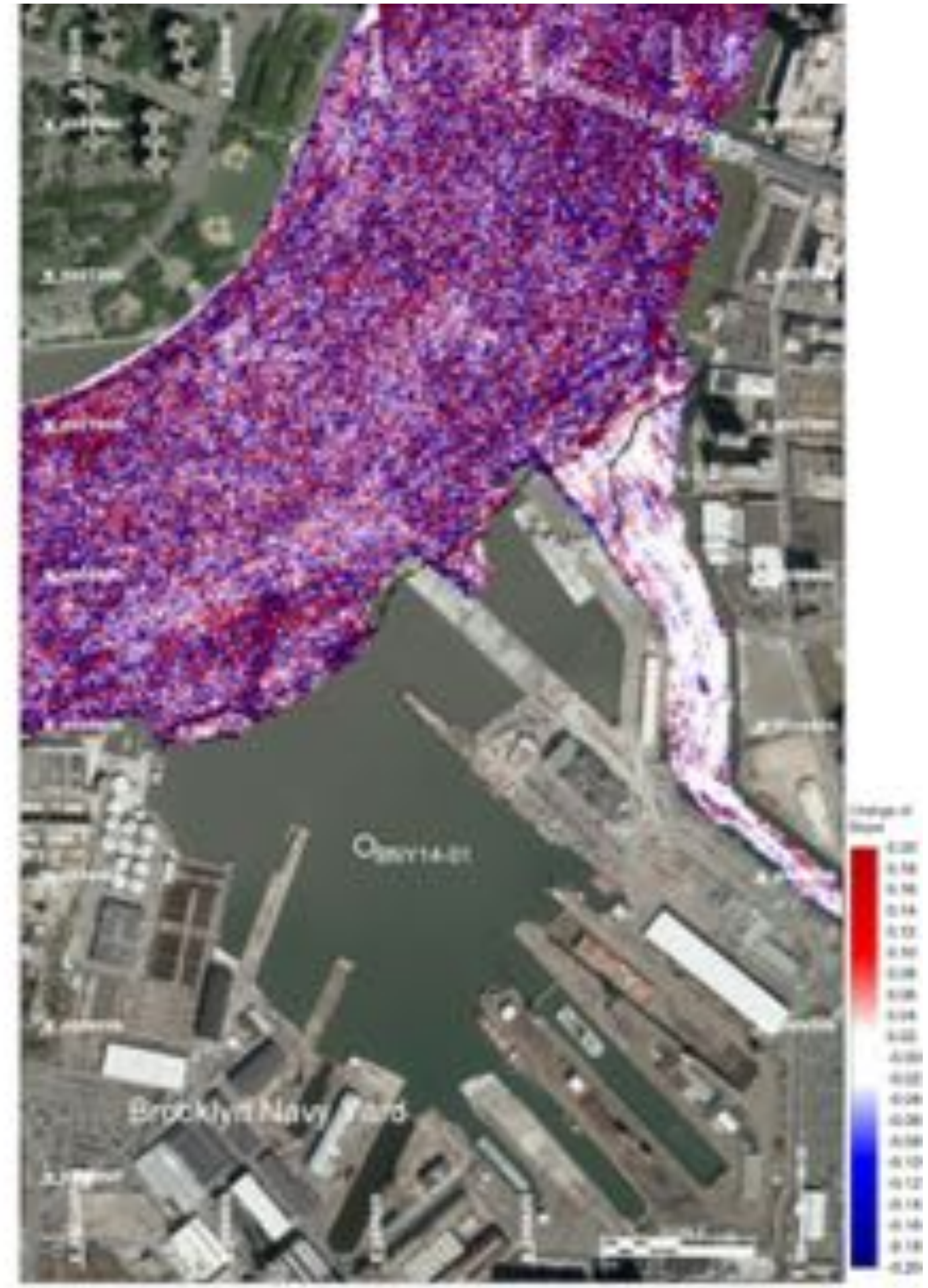

Figure 108. Bathymetric analysis for the Brooklyn Navy Yard (derivative maps for Area 5). Data from NOAA survey H11353 (2004) and USACE survey 2676 (2004) were combined in a 1m x 1m grid using a triangular linear interpolation. (Left) 2D first order derivative filter – slope. (Right) 2D second order derivative filter – change in slope.

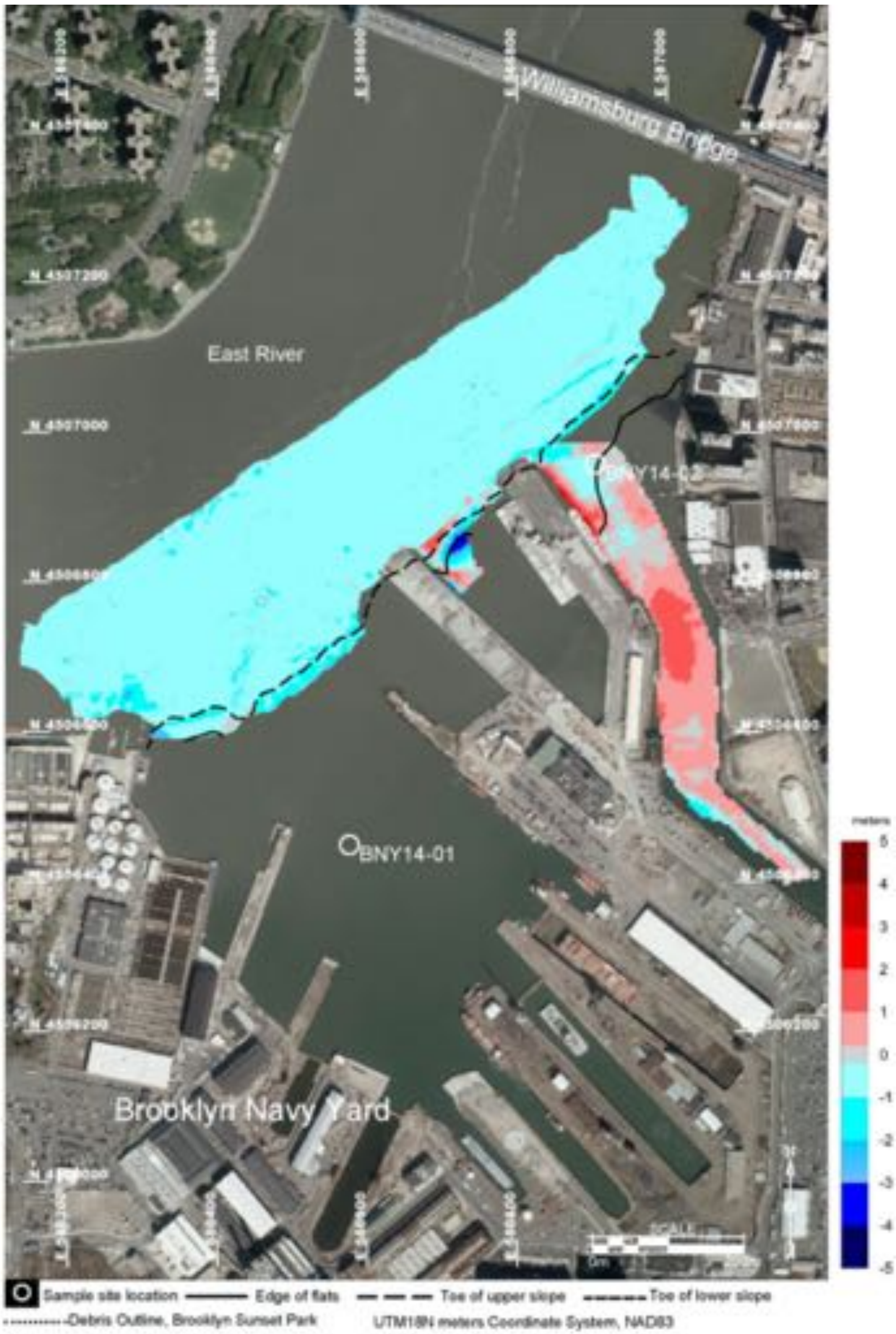

Figure 109. Bathymetry elevation difference map 2015 minus 2006 for the Brooklyn Navy Yard. The 2015 bathymetry includes multibeam bathymetry from e4sciences. The 2006 bathymetry includes NOAA survey H11353 (2004) and USACE survey 2676 (2004). The map displays both results of the difference in bathymetry for the 5m x 5m grid in the ultrashallow area, and the 1m x 1m grid in the deeper area. All grids were obtained with triangular linear interpolations.

5.5.2 Sediments (side-scan, seismic, cross sections, isopachs, grab samples)

Figure 110 displays the orthosonograph of Brooklyn Navy Yard insonified from the west and north. Figure 111 is its pair insonified from the east and the south.

Figure 112 is a sub-bottom seismic cross from northwest to southeast through the Brooklyn Navy Yard. Figure 113 is the acoustic silt isopach.

Table 25 lists the grain size mean and standard deviation.

Table 25. Brooklyn Navy Yard grain size

Sample	Mean	Median	Std. Deviation
	Φ		
BNY14-01	8.3	8.5	2.5
BNY14-02	7.7	7.0	2.0

Table 26 lists the measurement of lead, beryllium, and cesium.

Table 26. Brooklyn Navy Yard Pb, ^{7}Be, and ^{137}Cs

Sample	Sample Date	Sample Time	Pb (ICPMS)	^{7}Be	^{7}Be Qualifiers	^{137}Cs	^{137}Cs Qualifiers
			mg/Kg	pCi/g		pCi/g	
BNY14-01	11/4/14	10:48	34	0.346	U	0.193	U
BNY14-02	11/4/14	10:21	75	-0.013	U	0.191	U
U = Result is less than the sample detection limit							

Table 27 lists the compressional-wave velocity.

Table 27. Brooklyn Navy Yard acoustic velocity

Sample	Average P Velocity	Average P Velocity
	[m/s]	[ft/s]
BNY14-01	1,479.7	4,853.4
BNY14-02	1,475.4	4,839.4

Table 28 lists the XRF results for other elements in the sediments.

Table 28. Brooklyn Navy Yard XRF

Sample	S Avg	S Max	Fe Avg	Fe Max	Hg Avg	Hg Max	Zn Avg	Zn Max	Pb Avg	Pb Max	As Avg	As Max	Mn Avg	Mn Max
Push-Core	ppm													
BNY14-01	2,475.18	5,923.88	15,296.92	18,819.16	< LOD	< LOD	87.91	190.50	95.80	314.05	20.66	32.46	184.09	250.64
BNY14-02	2,366.23	3,711.65	15,011.39	17,421.63	< LOD	< LOD	80.08	100.17	67.67	88.36	< LOD	< LOD	128.96	222.34
BNY14-01	2,475.18	5,923.88	15,296.92	18,819.16	< LOD	< LOD	87.91	190.50	95.80	314.05	20.66	32.46	184.09	250.64
*<LOD = below Limit Of Detection														

Figure 110. Brooklyn Navy Yard orthosonograph insonified from the west.

Figure 111. Brooklyn Navy Yard orthosonograph insonified from the east.

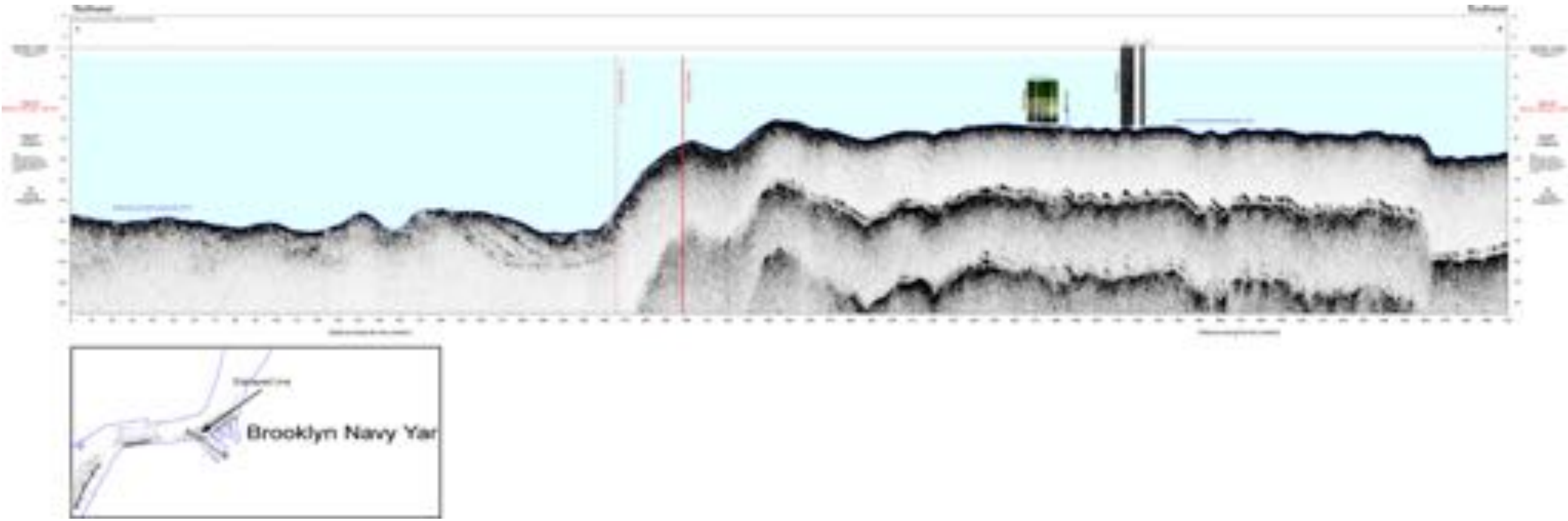

Figure 112. Seismic cross section, Brooklyn Navy Yard.

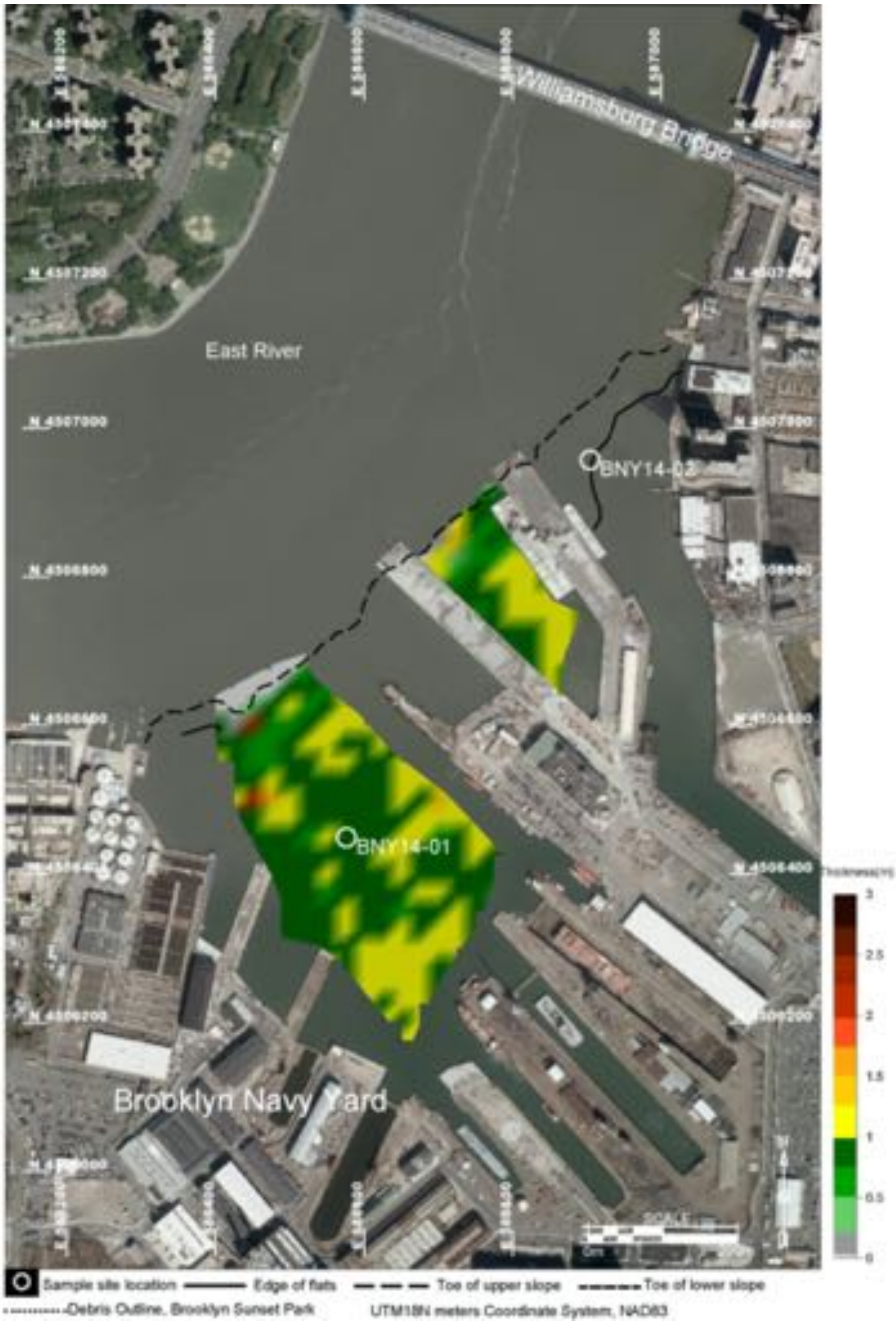

Figure 113. Acoustic silt isopach map for the Brooklyn Navy Yard.

5.5.3 Bottom classification (SPI, benthic classification)

Figure 114 displays the geological and structural substrate for Brooklyn Navy Yard. Figure 115 plots the density of individual organisms per square meter. Figure 116 plots the composite bottom classification.

Six analyzable images were collected from the Brooklyn Navy Yard (BNY) area. Average penetration depth was 14.28cm. Two sites had aRPD measurements >3.75, two sites had aRPD between 1.51cm and 3.00cm, and two sites had aRPD >0 but below 1.50cm. No anoxia was observed at the sediment-water interface and no methane was present within the sediment. Major modal grain size was >4 phi class for all images and small tubes were present in the six images analyzed. Three replicates from the same site with shallow aRPD depth measurements were observed to have only Stage I organisms. No epifauna were observed. OSI values ranged from a value of 3 (at the location with shallow aRPD depth) to 11 at locations where the aRPD depth was greater and Stage III microvoids were present. This area is an active, deep water marina and fine, anoxic black sediments are resuspended frequently through boating activities causing localized disturbances; however, surface roughness was attributed to biological activities of small Stage I worm tubes. Two samples were collected from grabs to test for sediment texture. Both sediment samples from BNY were black, silty material and the samples from these locations had >96% fines.

The lowermost East River, in the vicinity of the Brooklyn Navy Yards, represents another anthropogenically-impacted area. The East River is estuarine in nature and is home to over 100 different taxa (Sweeney & Sañudo-Wilhelmy 2004; Baard, Jackson, & Melnick 2005; Buck, Gobler, & Sañudo-Wilhelmy 2005; Gobler & Buck 2006). Organisms commonly found throughout the East River are able to tolerate a variety of harsh conditions—both natural and human-related. The sediments of the East River are a mix of cobbles, gravels, sands, silts and mud. The organisms that inhabit these sediments, especially in the vicinity of the lower River include small nematodes, polychaetes, oligochaetes, and a variety of arthropods (e.g. benthic copepods, cumaceans, amphipods, isopods, decapods) and mollusks (both gastropods and bivalves). The more pollution-tolerant benthos tend to occur in the greatest densities. The majority of the soft-bottom benthic assemblages are located in areas where fine sediments accumulate, including but not limited to areas near piers and pilings and in low-velocity sections of the River.

Epibenthic organisms commonly found in the East River include hydrozoans, anthozoans, nemerteans, amphipods, tunicates, and a variety of mussels and crabs, including the horseshoe crab. In general, submerged surfaces (i.e. pilings, rocks, piers) are often inhabited by a more diverse assemblage of fouling organisms, including mussels, encrusting polychaetes, and tunicates (Ayers, 1951; Gosner, 1969; Abdus-Samad, 2013).

In addition, the site with very low calculated OSI values in BNY is a region of both high sediment accumulation rates and active dredging. The dredging lowers the site depth and makes it a sediment sink, contributing to the high sedimentation rates. In contrast, the healthy site in BNY is in a relatively quite spot without dredging or fast sediment accumulation. The contrast in the health of the benthic communities between these two sites strongly supports our hypothesis that physical disturbance is a major factor affecting the observed health of benthic communities in the harbor

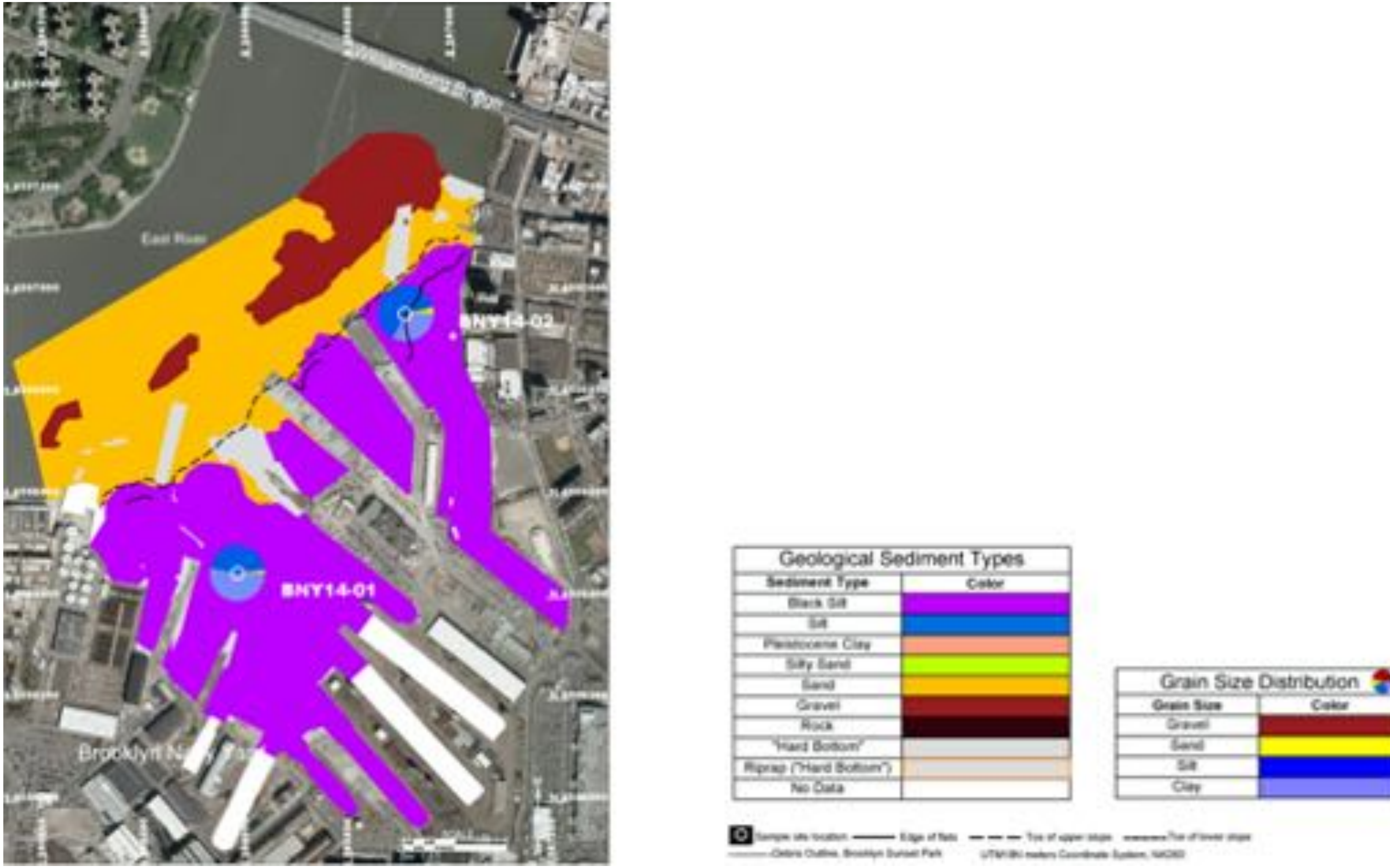

Figure 114. Bottom sediment type and geological substrate map for the Brooklyn Navy Yard.

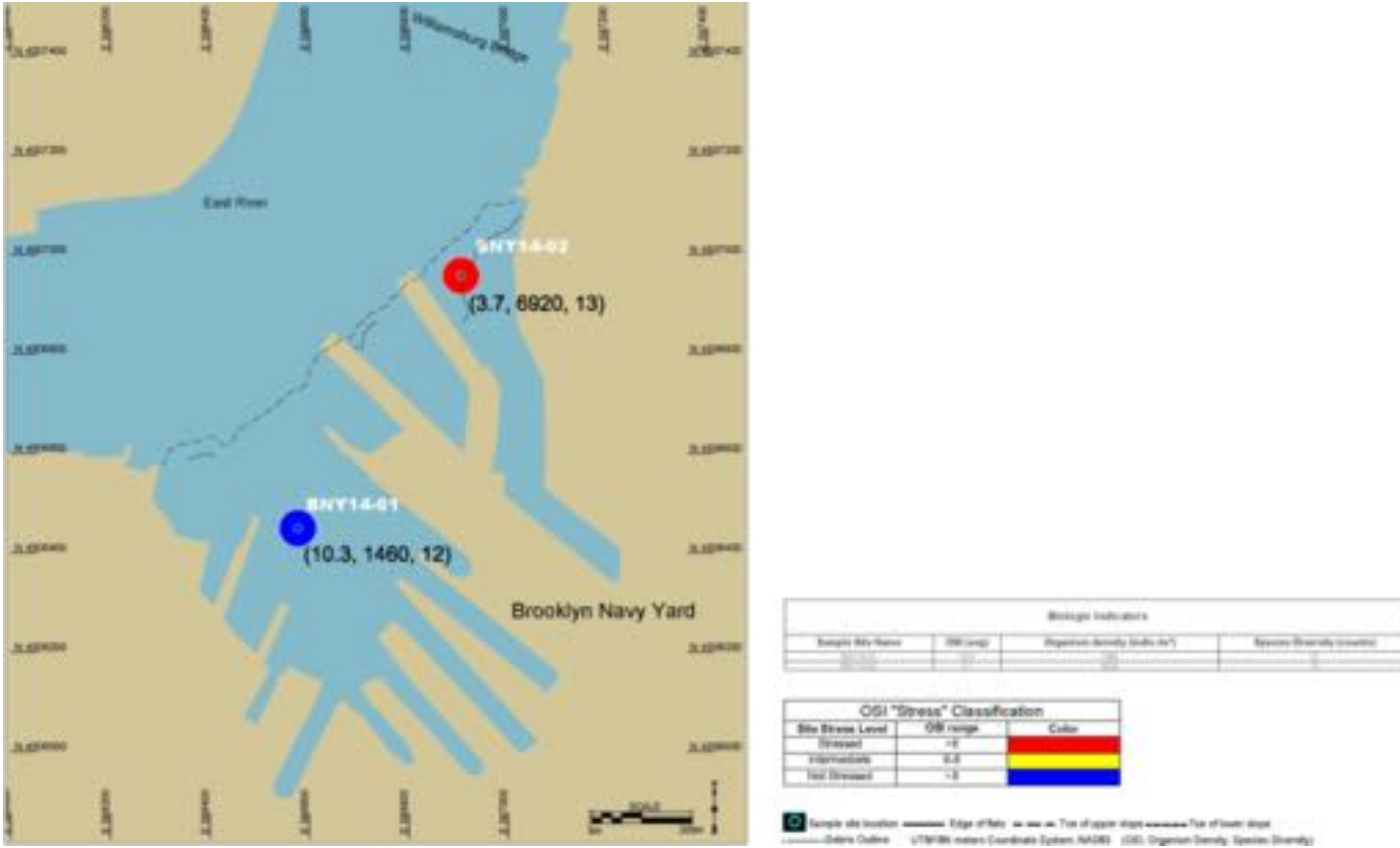

Figure 115. Organism density map for Brooklyn Navy Yard. The numbers at each site represent the triplet (OSI, organism density per square meter, diversity as total number of species). In the cases of no measurement the space is left blank.

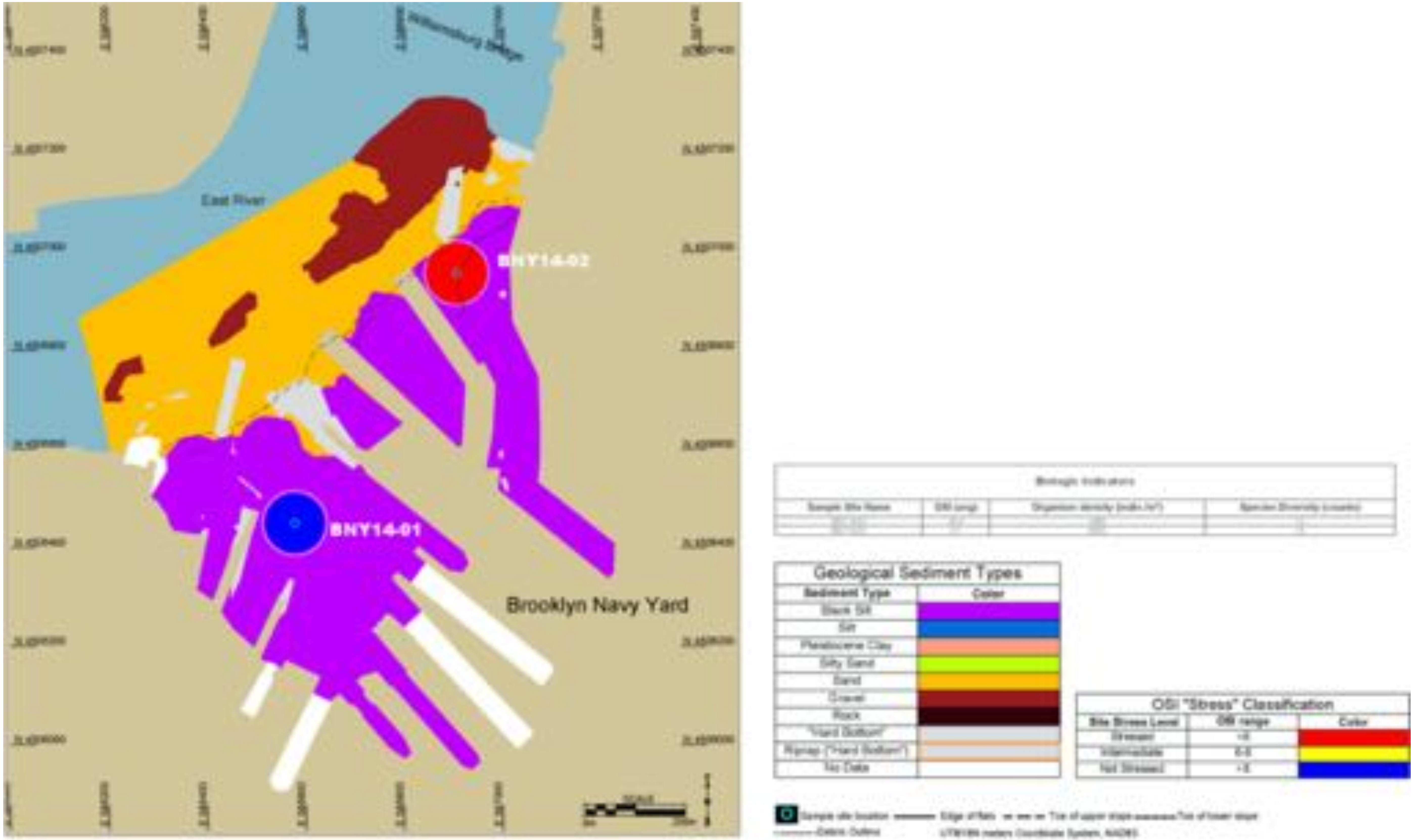

Figure 116. Composite bottom classification map for the Brooklyn Navy Yard.

5.6 Area Report 6. West Manhattan waterfront South (Harrison St. to 17th St.)

Figure 117 is a location photo for West Manhattan waterfront South.

5.6.1 Morphology (Bathymetry, bathymetry analysis)

Figure 117 is a location photograph for West Manhattan waterfront South. Note the structures include piers with slips in between the piers.

Figure 118 is the bathymetry for West Manhattan waterfront South. Single and multibeam data from e4sciences (2015) were combined in 5m x 5m and 1m x 1m grids, respectively, using a triangular linear interpolation. Historical data from NOAA surveys F00573 (2009) and F00598 (2012), and USACE survey 4126 (2014), were combined in a 1m x 1m grid using a triangular linear interpolation. 2D first and second order derivative filters were applied to the 2014 historical bathymetry. Figure 119 plots the derivative maps for the bathymetry. Figure 120 is the difference map between 2015 and 2014. The map displays both results of the difference in bathymetry for the 5m x 5m grid in the ultrashallow area, and the 1m x 1m grid in the deeper area. All grids were obtained with triangular linear interpolations.

Figure 117. Location photo for West Manhattan waterfront South.

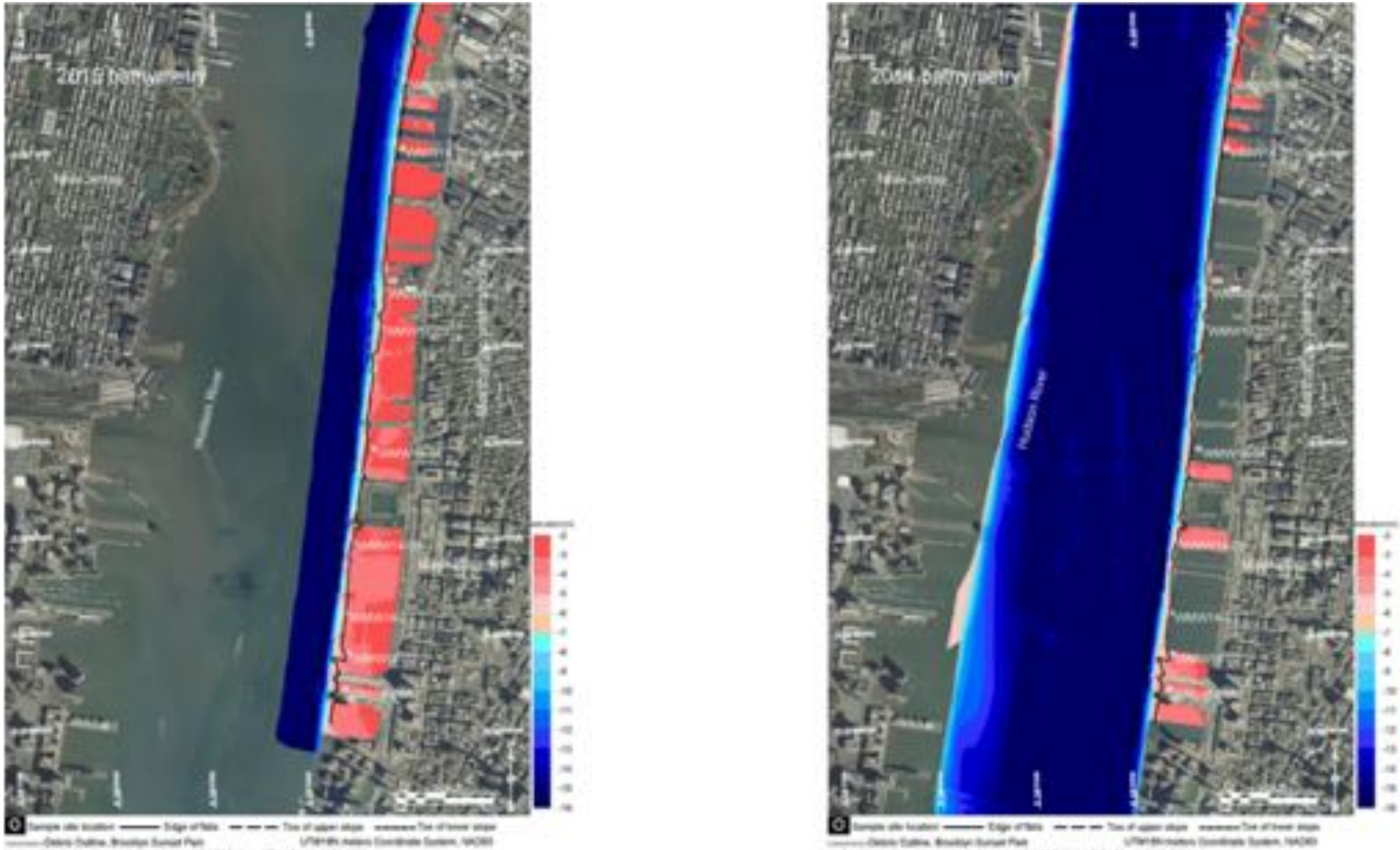

Figure 118. Bathymetric and location map for West Manhattan waterfront South. (Left) Single and multibeam data from e4sciences (2015) were combined in 5m x 5m and 1m x 1m grids, respectively, using a triangular linear interpolation. (Right) Historical data from NOAA surveys F00573 (2009) and F00598 (2012), and USACE survey 4126 (2014), were combined in a 1m x 1m grid using a triangular linear interpolation.

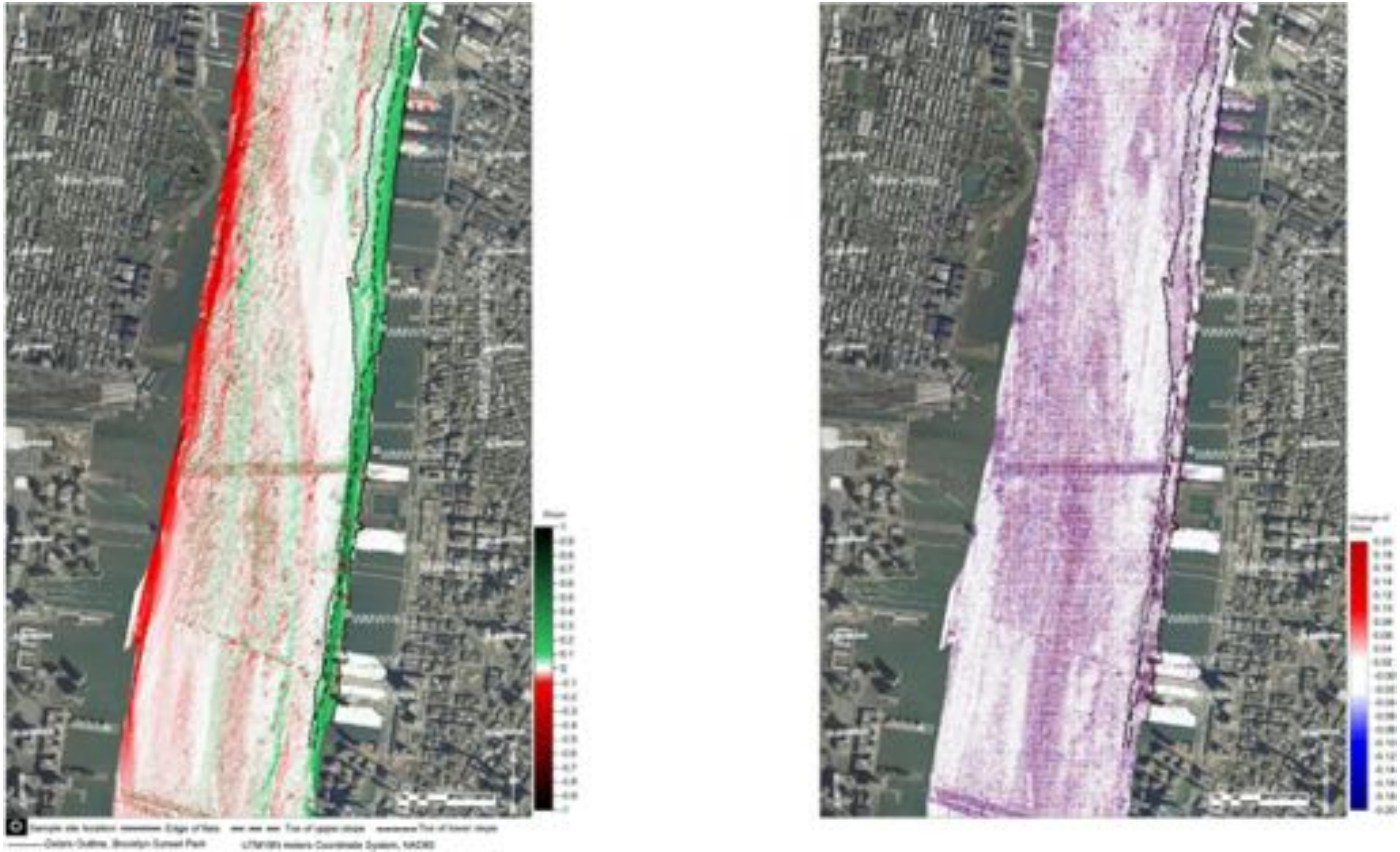

Figure 119. Bathymetric analysis for West Manhattan waterfront South (derivative maps for Area 6). Data from NOAA surveys F00573 (2009) and F00598 (2012) and USACE survey 4126 (2014) were combined in a 1m x 1m grid using a triangular linear interpolation. (Left) 2D first order derivative filter – slope. (Right) 2D second order derivative filter – change in slope.

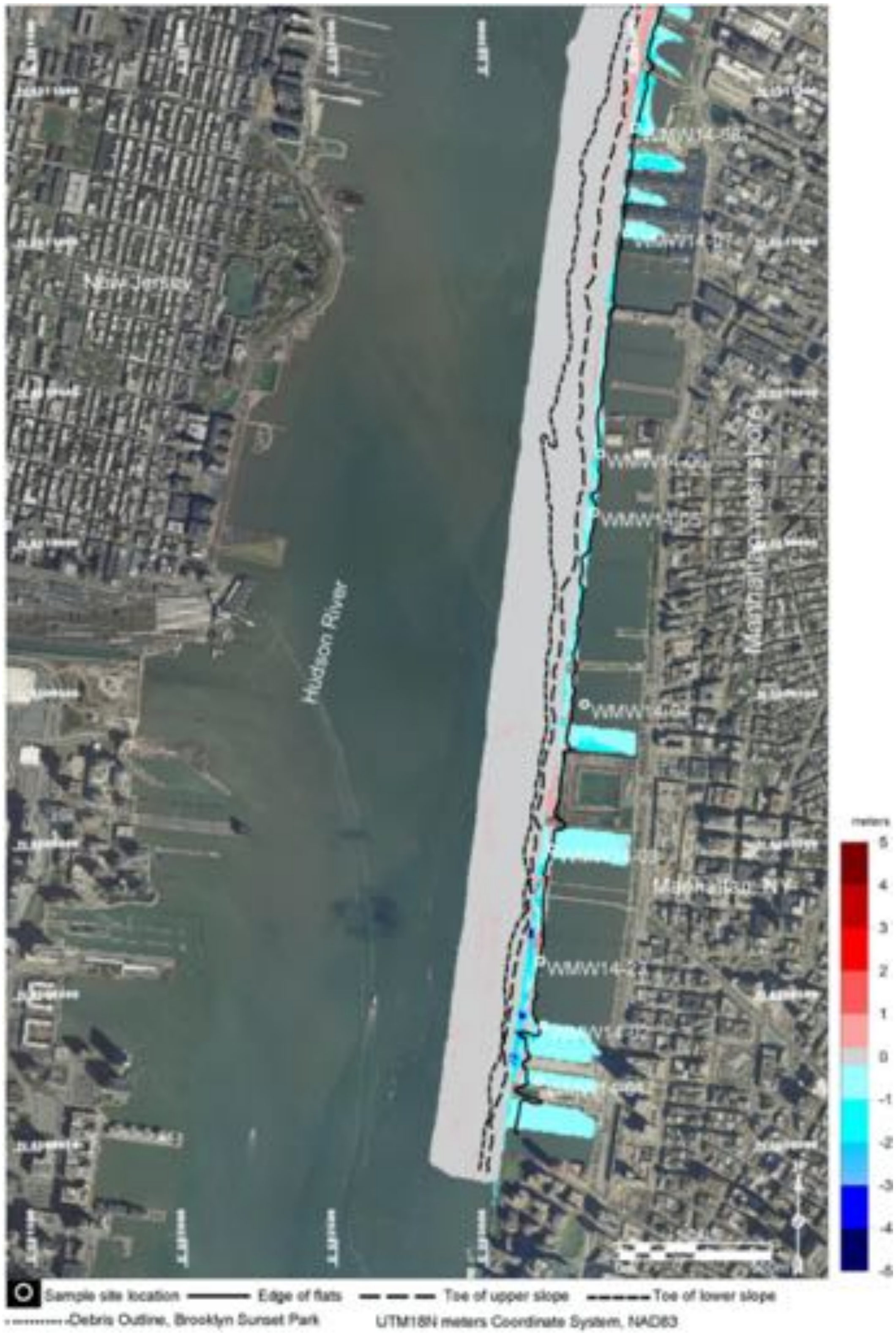

Figure 120. Bathymetry elevation difference map 2015 minus 2014 for West Manhattan waterfront South. The 2015 bathymetry includes single and multibeam bathymetries from e4sciences. The 2014 bathymetry includes NOAA surveys F00573 (2009) and F00598 (2012) and USACE survey 4126 (2014). The map displays both results of the difference in bathymetry for the 5m x 5m grid in the ultrashallow area, and the 1m x 1m grid in the deeper area. All grids were obtained with triangular linear interpolations.

5.6.2 Sediments (side-scan, seismic, cross sections, isopachs, grab samples)

Figure 121 displays the orthosonograph of West Manhattan waterfront South insonified from the west and north. Figure 122 is its pair insonified from the east and the south.

Figure 123 is a sub-bottom seismic cross from west to east across West Manhattan waterfront South. Figure 124 is the acoustic silt isopach.

Table 29 lists the grain size mean and standard deviation.

Table 29. West Manhattan waterfront South grain size

Sample	Mean	Median	Std. Deviation
	Φ		
WMW14-01	6.8	7.0	3.0
WMW14-02	6.5	6.5	2.0
WMW14-03	6.3	6.0	1.5
WMW14-04	6.8	6.5	2.1
WMW14-05	6.3	5.5	2.3
WMW14-06	6.5	6.0	2.3

Table 30 lists the measurement of lead, beryllium, and cesium.

Table 30. West Manhattan waterfront South, Pb, ^{7}Be, and ^{137}Cs

Sample	Sample Date	Sample Time	Pb (ICPMS)	^{7}Be	^{7}Be Qualifiers	^{137}Cs	^{137}Cs Qualifiers
			mg/Kg	pCi/g		pCi/g	
WMW14-01	11/5/14	6:45	42	0.193	U	0.130	U
WMW14-02	11/5/14	6:58	33	0.440	U	0.070	U
WMW14-03	11/5/14	7:20	36	-0.395	U	0.132	U
WMW14-04	11/5/14	7:36	38	0.000	U	0.047	U
WMW14-05	11/5/14	7:58	30	-0.126	U	0.108	U
WMW14-06	11/5/14	8:13	39	0.515	U	0.134	U
U = Result is less than the sample detection limit							

Table 31 lists the measured compressional-wave velocity.

Table 31. West Manhattan waterfront South, acoustic velocity

Sample	Average P Velocity	Average P Velocity
	[m/s]	[ft/s]
WMW14-01	1,517.6	4,977.6
WMW14-02	1,490.8	4,889.7
WMW14-03	1,479.7	4,853.3
WMW14-04	1,498.2	4,914.0
WMW14-05	1,612.6	5,289.4
WMW14-06	1,479.3	4,852.0

Table 32 lists the XRF results for other elements.

Table 32. West Manhattan waterfront South, XRF

Sample	S Avg	S Max	Fe Avg	Fe Max	Hg Avg	Hg Max	Zn Avg	Zn Max	Pb Avg	Pb Max	As Avg	As Max	Mn Avg	Mn Max
Push-Core	ppm													
WMW14-01	2,840.34	3,938.64	18,878.75	33,985.56	< LOD	< LOD	71.00	93.82	30.59	40.55	8.98	9.88	257.57	428.78
WMW14-02	1,862.07	2,355.39	13,532.28	19,290.83	< LOD	< LOD	63.24	91.14	32.90	41.79	< LOD	< LOD	155.02	218.74
WMW14-03	1,559.93	1,974.02	15,368.48	17,991.79	< LOD	< LOD	58.15	65.66	27.78	33.82	7.84	7.96	189.96	310.22
WMW14-04	2,398.99	3,269.89	16,175.61	20,124.38	< LOD	< LOD	68.40	84.41	34.94	48.52	< LOD	< LOD	195.92	259.46
WMW14-05	2,192.80	2,483.74	16,066.76	21,822.67	< LOD	< LOD	63.73	85.51	30.80	43.37	< LOD	< LOD	156.94	217.91
WMW14-06	1,396.98	2,402.15	14,160.51	16,103.13	< LOD	< LOD	57.33	68.00	29.92	39.82	10.16	10.16	166.11	245.56
*<LOD = below Limit Of Detection														

Figure 121. West Manhattan waterfront South orthosonograph insonified from the west.

Figure 122. West Manhattan waterfront South orthosonograph insonified from the east.

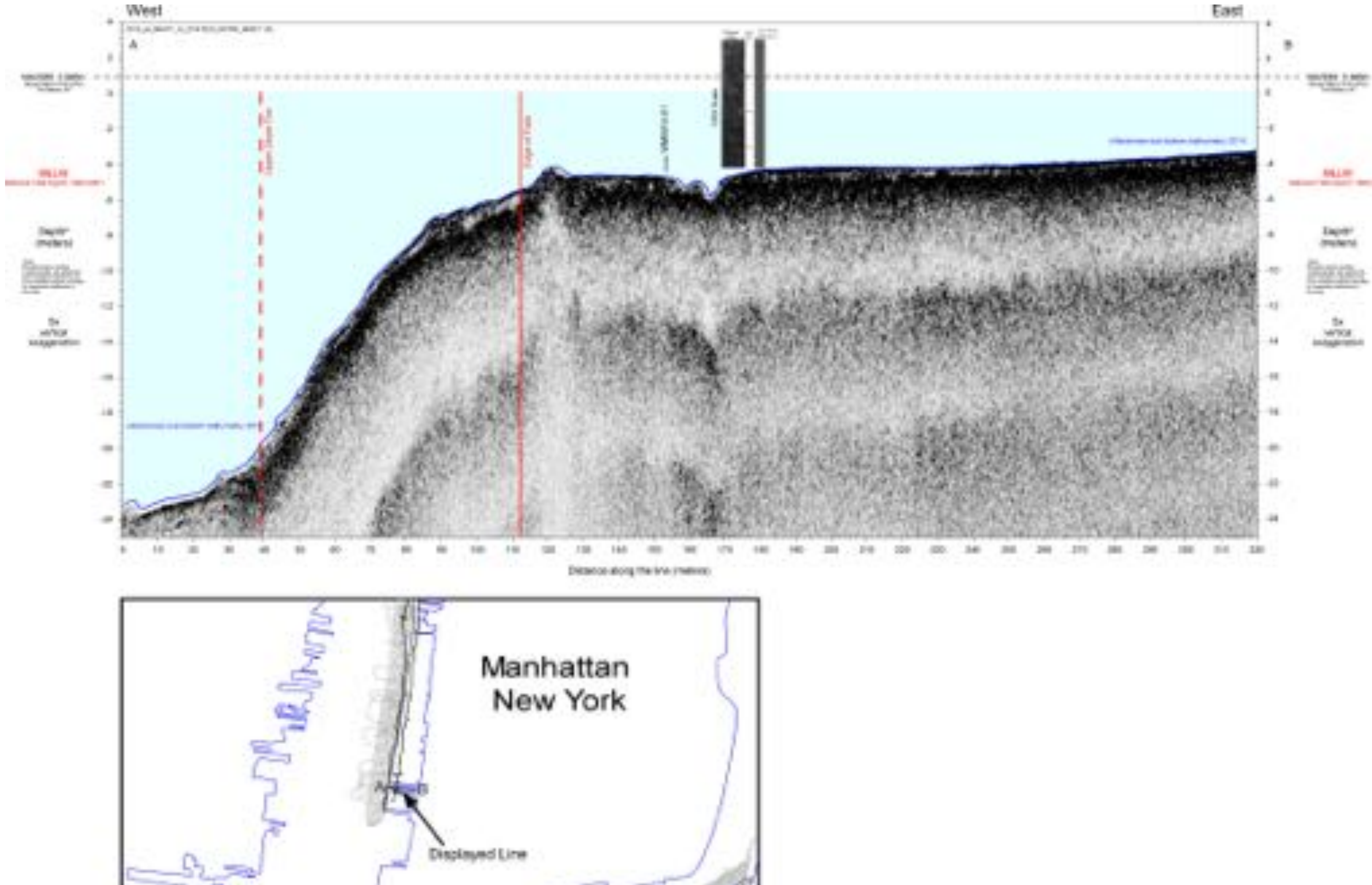

Figure 123. Seismic cross section, West Manhattan waterfront South.

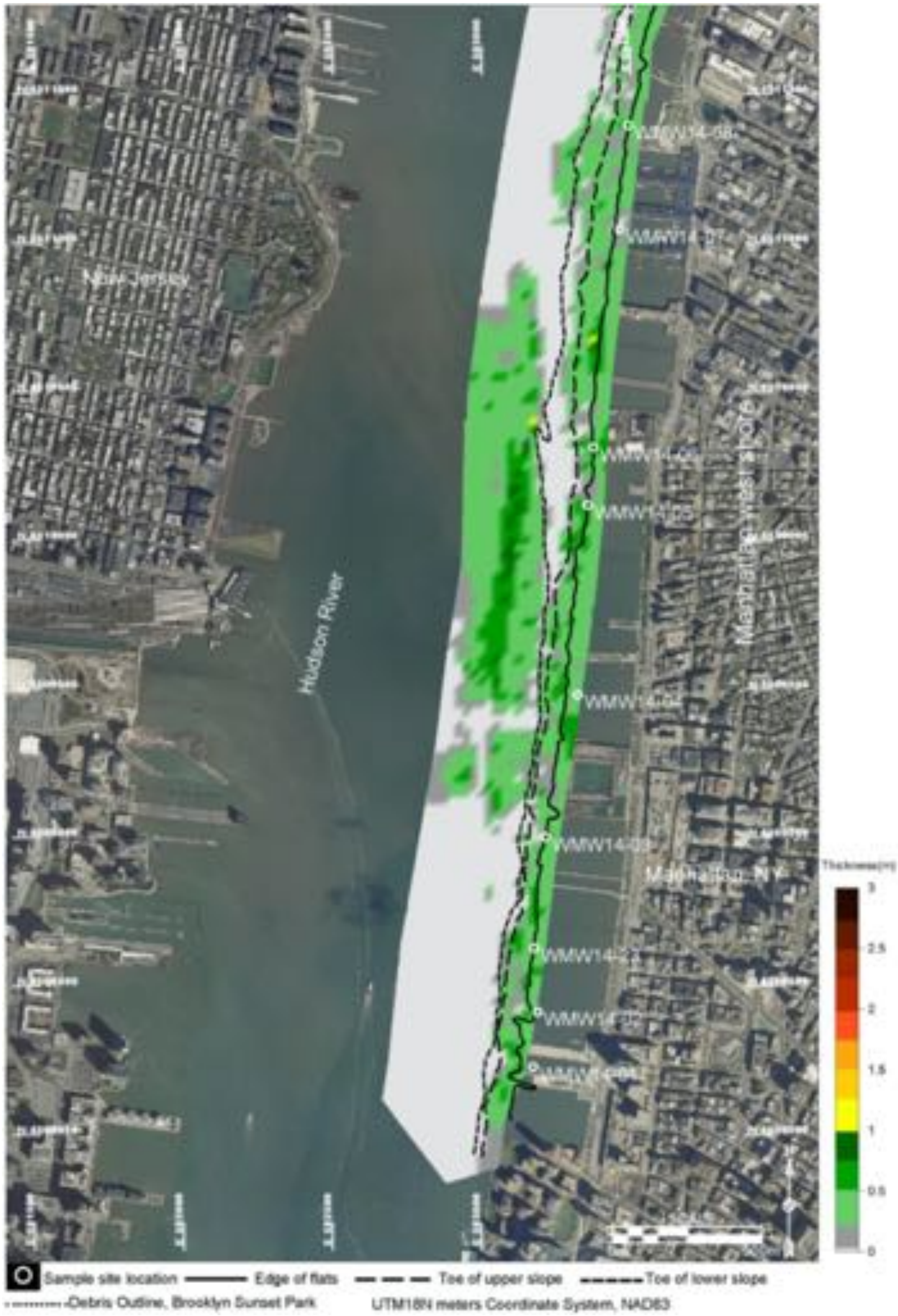

Figure 124. Acoustic silt isopach map for West Manhattan waterfront South.

5.6.3 Bottom classification (SPI, benthic classification)

Figure 125 displays the geological and structural substrate for West Manhattan waterfront South. Figure 126 plots the density of individual organisms per square meter. Figure 127 plots the composite bottom classification.

West Manhattan waterfront (WMW) South shoreline where these samples were collected is anthropogenically-structured, hardened, and supported by pilings, with some sites sampled in active slips and marinas. Six grab samples (WMW14-01 to 14-06) were collected and sediment from these grabs was analyzed for grain size analysis. These sites had >50% fine sediment, with several having >85% fines. Sites within the WMW South area (and North area) tended to have the highest percentages of silt and clay compared with those of the WMW middle area. Despite some differences in sediment type, overall camera penetration was similar among the three areas when compared with a mean value between 12 and 14cm camera penetration depth. The aRPD at the South and Middle sites had greater depth measured than sites sampled at WMW North. Of the twelve WMW South images analyzed, nine had aRPD depths >3.75cm and only one had an aRPD depth of less than 1.0cm. Epifauna and methane were not observed at any of the WMW sites. Major modal grain size for the three areas had a phi class >4. Surface roughness for the three WMW areas was attributed to biological activities and the majority of images analyzed had visible worm tubes, voids, and successional stage was classified as I on III – Stage I assemblages are occurring at the same place and time as evidence of Stage III organisms. Small burrows within the sediment were also observed and sediment was oxidized at the surface.

All of area 6 was included in the Hudson River Park and Hudson River Estuarine Sanctuary in 1998. The establishment of these 400 water-acres of protected habitat has severely limited and reduced boat traffic in the area, allowing healthy benthic habitat to grow and spread north in both this and area 7.

Geological Sediment Types	
Sediment Type	**Color**
Black Silt	
Silt	
Pleistocene Clay	
Silty Sand	
Sand	
Gravel	
Rock	
"Hard Bottom"	
Riprap ("Hard Bottom")	
No Data	

Grain Size Distribution	
Grain Size	**Color**
Gravel	
Sand	
Silt	
Clay	

Figure 125. Bottom sediment type and geological substrate map for West Manhattan waterfront South.

Biologic Indicators			
Sample Site Name	OSI (avg)	Organism density (indiv./m²)	Species Diversity (counts)
[illegible]	[illegible]	[illegible]	[illegible]

OSI "Stress" Classification		
Site Stress Level	OSI range	Color
Stressed	<6	
Intermediate	[illegible]	
Not Stressed	>6	

Figure 126. Organism density map for West Manhattan waterfront South. The numbers at each site represent the triplet (OSI, organism density per square meter, diversity as total number of species). In the cases of no measurement the space is left blank.

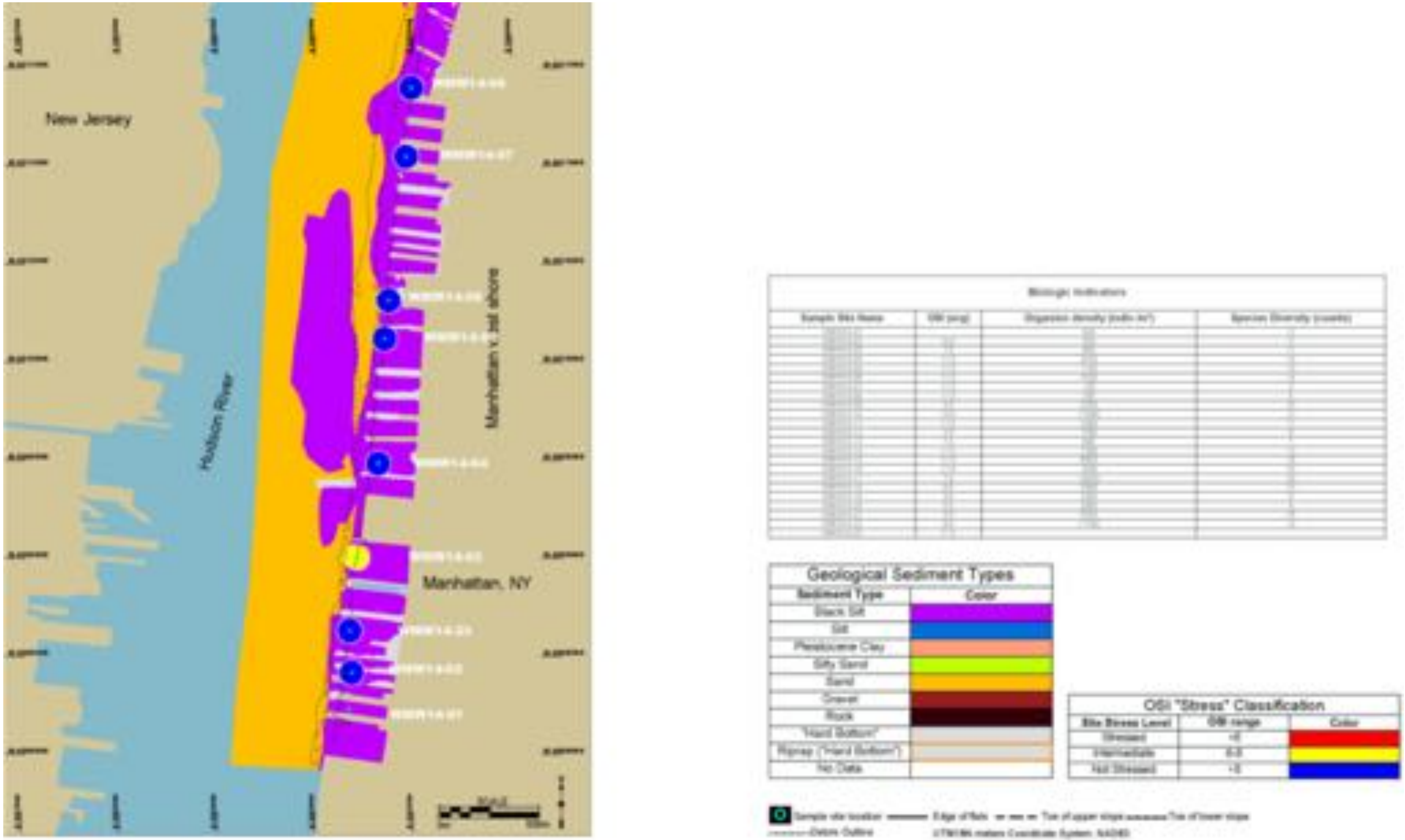

Figure 127. Composite bottom classification map for West Manhattan waterfront South.

5.7 Area Report 7. West Manhattan waterfront Middle (17th St. to 57th St.)

5.7.1 Morphology (Bathymetry, bathymetry analysis)

Figure 128 is a location photograph for West Manhattan waterfront Middle. Note the structures include piers with slips in between the piers.

Figure 129 is the bathymetry for West Manhattan waterfront Middle. Single and multibeam data from e4sciences (2015) were combined in 5m x 5m and 1m x 1m grids, respectively, using a triangular linear interpolation. Historical data from NOAA surveys F00573 (2009) and F00598 (2012), and USACE survey 4126 (2014), were combined in a 1m x 1m grid using a triangular linear interpolation. 2D first and second order derivative filters were applied to the 2014 historical bathymetry. Figure 130 plots the derivative maps for the bathymetry. Figure 131 is the difference map between 2015 and 2014. The map displays both results of the difference in bathymetry for the 5m x 5m grid in the ultrashallow area, and the 1m x 1m grid in the deeper area. All grids were obtained with triangular linear interpolations.

Figure 128. Location photo for West Manhattan waterfront Middle.

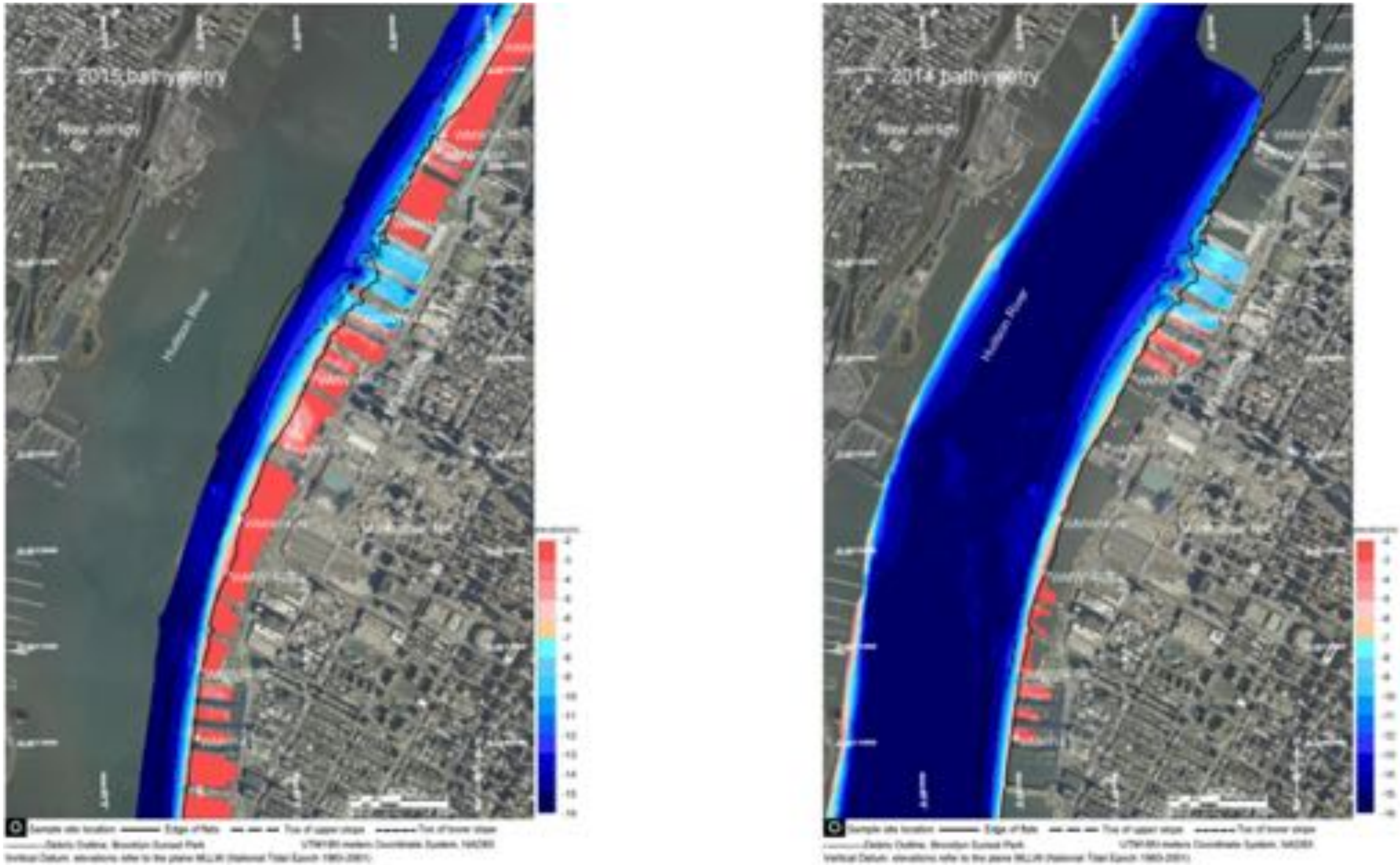

Figure 129. Bathymetric and location map for West Manhattan waterfront Middle. (Left) Single and multibeam data from e4sciences (2015) were combined in 5m x 5m and 1m x 1m grids, respectively, using a triangular linear interpolation. (Right) Historical data from NOAA surveys F00573 (2009) and F00598 (2012), and USACE survey 4126 (2014), were combined in a 1m x 1m grid using a triangular linear interpolation.

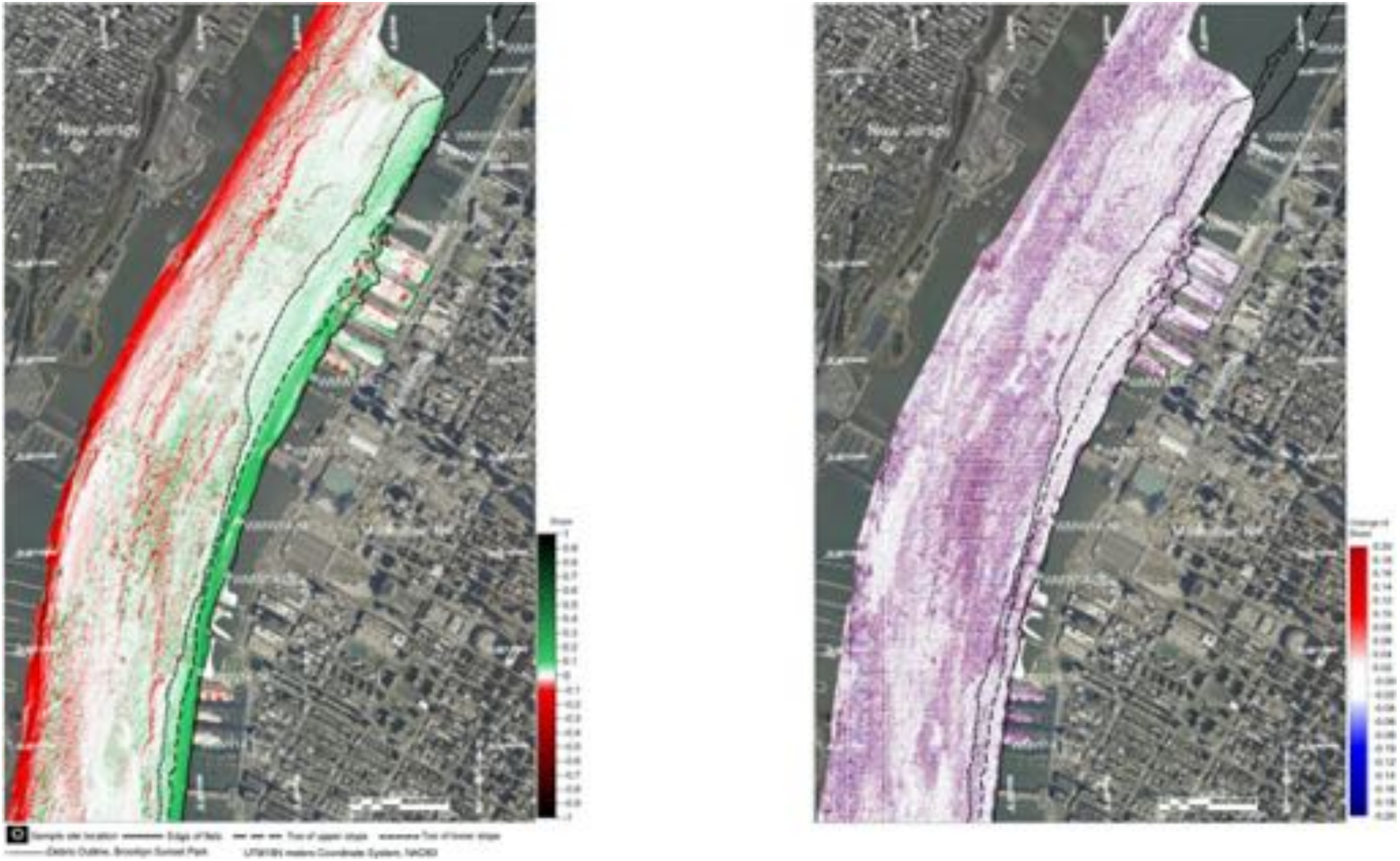

Figure 130. Bathymetric analysis for West Manhattan waterfront Middle (derivative maps for Area 7). Data from NOAA surveys F00573 (2009) and F00598 (2012) and USACE survey 4126 (2014) were combined in a 1m x 1m grid using a triangular linear interpolation. (Left) 2D first order derivative filter – slope. (Right) 2D second order derivative filter – change in slope.

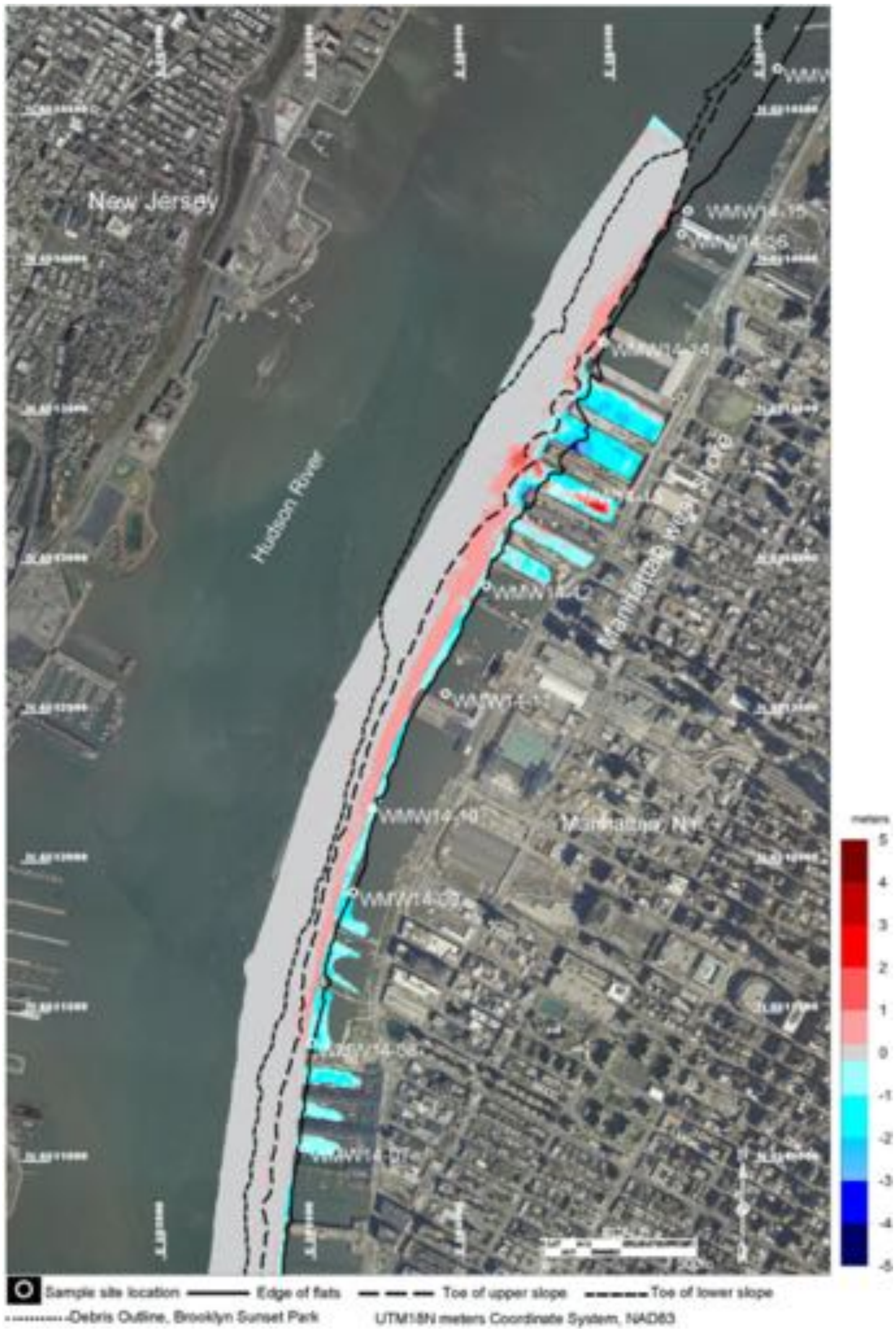

Figure 131. Bathymetry elevation difference map 2015 minus 2014 for West Manhattan waterfront Middle. The 2015 bathymetry includes single and multibeam bathymetries from e4sciences. The 2014 bathymetry includes NOAA surveys F00573 (2009) and F00598 (2012) and USACE survey 4126 (2014). The map displays both results of the difference in bathymetry for the 5m x 5m grid in the ultrashallow area, and the 1m x 1m grid in the deeper area. All grids were obtained with triangular linear interpolations.

5.7.2 Sediments (side-scan, seismic, cross sections, isopachs, grab samples)

Figure 132 displays the orthosonograph of West Manhattan waterfront Middle insonified from the west and north. Figure 133 is its pair insonified from the east and the south.

Figure 134 is a sub-bottom seismic cross from west to east across West Manhattan waterfront Middle. Figure 135 is the acoustic silt isopach.

Table 33 lists the grain size mean and standard deviation. Note the small variation of mean size and standard deviation with location.

Table 33. West Manhattan waterfront Middle grain size

Sample	Mean	Median	Std. Deviation
	Φ		
WMW14-07	6.5	6.5	1.5*
WMW14-08	6.5	6.5	3.3
WMW14-09	5.2	4.5	2.0
WMW14-10	5.3	4.0	2.5*
WMW14-11	6.7	6.5	2.8
WMW14-12	6.2	6.0	2.3
WMW14-13	7.3	7.0	2.7
WMW14-14	7.3	7.5	3.5

Table 34 lists the measurement of lead, beryllium, and cesium.

Table 34. West Manhattan waterfront Middle, Pb, ^{7}Be, and ^{137}Cs

Sample	Sample Date	Sample Time	Pb (ICPMS)	^{7}Be	^{7}Be Qualifiers	^{137}Cs	^{137}Cs Qualifiers
			mg/Kg	pCi/g		pCi/g	
WMW14-07	11/5/14	8:30	53	0.000	U	0.036	U
WMW14-08	11/5/14	8:49	33	0.500	U	0.099	U
WMW14-09	11/5/14	9:07	53	-0.011	U	0.143	U
WMW14-10	11/5/14	9:25	33	0.009	U	-0.071	U
WMW14-11	11/5/14	9:46	33	0.167	U	0.072	U
WMW14-12	11/5/14	10:15	30	0.538	U	0.128	U
WMW14-13	11/5/14	10:32	34	0.200	U	0.113	U
WMW14-14	11/5/14	10:49	33	0.866	U	0.116	U
U = Result is less than the sample detection limit							

Table 35 lists the measurements of compressional-wave velocity.

Table 35. West Manhattan waterfront Middle, acoustic velocity

Sample	Average P Velocity	Average P Velocity
	[m/s]	[ft/s]
WMW14-07	1,474.5	4,836.4
WMW14-08	1,597.7	5,240.3
WMW14-09	1,501.0	4,923.4
WMW14-10	1,537.6	5,043.4
WMW14-11	1,507.2	4,943.5
WMW14-13	1,480.8	4,857.1
WMW14-14	1,527.8	5,011.3

Table 36 lists the XRF results for other elements in the sediments.

Table 36. West Manhattan waterfront Middle, XRF.

Sample	S Avg	S Max	Fe Avg	Fe Max	Hg Avg	Hg Max	Zn Avg	Zn Max	Pb Avg	Pb Max	As Avg	As Max	Mn Avg	Mn Max
Push-Core	ppm													
WMW14-07	1,890.30	2,531.89	14,497.13	19,080.23	< LOD	< LOD	66.79	96.88	34.75	50.75	9.68	9.90	188.63	375.74
WMW14-08	1,331.80	1,930.06	16,466.36	18,574.70	< LOD	< LOD	69.51	88.67	32.15	36.32	< LOD	< LOD	259.99	302.67
WMW14-09	1,792.54	2,443.91	12,539.93	16,755.08	< LOD	< LOD	66.70	83.40	45.93	57.28	< LOD	< LOD	164.90	220.78
WMW14-10	1,718.37	2,392.69	13,151.56	33,724.63	< LOD	< LOD	82.79	138.80	57.53	107.43	11.86	11.86	184.23	470.18
WMW14-11	954.41	1,869.13	13,805.10	20,396.61	< LOD	< LOD	57.55	68.65	28.17	35.96	< LOD	< LOD	191.33	514.01
WMW14-12	2,236.74	3,309.65	14,962.11	17,465.85	< LOD	< LOD	67.40	85.76	38.63	45.01	< LOD	< LOD	196.44	240.83
WMW14-13	1,617.00	2,118.30	18,404.64	21,056.17	< LOD	< LOD	72.18	83.91	33.01	39.60	9.68	10.23	310.89	432.38
WMW14-14	1,348.17	2,404.99	15,550.09	17,345.06	< LOD	< LOD	64.43	74.42	31.44	36.30	< LOD	< LOD	200.55	282.46
*<LOD = below Limit Of Detection														

Figure 132. West Manhattan waterfront Middle orthosonograph insonified from the west.

Figure 133. West Manhattan waterfront Middle orthosonograph insonified from the east.

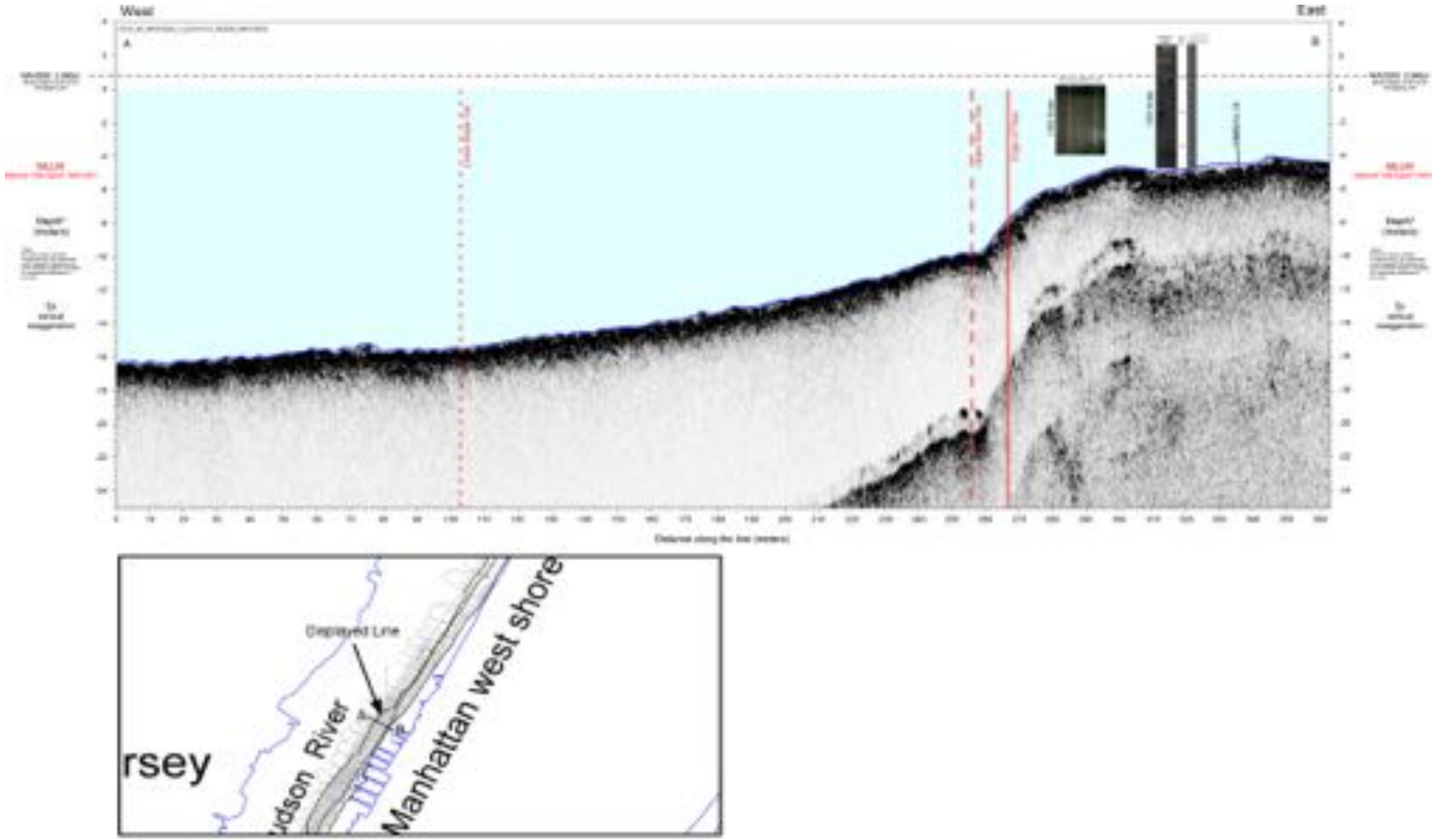

Figure 134. Seismic cross section, West Manhattan waterfront Middle.

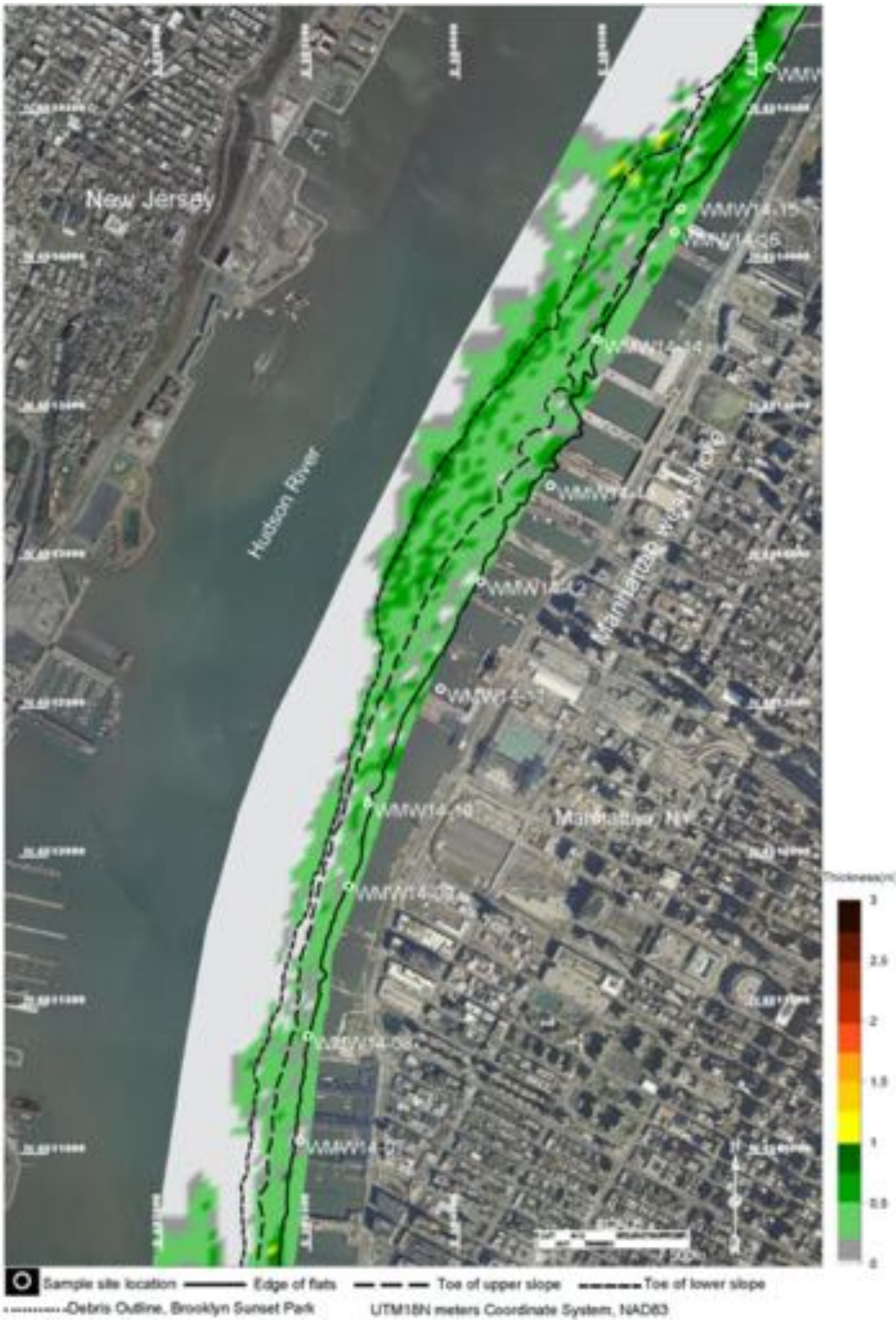

Figure 135. Acoustic silt isopach map for West Manhattan waterfront Middle.

5.7.3 Bottom classification (SPI, benthic classification)

Figure 136 displays the geological and structural substrate for West Manhattan waterfront Middle. Figure 137 plots the density of individual organisms per square meter. Figure 138 plots the composite bottom classification.

The West Manhattan waterfront (WMW) Middle shoreline where these samples were collected is anthropogenically-structured, hardened, and supported by pilings with some locations sampled in active slips and marinas. Eight grab samples (WMW14-07 to 14-14) were collected and sediment from these grabs was analyzed for grain size analysis. These samples had >50% fine sediment with several having >85% fines. Sites with sandier sediment were located within the mid-section of WMW where the North and South sections tended to have the highest percentages of silt and clay. Despite more sand being present at the middle WMW sites, overall camera penetration was similar among the three sections when compared with a mean value between 12 and 14cm camera penetration depth. The aRPD at the South and Middle sites had greater depth measured than sites sampled at WMW North. Of the fifteen sites sampled in WMW middle, eight had aRPD depth >3.75cm with only three sites having an aRPD depth less than 1.0cm. Epifauna and methane were not observed at the WMW sites for the middle area. Major modal grain size for the MWM areas had a phi class >4. Surface roughness for the three MWM areas was attributed to biological activities and the majority of images analyzed had visible worm tubes, voids; successional stage was classified as I on III – Stage I assemblages are occurring at the same place and time as evidence of Stage III organisms. Small burrows within the sediment were also observed and sediment was oxidized at the surface.

Much of this area is also included in the Hudson River Estuarine Sanctuary. Sites in a similar region were classified as “stressed” by Hale et al. (2007). The spread of healthy benthic habitat north along the west side of Manhattan is a testament to the commitment of the City to improving water treatment and educating the public to help maintain a healthy NY Harbor.

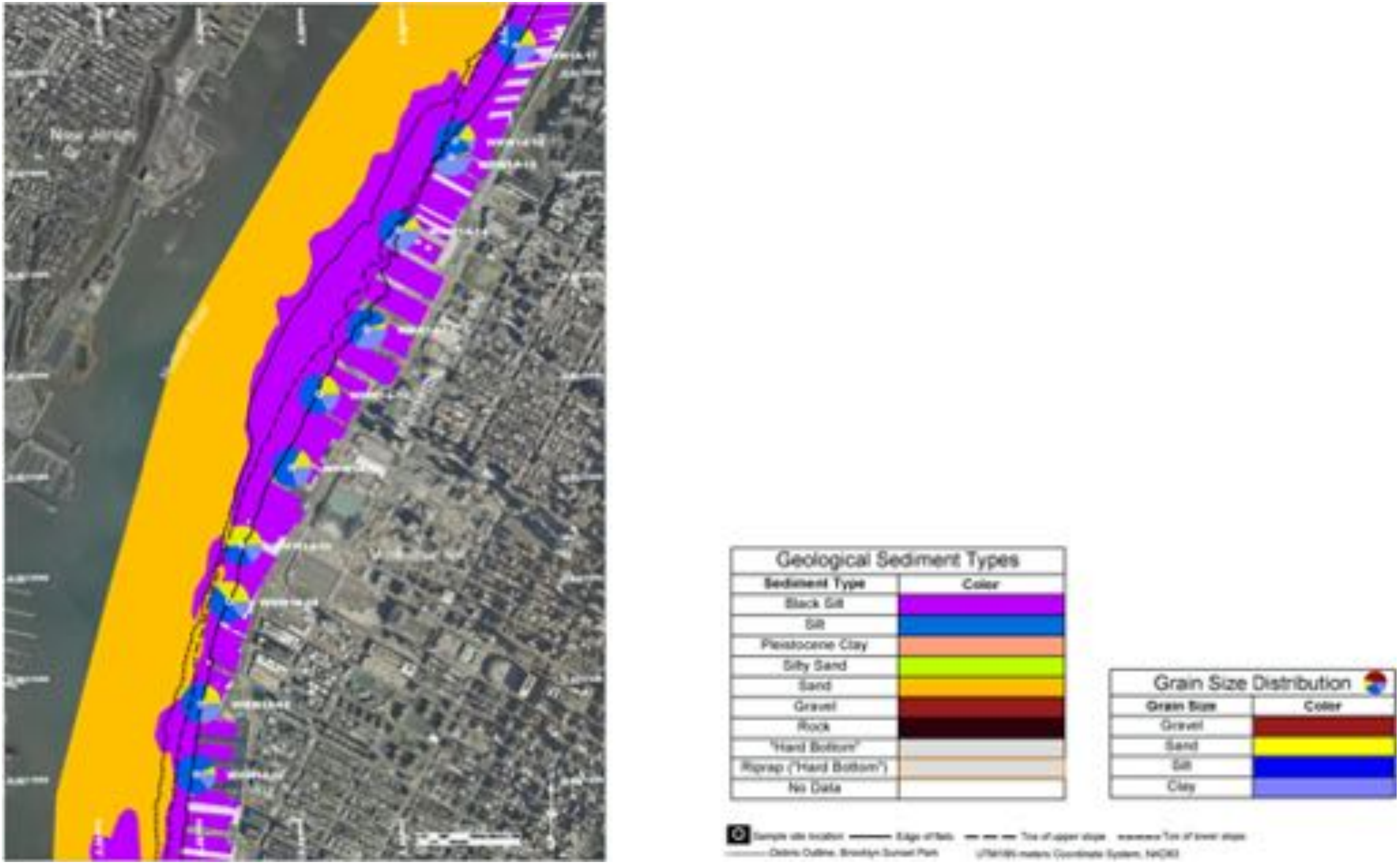

Figure 136. Bottom sediment type and geological substrate map for West Manhattan waterfront Middle.

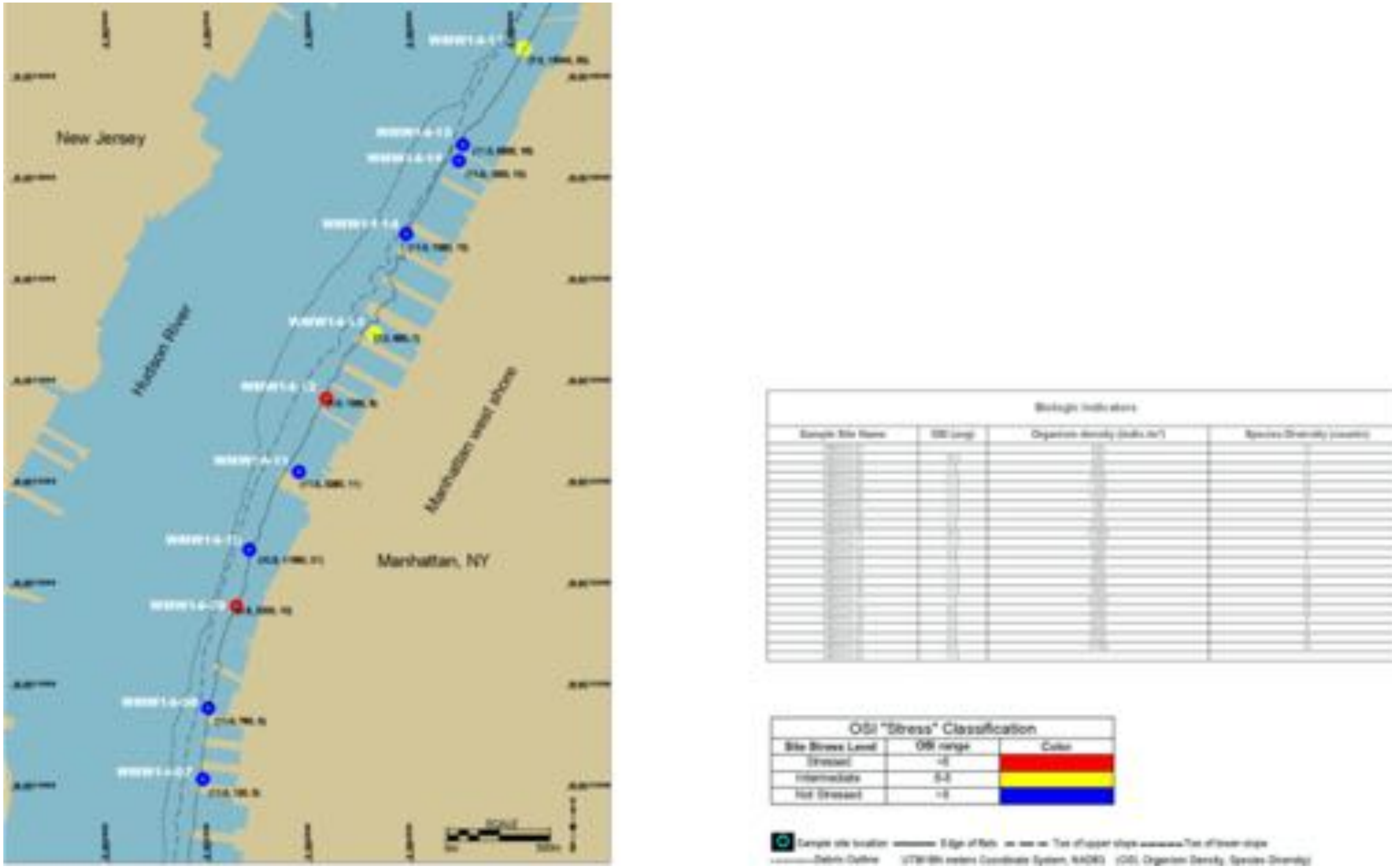

Figure 137. Organism density map for West Manhattan waterfront Middle. The numbers at each site represent the triplet (OSI, organism density per square meter, diversity as total number of species). In the cases of no measurement the space is left blank.

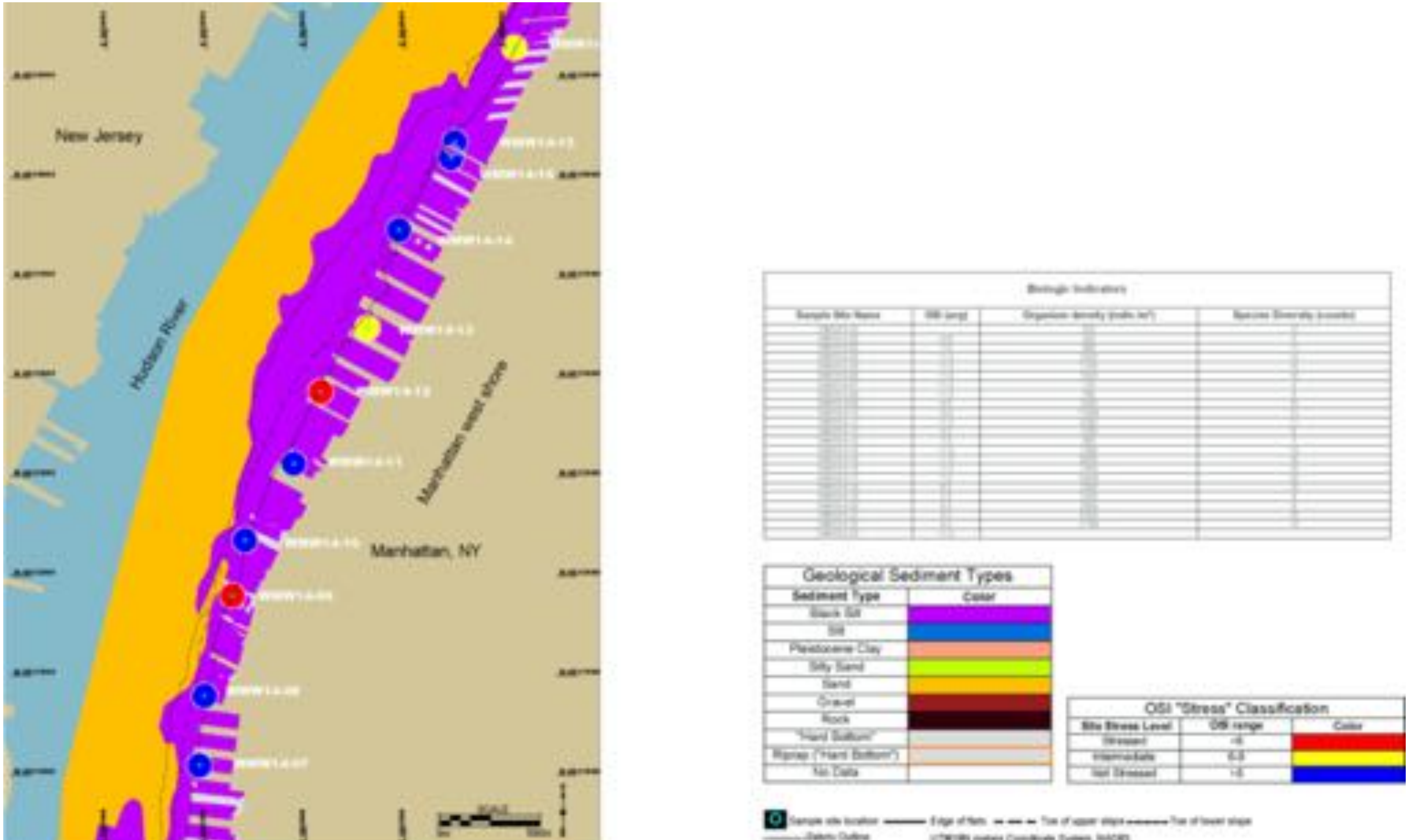

Figure 138. Composite bottom classification map for West Manhattan waterfront Middle.

5.8 Area Report 8. West Manhattan waterfront North (57^{th} St. to 109^{th} St.)

5.8.1 Morphology (Bathymetry, bathymetry analysis)

Figure 139 is a location photograph for West Manhattan waterfront North. Note the structures include a marina with slips between the piles.

Figure 140 is the bathymetry for West Manhattan waterfront North. Single and multibeam data from e4sciences (2015) were combined in 5m x 5m and 1m x 1m grids, respectively, using a triangular linear interpolation. Historical data from NOAA surveys F00573 (2009) and F00598 (2012), and USACE survey 4126 (2014), were combined in a 1m x 1m grid using a triangular linear interpolation. 2D first and second order derivative filters were applied to the 2014 historical bathymetry. Figure 141 plots the derivative maps for the bathymetry. Figure 142 is the difference map between 2015 and 2014. The map displays both results of the difference in bathymetry for the 5m x 5m grid in the ultrashallow area, and the 1m x 1m grid in the deeper area. All grids were obtained with triangular linear interpolations.

Figure 139. Location photo for West Manhattan waterfront North.

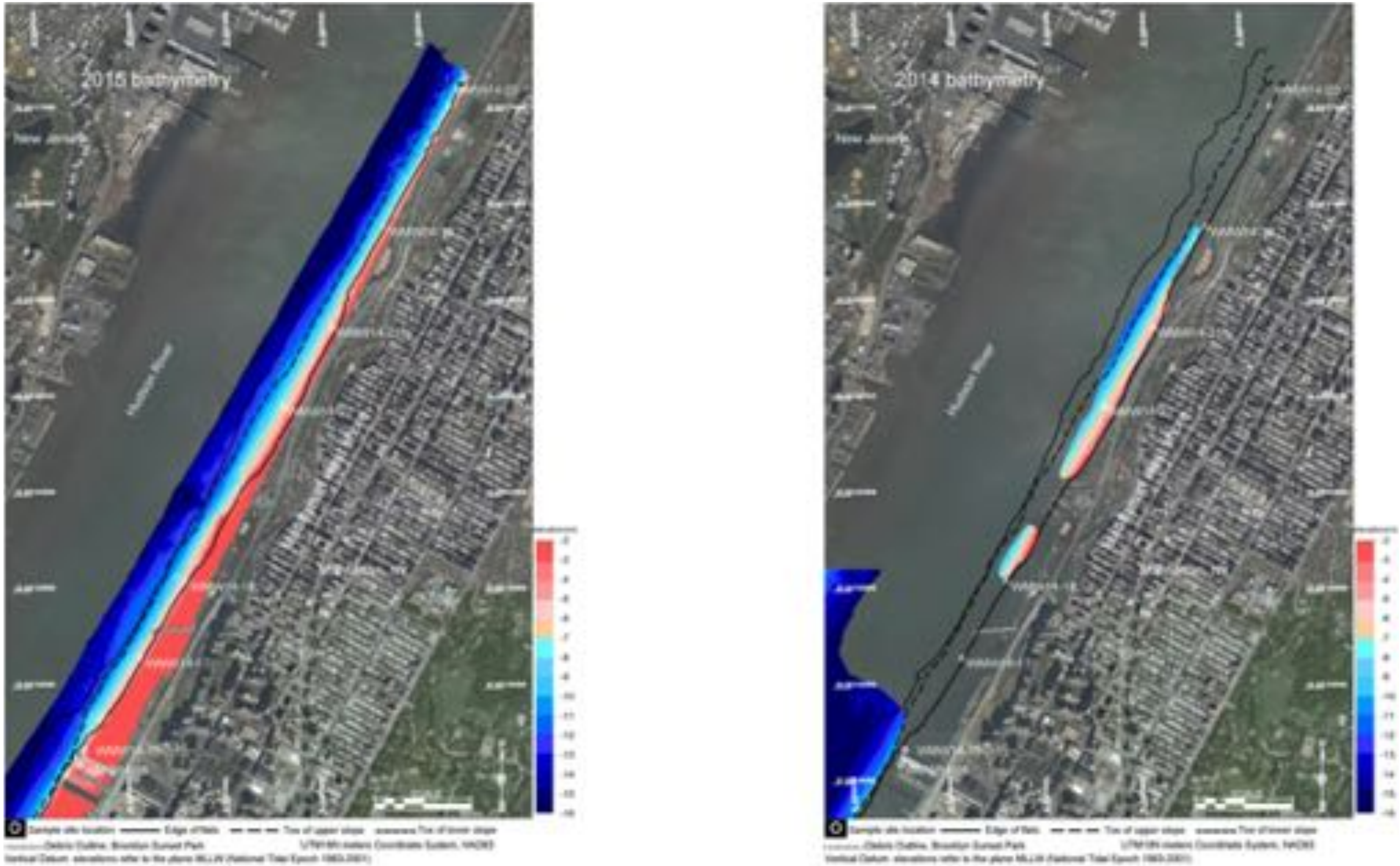

Figure 140. Bathymetric and location map for West Manhattan waterfront North. (Left) Single and multibeam data from e4sciences (2015) were combined in 5m x 5m and 1m x 1m grids, respectively, using a triangular linear interpolation. (Right) Historical data from NOAA surveys F00573 (2009) and F00598 (2012), and USACE survey 4126 (2014), were combined in a 1m x 1m grid using a triangular linear interpolation.

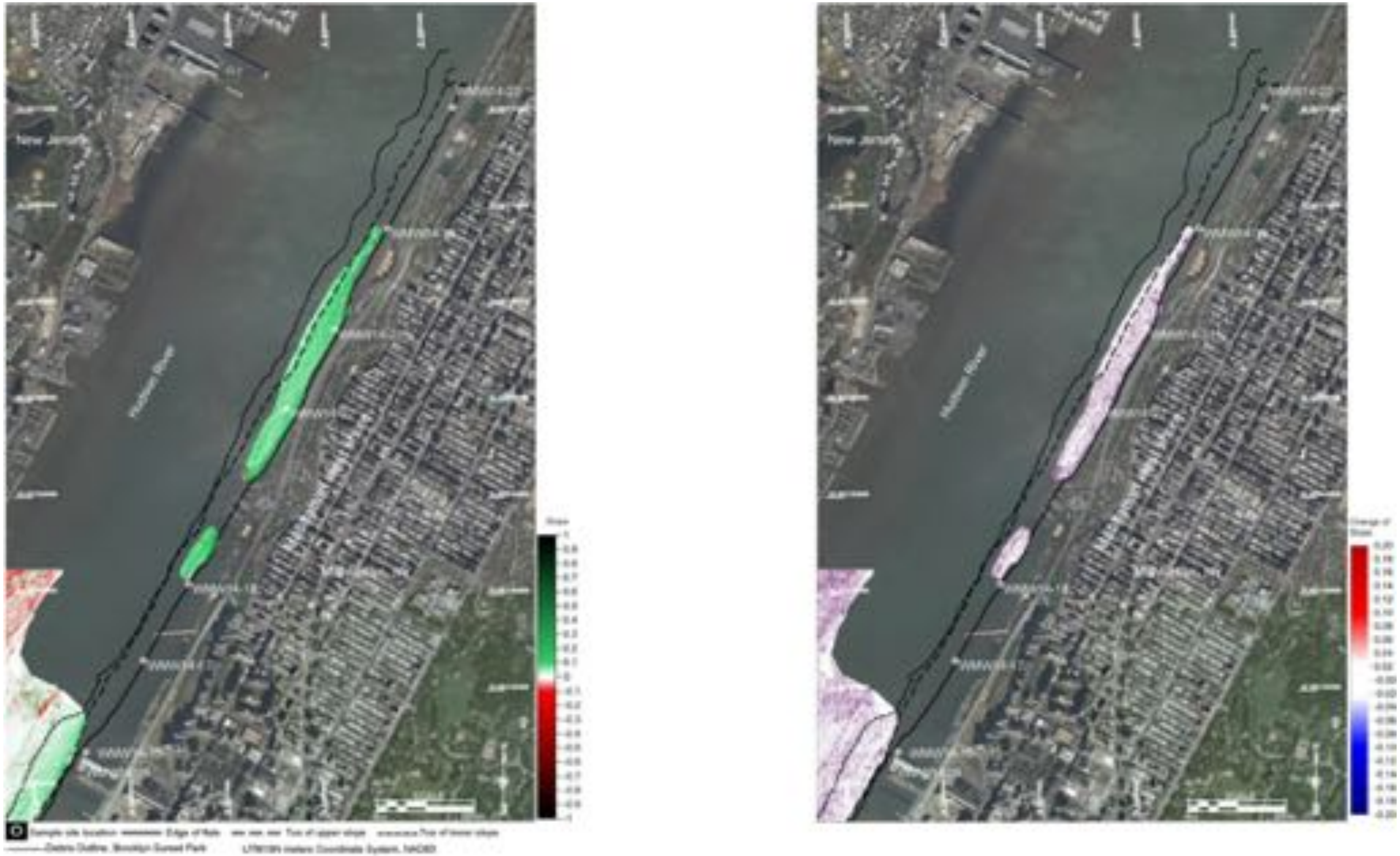

Figure 141. Bathymetric analysis for West Manhattan waterfront North (derivative maps for Area 8). Data from NOAA surveys F00573 (2009) and F00598 (2012) and USACE survey 4126 (2014) were combined in a 1m x 1m grid using a triangular linear interpolation. (Left) 2D first order derivative filter – slope. (Right) 2D second order derivative filter – change in slope.

Figure 142. Bathymetry elevation difference map 2015 minus 2014 for West Manhattan waterfront North. The 2015 bathymetry includes single and multibeam bathymetries from e4sciences. The 2014 bathymetry includes NOAA surveys F00573 (2009) and F00598 (2012) and USACE survey 4126 (2014). The map displays both results of the difference in bathymetry for the 5m x 5m grid in the ultrashallow area, and the 1m x 1m grid in the deeper area. All grids were obtained with triangular linear interpolations.

5.8.2 Sediments (side-scan, seismic, cross sections, isopachs, grab samples)

Figure 143 displays the orthosonograph of West Manhattan North insonified from the west and north. Figure 144 is its pair insonified from the east and the south.

Figure 145 is a sub-bottom seismic cross from west to east across West Manhattan waterfront North. Figure 146 is the acoustic silt isopach.

Table 37 lists the grain size mean and standard deviation. Note the variation of mean size and standard deviation with location.

Table 37. West Manhattan waterfront North grain size

Sample	Mean	Median	Std. Deviation
	Φ		
WMW14-15	7.0	6.5	3.3
WMW14-16	8.0	8.0	3.0
WMW14-17	7.0	7.0	3.0
WMW14-18	7.5	7.0	2.0
WMW14-19	5.7	6.0	1.0
WMW14-20	3.2	5.5	5.0
WMW14-21	7.3	2.5	2.5
WMW14-22	7.5	7.5	3.0

Table 38 lists the measurement of lead, beryllium, and cesium.

Table 38. West Manhattan waterfront North Pb, ^{7}Be, and ^{137}Cs

Sample	Sample Date	Sample Time	Pb (ICPMS)	^{7}Be	^{7}Be Qualifiers	^{137}Cs	^{137}Cs Qualifiers
			mg/Kg	pCi/g		pCi/g	
WMW14-15	11/5/14	11:07	34	0.056	U	0.108	U
WMW14-16	11/5/14	11:25	35	1.090	U	0.100	U
WMW14-17	11/5/14	11:45	94	-0.031	U	0.254	
WMW14-18	11/5/14	12:35	120	-0.011	U	0.016	U
WMW14-19	11/5/14	13:20	29	0.014	U	0.514	
WMW14-20	11/5/14	13:45	36	0.468	U	0.141	U
WMW14-21	11/5/14	14:30	78	0.000	U	0.009	U
WMW14-22	11/5/14	15:05	140	0.110	U	0.000	U
U = Result is less than the sample detection limit							

Table 39 lists the measurement of compressional-wave velocity in the sediments.

Table 39. West Manhattan waterfront North, acoustic velocity

Sample	Average P Velocity	Average P Velocity
	[m/s]	[ft/s]
WMW14-15	1,490.5	4,889.0
WMW14-16	1,513.1	4,962.9
WMW14-17	1,525.1	5,002.4
WMW14-19	1,503.8	4,932.5
WMW14-22	1,485.4	4,872.0

Table 40 lists the XRF results for other elements in the sediments.

Table 40. West Manhattan waterfront North XRF

Sample	S Avg	S Max	Fe Avg	Fe Max	Hg Avg	Hg Max	Zn Avg	Zn Max	Pb Avg	Pb Max	As Avg	As Max	Mn Avg	Mn Max
Push-Core	ppm													
WMW14-15	1,965.13	2,531.89	12,859.55	17,041.14	< LOD	< LOD	57.86	70.64	28.24	31.76	< LOD	< LOD	141.18	185.17
WMW14-16	1,502.57	1,708.81	14,856.15	18,254.43	< LOD	< LOD	59.96	70.37	31.07	35.30	< LOD	< LOD	277.54	372.27
WMW14-17	2,492.41	3,725.79	15,600.12	18,215.87	< LOD	< LOD	121.77	134.44	90.53	113.04	< LOD	< LOD	167.37	240.35
WMW14-18	6,618.74	10,543.05	20,460.28	21,353.52	< LOD	< LOD	171.32	195.48	111.20	118.65	13.34	13.53	192.73	236.54
WMW14-19	3,295.98	6,847.52	18,077.22	22,331.66	< LOD	< LOD	132.63	226.02	98.08	166.50	24.54	41.26	190.37	288.13
WMW14-20	2,723.93	6,325.06	17,200.53	21,699.21	< LOD	< LOD	66.07	84.65	34.19	45.02	< LOD	< LOD	291.30	382.64
WMW14-21	2,673.01	4,159.25	18,169.61	21,992.74	< LOD	< LOD	126.15	158.81	107.70	156.56	19.00	22.68	206.65	265.36
WMW14-22	2,025.20	3,901.10	16,042.07	18,906.12	< LOD	< LOD	183.93	451.08	155.05	422.45	14.86	17.15	126.15	182.66

*<LOD = below Limit Of Detection

Figure 143. West Manhattan waterfront North orthosonograph insonified from the west.

Figure 144. West Manhattan waterfront North orthosonograph insonified from the east.

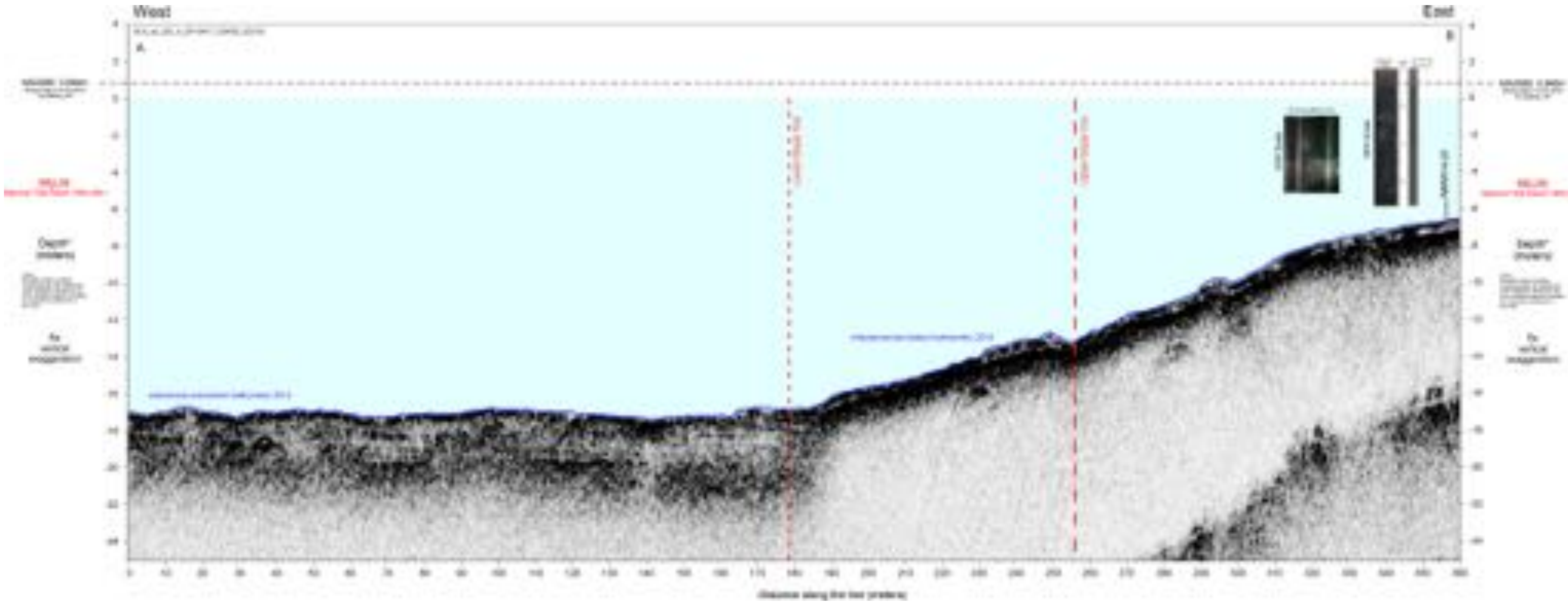

Figure 145. Seismic cross section, West Manhattan waterfront North.

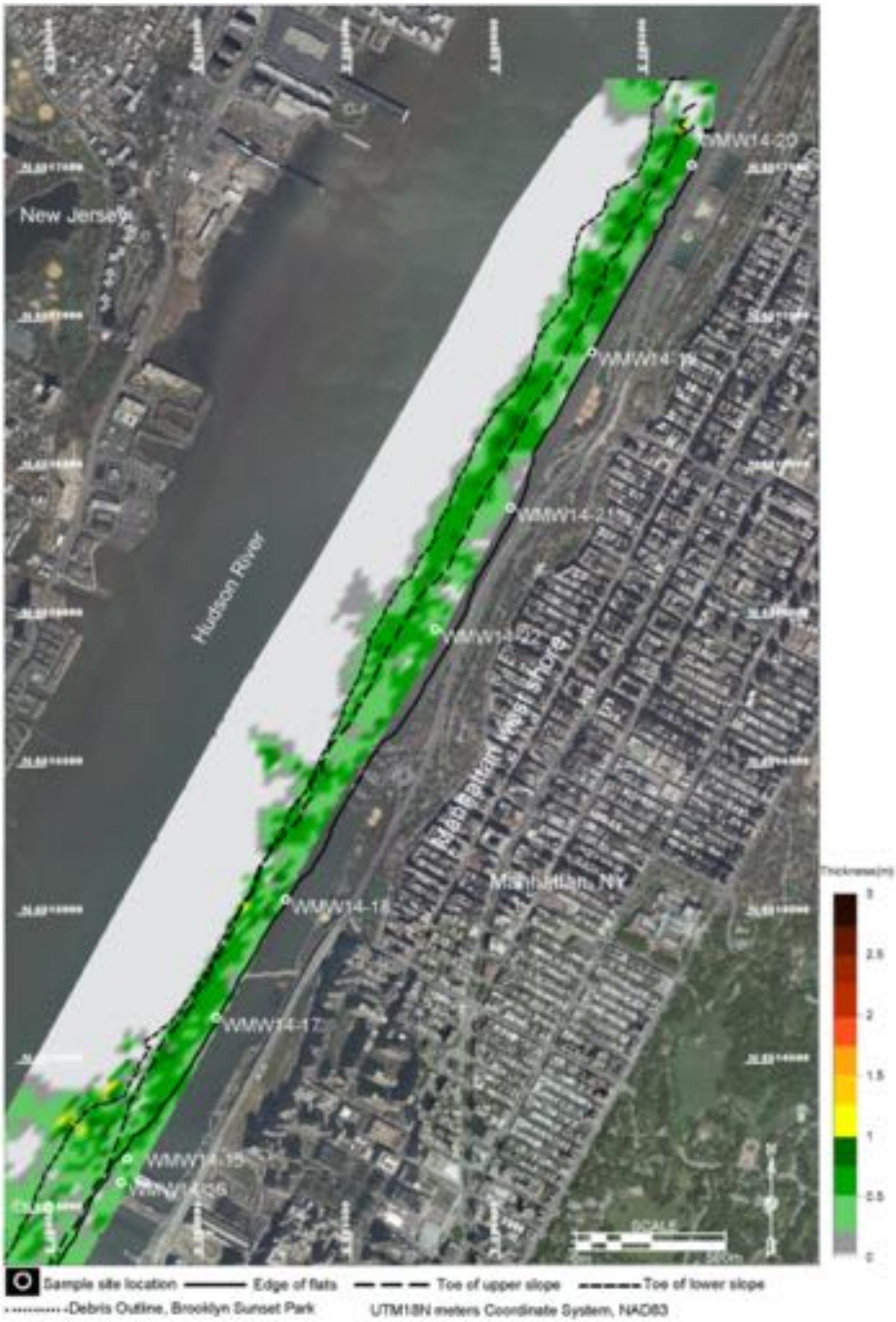

Figure 146. Acoustic silt isopach map for West Manhattan waterfront North.

5.8.3 Bottom classification (SPI, benthic classification)

Figure 147 displays the geological and structural substrate for West Manhattan waterfront North. Figure 148 plots the density of individual organisms per square meter. Figure 149 plots the composite bottom classification.

The West Manhattan waterfront (WMW) North shoreline where these samples were collected is anthropogenically-structured, hardened, and supported by pilings with some locations sampled in active slips and marinas. Eight grab samples (WMW14-15 to 14-22) were collected and sediment from these grabs was analyzed for grain size analysis. These samples had >50% fine sediment with several having >85% fines. Sites with sandier sediment were located within the mid-section of WMW where the North and South sections tended to have the highest percentages of silt and clay. Despite more sand being present at the middle WMW sites, overall camera penetration was similar among the three sections when compared with a mean value between 12 and 14cm camera penetration depth. The aRPD at the South and Middle sites had greater depth measured than sites sampled at WMW North. WMW North sites had lower aRPD values ranging between 0.2 to 2.25cm and only four of the 10 sites sampled in this area had aRPD values >3.75cm. Epifauna and methane were not observed at the WMW North sites. Major modal grain size for the three areas had a phi class >4. Surface roughness for the three WMW areas was attributed to biological activities and the majority of images analyzed had visible worm tubes, voids, and successional stage was classified as I on III – Stage I assemblages are occurring at the same place and time as evidence of Stage III organisms. Small burrows within the sediment were also observed and sediment was oxidized at the surface.

The northernmost sites along the WMW (area 8 – this area) were the least health, the most stressed and had the lowest calculated OSI values. The shallow benthic zone in this area is narrow, with high force from current due to the narrow shelf. There is also increased use of the shallows and increased boat traffic relative to the further south regions of Manhattan's western shore. All of these contribute to the stresses on benthic communities in this area, and contrast with the healthier, less stressed communities observed in habitats further south along WMW.

Figure 147. Bottom sediment type and geological substrate map for West Manhattan waterfront North.

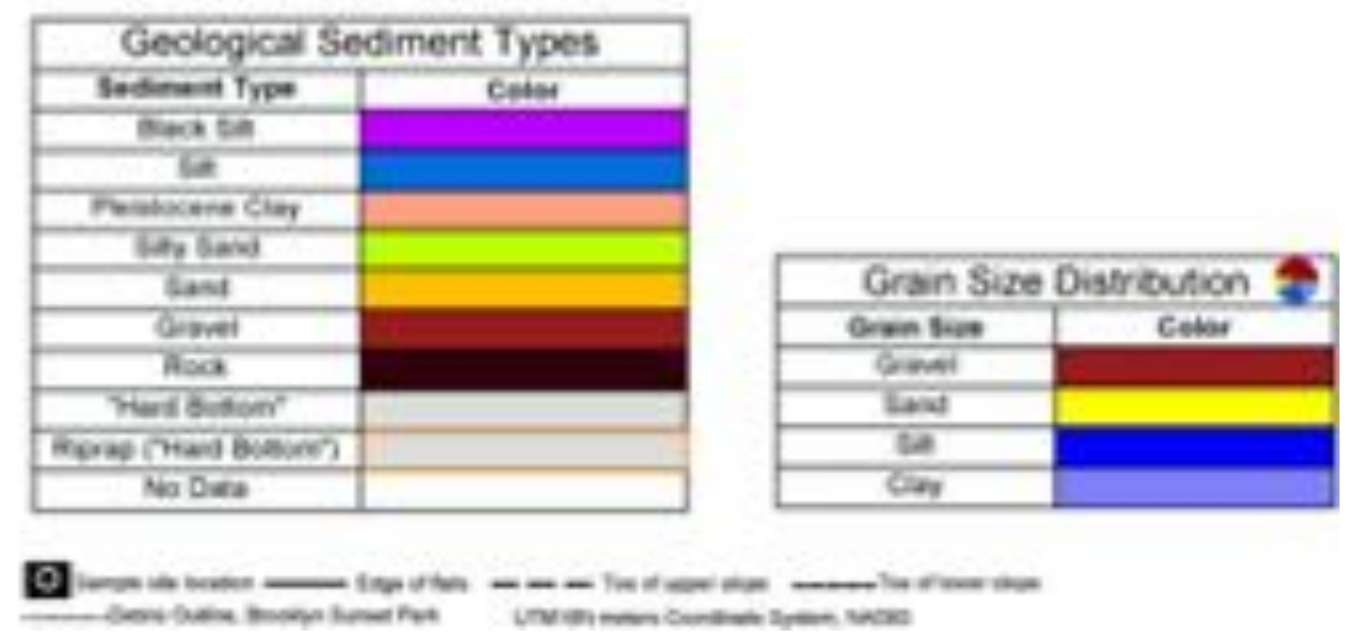

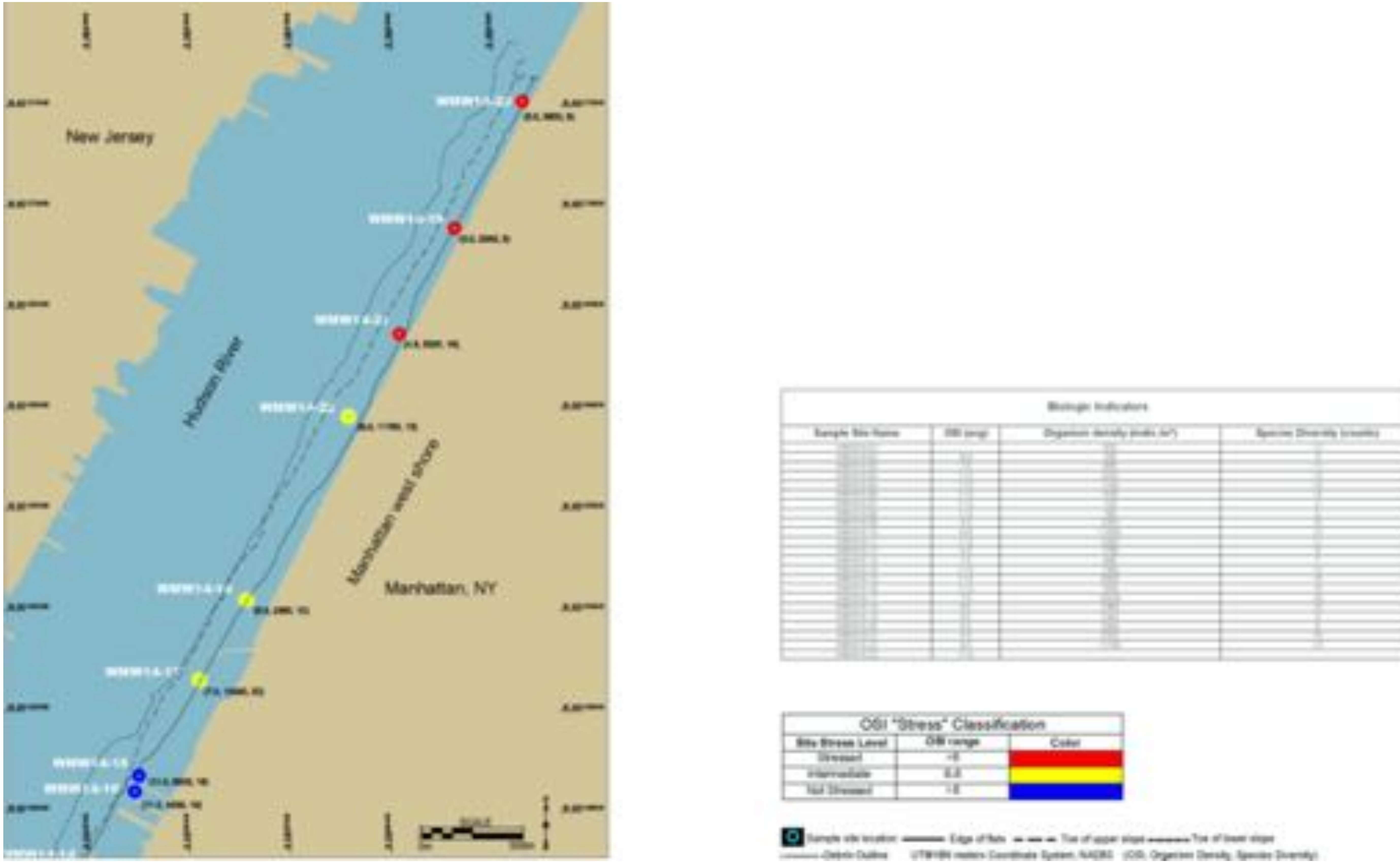

Figure 148. Organism density map for West Manhattan waterfront North. The numbers at each site represent the triplet (OSI, organism density per square meter, diversity as total number of species). In the cases of no measurement the space is left blank.

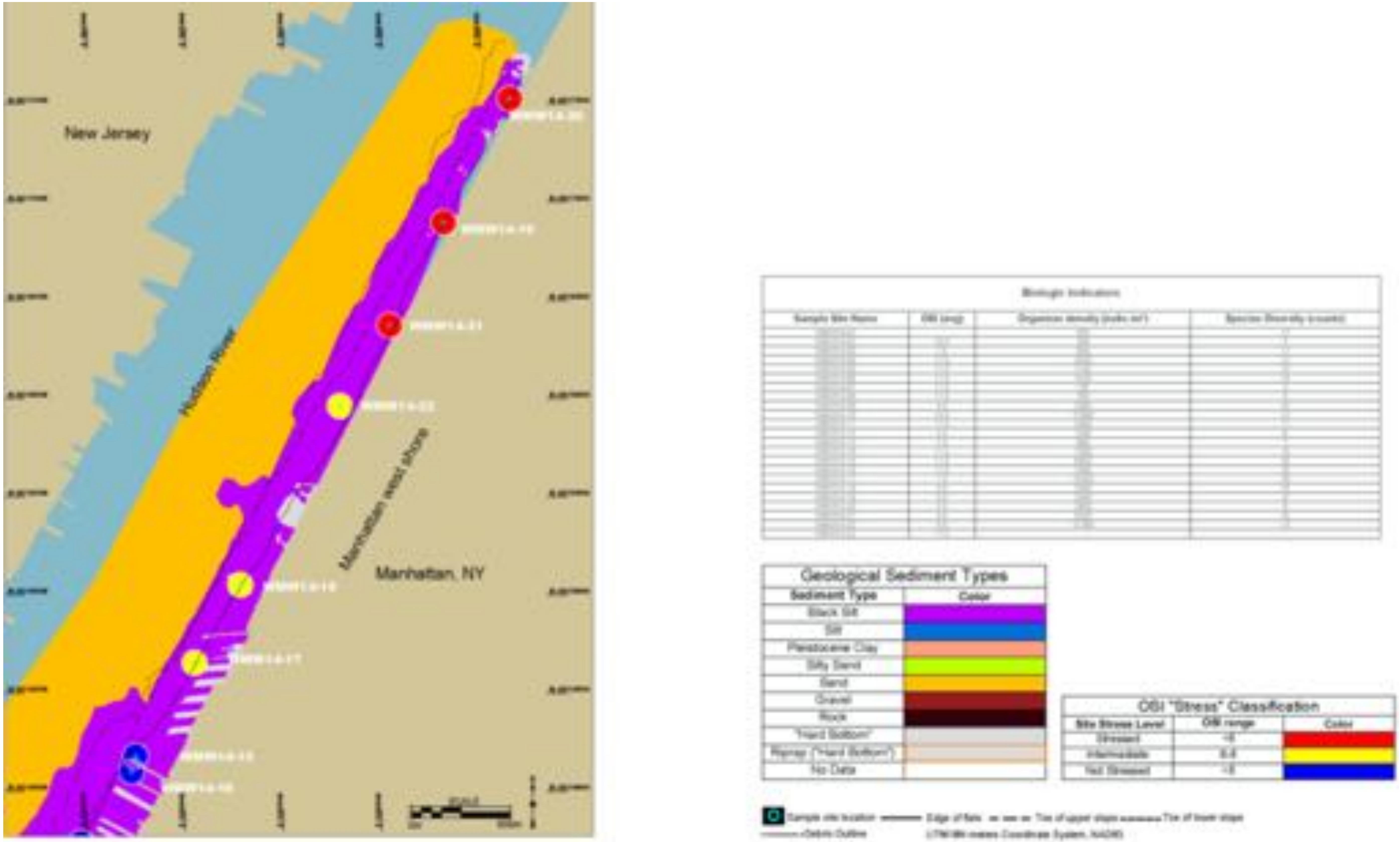

Figure 149. Composite bottom classification map for West Manhattan waterfront North.

6.0 Conclusions

The New York State Department of Environmental Conservation (DEC) monitors the Hudson River Estuary. The New York City Department of Environmental Protection (DEP) has partnered with the DEC to map the shallow waters in the Hudson and East Rivers.

The DEP assigned e4sciences (e4) to map the sediment strata, the shoreline structures, and the benthic faunal communities on both the western shoreline of Manhattan and the northwestern shore of Brooklyn. e4 measured the bathymetry, sonar reflectivity, seismic reflectivity, Sediment Profile Images (SPIs), sediment chemistry, grain size, infrastructure, and benthic species.

e4 developed detailed bathymetric, acoustic-reflectivity, benthic-organism, and acoustic-character maps of the shallow portions of the Upper Bay of New York Harbor. The area of investigation is divided into eight areas:

1. Bay Ridge Flats
2. Governors Island
3. Sunset Park waterfront
4. Brooklyn Bridge Park
5. Brooklyn Navy Yard
6. West Manhattan waterfront South (Harrison St. to 17th St.)
7. West Manhattan waterfront Middle (17th St. to 57th St.)
8. West Manhattan waterfront North (57th St. to 109th St.)

1. e4 collected and analyzed sediment cores and grab samples to determine grain size distribution, benthic invertebrate faunal communities, and sediment chemistry. e4 collected and analyzed Sediment Profile Imagery (SPI) to determine fine-scale structures, infaunal activity, and water chemistry at the sediment-water interface. e4 integrated geological, chemical, and biological data with sub-bottom datasets to derive sediment accumulation rates and integrated bottom classifications. e4 integrated newly collected data and analyses with previous work conducted in the harbor. The current analysis included measures of change over time, to the extent that previous work spatially and analytically overlaps areas of investigation in this project.

2. The survey, SPI drop, and sample site results show that five areas – Bay Ridge Flats, Brooklyn Bridge Park, Sunset Park waterfront, West Manhattan waterfront South, and West Manhattan waterfront Middle – are overall healthy, lightly stressed, ecosystems. They reflect the diversity of ecosystems in NY Harbor.

3. The other three areas – Governors Island, Brooklyn Navy Yard, and West Manhattan waterfront North – are a mixture of healthy and stressed sites, with many of the healthier communities in these areas confined to regions of relatively low rates of sediment accumulation.

4. Healthy communities exist in both coarse and fine-grained sediments. Communities in sandier areas are more stable and better established. Healthy communities in siltier areas are more variable and, we hypothesize, sensitive to change in sediment accumulation rate and physical disturbance.

5. e4sciences compared the current results with data collected 10 or more years ago. Seasonal spring to fall variations notwithstanding, e4sciences observed that the western shorelines of Manhattan and Brooklyn are generally healthy and have been improving since 1993. Efforts to remove polluted silts, increase park areas (with corresponding reductions in boat traffic), and clean the water have begun to show measurable success.

6. On the southwest shore of Manhattan, our study showed the most benthic habitat quality improvement when compared with historical data. This is most likely the consequence of New York City's continued efforts to improve water quality with advanced sewage treatment programs and education of the public, with additional benefits accruing to the local benthic community from the establishment of the Hudson River Estuarine Sanctuary in 1998.

7. Analyses of the benthic communities show a strong association with sediment type, specifically grain size. Sonic reflectivity in the orthosonographs, benchmarked by cores and grab samples, distinguishes the differences between the sandy environments and the silty environments.

8. The current results, when compared with data collected 10 or more years ago, indicate that benthic habitat quality within open water areas such as Bay Ridge Flats and Governors Island remained stabilized with many Organism-Sediment Index (OSI) values greater than 6.

9. Observations of healthy communities on the western shore of Manhattan increased and e4 observed healthy sites further north in this area than had been previously reported.

10. We found pockets of stressed habitats in Brooklyn Navy Yard, at the mouth of the Gowanus Canal, within berthing slips of West Manhattan waterfront North, and in sediment traps around the shore of Governors Island and on the slopes of Bay Ridge Flats. These areas are active both from natural tidal forces and from sediment movement related to human use of the harbor. Many have been previously identified as stressed habitats.

11. The more diverse and well-established communities live in the sandier environments with better circulation. Healthy communities can still be found in the siltier, finer-grained sediments, but these are more variable and sensitive to change.

12. The contour map of the black silt shows that siltier environments are generally restricted to the inner confines of the piers and the leeward sides of structures and outcrops, such as Governors Island.

13. Opportunistic benthic organisms can be found in Sunset Park waterfront, the Brooklyn Navy Yard, West Manhattan waterfront North, and sediment traps on the shore of Governors Island and the slopes of Bay Ridge Flats.

14. In our SPI analyses, we observed small opportunistic tube-dwelling polychaetes or oligochaetes, identified as Stage I successional species. They are among the first macrofaunal components to colonize newly disturbed sediments.

15. These worms may reach high densities of greater than $10^5/m^2$ within a few days to weeks after disturbance of the bottom. The pioneering species that colonize a disturbed bottom may vary, depending on substratum, but the opportunists are the initial species to occupy organically enriched habitat. They oxidize the sediment-water interface and they pave the way for later successional stage species (Stage II and Stage III). The pioneering species feed

near the sediment surface or from the water column. They construct tube walls or shells that isolate them from the poor quality sediment often low in oxygen and high in organic content.

16. In Bay Ridge Flats, Brooklyn Bridge Park, Governors Island, West Manhattan waterfront South, and West Manhattan waterfront Middle, infaunal amphipods, gastropods, and other sediment feeders represent equilibrium stage (Stage III) or successional end-stage species. e4 found shallow-dwelling bivalves (*Mulinia lateralis*, *Tellina agilis*), grazing gastropods (*Illyanassa* sp.), and a few species of tubicolous amphipods (*Ampelisca sp.*).

17. Stage III assemblages include maldanid, nepthyd, and lumbrinerid polychaetes, nuculanid clams, and *Molpadia* tunicates. These areas have deeply oxygenated sediment surfaces where the redox discontinuity commonly reaches depths of over 10 cm.

18. e4sciences used bathymetry, sonar reflectivity, and seismic reflectivity to characterize site sediments, their properties, and their thicknesses. A contour map shows the thickness and spatial distribution of the black silt. Pleistocene sediments are exposed in Bay Ridge Flats and the northeastern shore of Governors Island. Bay Ridge Flats have retained their morphology over two hundred years.

19. The schist of the Hartland Formation is exposed in Governors Island. The Fordham gneiss is exposed in Brooklyn Bridge Park underneath the Manhattan Bridge. Rock is relatively shallow on the west shore of Manhattan.

20. The fish in New York Harbor prefer the areas of high vorticity. The orthosonographs show schools of fish are observed in those areas around Governors Island, Manhattan, and Bay Ridge Flats.

21. Appendices contain the raw and processed digital data with their corresponding shapefiles and metadata.

22. The metadata describes the data type, size, and geographic extent of both the raw and processed data. The metadata follows the Federal Geographic Data Committee standards.

23. e4sciences provided license-free viewers for side-scan sonar and sub-bottom reflection seismology.

24. e4sciences identified controlling factors for the spatial distribution of the benthic communities as (a) the geological or structural substrate, (b) well-circulating cleaner water, and (c) anthropogenic disturbance.

25. Water quality and the presence of pathogens, pollutants, and suspended sediments are important. The amount of pollutants has been reduced in the past forty years. Suspended sediment load is declining. These trends have contributed to improved benthic community health in the Upper Bay areas of New York Harbor.

26. e4sciences did not observe completely anoxic conditions in the benthic zone at any of our sample sites.

27. e4sciences found that the areas of investigation are lightly stressed at worst, and are healthier than observed in previous work conducted in the 1970's and 1990's.

7.0 References

Abdus-Samad, S. 2013. The Effect of the Composition of Concrete on Biodiversity and Ecology on Benthic Organisms. *New York Harbor School*, 1-23.

Able, K. and Duffy-Anderson, J. 1999. Effects of Municipal Piers on the Growth of Juvenile Fishes in the Hudson River Estuary: A Study across a Pier Edge. *Marine Biology*, 133, 409–418.

Able, K. and Duffy-Anderson, J. 2005. A Synthesis of Impacts of Piers on Juvenile Fishes and Selected Invertebrates in the Lower Hudson River. Institute of Marine and Coastal Sciences, Rutgers.

Able, K. and Duffy-Anderson, J. 2006. Impacts of Piers on Juvenile Fishes in the Lower Hudson River. *The Hudson River Estuary*, Cambridge University Press, 428-440.

Able, K., Manderson, J., and Studholme, A. 1998. The Distribution of Shallow Water Juvenile Fishes in an Urban Estuary : The Effects of Manmade Structures in the Lower Hudson River. *Estuaries*, 21 (48), 731–744.

Adams, D. and Benyi, S. 2003. Sediment Quality of the NY/NJ Harbor System: a 5-year Revisit. U.S. EPA-Region 2, Division of Science and Assessment.

Adams, D.A., O'Connor, J.S. and S.B. Weisberg (1998). Sediment quality of the NY/NJ harbor system: An investigation under the Regional Environmental Monitoring and Assessment Program (R-EMAP). *Final Report*. EPA/902-R-98-001, March 1998.

Austin, H., & Findlay, S. 1989. Benthic bacterial biomass and production in the Hudson River estuary. *Microbial Ecology*, 18 (2), 105-116.

Ayers, J. 1951. The Average Rate of Fouling of Surface Objects and of Submerged Objects in the Waters Adjacent to New York Harbor. *Office of Naval Research, Status Rept*.

Baard, E., Jackson, T., and Melnick, R. 2005. *The East River*. Arcadia Publishing.

Baldigo, B., Sloan, R., Smith, S., Denslow, N., Blazer, V., and Gross, T. 2006. Polychlorinated Biphenyls, Mercury, and Potential Endocrine Disruption in Fish from the Hudson River, New York, USA. *Aquatic Sciences*, 68 (2), 206–228. doi:10.1007/s00027-006-0831-8.

Baskerville, C.A. 1994. Bedrock and Engineering Geologic Maps of New York County and parts of Kings and Queens Counties, New York, and parts of Bergen and Hudson Counties, New Jersey: U.S. Geological Survey, Miscellaneous Investigations Series Map I-2306, scale 1:24000.

Baskerville, C.A.1992. Bedrock and Engineering Geologic Maps of Bronx County and parts of New York and Queens Counties, New York: U.S. Geological Survey, Miscellaneous Investigations Series Map I- 2003, scale 1:24000.

Bell, R., Flood, R., and Carbotte, S. 2003. Hudson River Estuary Program Benthic Mapping Project: New York State Department of Environmental Conservation Phase II.

Bell, R.E., Flood, R.D., Carbotte, S., Ryan, W.B.F., McHugh, C., Cormier, M., Versteeg, R., Bokuniewicz, H., Ferrini, V.L., Thissen, J., Ladd, J.W., and Blair, E.A. 2006. Benthic Habitat Mapping in the Hudson River Estuary. *The Hudson River Estuary*, Cambridge Univ Press, 51-64.

Bell, R.E., Flood, R.D., Carbotte, S., Ryan, W.B.F., McHugh, C., Cormier, M., Versteeg, R., Bokuniewicz, H., Ferrini, V.L., and Thissen, J. 2000. Hudson River Estuary Program Benthic Mapping Project, Phase 1 Final Report NYSDEC Under Contract C003843.

Bell, R.E., Flood, R.D., Carbotte, S., Ryan, W.B.F., Nitsche, F.O., Chilrud, S., Arko, R., Ferrini, V., Slagle, A., Bertinato, C. and Turrin, M. 2003. Hudson River Estuary Program Benthic Mapping Project, Phase 2 Report to NYSDEC under contract C004092.

Bell, R.E., Flood, R.D., Carbotte, S.M., Ryan, W.B.F., Nitsche, F.O., Chilrud, S., Arko, R., Ferrini, V., Slagle, A., Bertinato, C., and Turrin, M. 2004a. Hudson River Estuary Program Benthic Mapping Project Phase III Report 1, report to NYSDEC under contract C004092.

Bell, R.E., Flood, R.D., Carbotte, S.M., Ryan, W.B.F., Nitsche, F.O., Chilrud, S., Arko, R., Ferrini, V., Slagle, A., Bertinato, C., and Turrin, M. 2004b, New York Harbor Area subreport, Lucent Technologies Environmental Benefit Plan project, report to NYSDEC.

Benyi, S., Hollister, J., Kiddon, J., and Walker, H. 2009. A Process for Comparing and Interpreting Differences in Two Benthic Indices in New York Harbor. *Marine Pollution Bulletin*, 59 (1-3), 65–71. doi:10.1016/j.marpolbul.2008.11.009.

Berger, N., Haseltine, M., Boehm, J., and Goreau, T. 2006. Increased Oyster Growth and Survival Using Biorock Technology. *Innovative Methods of Marine Ecosystem Restoration*, 12, 141-150. doi: 10.1201/b14314-13.

Blackford, E. 1885. The Oyster Beds of New York. *Transactions of the American Fisheries Society*, 14 (1), 85–89. doi:10.1577/1548-8659.

Blackford, E. 1887. *Report of the Oyster Investigation and Shell-Fish Commission for the Year Ending November 30th, 1887.* The Troy Press Company Printers.

Blackford, E. 1888. *Report of the Oyster Investigation and of Survey of Oyster Territory for the Years 1885 and 1886.* Argus Company Printers.

Boesch, D. and Rabalais, N. 1991. Effects of Hypoxia on Continental Shelf Benthos: Comparisons between the New York Bight and the Northern Gulf of Mexico. *Geological Society, London, Special Publications*, 58 (1), 27–34. doi:10.1144/GSL.SP.1991.058.01.02.

Bopp, R.F., Simpson, H.J., Olsen, C.R., and Kostyk, N. 1981. Polychlorinated Biphenyls in Sediments of the Tidal Hudson River, New York. *Environmental Science & Technology*, 15 (2), 210-216. doi:10.1021/es00084a007.

Bragin, A.B., Woolcott, C., and Misuik, J. 2009. A Study of the Benthic Macroinvertebrate Community of an Urban a Estuary: New Jersey's Hackensack Meadowlands. *New Jersey Meadowlands Commission*.

Bricelj, V., Ford, S., Borrero, F., Perkins, F., Rivera, G., Hillman, R., Elston, R.A., and Chang, J. 1992. Unexplained Mortalities of Hatchery Reared, Juvenile Oysters, Crassostrea Virginica. *Journal of Shellfish Research*, 11, 331-347.

Brinkhuis, B. 1980. *Biological Effects of Sand and Gravel Mining in the Lower Bay of New York Harbor: An Assessment from the Literature*. Marine Sciences Research Center, Stony Brook University.

Buck, N., Gobler, C., and Sañudo-Wilhelmy, S. 2005. Dissolved Trace Element Concentrations in the East River-Long Island Sound System: Relative Importance of Autochthonous versus Allochthonous Sources. *Environmental Science & Technology*, 39 (10), 3528-3537.

Camargo, J.A. and Alonso, A. 2006. Ecological and Toxicological Effects of Inorganic Nitrogen Pollution in Aquatic Ecosystems: A Global Assessment. *Environment International*, 32 (6), 831-49. doi:10.1016/j.envint.2006.05.002.

Carbotte, S.M., Bell, R.E., Ryan, W.B.F., McHugh, C., Slagle, A., Nitsche, F.O., and Rubenstone, J. 2004. Environmental Change and Oyster Colonization within the Hudson River Estuary linked to Holocene Climate. *Geo-Marine Letters*, 24, 212-224.

Carpenter, D. and Welfinger-Smith, G. 2011. The Hudson River: A Case Study of PCB Contamination. *Water and Sanitation-Related Diseases and the Environment: Challenges, Interventions, and Preventative Measures*. doi: 10.1002/9781118148594.ch25.

Cerrato, R. 2006. Long-Term and Large-Scale Patterns in the Benthic Communities of New York Harbor. *The Hudson River Estuary*, Cambridge University Press, 242-265.

Cerrato, R.M. and Flood, R.D. 2009. Initial Investigations of Acoustic and Faunal Associations in the Hudson River Estuary. Report attached to Flood, R.D. and R.M. Cerrato, 2010, Scales and Significance of Sediment Variability in the Hudson River, Report to the Hudson River Foundation.

Chenery, M. 2002. Population Dynamics of Blue Crab (Callinectes Sapidus) in the Hudson River, New York. Thesis submitted to the Faculty of the Graduate School of the University of Maryland.

Dalton, D. 2006. Baykeeper Volunteer Oyster Restoration Program Achieves Historic Milestone. NYNJ Baykeeper Estuarian, Spring 2006, 1-4. http://nynjbaykeeper.org/wp-content/uploads/2013/05/springvol.pdf.

DePaola, A., Kaysner, C., Bowers, J., and Cook, D. 2000. Environmental Investigations of Vibrio Parahaemolyticus in Oysters after Outbreaks in Washington, Texas, and New York (1997 and 1998). *Applied and Environmental Microbiology*, 66 (11), 4649-4654.

Diaz, R.J. and Schaffner, L.C. 1988. Comparison of Sediment Landscapes in the Chesapeake Bay as seen by Surface and Profile Imaging. *Understanding the estuary; Advances in Chesapeake Bay research*. Chesapeake Research Consortium.

Diaz, R.J., Solan, M. and Valente, R.M. 2004. A review of approaches for classifying benthic habitats and evaluating habitat quality. *Journal of Environmental Management*, 73, 165-181.

Drake, A.A. Jr.,Volkert, R.A., Monteverde, D.H., Herman, G.C., Houghton,H.F., Parker, R.A., and Dalton, R.F. 1996. Bedrock Geologic Map of Northern New Jersey, Scale 1 to 100,000, 8 cross sections, 4 sheets, each size 58x41, I-2540-B.

Drake, S. and Kim, Y. 2011. Gowanus Canal Sponge Park^{TM}. *Ecological Restoration*, 29, 392-40.

Duffy-Anderson, J., Manderson, J., and Able, K. 2003. A Characterization of Juvenile Fish Assemblages Around Man-Made Structures in the New York–New Jersey Harbor Estuary, USA. *Bulletin of Marine Science*, 72 (3), 877-889.

EPA/902-R-03-002 2003. Sediment Quality of the NY/NJ Harbor System: A 5-Year Revisit 1993/4 – 1998 (http://www.epa.gov/emap/remap/html/docs/NY_NJHarbor98.pdf).

Ernst, A., and Dietrich, J. 2006. *Guide to Benthic Invertebrates of the Hudson River Park*. Center for the Environment Cornell University.

Farley, C. 1988. Histochemistry as a Tool for Examining Possible Pathologic Cause-and-effect Relationships between Heavy Metal and Inflammatory Lesions in Oysters, Crassostrea Virginica. *Marine Environmental Research*, 24 (1-4), 271–275. doi:10.1016/0141-1136(88)90319-4.

Farrell, S. 2012. The Gowanus Canal: Local Politics of 'Superfunding' Status. In *The World in Brooklyn:Gentrification, Immigration, and Ethnic Politics in a Global City.*

Feldman, R. 2001. Taxonomic and Size Structures of Phytophilous Macroinvertebrate Communities in Vallisneria and Trapa Beds of the Hudson River, New York. *Hydrobiologia*, 452 (1), 233-245.

Fisher, R.A., Corbet, S.A. and C.B. Williams (1943). The relation between the number of species and the number of individuals in a random sample of an animal population. *Journal of Animal Ecology*, 12(1), 42-58.

Flood, R.D. and R.M. Cerrato. 2010. Scales and Significance of Sediment Variability in the Hudson River, Final Report to the Hudson River Foundation.

Flood, R.D., Revised Multibeam Bathymetry, Sun-Illuminated Bathymetry, and Multibeam Backscatter Data Files, Report to NYSDEC Under MOU05120.

Folk, R.L. 1974. The Petrology of Sedimentary Rocks. The Walter Geology Library, Hemphill Publishing.

Franz, D. 1982. An Historical Perspective on Mollusks in Lower New York Harbor, with Emphasis on Oysters. *Ecological Stress and the New York Bight: Science and Management*, 181-197.

Franz, D. and Harris, W. 1988. Seasonal and Spatial Variability in Macrobenthos Communities in Jamaica Bay, New York - An Urban Estuary. *Estuaries*, 11 (1), 15–28.

Fung, M., and Levinton, J. 2005. Dispersal and Colonization of Limnodrilus Hoffmeisteri in a Hudson River Tidal Marsh Cove. Final Report of the Tibor T. Polgar Fellowship Program.

Galimany, E., Rose, J., Dixon, M., and Wikfors, G. 2013. Quantifying Feeding Behavior of Ribbed Mussels (Geukensia demissa) in Two Urban Sites (Long Island Sound, USA) with Different Seston Characteristics. *Estuaries and Coasts*, 36, 1265–1273.

Gardner, K., Nystroem, G., and Aulisio, D. 2007. Leaching Properties of Estuarine Harbor Sediment before and after Electrodialytic Remediation. *Environmental Engineering Science*, 24 (4), 424-433. doi:10.1089/ees.2006.05108.

Germano, J., Rhoads, D., Valente, R., Carey, D., and Solan, M. 2011. The Use of Sediment Profile Imaging (SPI) for Environmental Impact Assessments and Monitoring Studies: Lessons Learned from the Past Four Decades. *Oceanography and Marine Biology: An Annual Review*, 49, 247-310.

Gobler, C. and Buck, N. 2006. Nitrogen and Silicon Limitation of Phytoplankton Communities Across an Urban Estuary: The East River-Long Island Sound System. *Estuarine, Coastal and Shelf Science*, 68 (2), 127-138.

Gosner, K. 1969. Biological Fouling On Navigational Buoys In Hudson-River Estuary. *Bulletin New Jersey Academy Of Science*, 14 (1-2), 49.

Goto, D. and Wallace, W. 2010. Relative Importance of Multiple Environmental Variables in Structuring Benthic Macroinfaunal Assemblages in Chronically Metal-Polluted Salt Marshes. *Marine Pollution Bulletin*, 60 (3), 363–75. doi:10.1016/j.marpolbul.2009.11.002.

Goto, D. and Wallace, W. G. W. 2011. Altered Feeding Habits and Strategies of a Benthic Forage Fish (Fundulus Heteroclitus) in Chronically Polluted Tidal Salt Marshes. *Marine Environmental Research*, 72 (1-2), 75–88. doi:10.1016/j.marenvres.2011.06.002.

Grizzle, R., Ward, K., Lodge, J., Suszkowski, D., and Mosher-Smith, K. 2012. *Oyster Restoration Research Project (ORRP) Final Technical Report Orrp Phase I : Experimental Oyster Reef Development and Performance Results*.

Grothues, T. and Able, K. 2010. Association of Adult Fishes with Piers in the Lower Hudson River: Hydroacoustic Surveys for an Undersampled Resource. *Institute of Marine and Coastal Sciences*.

Grothues, T. and Able, K. 2013. *Impacts of Shoreline Modifications on Fishes and Crabs in New York Harbor*.

Hale, S., Benyi, S., Strobel, C., Kiddon, J., Hollister, J., Walker, H., and Heltshe, J. 2007. Benthic Indices: Developing, Evaluating, and Using Measures of Benthic Condition for Northeast Coastal Waters (ECO MYP). Poster presentation, Environmental Protection Agency (EPA) Atlantic Ecology Division Peer Review Poster Sessions, September 25th-28th, 2007. PDF at: http://www.epa.gov/aed/html/comm/posters/Hale_peer07FINAL.pdf. (accessed September 1, 2015.)

Harris, J. and Mass, A. 2008. Bronx River Pilot Oyster Reef Placement Report 2007 Season. *City of New York Parks and Recreation Natural Resources Group*.

Hoellein, T., Arango, C., and Zak, Y. 2011. Spatial Variability in Nutrient Concentration and Biofilm Nutrient Limitation in an Urban Watershed. *Biogeochemistry*, 106, 265–280.

Hoellein, T., Zarnoch, C., Branco, B., Bruesewitz, D., and Gardner, W. 2013. *The Influence of Oyster Restoration on Nitrogen Cycling in the Hudson-Raritan Estuary: Final Report to the Hudson River Foundation*, 1–52.

Ingersoll, E. 1881. A Report on the Oyster-industry of the United States. Department of the Interior, Tenth Census of the United States.

Iocco, L.E., Wilber, P., Diaz, R., Clarke, D.G., and Will, R.J. 2000a, Benthic Habitats of the New York/New Jersey Harbor: 1995 Survey of Jamaica, Upper, Newark, Bowery, and Flushing Bays, Final Report, NOAA Coastal Services Center, NOAA/CSC/2123-CD.

Iocco, L.E., Wilber, P., and Diaz, R. 2000b. Benthic Habitats of Selected Areas of the Hudson River, NY Based on Sediment Profile Imagery, report from NOAA's Coastal Services Center to NYSDEC.

Kelaher, B., Levinton, J., Oomen, J., Allen, B., and Wong, W. 2003. Changes in Benthos Following the Clean-up of a Severely Metal-polluted Cove in the Hudson River Estuary: Environmental Restoration or Ecological Disturbance? *Estuaries*, 26 (6), 1505–1516.

Kenna, T.C. and Nitsche, F.O. 2011. Using X-Ray Fluorescence Spectrometry to Rapidly Measure Metal Distributions in Hudson River Sediment Cores, Final Report to NYSDEC Contract C006787.

Kenna, T.C., Nitsche, F.O., Herron, M.M., Mailloux, B.J., Peteet, D., Sritrairat, S., Sands, E. and Baumgarten, J. 2010. Evaluation and Calibration of a Field Portable X-Ray Fluorescence Spectrometer for Quantitative Analysis of Siliciclastic Soils and Sediments. *Journal of Analytical Atomic Spectrometry*, 26 (2), 395-405.

Kim, J. K., Kraemer, G. P., and Yarish, C. 2014. Field Scale Evaluation of Seaweed Aquaculture as a Nutrient Bioextraction Strategy in Long Island Sound and the Bronx River Estuary. *Aquaculture*, 433, 148–156. doi:10.1016/j.aquaculture.2014.05.034.

Kratzer, E. B., Jackson, J. K., Arscott, D. B., Aufdenkampe, A. K., Dow, C. L., Kaplan, L. A., Newbold, J.D., and Sweeney, B. W. 2014. Drinking-water-supply Watersheds Macroinvertebrate Distribution in Relation to Land Use and Water Chemistry in New York City Drinking-water-supply Watersheds. *Journal of the North American Benthological Society*, 25 (4).

Kratzer, E., Jackson, J., and Arscott, D. 2006. Macroinvertebrate Distribution in Relation to Land Use and Water Chemistry in New York City Drinking-water-supply Watersheds. *Journal of the North American Benthological Society*, 25 (4), 954–976.

Larson, M. and Mankiewicz, P. 2006. Restoring Soundview Park HEP Priority Restoration Site LI10. *The Tidal Exchange: The Newsletter of the New York-New Jersey Harbor Estuary Program*, 1.

Llanso, R., Southerland, M., Volstad, J., Strebel, D., and Mercurio, G. 2003. Hudson River Estuary Biocriteria Project Final Report. New York State Department of Environmental Conservation.

Long, E., Wolfe, D., Stern, E., and Thursby, G. 1993. Sediment Toxicity in the Hudson-Raritan Estuary: Distribution and Correlations with Chemical Contamination. *Estuaries*, 19 (4), 901-912.

Lovegreen, J. R. 1974. Paleodrainage History of the Hudson Estuary: New York, NY, Columbia University Department of Geological Sciences Master's Thesis, 151 p., 8 pl.

Mackenzie, C.L. 2007. Causes Underlying the Historical Decline in Eastern Oyster (Crassostrea Virginica Gmelin, 1791) Landings. *Journal of Shellfish Research*, 26 (4), 927–938. doi:10.2983/0730-8000(2007)26[927:CUTHDI]2.0.CO;2.

Maher, N. and Cerrato, R. 2004. Feasibility of Mapping Benthic Biotopes in the Hudson River, Final Report to Lamont-Doherty Earth Observatory of Columbia University. Appendix 9 to Bell et al., 2004, Hudson River Estuary Program Benthic Mapping Project Phase III Report 1, Report to NYSDEC Under Contract C004092.

Maher, N.P. 2006. A New Approach to Benthic Biotope Identification and Mapping. Ph.D. Thesis, Marine Sciences Research Center, Stony Brook University, Stony Brook, NY.

McHugh, C.M.G., Pekar, S.F., Christie-Blick, N., Ryan, W.B.F., Carbotte, S., and Bell, R. 2004. Spatial Variations in a Condensed Interval Between Estuarine and Open Marine Settings: Holocene Hudson River Estuary and Adjacent Continental Shelf. *Geology*, 32 (2): 169-172.

Merguerian, C. and Baskerville, C. A. 1987. The Geology of Manhattan Island and the Bronx, New York City, New York, p. 137-140 in Roy, D. C., ed., Northeastern Section of the Geological Society of America, *Centennial Fieldguide*, 5, 481.

Merguerian, C. and Merguerian, M. 2004. Geology of Central Park – From Rocks to Ice. Hanson, G. N., *chm*., Eleventh Annual Conference on Geology of Long Island and Metropolitan New York, 17 April 2004, State University of New York at Stony Brook, NY, Long Island Geologists Program with Abstracts.

Moss, C.J. 2010. Newly Mapped Walloomsac Formation in Lower Manhattan and New York Harbor and the Implications for Engineers. Hanson, G. N., chm., Fifteenth Annual Conference on Geology of Long Island and Metropolitan New York, April 2010, State University of New York at Stony Brook, NY, Long Island Geologists Program with Abstracts.

Murphy, W., Ward, W.B., R. Fleming, S. Beda., G. Fleming, B. Boyd, and B.A. Baker 2004. Seasonal variations in the acoustical properties of black silt in the New York and New Jersey Harbor, Eleventh Conference on the Geology of Long Island and Metropolitan New York, April, 2004.

Nitsche, F.O. and Kenna, T.C. 2010. Hudson River Shallow Water Mapping: Sediment Sampling. Report submitted to Fugro as part of a Final Report to NOAA Coastal Services Center.

Nitsche, F.O. and Kenna, T.C. 2011. Detailed Analysis of Deposition in the Hudson River Estuary Through Integration of Geochemical and Geophysical Data, Final Report to NYSDEC Contract C006787.

Nitsche, F.O., Bell, R., Carbotte, S.M., Ryan, W.B.F., and Flood, R. 2004. Process-related Classification of Acoustic Data from the Hudson River Estuary. *Marine Geology*, 209 (1-4), 131-145.

Nitsche, F.O., Bell, R., Carbotte, S.M., Ryan, W.B.F., Slagle, A., Chillrud, S., Kenna, T., Flood, R., Ferrini, V., Cerrato, R., McHugh, C., and Strayer, D. 2005. Integrative Acoustic Mapping Reveals Hudson River Sediment Processes and Habitats, *EOS*, 86 (24), 225-229.

Nitsche, F.O., Carbotte, S., Ryan, W.B.F., and Bell, R. 2005. A Seabed Classification Approach based on Multiple Acoustic Sensors in the Hudson River Estuary. *High Resolution Morphodynamics and Sedimentary Evolution of Estuaries*, Springer, 33-55.

Nitsche, F.O., Kenna, T.C., and Haberman, M. 2010. Quantifying 20th Century Deposition in Complex Estuarine Environment: An example from the Hudson River. *Estuarine, Coastal and Shelf Science*, 89 (2), 163-174.

Nitsche, F.O., Ryan, W.B.F., Carbotte, S.M., Bell, R.E., Slagle, A., Bertinado, C., Flood, R., Kenna, T., and McHugh, C. 2007. Regional Patterns and Local Variations of Sediment Distribution in The Hudson River. *Estuary, Estuarine, Coastal and Shelf Science*, 71, 259-277.

Northern Ecological Associates. 2007. *Bronx River Watershed Management Plan (Volume 2) Wetland Field Assessment And Management Plan* (Vol. 2). Westchester County Department Of Planning.

NYCDEP. 2007. *Gowanus Canal Waterbody / Watershed Facility Plan Report*. Bureau of Engineering Design and Construction.

NYSDEC. 2015. *Biomonitoring: Biomonitoring in New York State*. www.dec.ny.gov/chemical/23847.html (accessed, September 10, 2015).

Pekar, S.F., McHugh, C.M.G., Christie-Blick, N., Jones, M., Carbotte, S.M., Bell, R.E. and Lynch-Stieglitz, J. 2004. Estuarine Processes and their Stratigraphic Record: Paleosalinity and Sedimentation Changes in the Hudson Estuary (North America). *Marine Geology*, 209 (1-4), 113-129.

Radosh, D. and Reid, R. 1980. *Benthic Macrofauna of Romer Shoal (Raritan Bay) in Relation to Sand Mining*. U.S. Department of Commerce, National Oceanic and Atmospheric Administration, National Marine Fisheries Service, Northeast Fisheries Center, Sandy Hook Laboratory.

Ravit, B., Walsh, S., Miskewitz, R., Quierolo, S., Comi, M., Lynn, C., and Steimle, F. 2011. *The Eastern Oyster (Crassostrea virginica) in the Hudson-Raritan Estuary: Restoration versus Shellfishery Regulation*.

Rhoads, D.C. 1974. Organism Sediment Relations on the Muddy Sea Floor. *Oceanography and Marine Biology Annual Review*, 12, 263-300.

Rhoads, D.C. and Germano, J.D. 1986. Interpreting Long-term Changes in Benthic Community Structure: A New Protocol. *Hydrobiologia*, 142: 291-308.

Sanderson, E. and LaBruna, D. 2005. Mapping the Historical Ecology and Reconstructing Historical Flora of the Lower Bronx River : A Guide Ecosystem Restoration and Outreach (p. 126). Wildlife Conservation Society.

Slagle, A., Carbotte, S., Nitsche, F., Ryan, W., and Bell, R. 2004. Spatial and Temporal Variability of Sedimentary Environments in the Hudson River Estuary. American Geophysical Union Spring Meeting Abstracts.

Slagle, A., Carbotte, S., Ryan, W., Bell, R., Nitsche, F., and McHugh, C. 2002. Changes in Depositional Setting Reflect Rising Sealevel in Latest Holocene Sediments of the Hudson River. American Geophysical Union Fall Meeting Abstracts, 1–2.

Slagle, A.L., Ryan, W.B.F., Carbotte, S.M., Bell, R., Nitsche, F.O., and Kenna, T. 2006, Late-stage Estuary Infilling Controlled by Limited Accommodation Space in the Hudson River. *Marine Geology*, 232 (3-4), 181-202.

Steimle, F., Caracciolo, J., and Pearce, J. 1982. Impacts of Dumping on New York Bight Apex Benthos. *Ecological Stress and the New York Bight: Science and Management*.

Strayer, D.L. and Malcom, M.M. 2004. Combining Geophysical and Biological Information to Define Benthic Habitats in the Hudson River. Appendix 8 to Bell et al. 2004, Hudson River Estuary Program Benthic Mapping Project Phase III Report 1, Report to NYSDEC Under Contract C004092.

Strayer, D.L., Malcolm, M.M., Bell, R.E., Carbotte, S.M., Nitsche, F.O. 2006. Using Geophysical Information to Define Benthic Habitats in a Large River. *Freshwater Biology*, 51, 25–38.

Stringer, M. 2002. NY / NJ Baykeeper Oyster Growth Study Year 2002 Report, 1–13.

Sweeney, A. and Sañudo-Wilhelmy, S. 2004. Dissolved Metal Contamination in the East River–Long Island Sound System: Potential Biological Effects. *Marine Pollution Bulletin*, 48 (7-8), 663-670.

USACE. 1999a. Final Environmental Impact Statement (FEIS) for the New York and New Jersey Harbor Study.

USACE. 1999b. Feasibility Report for New York and New Jersey Harbor Navigation Study, volume 2-Appendix F.

USACE. 1999c. Biological Monitoring Program 1998-1999, New York and New Jersey Harbor Navigation Study.

USACE. 2006. Harborwide Benthic Monnitoring Program Final Report. New York and New Jersey Harbor Deepening Project.

USACE. 2012. Sediment Distribution and Benthic Community Characterization in New York/New Jersey Harbor. Application of Adult and Juvenile Winter Flounder Data to Habitat Uses in New York/New Jersey Harbor. *NY and NJ Harbor Deepening Project*, App. B-2.

Wentworth, C.K. 1922. A Scale of Grade and Class Terms of Clastic Sediments. *Journal of Geology*, 30, 377-392.

Yeung, C. and McConnaughey, R.A. 2008. Using Acoustic Backscatter from a Sidescan Sonar to Explain Fish and Invertebrate Distributions: Case Study in Bristol Bay, Alaska. *ICES Journal of Marine Science*, 65, 242–254.